

*Microwave Detection of Fatigue Cracks in
Specially Prepared Steel Specimens*

Final Report

Submitted to:

**Virginia Transportation Research Council
530 Edgemont Road
Charlottesville, VA 22903**

by

**N. Qaddoumi, M. Frank, N. Bertrand, R. Mirshahi, S. Ganchev and R. Zoughi
Applied Microwave Nondestructive Testing Laboratory
Electrical Engineering Department
Colorado State University
Ft. Collins, CO 80523
(970) 491-0637**

September 1998

VTRC 99-CR3

Abstract

In the aging highway systems the problems of fatigue-induced damage and cracking in metal structures are very severe. Many such systems are operating even beyond their design lifetime, which requires more than the originally prescribed inspection cycles. In order to reduce the cost, increase testing efficiency and reliability, which subsequently improve the safety of steel bridge members, it is necessary to develop a highly reliable, fast and relatively inexpensive NDE technique. Currently, NDE methods for detecting fatigue cracks include visual inspection or the use of dye penetrant and magnetic particles. These techniques are labor-intensive, time-consuming and hazardous. Subsequently, other techniques are needed to detect and evaluate fatigue cracks in a bridge with minimal time for scanning and minimal safety precautions. These techniques should be able to detect cracks under paint well before any visible change (rust stain) appears on the paint surface. Additionally, these techniques should be able to detect surface breaking cracks on unpainted weathering steel as well as cracks filled with rust or paint. A solution to these problems is the use of different types of microwave sensors and testing methods for exposed, covered and filled crack detection. Microwave based NDE methods are capable of providing many practically useful features for this purpose. Open-ended coaxial line probes were used, at various frequencies, to detect the presence of cracks on weld joints and at critical locations. Many prescribed samples with known defects were obtained from the sponsor to conduct these microwave measurements. The detailed results of this investigation are presented in this report and the subsequent appendices.

Introduction

Detection of surface fatigue cracks on metals is an important concern in many applications [1-3]. Since 1991, several new microwave approaches for surface crack detection have been developed, and extensive measurements have been conducted at the Applied Microwave Nondestructive Testing Laboratory (*amntl*) in the Electrical Engineering Department at Colorado State University. We have established that an open-ended rectangular waveguide probe and an open-ended coaxial line probe operating in a certain frequency range, polarization and excitation mode can be used effectively for surface crack detection [4-26]. Each probe type (i.e. rectangular waveguide probe or coaxial line probe) has its own advantages and disadvantages when used for crack detection on metallic surfaces. The potential direct benefit of this study is to determine the potential practical capabilities of microwave NDE techniques for the detection of various cracks in specially prepared steel specimens. Coupled with other suitable NDE techniques, this will increase the reliability of inspections and the safety of bridge structures, and should reduce the cost of inspection. The general advantages of the microwave methods using open-ended rectangular waveguides are summarized as:

1. novelty of the approach compared to conventional NDE techniques. This is a fresh look at fatigue crack detection. The yet to be tapped capabilities of this technique, once fully developed, have the potential of making it popular and a prominently used method for crack detection and evaluation,

2. the method is fast, reliable and relatively inexpensive,
3. the sensor may or may not be in contact with the surface under examination,
4. cracks may be filled or covered with dielectric materials such as paint, dirt, rust, etc.,
5. the same probe which detects and characterizes the properties of a crack under coating, may also (without significant alteration to its design) measure the thickness of the coating and its material characteristics,
6. cracks may be on non-ferromagnetic as well as ferromagnetic metals,
7. microwave techniques work with coarse-grained materials,
8. the detected signal is only due to surface cracks and not to interior flaws. Hence, signal interpretation is easier compared to techniques in which one must discriminate between signals due to interior and surface flaws,
9. the technique may be applied to curved and other complicated surfaces depending on the degree of surface curvature,
10. crack orientation, edge and tip locations can be identified,
11. no special operator skills, in the fields of microwaves or signal interpretation, are needed for successful crack detection,
12. very little (if any) surface preparation is required,
13. the technique is environmentally compliant and operator friendly and safe,
14. the required microwave power is in the low milliwatt range,
15. such a system may be battery operated and portable,
16. the results are obtained in real-time,

17. the technique is not a source of high electromagnetic noise pollution (interference), and at the same time it is insensitive to external electromagnetic sources of interference,
18. adaptable to automatic (no operator involvement) detection schemes.

Open-ended coaxial probes are also capable of providing many of the above features and advantages. As will be mentioned later, this probe was primarily used in the current study. Consequently, its particular advantageous features will be summarized along with the probe description later.

Purpose & Scope

The primary objective of this research endeavor was to investigate and assess the capabilities and limitations of microwave nondestructive testing methods for the detection of exposed, covered and filled surface breaking cracks in laboratory environment, using specially prepared steel specimens. This included investigating the use of rectangular waveguide and open-ended coaxial probes operating at a multitude of frequencies. The ultimate goal (of the sponsor) is to make comparative evaluation of the potential of microwave detection techniques with other more standard detection techniques.

To accomplish the goal of this research project, the following specific tasks were performed:

1. **Obtained Reference Steel Specimens** - Special steel specimens with cracks of various dimensions and relative location with respect to weld joints were prepared and provided by the sponsor (VTRC). Some of these specimens included cracks on rusted steel specimens as well as cracks under paint. Subsequently, these specimens were used to determine the capabilities and limitations of these microwave method(s).
2. **Designed and Assembled Microwave Measurement Systems** - Several laboratory microwave sensors were assembled with characteristics appropriate for testing the provided steel specimens. These sensors primarily employed open-ended coaxial line probes. As will be explained shortly, open-ended rectangular waveguide probes, due to their inherent physical and dimensional characteristics with respect to the specimen characteristics, were found to be of very limited use. The utility of several measurement parameters proportional to the phase and magnitude of the reflection coefficient, standing wave properties and the operating frequency was investigated.
3. **Conducted Laboratory Measurements** - The performance characteristics of the microwave sensors were tested in the laboratory on the reference specimens when the cracks were exposed, filled and under coatings of paint and rust.
4. **Measurement-Parameter Optimization** - Based on the results of task 3, measurement parameters were optimized for increased detection sensitivity. To

accomplish this task, a multitude of measurements on each specimen in hand at CSU was conducted at once because we couldn't have all the specimens simultaneously.

5. Data Analysis - The results of these measurements are analyzed/reported in such a way that they can be easily compared with the measurement results of other NDE methods on the same specimens (for the purpose of this comparative study.

Methods and Materials

To achieve the goals set forth, several steel specimens in which cracks with different induced properties were obtained from the sponsor. Each sample had either a name describing its use (and its structure) or a number indicating its properties including the properties of the cracks. Some of these specimens were tested and then returned to the sponsor to be either corroded or painted and were tested again. The complete description of the specimens will be given in the results section. However, the following paragraphs provide for a succinct description of the two microwave measurement techniques mentioned earlier. For a more detailed description, the reader is encouraged to consult references [7,8,9,13,20,21,25,26].

Several sensors, employing either an open-ended rectangular waveguide probe or an open-ended coaxial line probe, were investigated for use in the inspection of the cracked steel

specimens. Using Open-ended rectangular waveguides, the dominant mode approach, experiments are conducted by moving the cracked metal surface over the aperture of the open-ended rectangular waveguide while monitoring the standing wave characteristics inside the waveguide. From previous works [4-24] it was observed that when the crack length is parallel to the broad dimension of the waveguide (i.e. orthogonal to the electric field of the dominant TE_{10} mode) the standing wave experiences a pronounced shift in location when the crack is inside the aperture of the waveguide compared to when the crack is outside the aperture (a short circuit condition). This shift indicates changes in the reflection coefficient properties of the metal surface perturbed by the crack. It was also observed that the shift is highly dependent on the relative location of the crack within the waveguide aperture (i.e. whether the crack is at the edge or at the center of the aperture). Figures 1a-b show the geometry of a crack with a width of W , a depth of D and a waveguide aperture with dimensions a and b when the crack length is parallel to the broad dimension of the waveguide. The scanning distance, is the distance that the probe moves with respect to an arbitrary point on the surface of the specimen while recording data. It was also observed that when the crack is not parallel to the broad dimension of the waveguide, the level of change in the standing wave decreased, and when the crack becomes parallel to the smaller dimension of the waveguide (parallel to the dominant TE_{10} mode electric field) there was no measurable perturbation in the characteristics of the standing wave. This is due to the fact that in this case the surface currents are parallel to the crack length and are insignificantly disturbed by the crack. "*Crack characteristic signal*" is referred to the detector voltage (the recorded signal) variations as a function of scanning distance, i.e. when a waveguide aperture is scanned over a crack.

Open-ended rectangular waveguide probes can also be used to detect cracks using the higher-order mode detection technique [6,9,13]. In an open-ended rectangular waveguide, only the dominant TE_{10} mode may propagate, all other modes are evanescent and decay exponentially. When no crack is present on the specimen surface, only the TE_{10} mode exists in the waveguide. However, the geometry of the crack perturbs the field distribution at the waveguide aperture during a scan, thus higher-order modes are generated [9]. These modes do not propagate and to pick them up, the probe has to be located very close to the aperture of the waveguide.

An open-ended coaxial probe or sensor is referred to a coaxial transmission line whose one end is cut and is exposed to free-space or any other material that is immediately adjacent to it. In this way, the fields present at this open aperture can interact with the material which is exposed to the aperture. Figures 2a-b show the side and plan views of an open-ended coaxial probe. These types of probes have been used extensively in dielectric property characterization of materials as well as inspection of biological tissues. An open-ended coaxial line is an inefficient antenna (from communications point of view), however the fields in the vicinity of its aperture may be used to interrogate its surrounding environment. The fields outside of an open-ended coaxial line may be considered to be non-propagating and be of the fringing type (or quasi-static). Open-ended coaxial lines, unlike other types of transmission lines (e.g. waveguides), have a large operating bandwidth when operating in their dominant transverse electromagnetic (TEM) mode. One may take advantage of this important feature when trying to optimize the utility of

this sensor as a nondestructive testing probe. Some of the features of this probe are [25,26]:

1. open-ended coaxial line probes are simple in design and easy to use,
2. the probe footprint is relatively small (a few millimeters in diameter), allowing a detailed inspection of a given area,
3. coaxial lines provide for a wide range of operating frequencies (compared to waveguides),
4. introduction of bends along the length of a coaxial line makes it suitable for accessing hard to reach areas such as inside holes, near edges and in and around weld joints,
5. the required input microwave power is in the low milliwatt range, and due to the radiation inefficiency associated with this sensor, there is no radiation hazard, in addition to the fact that edge effects are also minimized for the same reason,
6. the signal associated with the detection of a crack is quite distinctive, and consequently detection of a crack does not require much signal processing, unless a crack is in a “noisy” environment (i.e. rough surfaces) in which case simple feature extraction techniques may be employed,
7. coaxial line geometrical characteristics as well as the frequency of operation may be optimized for robust crack detection.

When operating in its dominant TEM mode, the electric and magnetic fields inside the coaxial line are orthogonal to each other, hence the TEM mode. The fields at the aperture of an open-ended coax are shown in Figure 3. When inspecting a metal surface by an

open-ended coaxial aperture, the coaxial line is considered to be short-circuited. This means that microwave currents will be induced on the surface of the metal plate. These currents follow the electric field lines and their amplitudes decrease as a function of distance away from the inner conductor (towards the outer conductor) [25]. Figure 4 pictorially describes the process of current distribution perturbation as half of the coaxial aperture scans a crack. Namely, a surface breaking crack on a conductor surface perturbs the current flow as the crack moves from the outer conductor towards the inner conductor. Since the current distribution has axial direction and the crack does not, as the crack moves from the outer conductor to the inner conductor, the current distribution becomes increasingly perturbed (Figure 4a-c). In addition, the magnitude of the surface currents increases as a function of decreasing distance from the inner conductor. Moreover and unlike open-ended rectangular waveguide aperture probes, the electric field polarization is axial which makes crack detection much more independent of the crack relative orientation than open-ended waveguide probes. This is an important feature of this probe. When the crack coincides with the inner conductor the current distribution is minimally (hardly any) perturbed, and a similar situation to that of the short-circuited case when the crack is outside the aperture occurs (Figure 4d). As the crack continues to move towards the outer conductor, on the other side, the opposite is repeated.

As explained above, during the scanning process, the coaxial line is first exposed to a short circuited load (e.g. when the crack is outside of the aperture) and then to a load whose reflection properties continually change as a function of the location of crack within the aperture (e.g. as more and more currents are perturbed). Monitoring a signal proportional

to this varying reflection coefficient gives an indication of the presence of the crack [25,26]. This distinct signal is referred to as the “*coax crack characteristic signal*”, and it gives a clear indication of the presence of a crack. Figure 5 shows a typical coax crack characteristic signal for a machined slot with a width of 0.2 mm and depth of 0.4 mm using coax # 3 (see Table I) at a frequency of 9 GHz. It is important to note that this is a typical signal for a machined slot in a flat and smooth aluminum specimen. The introduction of a slight liftoff and coatings such as rust and paint along with sever surface roughness (such as weld joints) alters the shape of this signal. In such cases the two distinct sides of this signal combine together producing one signal or “a bump or a dip” in between the two short circuit regions. Also, in these cases, the short circuit regions do not remain as flat and uniform, as shown in Figure 5.

At the beginning of this research endeavor the intention of the investigating team was to use both the open-ended rectangular waveguide and the open-ended coaxial probes to detect the presence of surface cracks on metals. This was suggested by the proposers since at that time they did not know the exact characteristics of the specimens which would be produced by the sponsor. Upon receiving the specimens it became clear that the rectangular waveguide probes could not be used because of the fact that most of the cracks were in welds or very close to them. Hence, because of the limited space available for the rectangular waveguide probe to conduct the needed scans this probe was found not to be very suitable for these specific specimens. As Indicated in Figure 1, rectangular waveguides are terminated into flanges. These flanges vary in dimensions depending on the frequency band at which the waveguide operates. For example, for X-band (8.2 GHz -

12.4 GHz) the flange is (42 mm x 42 mm) and for V-band (50 GHz – 75 GHz) is (18 mm x 18mm). Also, for a waveguide probe without a flange, the wall thickness of the waveguide is usually larger than the distance between cracks parallel to weld joints and the weld joints themselves. On the other hand, open-ended coaxial lines have smaller aperture dimensions as shown in Table I (outer diameters between 1 mm - 9 mm). Thus, the use of an open-ended coaxial line probe was the clear and direct approach for this investigation. The probing area of a coaxial line is relatively small and the space required is minimal. Several coaxial line probes were made and used throughout this project. Coaxial lines in general have a wide frequency of operation. The lower limit is dc (i.e. 0 Hz) and the size of the internal and the external conductors and the dielectric properties of the insulator in between determine the upper frequency limit. The dimensions and the upper frequency of operation (cutoff frequency of a coax) of several coaxial line probes are listed in Table I. As the table indicates, as the dimensions of the coaxial line become smaller, the upper frequency of operation increases. However, as the size gets smaller, maintaining a good contact between the coaxial line probe and the sample becomes more difficult. Setups with frequencies of operation covering several microwave frequency bands (X-, Ku-, K- and Ka-bands, 8.2-40 GHz) were assembled and used. Ultimately, measurements were conducted in X-, K- and Ka-frequency bands.

Although open-ended waveguide probes were not used, it must be noted that the detection scheme used for the coaxial probe is very similar to those of waveguide probes. The only difference is the interrogating probe (i.e. open-ended waveguide vs. open-ended coax).

Therefore, the investigating team's extensive expertise in using waveguide probes were directly utilized to increase the potential success of using coaxial probes.

In Table I, the coaxial probe length, D , provides for an arbitrary distance/phase which the incident and reflected signals travel from the microwave source and to the detector, respectively. Coupled with the frequency of operation and the location of the detector on the standing wave, this dimension can be used to enhance the measurement sensitivity (particularly for a fixed detector location and a fixed frequency of operation). Thus, fixed Gunn diode microwave sources and fixed location detectors may be used and the overall phase properties of the reflected signal may be adjusted by changing D .

Another issue that must be mentioned is that when detecting cracks on welds, due to the lack of relatively smooth scanning surface, the measurement results can significantly be different in shape compared to the results shown in Figure 5. In some cases where the crack is between two weld "humps", this probe may not be able to detect the crack.

Finally, the cracks in the samples provided by the sponsor were very tight cracks.

Therefore, the sensitivity of this microwave technique also is influenced by this fact. Open cracks (however small the opening may be) are easier to detect than completely closed cracks.

Results and Discussions

An extensive experimental effort was carried out during this investigation. Several specimens provided by the sponsor were tested using many microwave inspection systems. The measurements were conducted by placing the specimen on a table that is driven by a uniaxial stepper motor and scanning a coaxial line probe over these specimens as the table moves. Figure 6 shows the typical measurement setup used in the investigation. In addition, the influence of frequency on the ability to detect cracks was also investigated. The general sensor setup used in this investigation consisted of a simple integrated system employing a Gunn oscillator, as the microwave signal source, and a simple diode detector positioned at a fixed location on the standing wave pattern within a rectangular waveguide. The waveguide is terminated into a waveguide to coax transition to which a coaxial line probe (like the one shown in Figure 2a) is connected, as shown in Figure 6. In these measurements, a dc voltage proportional to the properties (phase and/or magnitude) of the reflection coefficient at the coaxial probe aperture is used to generate single line scans of the specimens with defects/cracks (i.e. to obtain crack characteristic signals), similar to that shown in Figure 5. The results show the detected output voltage as a function of scanning distance. In the subsequent sections, the results of the different experiments performed on many specially prepared samples are presented. Since numerous scans of these cracks were obtained, the representative results are explicitly shown and discussed in the various sections of this report. However, for completeness, all scan data are provided in various appendices at the end of this report. The important parameters of the data sets in each appendix are fully listed as well. The results will be

presented in the order they were obtained as the investigation progressed. The results will be presented for each group of samples received together.

Sample Group A:

This group includes the first set of samples received from the sponsor at the beginning of the investigation. This group includes the following samples:

- 1- A pipe sample with three cracks in it (Figure 7), the pipe sample had three cracks, or defects for the purpose of this report, on the welded joint. Crack one was a centerline indication with a length of 10 mm. Crack two was a toe indication with a length of 10 mm. The third crack was a transverse indication with a length of 11 mm.

- 2- Two flat plate samples each was made of two pieces of metal welded together, these samples are denoted as PL1497 and PL1498. Each sample had two cracks parallel to the weld line (Figures 8 and 9). Sample PL1497 had two cracks on the center of the weld, and both were on the top of the sample. Crack one was a centerline indication with a length of 36.8 mm, and crack two was a transverse indication with a length of 11 mm. Sample PL1498 also had two cracks along the edge of the weld. Crack two was on the bottom of the sample, while crack one

was on the top. Crack one was a toe indication with a length of 61 mm, and crack two was a root indication with a length of 24 mm.

- 3- Two T-shaped samples each made of two plates (A and B) where plate B was welded perpendicularly to the middle of plate A, with each sample containing two cracks (Figures 10 and 11), these samples are called T1495 and T1496. Sample T1495 had two cracks that were on the weld. Crack one was a centerline indication with a length of 64 mm, and crack two was a transverse indication with a length of 5.8 mm. Sample T1496 also had two cracks that run along the edge of the weld. Crack one was a toe indication with a length of 71 mm, and crack two is a root indication with a length of 34 mm.

These samples have center line/root/toe indication cracks (parallel to the welding direction), as well as transverse indication cracks (perpendicular to the welding direction). Throughout these measurements and as a function of the location of a given crack with respect to the weld in which it appeared, we tried scanning locations where the rough nature of the weld surface caused as minimal as possible of measurement/scanning difficulty. Depending on the orientation of a crack with respect to the weld surface in which it appeared, this was not always possible. A phase sensitive sensor utilizing a coaxial line probe, operating within the X-band (8.2 GHz - 12.4 GHz) frequency range was used to inspect these specimens. The frequency of operation was varied within the band to optimize the crack detection sensitivity. The detailed experimental results on this set and on all the other sets are presented in the appendices. Each appendix is named after

the group name for which the data was obtained (i.e. the detailed results for this group will be in appendix A). The pipe sample (sample 1 of group A) had three cracks as described above. Line scans, close to the cracks, were performed and a voltage that is primarily related to the phase of the reflection coefficient at the aperture of the coaxial line was recorded. Figure 12 shows the results obtained from an incontact scan of the first crack on the sample. The scan was conducted at a frequency of 11.9 GHz using coax #3 (refer to Table I). The presence of the crack is indicated by the dip at the middle of the scan. As can be seen, when no crack is present variations in the detected signal are minimal, however, once the crack is “seen” by the aperture a sudden deep dip is observed. The shape and level of the signal that indicates the presence of a crack depend on several factors. Frequency of operation, any slight liftoff, coaxial line dimensions and properties of the crack (i.e. width or opening and depth). Figures 13 and 14 show the results obtained from scanning the second and third cracks on the sample using the same sensor and frequency of operation used to detect the first crack. The results clearly indicate that the presence of these cracks on the pipe sample was detected and the shape of the crack characteristic signal, in Figure 14, is similar to that obtained for machined notches, as shown in Figure 5 and references [25,26]. The shape of the crack characteristic signal can be explained by understanding the mechanism by which the fields of the coax interact with the cracked metallic surface. As explained earlier, during the scanning process, the coaxial line is first exposed to a short circuited load (e.g. when the crack is outside of the aperture) and then to a load whose reflection properties continually change as a function of the location of crack within the aperture (e.g. as more and more currents are perturbed). Once, the crack lines up with the inner conductor, minimal perturbation

occurs. As the crack moves toward the outer conductor, the opposite is repeated. Figure 14 shows a signal that one would expect to obtain from a coaxial line probe scanning over a crack. However, Figures 12 and 13 show somewhat different characteristic signals from each other and from that of crack 3 (Figure 14). The difference is due to the presence of inevitable slight different liftoff associated with each measurement as well as the differences in the shapes and dimensions of the cracks. In addition, the local surface roughness significantly contributes to the apparent differences in these figures. However, what is important is the fact that these tight (closed) cracks are detected in this sample.

The same setup used to detect the cracks on the pipe specimen was used to inspect the two flat plate samples PL1497 and PL1498 of this group. Figure 15 presents the results obtained from scanning the first crack in sample PL1497 at 11.9 GHz. The crack was relatively close to the weld line and this made it relatively difficult to scan across the crack. Thus, this scan and many others were conducted, on this sample, by positioning the probe in between the crack and the weld line and then moving it across the crack. That is why the signal indicating the presence of the crack is close to the beginning of the scan. The presence of the crack is indicated by the peak obtained between 0.5 mm and 1 mm on the scanning distance axis. The cracks on the PL1498 were on the weld line and consequently there was no way, at that time, to scan across the cracks.

The T-plate specimens (T1495 and T1496) were inspected next. Specimen T1495 had a crack on side B that is perpendicular to the weld line. Figure 16 shows two 4 mm-long scans of the first crack on this specimen at a frequency of 11.9 GHz twice with the crack

present and once over an area devoid of cracks. The presence of the crack is detected as indicated in Figure 16. The two scans of the crack, shown in Figure 16, were conducted to check the repeatability. The signal detected due to the presence of the crack is clearly distinct from the signals obtained from outside the crack region (and from the region with no crack denoted as “control run”). The results indicate the sensitivity of the probe to the presence of the crack, as well as the repeatability associated with this technique once a crack is detected. The cracks on the second specimen T1496 were on plate A and were very close to the weld line. Again there was not enough space to scan across the crack. Later on in the study, we were able to modify the scanning procedure and were able to detect such cracks, as will be explained later.

Thus far, whenever a crack is scanned across its opening, its presence has been detected. The presence of a crack is indicated by a sudden change in the level of the detected signal. The detailed results obtained for these samples are presented in Appendix A. Up to this point only one setup operating at X-band had been used. Also, all measurements conducted so far have been conducted by scanning the coaxial line across the crack (as opposed to along the crack).

Sample Group B:

The samples of group A were sent back to the sponsor to induce a thin layer of rust on top of the surfaces of the specimens. Two sets of rusted samples were sent back to CSU, namely:

- 1- Samples PL1497 and PL1498 after a layer of rust had been induced on them.
- 2- Samples T1495 and T1496 after a layer of rust had been induced on them.
- 3- Pipe sample after a layer of rust had been induced on it.

As mentioned before, these samples include center line/root/toe indication cracks (parallel to the welding direction), as well as transverse indication cracks (perpendicular to the welding direction). As these samples were received, after a thin layer of rust was induced on their surfaces, the same setup used with group A (i.e. at X-band) was used to inspect the surfaces of these specimens; however, the results were not very promising at this band. Consequently, two sensors operating at higher frequency bands, namely K-band (18 GHz - 26.5 GHz) and Ka-band (26.5 GHz- 40 GHz), were built and used.

K-Band Results:

Since the objective of this research endeavor was to assess the capabilities and limitations of this newly developed technique, the investigating team was also learning while trying different techniques and setups suitable for the provided samples. The flat plate samples PL1497 and PL1498 were tested first after a thin layer of rust was induced on the surface of each specimen. Figure 17 shows the results obtained from two 3 mm-long scans of the first crack on PL1497 conducted at 24 GHz using coax #3. The two scans shown in the figure are for when the first crack is scanned and when a similar area devoid of cracks is scanned. The presence of the crack is indicated by the spike at the location of the crack in the scan. When compared to Figure 15 (e.g. the same crack not rusted and at 11.9 GHz) the results indicate that the presence of the crack is detected, however, the apparent shape of the signal has been modified as expected. It is important to note that detection is the primary goal. Figure 18 shows the results obtained from a 4 mm-long scan of the second crack on the specimen using the same setup used for detecting the first crack. As the figure indicates the presence of the crack is detected in the middle of the scan. Figure 19 shows the result of subtracting the signals obtained from scanning over the crack and away from the crack in Figure 18. Again, the presence of the crack is observed at the middle of the graph. Moreover, the graph resembles more the expected shape of the signal also. The same setup was then used to scan the cracks on the other rusted plate sample PL1498. We tried to scan across the cracks on the weld line without success (even before rusting the sample we were not able to scan across cracks on this specimen).

Cracks on the T-shaped samples (T1495 and T1496) were scanned next. The first crack on T1495 was scanned first and no conclusive results were obtained. Figure 20 shows the results obtained from a 3 mm-long scan of the second crack on sample T1495. The scan of the area that is devoid of cracks was uniform and the presence of the crack is detected by the large dip on the graph. Figure 20 indicates that a crack, under a thin layer of coating (i.e. rust or paint) may be detected using this technique. However, the crack characteristic signal tends to broaden since the crack is effectively exposed to the coaxial line fields for a larger scanning distance [21,23,25]. Hence, this is the reason for the wider signal due to the crack in this case. Again we attempted to scan across the crack on sample T1496 without success.

Ka-Band Results:

The flat plate samples PL1497 and PL1498 were tested at Ka-band after a thin layer of rust had been induced on the surface of each specimen. Figure 21 shows the results obtained from three 3 mm-long scans conducted at 34.5 GHz using the coax # 3. Two of the scans were conducted over the first crack (for repeatability) and one scan was conducted over an area devoid of cracks. The presence of the crack is indicated by the dip at the location of the crack in the scan. The thin layer of rust also acts as a dielectric coating covering the crack. The results shown in Figure 21 are consistent with those previously obtained for covered notches using open-ended coaxial probes [25] and as explained in the previous paragraph. Figure 22 shows the results obtained from a 4 mm-

long scan of the second crack on the specimen using the same setup used to scan over the first crack. As the figure indicates the presence of the crack is detected. The same setup was used to scan the cracks on the other rusted plate sample PL1498. Again, we attempted to scan across the cracks on the weld line without success, as explained earlier.

The Ka-band setup was used to scan the cracks on the T-shaped samples (T1495 and T1496) next. Figure 23 presents the results obtained from a 3 mm-long scan of the first crack on sample T1495. The scan was repeated twice and the presence of the crack was detected both times. Figure 24 shows the results obtained from a 3-mm long scan of the second crack on sample T1495. The scan of the area that is devoid of cracks was uniform and the peak on the graph indicates the presence of the crack. Again, we attempted to scan across the cracks on sample T1496 without success.

The rusted pipe sample was also inspected using the K-band and Ka-band systems. The cracks on this rusted sample were not detected. The investigating team is under the impression that the cracks were masked out by the thick layer of rust on top of them. The rust layer may have been thicker than the depth of the cracks and consequently after rusting the specimen no cracks were present. Or, due to the thickness of the rust layer the results were influenced by variations in the rust layer thickness more than they were influenced by the presence of the cracks. Also, in this specimen the rust was quite non-uniform and rough.

Sample Group C:

This group includes two sets of samples:

- 1- Two flat plate samples each is made of two pieces of metal welded together, these samples are denoted as PL4295 and PL4296. Each sample had two cracks (Figures 25 and 26). Sample PL4295 had two cracks along the edge of the weld. Crack two was on the bottom of the sample, while crack one was on the top. Crack one was a toe indication with a length of 12 mm, and crack two was a root indication with a length of 20 mm. Sample PL4296 also had two cracks that were on the weld, and both were on the top of the sample. Crack one was a transverse indication with a length of 15 mm, and crack two was a centerline indication with a length of 21 mm.

- 2- Two T-shaped samples each is made of two plates (A and B) plate B was welded perpendicularly to the middle of plate A. Each sample had two cracks, these samples are called T4297 and T4298 (Figures 27 and 28). Sample T4297 had two cracks on the weld. Crack one is a transverse indication with a length of 13 mm, and crack two is a centerline indication with a length of 8 mm. Sample T4298 has two cracks along the edge of the weld. Crack one is a root indication with a length of 12 mm, and crack two is a toe indication with a length of 26 mm.

Up to this point, in this experimental investigation, we have been able to detect the presence of cracks if the sensor can be scanned across them without much change in the liftoff (most of the scans were made in contact or at very small liftoffs). However, as explained earlier, on some samples the presence of cracks was not detected because we were not able to conduct scans across the opening of these cracks. These cracks were either on the weld lines or very close to them. At this point of our investigation we decided to scan the coaxial line probe, with respect to the crack orientation, in another fashion to detect the presence of a crack. Figure 4 shows the interaction between the current distribution and a surface breaking crack as it moves from the outer conductor to the inner conductor (a to d) of an open-ended coaxial probe aperture to produce a crack characteristic signal. Using this fact if the crack is partially between the outer and inner conductors the current distribution will change (Figures 4 a-c) and consequently the crack will be detected. The scenario depicted in Figures 4 (a-c) can be obtained if a scan is conducted in the direction that is parallel to the crack. From here on some of the scans will be parallel to the crack length and some across the crack opening depending on the crack location. Thus, the characteristic signals will have the short circuit value as long as no cracks are present. Once a crack is present between the outer and inner conductors of the coaxial line, the signal level changes. This new level depends on the frequency of operation and the position of the crack with respect to the inner and outer conductors and the crack dimensions. Figure 29 shows the schematic of this scanning process. The figure indicates that using this procedure of scanning may also provide for determining the location of crack tips.

K-band Results:

The above discovery took place when the samples of group C were received. Also, since higher frequencies showed more potential in detecting the cracks under rust, two new mechanically-tuned Gunn oscillators, operating at K-band and Ka-band were used in the setups. These two can be used to mechanically change the frequency of operation. This provides for the ability to easily change the frequency of operation, within each band, in order to obtain frequencies with maximum sensitivity for crack detection. Consequently, plate sample PL4295 was inspected first. Figure 25a shows the position of the first crack on the sample, while Figure 25b shows the position of the second crack, on the other side of the sample. Figures 30 and 31 show two 14.5 mm-long scans of the first crack (12 mm long) on the specimen conducted using coax # 3, same as before, at 25.45 GHz and 25.9 GHz, respectively. Each scan begins with the coax located on an area devoid of cracks and then moves parallel to the length of the crack, as depicted in Figure 29. Both figures indicate that the level of the signal changes as the crack is “seen” by the aperture of the coaxial line. These two figures also demonstrate the practical utility of the frequency of operation as a detection optimization parameter. The presence of the crack is indicated by higher values of the detected signal, with respect to the no crack (i.e. short circuit) signal, at 24.45 GHz and by the lower values obtained at 25.9 GHz. In this way one may also be able to detect crack tip locations as well, much like the rectangular waveguide approach [18]. The setup was later used to scan the area close to the second crack. This crack is slightly away from the weld line and the scan was conducted across the opening of the crack. Figure 32 presents the results of a 7 mm-long scan obtained at 24 GHz using coax

5. As the figure indicates the crack is clearly detected. The level of the detected signal indicates that the diode was positioned close to a minimum on the standing wave pattern and that is why the measured values were small. A dc-amplifier can be used to obtain larger levels of signal while maintaining the signal to noise ratio associated with the measurement. The detailed results are presented in the appendices. The width of the signal due to the crack is approximately equal to the outer dimension of coax # 5 which is used in this experiment (the same is true for coax # 5 whose results are shown in Figures 33 and 34). The results of Figure 32 clearly show the fact that the crack is detected. Its shape is rather consistent with the presence of a slight liftoff and partially due to having a diode detector near a minimum on the standing wave pattern.

Plate sample PL4296 was inspected next. Figure 26 shows the position and orientation of the two cracks on the sample. Figures 33 and 34 show two 4 mm-long scans of the first crack, across the opening of the crack, using coax # 2, at 23.55 GHz and 23.05 GHz, respectively. Both figures indicate that the level of the signal changes as the crack is “seen” by the aperture of the coaxial line. These two figures indicate the tremendous potential of using coaxial line probes for surface breaking cracks detection since the detected signal, due to the presence of the crack, is very distinct. The same setup was then used to conduct a parallel scan of the second crack on the specimen. Figure 35 shows a 32 mm-long scan of the area close to the second crack (20 mm long) conducted at a frequency of 25 GHz. The presence of the crack is detected as the deep (lower values) region extending between 5-25 mm on the scanning distance axis. This figure also demonstrates that crack length determination can be accomplished by utilizing such a

measurement. The variations on the detected signal are due to scanning over different portions of the crack along its length where the crack properties as well as liftoff may vary.

Sample T4297 was inspected next. Figure 27 shows the position and orientation of the two cracks on the sample. Figures 36 and 37 show two 4 mm-long scans of the first crack, across the opening of the crack, using coax # 3, at 26.5 GHz and 24.5 GHz, respectively. The scans begin with the coax located on an area devoid of cracks and then moves across the opening of the crack. Both figures indicate that the level of the signal changes as the crack is “seen” by the aperture of the coaxial line (i.e. the crack has been detected). The same setup was then used to conduct a parallel scan of the second crack on the specimen. Figure 38 shows a 14 mm-long parallel scan of the area close to the second crack (8 mm long) at a frequency of 23.8 GHz. The presence of the crack is indicated by the hump shaped region in the middle of the scan as the coax goes over the one tip of the crack, then scans over its length and finally over the other tip of the crack.

Figure 28 shows the position and orientation of the two cracks on sample T4298. Figures 39 and 40 show two 30 mm-long scans of the first crack, parallel to the length of the crack, using coax # 3, at 24.8 GHz and 24.1 GHz, respectively. Each scan begins with the coax located on an area devoid of cracks and then moves parallel to the length of the crack. Both figures indicate that the level of the signal changes as the crack is “seen” by the aperture of the coaxial line. The same setup was then used to conduct a parallel scan to the second crack on the specimen. Figure 41 shows a 40 mm-long scan of the area

close to the second crack (26 mm long) conducted at a frequency of 25 GHz. The presence of the crack is detected as the deep (lower values) region extending between 10-35 mm on the scanning distance axis. On this figure we notice that there are two deep dips. These two dips were thought to be due to the probe going over the crack tips. However, this crack was later found to be made of two adjacent cracks. This issue will be discussed later.

Ka-band Results:

Plate sample PL4295 was inspected at Ka-band next. Figure 42 shows a 20 mm-long parallel scan of the first crack (12 mm long) on the specimen conducted using coax # 3 at 32.15 GHz. The scan begins with the coax located on an area devoid of cracks and then moves parallel to the length of the crack. The figure indicates that the level of the signal changes as the crack is “seen” by the aperture of the coaxial line. Although the crack is detected, due to the local surface roughness around this crack the detected signal is not as symmetrical as that shown in Figure 41. The Ka-band setup was then used to conduct a parallel scan of the area close to the second crack (20 mm long). Although this crack is slightly away from the weld line, the scan was conducted parallel to the length of the crack. Figures 43 and 44 show the results obtained at 31.4 GHz and 31.6 GHz, respectively. Again, the influence of the frequency of operation and local surface roughness is indicated by the change of the shape of the crack characteristic signal.

Plate sample PL4296 was inspected next. Figures 45 and 46 show two 6-mm long scans of the first crack, across the opening of the crack, using coax # 3, at 30.75 GHz and 31.1 GHz, respectively. Both figures indicate that the level of the signal changes as the crack is “seen” by the aperture of the coaxial line. The peak and dip in Figures 45 and 46, respectively, indicate the presence of the crack. For the given coaxial probe (#3) used in these experiments, the different frequencies cause the detector diode to be located at different locations on the standing wave. Thus, the various shapes associated with the coaxial line crack characteristic signals indicate the many different shapes that can be obtained. However, in all cases the crack is distinctly detected. The results also indicate that the crack may be detected at many different frequencies. The same setup was then used to conduct a parallel scan to the second crack on the specimen. Figure 47 shows a 30 mm-long scan of the area close to the second crack (21 mm long) conducted at a frequency of 31.1 GHz. The presence of the crack is detected in the region extending between 5-25 mm on the scanning distance axis.

Figure 48 shows two 6 mm-long scans of the first crack on sample T4297. These scans were conducted across the opening of the crack, using coax # 2, at 35.6 GHz. The scan was repeated twice for repeatability. The figure indicates that the level of the signal changes as the crack is “seen” by the aperture of the coaxial line. The same setup was used to conduct a parallel scan to the second crack on the specimen. Figure 49 shows a 14.5 mm-long parallel scan of the area close to the second crack (8 mm long) conducted at a frequency of 32.55 GHz using coax # 3. The figure indicates that the presence of the surface breaking crack is detected.

Sample T4298 was inspected next. Figures 50 and 51 show two 35 mm-long scans of the first crack, parallel to the length of the crack, using coax # 3, at 30.6 GHz and 31 GHz, respectively. The presence of the crack is indicated by the change of the signal level as the probe scans over the length of the crack. The same setup was then used to conduct a parallel scan to the second crack on the specimen. Figure 52 shows a 40 mm-long scan of the area close to the second crack (26 mm long) conducted at a frequency of 30.8 GHz. The measurement indicates that two cracks have been detected. After further investigation it was observed that this crack is made of two smaller cracks close to each other. The peaks (higher values) on the scanning distance axis indicate the presence of the cracks. Initially, when K-band was used we thought that the two distinct dips on Figure 41 were due to the tips of the crack. To confirm the results many other measurements were conducted on this specimen at different frequencies all of which leave us to believe that there are two cracks present in that location. Figure 53 shows the results of a 40 mm-long scan conducted using the same setup used in the first scan of these cracks, at a frequency of 31.13 GHz. The presence of the two cracks (forming the crack) is observed as two distinct dips. This observation must be compared to other techniques when detecting this crack.

Sample Group D:

This group includes the two sets of samples of group C after they were painted:

- 1- Samples PL4295 and PL4296 after a layer of paint has been applied to them (Figures 25 and 26).
- 2- Samples T4297 and T4298 after a layer of paint has been applied to them (Figures 27 and 28).

To investigate the capabilities and limitations of the technique at hand to detect the presence of surface breaking cracks under paint, several measurements on the prescribed specimens were conducted. K- and Ka-band systems were used because frequencies in these two bands demonstrated tremendous potential in detecting cracks including cracks under rust.

K-band Results:

The first inspected sample, after painting, was plate sample PL4295. Figure 54 shows a 20 mm-long parallel scan of the first crack (12 mm long) on the specimen conducted using coax # 2 at 24.8 GHz. The scan begins with the coax located on an area devoid of cracks and then moves parallel to the length of the crack. The figure indicates that the level of

the signal changes as the crack is scanned over by the aperture of the coaxial line. The setup was used to scan the area close to the second crack (20 mm long) next. This crack is slightly away from the weld line and the scan was conducted parallel to the length of the crack. Figure 55 shows the results obtained from a 25 mm-long scan at 23.66 GHz using coax # 2. The detailed results are presented in Appendix D.

The second sample inspected was plate sample PL4296. Figure 26 shows the position and orientation of the two cracks on the sample. Figures 56 and 57 show two 14.5 mm-long scans of the first crack parallel to the length of the crack using coax # 2, at 24.08 GHz and 23.44 GHz, respectively. Each scan begins with the coax located on an area devoid of cracks and then it moves parallel to the length of the crack. Both figures indicate that the level of the signal changes as the crack is scanned over by the aperture of the coaxial line. The influence of the frequency of operation on the measurement can be observed by noticing that the only difference between the two measurements shown in the two figures is the frequency of operation. As was shown before, a scan that is parallel to the length of the crack would start at a certain level (short circuit) this level changes as a crack is seen by the aperture. In this case, the presence of the crack is still detected, but due to the paint layer on top of the surface, the shape of the detected signal has changed. This is consistent with the results obtained from rusted samples measurements and the results obtained using open-ended rectangular waveguide probes for covered cracks [21,25]. The same setup was then used to conduct a parallel scan to the second crack on the specimen. Figures 58 and 59 show two 34 mm-long scans of the area close to the second crack (21 mm long) conducted at 24.4 GHz and 23.8 GHz using coax # 2. The presence of the

crack is detected as the hump (larger values) on Figure 58 or the deep (lower values) region extending between 5-25 mm on the scanning distance axis on Figure 59.

Sample T4297 was inspected next. Figure 27 shows the position and orientation of the two cracks on the sample. No conclusive results were obtained on the detection of the first crack under paint on this specimen using the K-band setup. This setup was then used to conduct a parallel scan to the second crack on the specimen. Figures 60 and 61 show two 25 mm-long scans of the area close to the second crack (8 mm long) conducted at 23.6 GHz and 22.6 GHz, respectively. The presence of the crack is indicated by the hump shaped region in the middle of the scan as the coax is moved over one tip of the crack, then over its length and finally over the other tip of the crack as shown in Figure 60. Figure 61 shows that the presence of the crack is indicated by the dip on the graph.

Figure 28 shows the position and orientation of the two cracks on sample T4298. Figures 62 and 63 show two 25 mm-long scans of the first crack, parallel to the length of the crack, using coax # 2, at 24.8 GHz and 23 GHz, respectively. The presence of the crack is detected in both cases. The same setup was then used to conduct a parallel scan to the second crack on the specimen. No conclusive results were obtained from these measurements at this frequency band. The detailed results are presented in Appendix D.

Ka-band Results:

Plate sample PL4295 was inspected at Ka-band next. Figure 64 shows a 20 mm-long scan of the first crack (12 mm long) on the specimen conducted using coax # 3 at 30.16 GHz. The scan begins with the coax located on an area devoid of cracks and then moves parallel to the length of the crack. The figure indicates that the level of the signal changes as the crack is “seen” by the aperture of the coaxial line. The same setup was then used to scan the area close to the second crack (20 mm long). Although this crack is slightly away from the weld line, the scan was conducted parallel to the length of the crack. Figures 65 and 66 show the results obtained at 32 GHz and 32.7 GHz, respectively. Again, the influence of the frequency of operation is indicated by the change of the shape of the crack characteristic signal.

Plate sample PL 4296 was inspected next. Figure 67 shows a 4 mm-long scan of the first crack, across the opening of the crack, using coax # 3, at 30.6 GHz. The figure indicates that the level of the signal changes as the crack is “seen” by the aperture of the coaxial line. This signal is consistent with the results obtained using coaxial probes for detecting cracks under coatings [25]. The presence of the crack is indicated at the middle of the scan. The same setup was then used to conduct a parallel scan to the second crack on the specimen. Figures 68 and 69 show two 40 mm-long parallel scans of the area close to the second crack (21 mm long) conducted at 31.8 GHz and 32 GHz, respectively. The presence of the crack is detected in the region extending between 5-25 mm on the scanning distance axis.

Figure 70 shows a 10 mm-long scan of the first crack on sample T4297. The scan was conducted across the opening of the crack, using coax # 3, at 31.36 GHz. The figure indicates that the level of the signal changes as the crack is “seen” by the aperture of the coaxial line. Although the crack is under a layer of paint, the presence of the crack is still distinctly detected. The same setup was then used to conduct a parallel scan to the second crack on the specimen. Figure 71 shows a 10 mm-long scan of the area close to the second crack (8 mm long) conducted at a frequency of 32.26 GHz. The Figure clearly indicates that the presence of the surface breaking crack is detected.

Sample T4298 was inspected next. Figure 72 shows a 20 mm-long scan of the first crack, parallel to the length of the crack, using coax # 3, at 31.7 GHz. The scan begins with the coax located on an area devoid of cracks and then moves parallel to the length of the crack. The same setup was then used to conduct a parallel scan to the second crack on the specimen. Figures 73 and 74 show two 40 mm-long scans of the area close to the second crack (26 mm long) conducted at 31.6 GHz and 32.13 GHz, respectively. The measurement indicates that two cracks have been detected, even under a layer of paint. The presence of the cracks is detected as the two dips (lower values) on Figure 73 and as the two peaks (higher values) on Figure 74.

Measurement Parameters Optimization

As mentioned above, the primary objective of this research endeavor was to investigate and assess the capabilities and limitations of newly developed microwave nondestructive testing methods for the detection and evaluation of exposed, covered and filled surface breaking cracks in laboratory environment, using specially prepared steel specimens. This included investigating the use of open-ended coaxial line probes operating at a multitude of frequencies. The results presented in the preceding sections were indicative of the measurements conducted at many frequencies throughout this investigation. However, most of the presented measurements were conducted at several frequencies of operation and using several coaxial line probes. In real life situations it is desired to use one setup, operating at a certain frequency and utilizing a certain coaxial probe. This capability is demonstrated next. Many of the measurements conducted on group C samples were repeated on group D samples (i.e. using the same setups including the frequency of operation and coaxial line probe). The results presented in the appendices of these two groups indicate that there are many combinations (frequency of operation/coax) that can be used to detect most of the cracks on these specimens. However, a sample of such a combination is presented here to illustrate the point. Ka-band setup operating at a frequency of 30.6 GHz was used to scan most of the cracks on the samples before and after paint. Coaxial line # 3 was used in all the measurements as well. Figures 75 – 84 present the results obtained from scanning different cracks on different specimens. Some of the presented characteristic signals were obtained by scanning across cracks (i.e. those figures showing short scanning distances) while others were obtained by scanning parallel

to the length of cracks (i.e. those figures showing long scanning distances). In all scans the presence of a crack is detected. Other frequencies (e.g. 32GHz) were used to inspect many cracks as can be seen in the appendices. These results have a very important practical ramification that a prototype can be built (utilizing these parameters for example) to inspect the presence of cracks on steel samples.

Conclusions

Extensive sets of microwave measurements for detecting various cracks in several specially prepared specimens were conducted. The issues of interest included crack detection capability and the influence of the frequency of operation. The microwave techniques used in these experiments utilized the open-ended coaxial line probes. These measurements covered a broad range of microwave and millimeter wave frequencies from 8.2 GHz to 40 GHz.

The cracks were also diverse in nature. They included cracks that were on smooth surfaces (away from the weld lines), very close to weld lines, and on the weld line. In addition some of these cracks were under rust or paint layers. Throughout the investigation it was clear that if a crack can be scanned across, its presence is detected. Also if a crack is too close to a weld line or is on a weld line, scanning parallel to it would reveal the crack detectable as well. Cracks under a layer of rust or a layer of paint were detected as well.

The influence of frequency, on detection capability, was investigated as well. Moreover, several cracks were scanned multiple times to show the repeatability associated with this technique. It was also demonstrated that using one near-optimal frequency of operation (for a given detection system configuration) it is possible to detect most (if not all) of the cracks in the specimens. Generally, cracks in different specimens were detected easily and repeatedly using this technique. This was shown to be true at numerous frequencies. Cracks under rust were not detected when frequencies in the X-band were used. The results showed that using frequencies in the K-band and the Ka-band revealed most of the cracks detectable. However, the obtained results show that the use of crack detection sensors operating at Ka-band frequencies gives the best results in general.

The local surface roughness and associated liftoff also influenced the results. This was primarily evident as the shape of the detected signals underwent some related changes. Cracks on welds present the most difficulty in detection due to this fact. For these cracks we used regions that presented the least possible surface roughness while scanning. Due to these reasons some of the cracks were not detected using this technique indicating the practical limitation associated with this technique. Cracks under paint were for the most part detected as well. It is possible that increased incident power may enhance these results as this was shown to be true for waveguide probes [22].

Overall, the results show that the use of open-ended coaxial line probes in microwave nondestructive surface crack detection is quite viable for detecting various cracks in the

specimens provided. The main goal in this investigation was to show the capabilities of this newly developed technique for the purpose of crack detection. However, this technique needs to be further optimized so that it may be applied to a whole host of cracks at a single frequency and system configuration. It must be noted that cracks on welds were detected once their location was known. For an unknown weld its entirety must be scanned (i.e. similar to other techniques). Nevertheless, the results are promising.

REFERENCES

1. Lozev, "Noncontact Nondestructive Detection and Evaluation of Fatigue Cracks in Steel Bridge Members," Research Proposal # VTRC96-RP-16.
2. Yeh, C.Y., "Detection and Sizing of Surface Cracks in Metals Using Open-Ended Rectangular Waveguides," Ph.D. Dissertation, Electrical Engineering Department, Colorado State University, 1994.
3. Feinstein, L. and R.J. Hruby, "Surface Crack Detection by Microwave Methods," 6th Symp. on Nondestructive Evaluation of Aerospace and Weapons Systems Components and Materials, San Antonio, Texas, 1967.
4. Yeh and R. Zoughi, " Surface Crack Detection on Metal Using a Novel Microwave Approach," ASNT Fall'92 Conference, Chicago, IL., November 16-20, 1992.
5. Yeh and R. Zoughi, "Metal Surface Crack Detection and Sizing Using a Novel Microwave Approach," Presented at the Special Session on "NDE and its Application in Fracture Mechanics," an ASME Conference, Denver, CO, July 25-29, 1993.

6. Yeh and R. Zoughi, "Higher Order Modes as Indicators of Fatigues Cracks on Metal Surfaces," ASNT Spring 1994 Conference, 3rd Annual Research Symposium Summaries, pp. 223-225, New Orleans, LA, March 21-25, 1994.
7. Yeh and R. Zoughi, " Microwave Detection of Finite Surface Cracks in Metals Sizing Using Rectangular Waveguide Sensors," Research in Nondestructive Evaluation, vol. 6, no. 1, pp. 35-55, 1994.
8. Yeh and R. Zoughi, "A Novel Microwave Method for Detection of Long Surface Cracks in Metals," IEEE Transactions on Instrumentation and Measurement, vol. 43, no. 5, pp. 719-725, October 1994.
9. Yeh, E. Ranu and R. Zoughi, "A Novel Microwave Method for Surface Crack Detection Using Higher Order Waveguide Modes," Materials Evaluation, vol. 52, no. 6, pp. 676-681, June 1994.
10. Yeh and R. Zoughi, "A Microwave Technique for Sizing Finite Cracks on Metal Surface Using Open-Ended Rectangular Waveguides," Proceedings of SPIE Symposium, Advanced Microwave and Millimeter Wave Detectors Conference, vol. 2275, pp. 112-118, San Diego, CA, July 24-29, 1994.
11. Yeh and R. Zoughi, "A Millimeter Wave Method for Detection of Finite Surface Cracks in Metal," Proceedings of SPIE Symposium, Advanced Microwave and

Millimeter Wave Detectors Conference, vol. 2275, pp. 103-111, San Diego, CA, July 24-29, 1994.

12. Yeh and R. Zoughi, "Sizing Technique for Slots and Cracks in Metals," *Materials Evaluation*, vol. 53, no. 4, pp. 496-501, 1995.
13. Huber and R. Zoughi, "Higher Order Modes as Indicators of Surface Cracks Under Stratified Dielectric Coatings Using an Open-Ended Waveguide," *Proceedings of the Review of Progress in Quantitative NDE*, vol. 14A, pp. 637-642, Snowmass, CO, August 1994.
14. Huber and R. Zoughi, "Microwave/mm-Wave Detection of Surface Cracks Under Stratified Dielectric Coatings Using an Open-Ended Waveguide," *Proceedings of the ASNT Fall '94 Conference*, pp. 180-182, Atlanta, GA, September 19-23, 1994.
15. Huber, "Electromagnetic Modeling of Exposed and Covered Surface Crack Detection Using Open-Ended Waveguides," Ph.D. Dissertation, Electrical Engineering Department, Colorado State University, 1995.
16. Zoughi, R. Salem, C. Huber, and H. Abiri, "Microwave/mm-Wave Detection of Surface Cracks Filled with a Dielectric Using an Open-Ended Waveguide," *ASNT*

Spring '95 Conference Paper Summaries, pp. 46-48, Las Vegas, NV, March 20-24, 1995.

17. Zoughi, R. Salem, C. Huber, S. Ganchev, and H. Abiri, "Application of Open-Ended Rectangular Waveguides for Detecting Surface Cracks," Proceedings of SPIE Symposium, Nondestructive Evaluation of Aging Infrastructure Conference, vol. 2456, pp. 269-280, Oakland, CA, June 6-8, 1995.
18. Ganchev, S.I., C. Huber, R. Runser, E. Ranu, and R. Zoughi, "Microwave Method for Locating Surface Crack Tips in Metals," *Materials Evaluation*, vol. 54, no. 5, pp.598-603, May 1996.
19. Zoughi, S. I. Ganchev, C. Huber, E. Ranu, and R. Runser, "A Novel Microwave Method for Filled and Covered Surface Crack Detection in Steel Bridge Members Including Crack Tip Identification," Final (Fourth Quarterly) Report, Federal Highway Administration (FHWA), Grant no. DTFH61-94-X-00023, p.187, Sept. 1995.
20. Huber, H. Abiri, S. I. Ganchev, and R. Zoughi, "Analysis of the Crack Characteristic Signal Using a Generalized Scattering Matrix Representation," *IEEE Transaction on Microwave Theory and Techniques*, vol. 45, no. 4, pp. 477-484, April 1997.

21. Huber, H. Abiri, S. I. Ganchev, and R. Zoughi, "Electromagnetic Modeling of Surface Crack Detection in Metals Under Dielectric Coatings using Open-Ended Rectangular Waveguides," *IEEE Transaction on Instrumentation and Measurement*, vol. 45, no. 11, pp. 2049-2057, November 1997.
22. Zoughi, S. Ganchev, and C. Huber, " Microwave Measurement-Parameter Optimization for Detection of Surface Breaking Hairline Cracks in Metals," *IEEE Nondestructive Testing and Evaluation*, vol. 14, pp. 323-337, 1998.
23. Qaddoumi, N., E. Ranu, R. Mirshahi, P. Stepanek, V. Otashevich, C. Huber and R. Zoughi, "Development of Equipment for and Quantitative Analysis of Microwave Detection and Evaluation of Fatigue Induced Surface Cracks in Steel," Final Report, Federal Highway Administration (FHWA), Grant no. DTFH61-94-X-00023, p. 519, January, 1998.
24. Qaddoumi, N., E. Ranu and R. Zoughi, "Portable Microwave System for Measurement of Fatigue Cracks," Final Report, SBIR 97-FH1 Subcontract Report, RLE Technologies, Inc., Ft. Collins, CO, p. 32, April 1998.
25. R. Zoughi, C. Huber, J. Easter and K. Hayes, "Microwave Detection of Surface Cracks in Metals Under Dielectric Coatings Using Open-Ended Coaxial Sensors: Preliminary Results" Special Topics Proceedings of *Nondestructive Evaluation of Infrastructure*, edited by H. Reis and B. Djordjevic, 1997.

26. Zoughi, R., K. Hayes and S. Ganchev, "Microwave Detection of Hairline Surface-Breaking Cracks in Metals Using Open-Ended Coaxial Sensors: Preliminary Results," *Proceedings of SPIE Symposium, Nondestructive Evaluation Techniques for Aging Infrastructure & Manufacturing Conferences*, vol. 2945, pp. 444-450, Scottsdale, AZ, December 2-5, 1996.

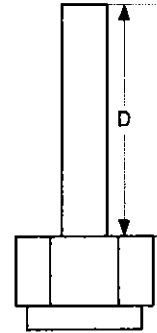
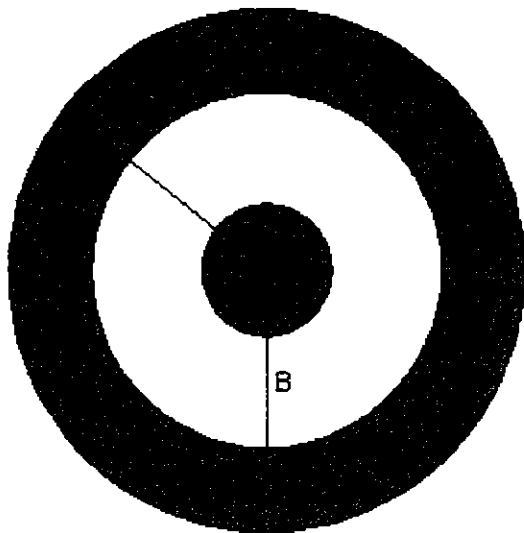


Table I: Dimensions and cutoff frequencies of coaxial line probes.

Coax #	A	B	C	D	Cut-off frequency
1	0.5 mm	1.5 mm	1.75 mm	40.0 mm	30.93 GHz
2*	0.5 mm	1.5 mm	1.75 mm	17.5 mm	30.93 GHz
3*	0.25 mm	0.75 mm	1.0 mm	19.5 mm	61.87 GHz
4	0.25 mm	0.75 mm	1.0 mm	22.8 mm	61.87 GHz
5*	0.5 mm	1.5 mm	1.75 mm	37.0 mm	30.93 GHz
6	0.25 mm	0.75 mm	1.0 mm	9.5 mm	61.87 GHz
7	1.0 mm	3.5 mm	4.0 mm	47.5 mm	13.75 GHz
8	1.75 mm	5.0 mm	9.5 mm	5.0 mm	9.16 GHz

* Indicates coaxes used in this investigation.

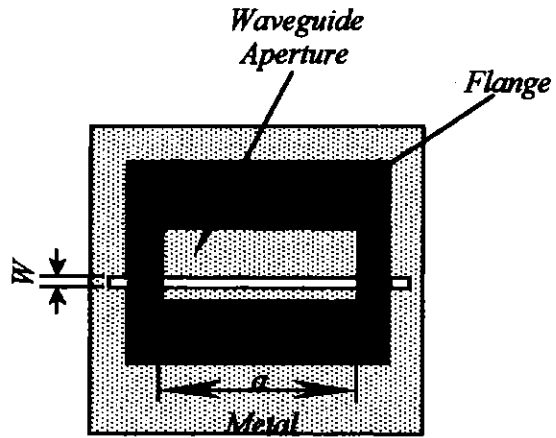


Figure 1a: Plan view of a flange-mounted open-ended rectangular waveguide scanning a metal surface with a crack [8].

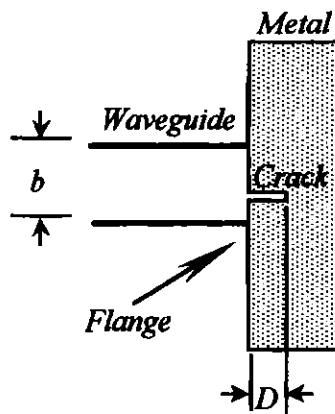


Figure 1b: Side view of a flange-mounted open-ended rectangular waveguide scanning a metal surface with a crack [8].

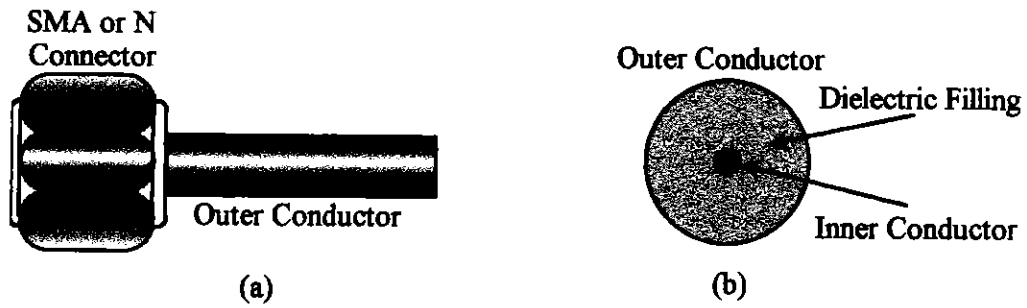


Figure 2: a) side view and b) plan view of an open-ended coaxial line/probe [25].

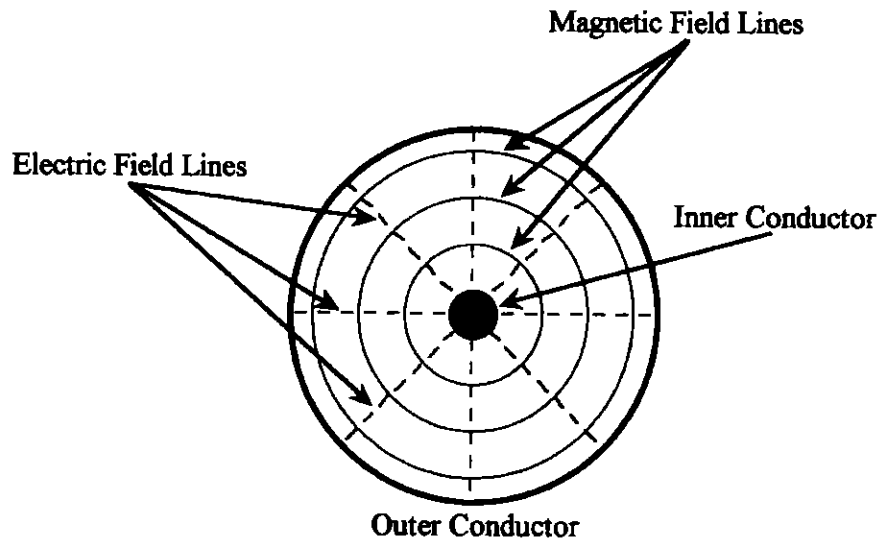


Figure 3: Dominant mode electric and magnetic field distributions of an open-ended coaxial line [25].

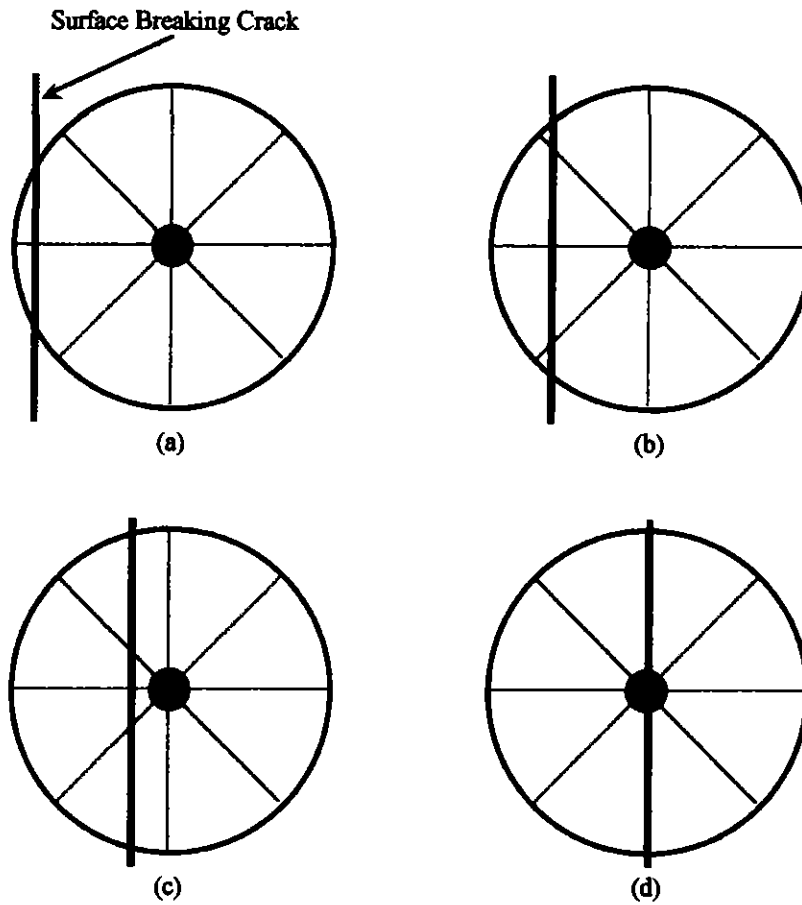


Figure 4: Interaction between current distribution and a surface breaking crack as it moves from the outer conductor to the inner conductor (a to d) of an open-ended coaxial probe aperture [25].

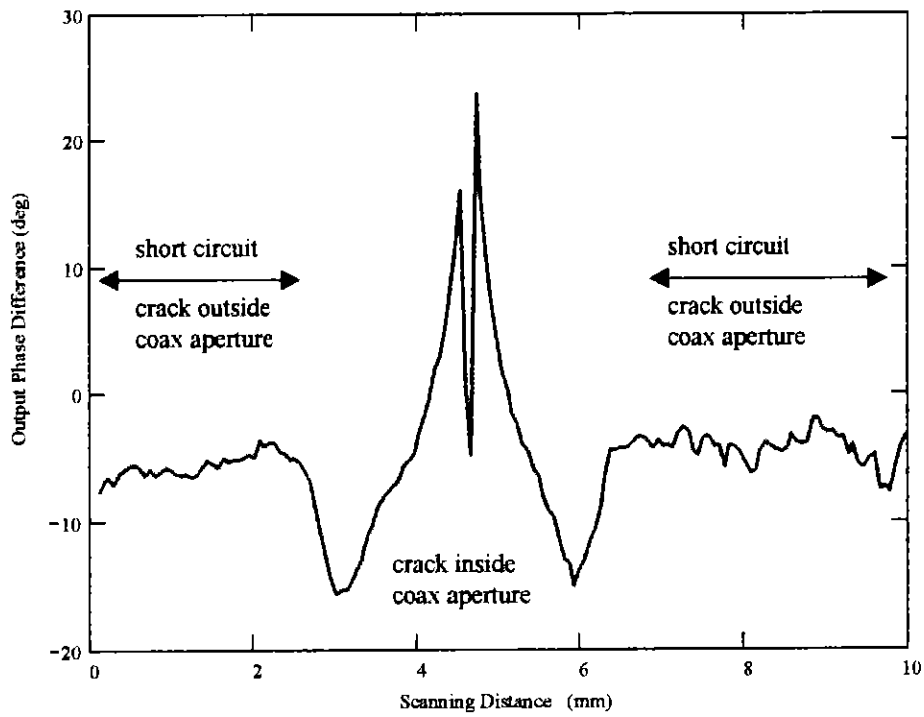


Figure 5: Crack characteristic signal of a machined notch at 9 GHz using coax # 3.

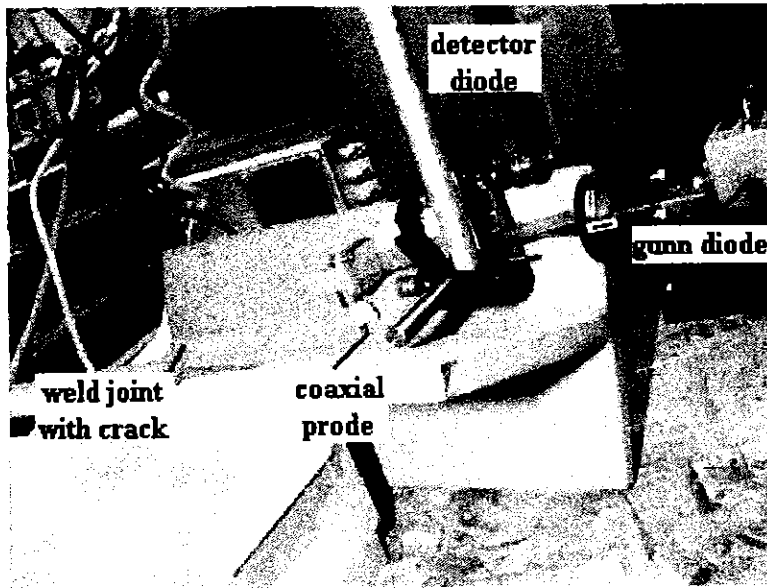


Figure 6: Typical coaxial line probe measurement setup.

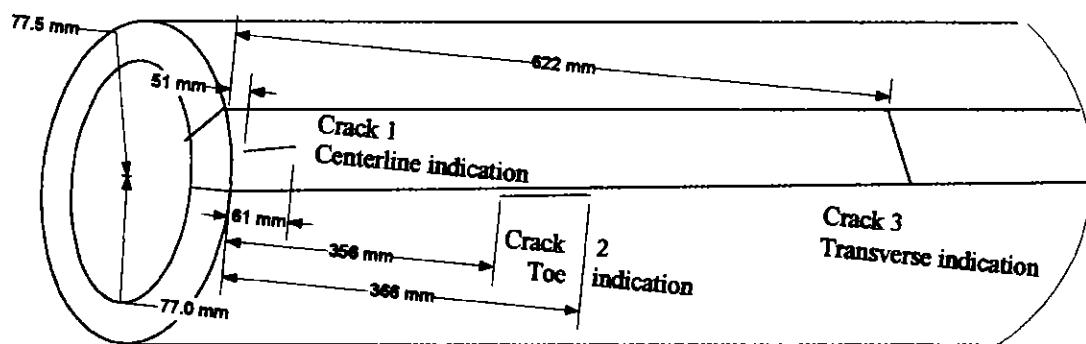
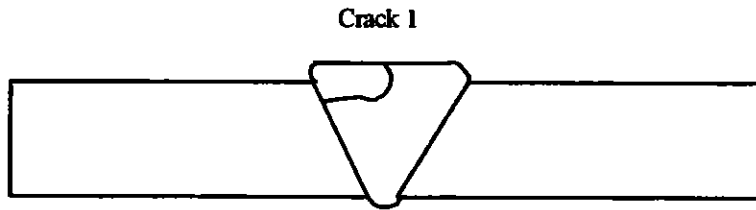
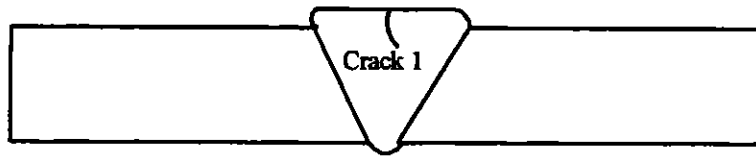
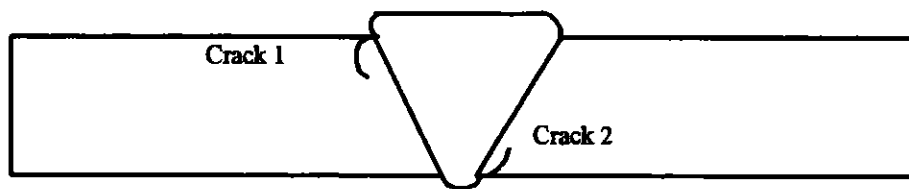


Figure 7: The geometry of the pipe sample.



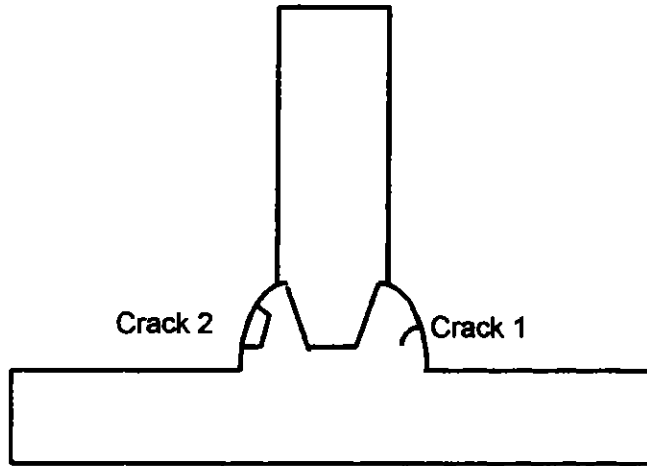
Defect No.	Defect Type	Defect Length(mm)	Distance From Datum (mm)	Max UT Indication db	Angle
1	Centerline Indication	36.8	99.8	N/A	N/A
2	Transverse Indication	11.0	279.9	N/A	N/A

Figure 8: The cross-section geometry of sample PL1497.



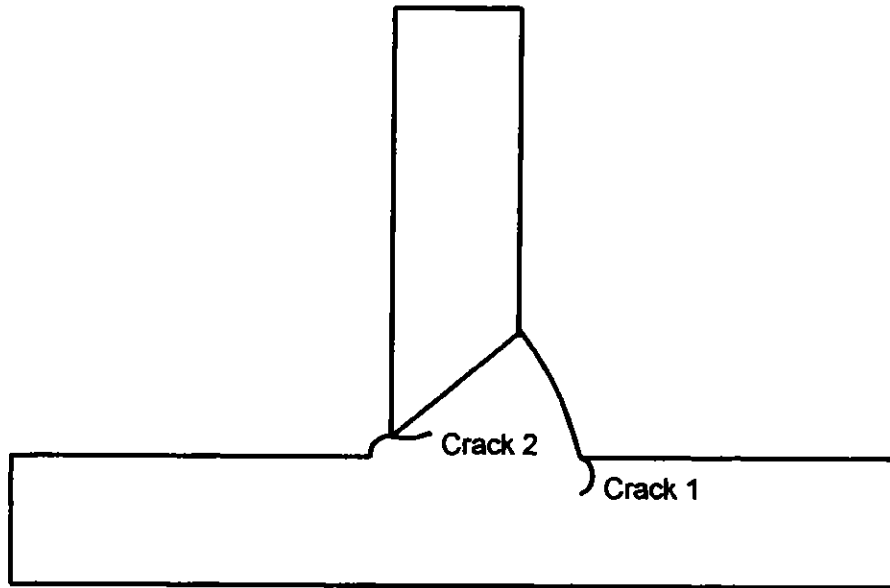
Defect No.	Defect Type	Defect Length(mm)	Distance From Datum (mm)	Max UT Indication db	Angle
1	Toe Indication	61.0	22.9	N/A	N/A
2	Root Indication	24.0	220	N/A	N/A

Figure 9: The cross-section geometry of sample PL1498 with two cracks.



Defect No.	Defect Type	Defect Length(mm)	Distance From Datum (mm)	Max UT Indication db	Angle
1	Centerline Indication	64	74.9	N/A	N/A
2	Transverse Indication	5.8	192.8	N/A	N/A

Figure 10: The cross-section geometry of sample T1495.



Defect No.	Defect Type	Defect Length(mm)	Distance From Datum (mm)	Max UT Indication db	Angle
1	Toe Indication	71.0	50.8	N/A	N/A
2	Root Indication	34.0	222.8	N/A	N/A

Figure 11: The cross-section geometry of sample T1496.

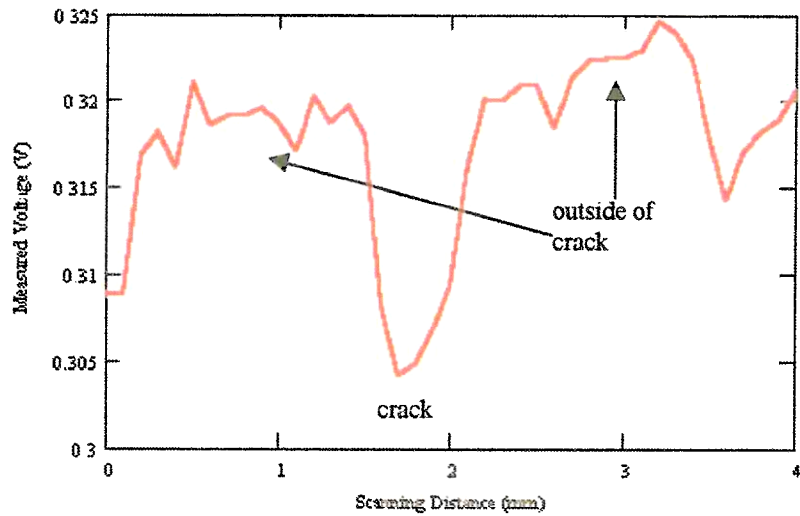


Figure 12 Crack characteristic signal for first crack on the pipe sample at 11.9 GHz using coax # 3

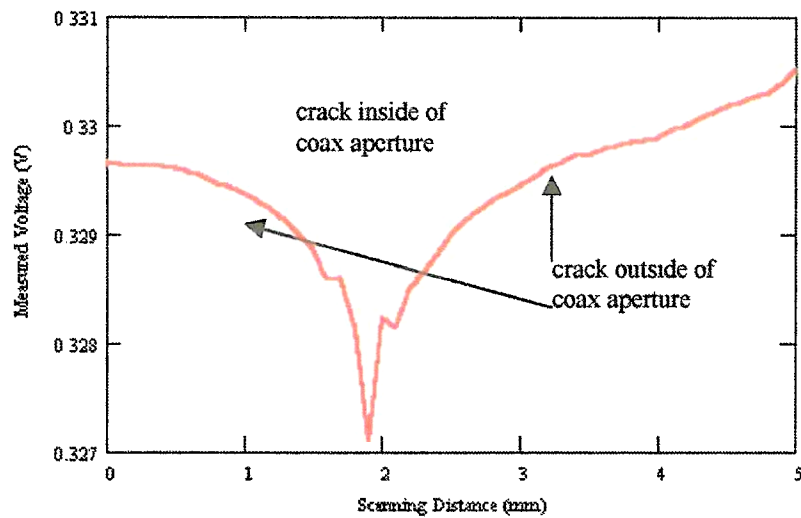


Figure 13 Crack characteristic signal for second crack on the pipe sample at 11.9 GHz using coax # 3

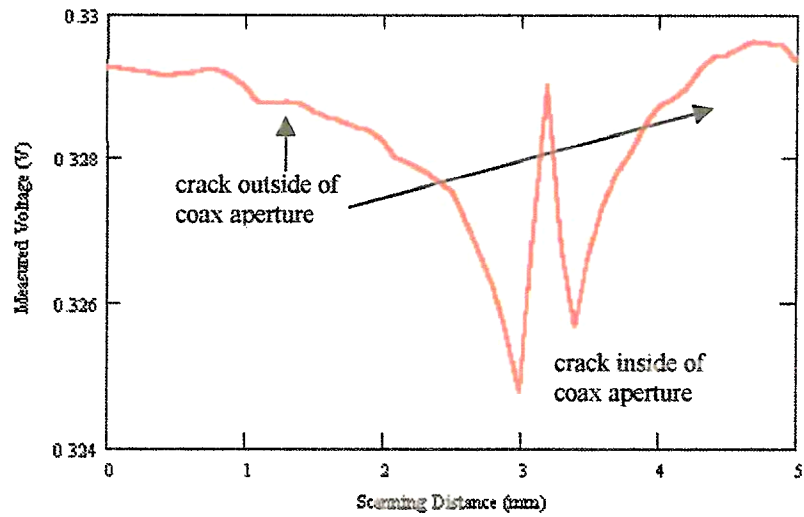


Figure 14 Crack characteristic signal for third crack on the pipe sample at 11.9 GHz using coax # 3

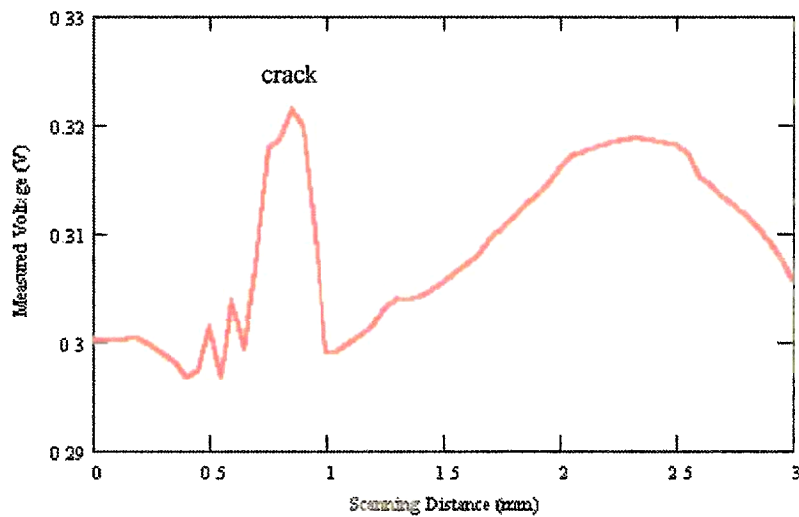


Figure 15 Crack characteristic signal of the first crack on sample PL1497 at 11.9 GHz using coax # 3

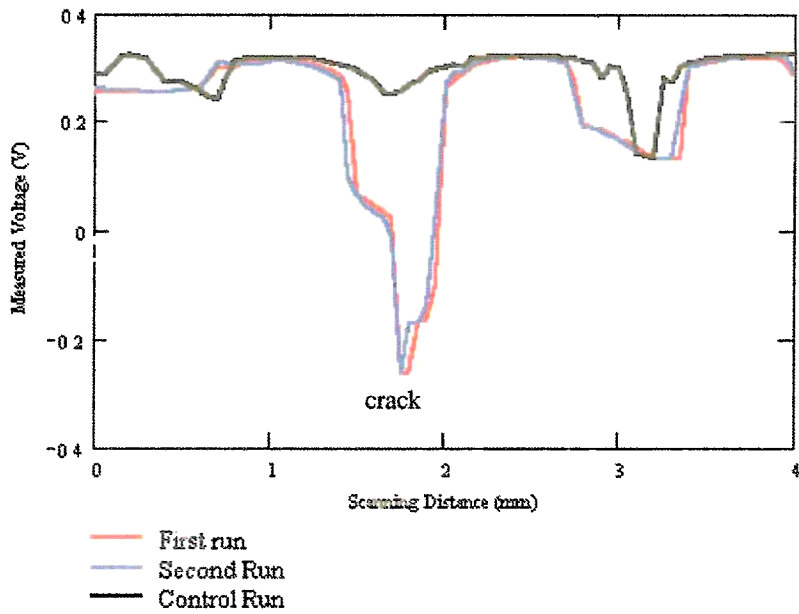


Figure 16 Crack characteristic signal of the first crack on sample T1495 at 11.9 GHz using coax # 3

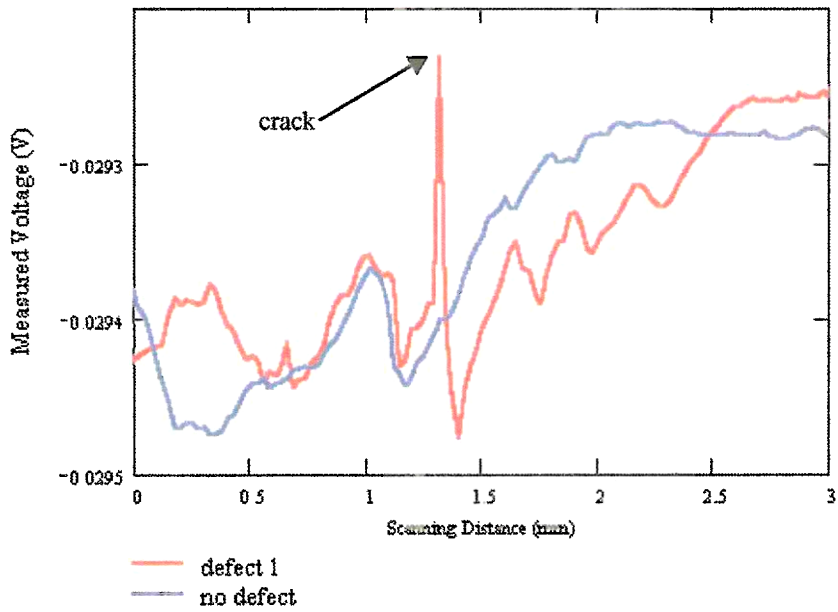


Figure 17. Crack characteristic signal of the first crack on sample PL1497 at 24 GHz using coax # 3

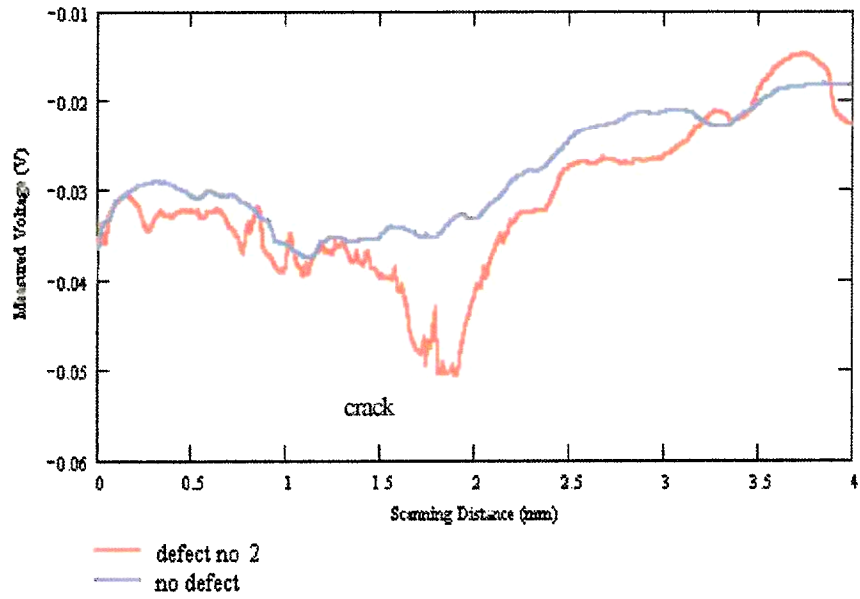


Figure 18 Crack characteristic signal of the second crack on sample PL1497 at 24 GHz using coax # 3

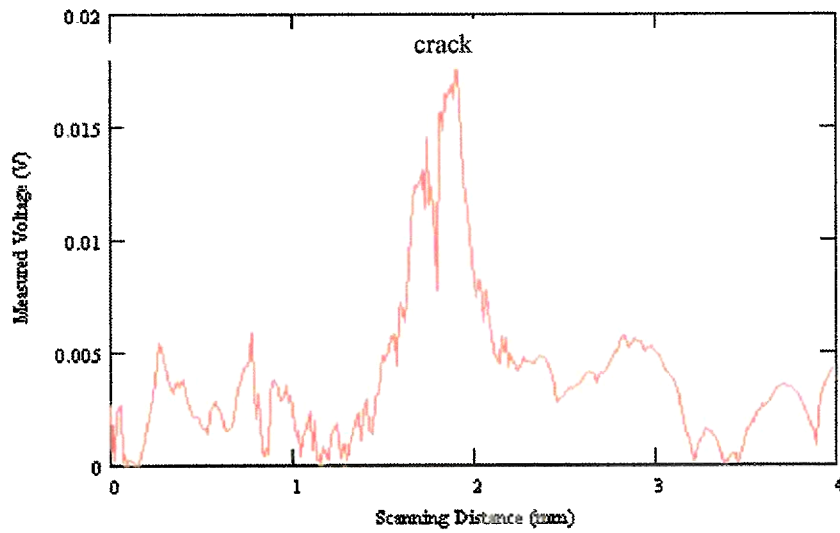


Figure 19 Difference between the two signals shown in Figure 18

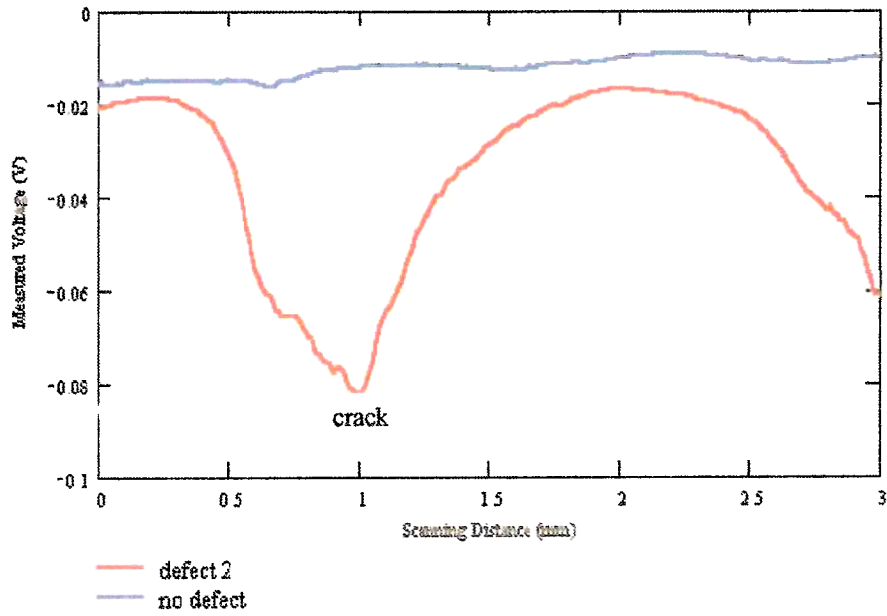


Figure 20 Crack characteristic signal of the second crack on sample T1495 at 24 GHz using coax # 3

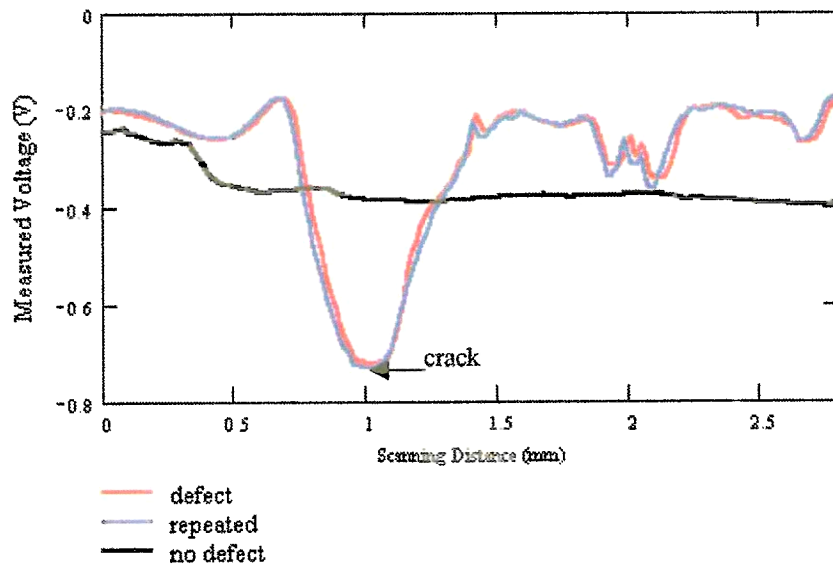


Figure 21: Crack characteristic signal of the first crack on sample PL1497 at 34.5 GHz using coax # 3

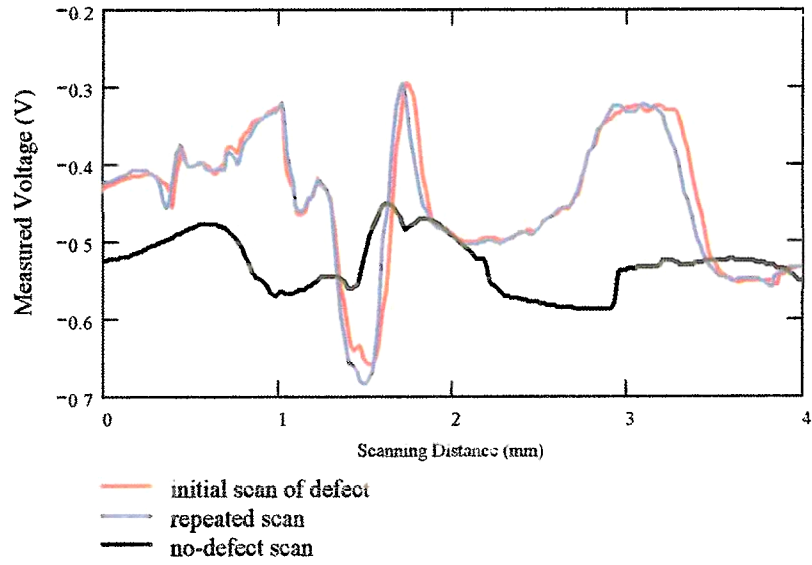


Figure 22: Crack characteristic signal of the second crack on sample PL1497 at 35 GHz using coax # 3

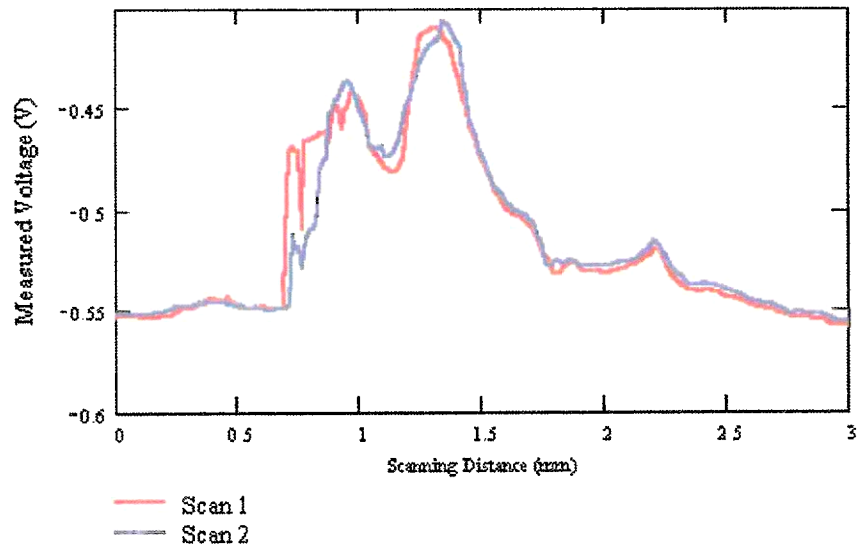


Figure 23: Crack characteristic signal of the first crack on sample T1495 at 35 GHz using coax # 3

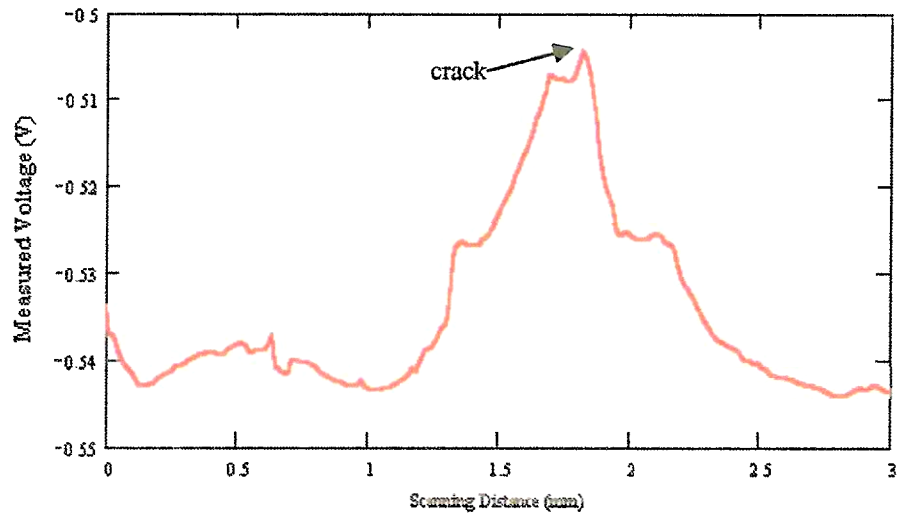


Figure 24 Crack characteristic signal of the second crack on sample T1495 at 35 GHz using coax # 3

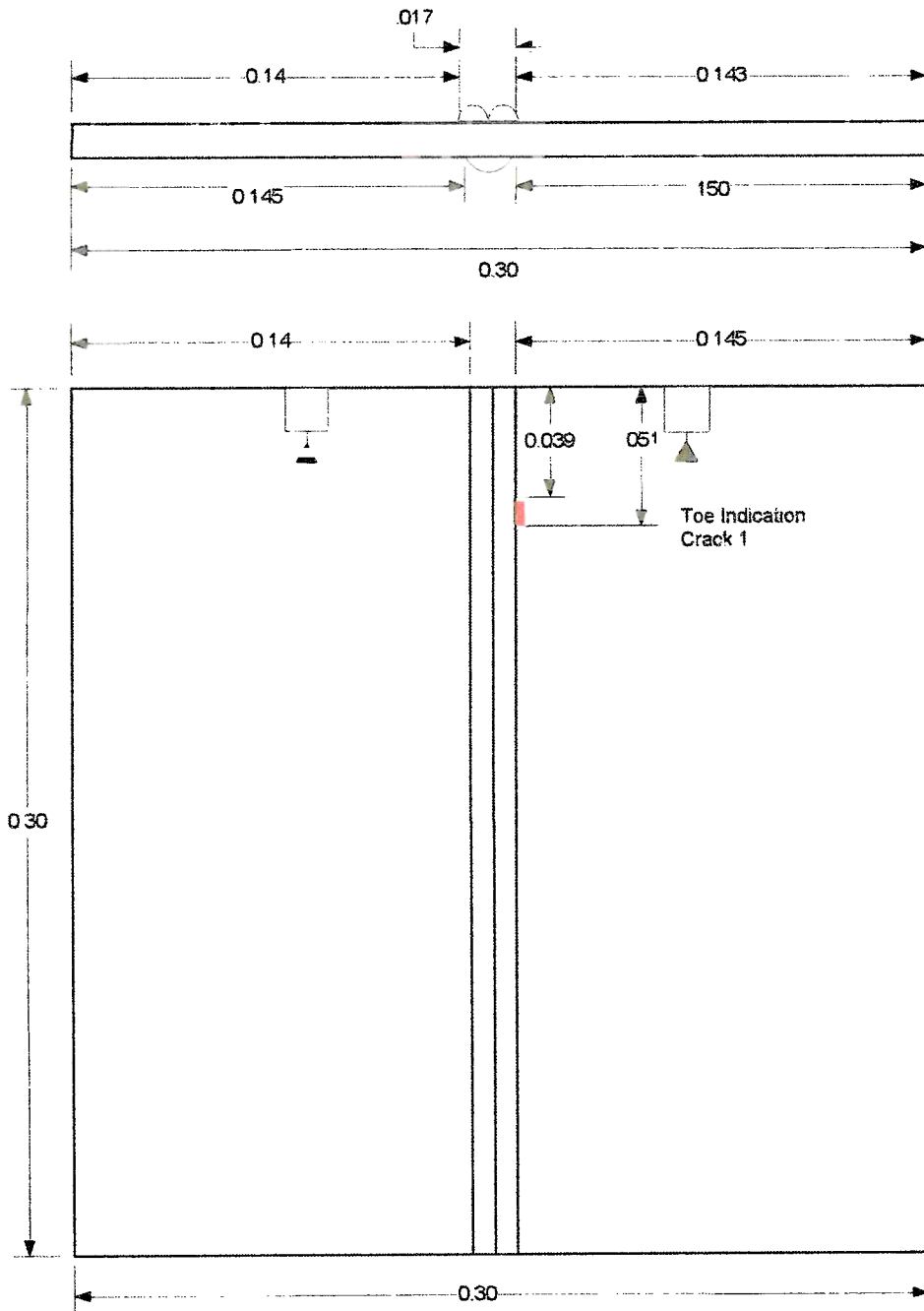


Figure 25a The side and top views of the geometry of sample PL4295 (dimensions are in mm)

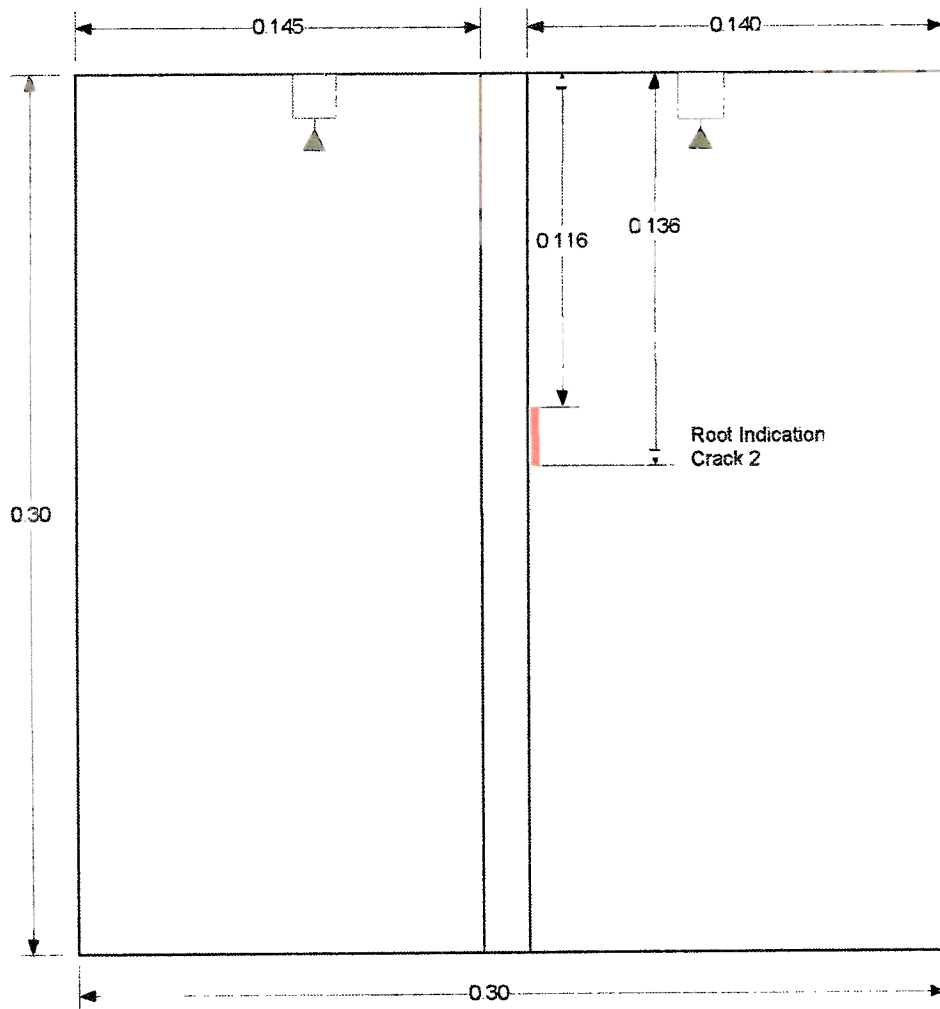


Figure 25b: The bottom view of the geometry of sample PL4295 (dimensions are in mm)

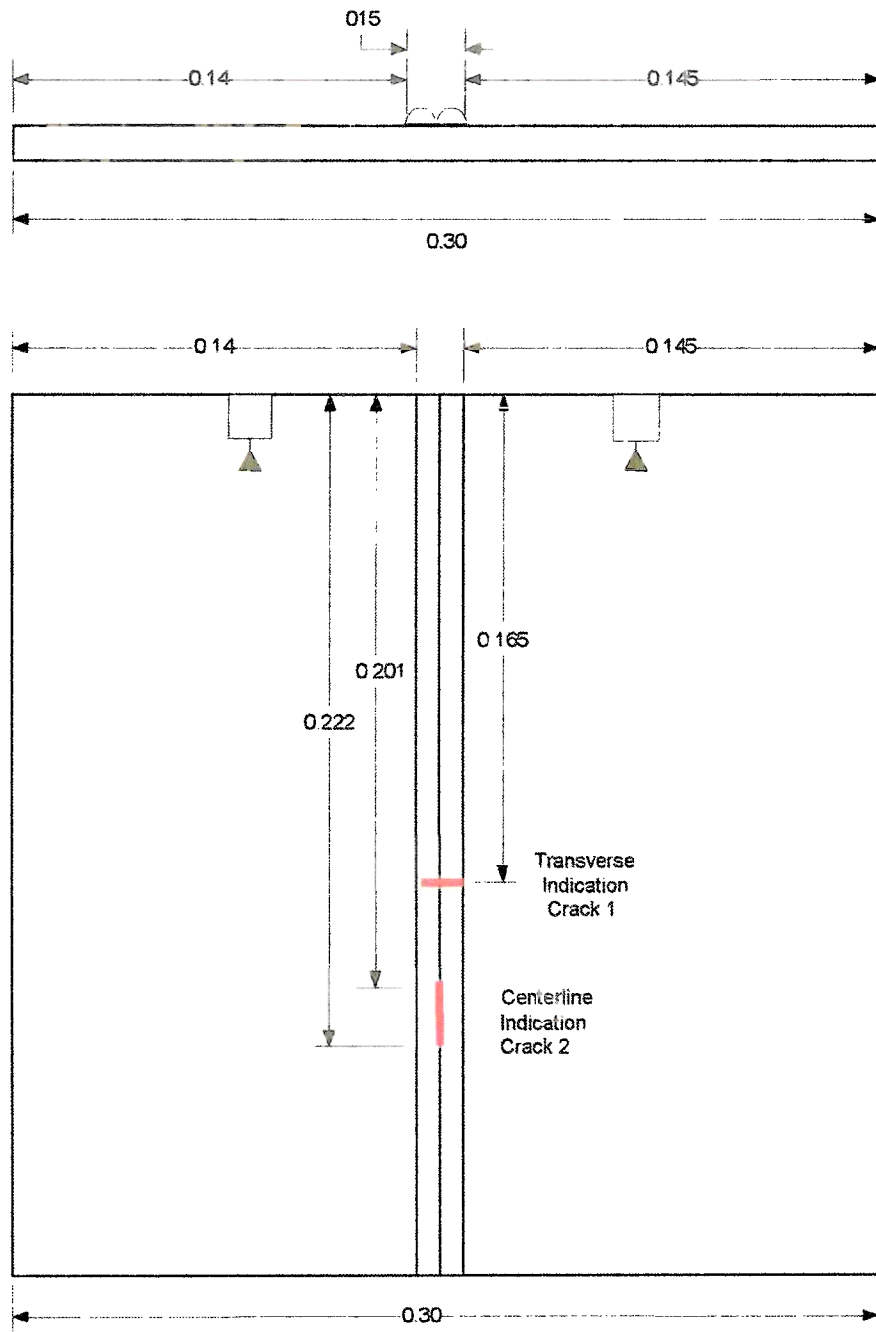


Figure 26: The side and top views of the geometry of the sample PL4296 (dimensions are in mm)

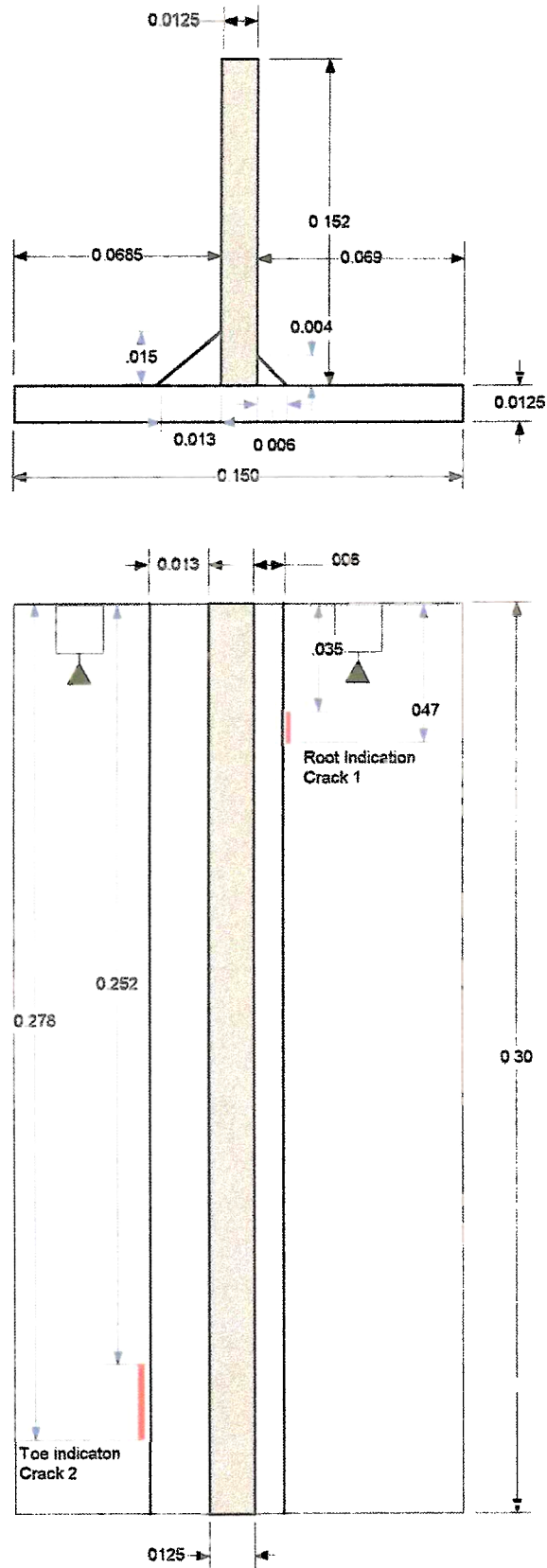


Figure 28. The side and top views of the geometry of sample T4298 (dimensions are in mm)

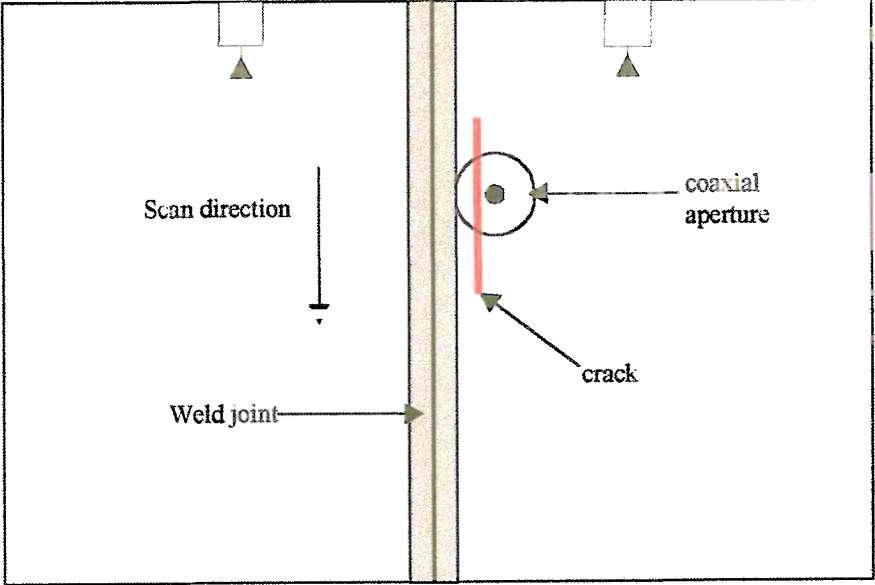


Figure 29 Schematic of a parallel scan using an open-ended coaxial probe aperture.

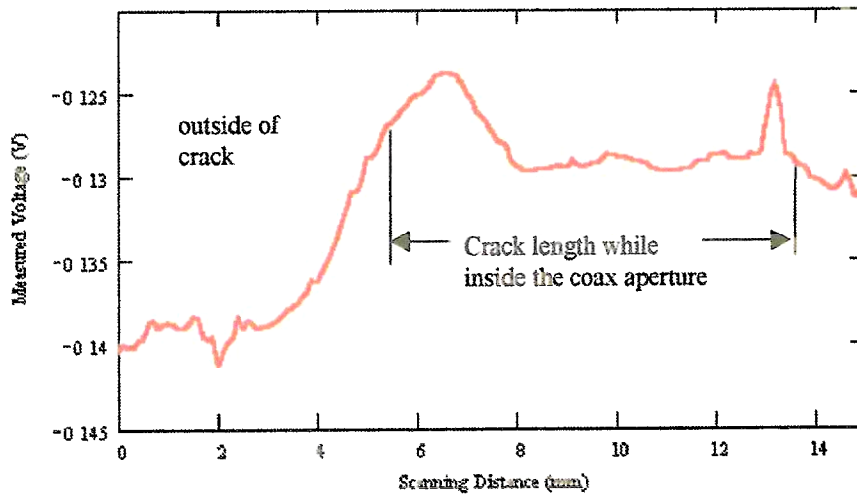


Figure 30 Crack characteristic signal of the first crack on sample PL4295 at 25.45 GHz using coax # 3

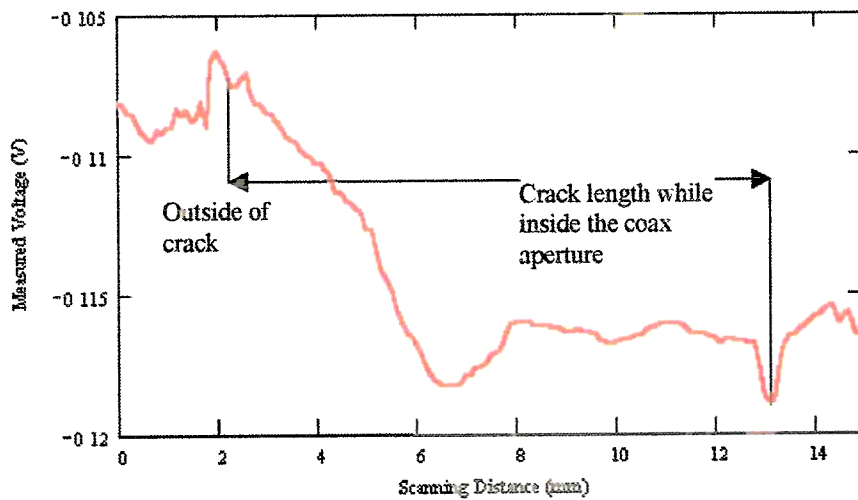


Figure 31 Crack characteristic signal of the first crack on sample PL4295 at 25.9 GHz using coax # 3

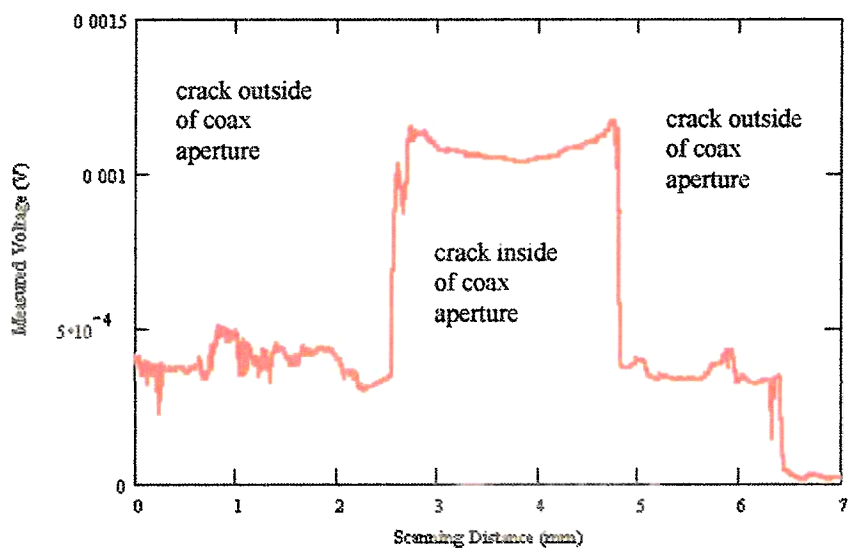


Figure 32 Crack characteristic signal of the second crack on sample PL4295 at 24 GHz using coax # 5

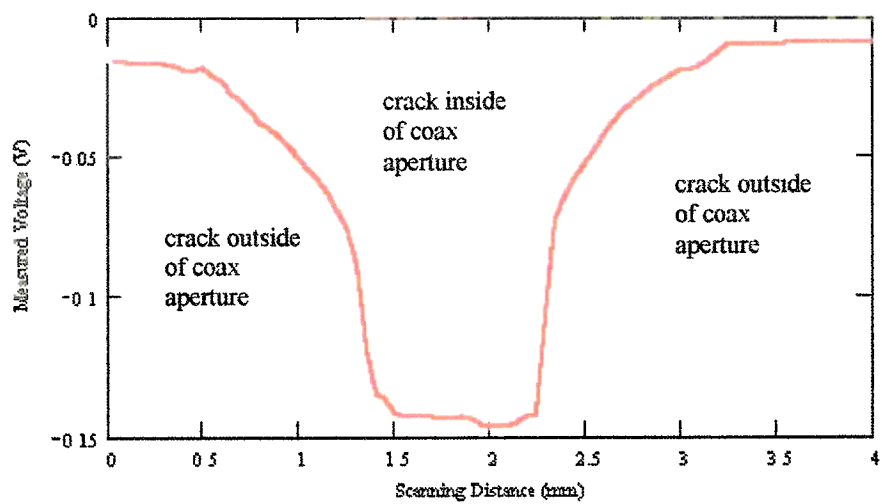


Figure 33 Crack characteristic signal of the first crack on sample PL4296 at 23.55 GHz using coax # 2

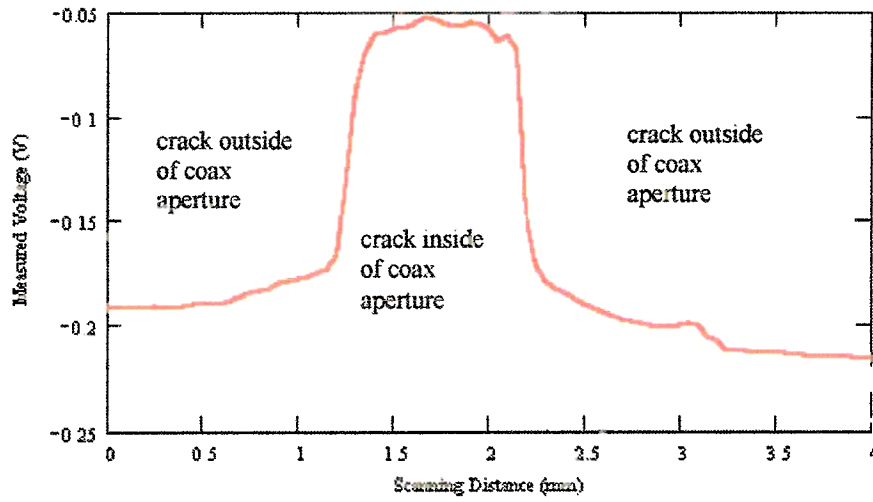


Figure 34. Crack characteristic signal of the first crack on sample PL4296 at 23.05 GHz using coax # 2

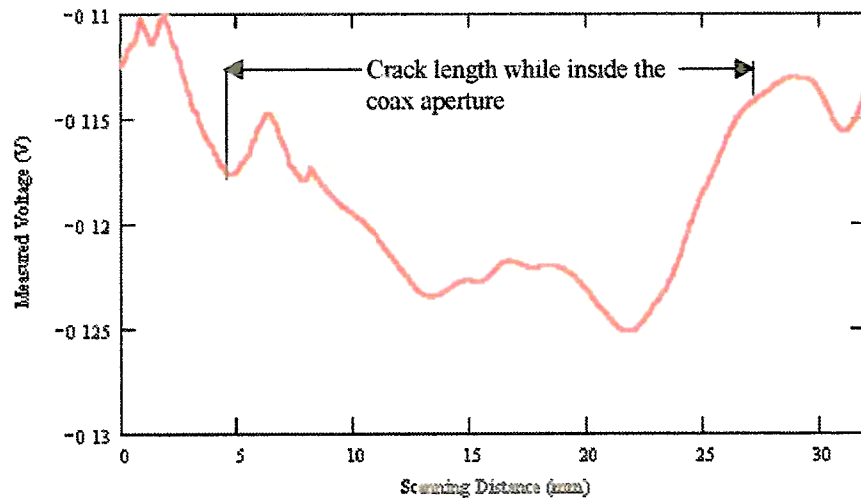


Figure 35. Crack characteristic signal of the second crack on sample PL4296 at 25 GHz using coax # 2

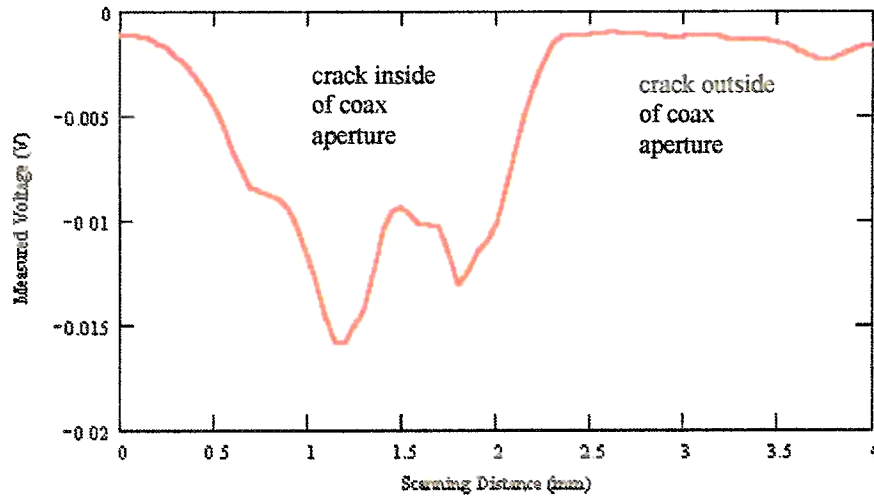


Figure 36 Crack characteristic signal of the first crack on sample T4297 at 26.5 GHz using coax # 3

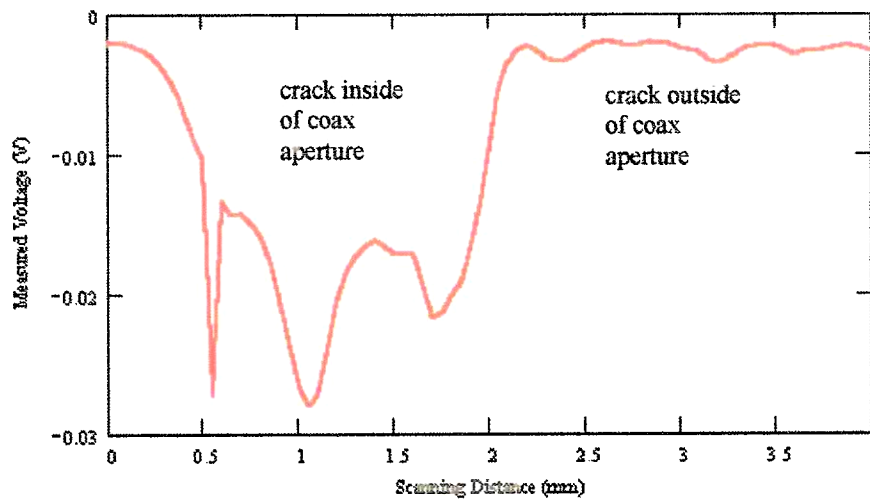


Figure 37 Crack characteristic signal of the first crack on sample T4297 at 24.5 GHz using coax # 3.

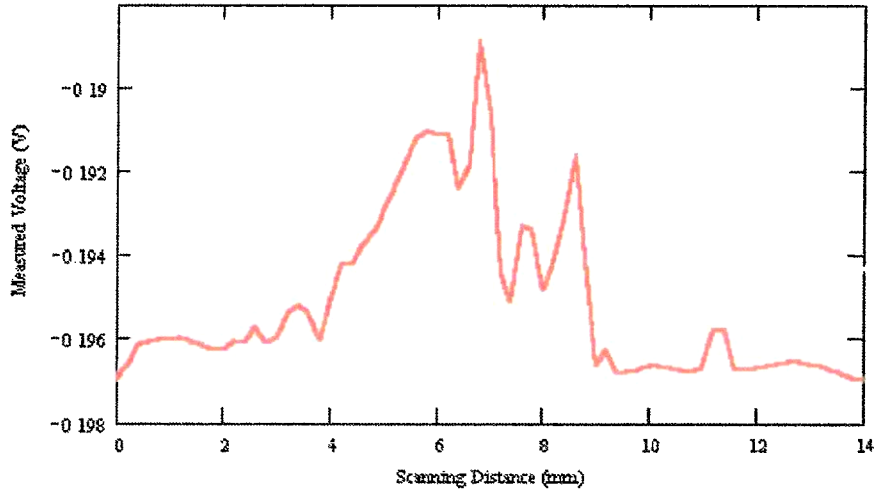


Figure 38 Crack characteristic signal of the second crack on sample T4297 at 23.8 GHz using coax # 3

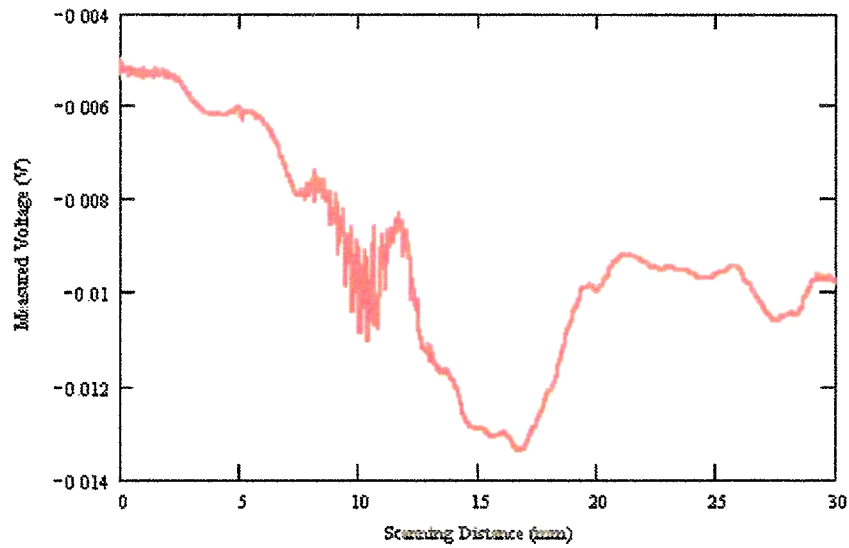


Figure 39: Crack characteristic signal of the first crack on sample T4298 at 24.8 GHz using coax # 3.

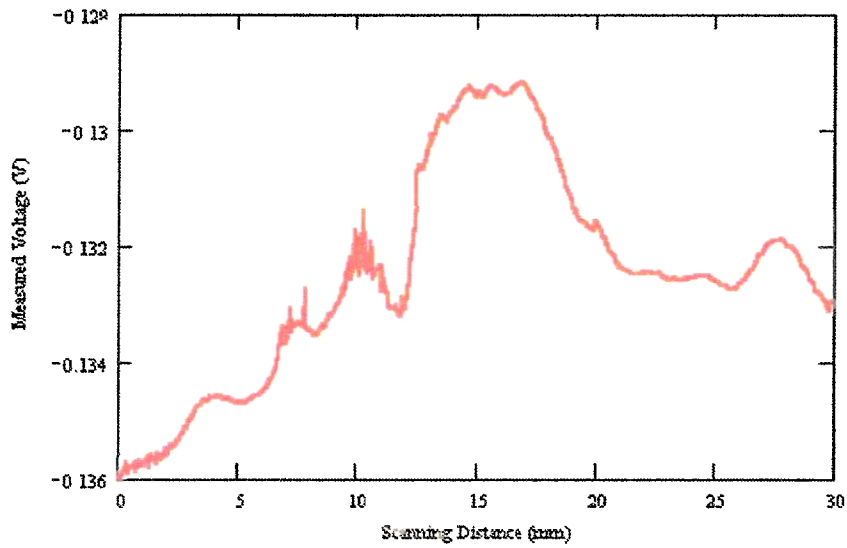


Figure 40. Crack characteristic signal of the first crack on sample T4298 at 24.12 GHz using coax # 3

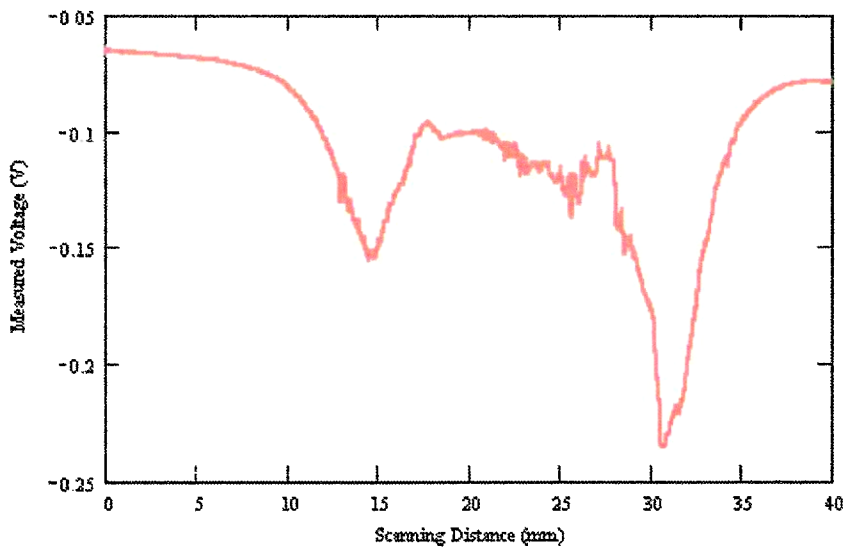


Figure 41. Crack characteristic signal of the second crack on sample T4298 at 25 GHz using coax # 3

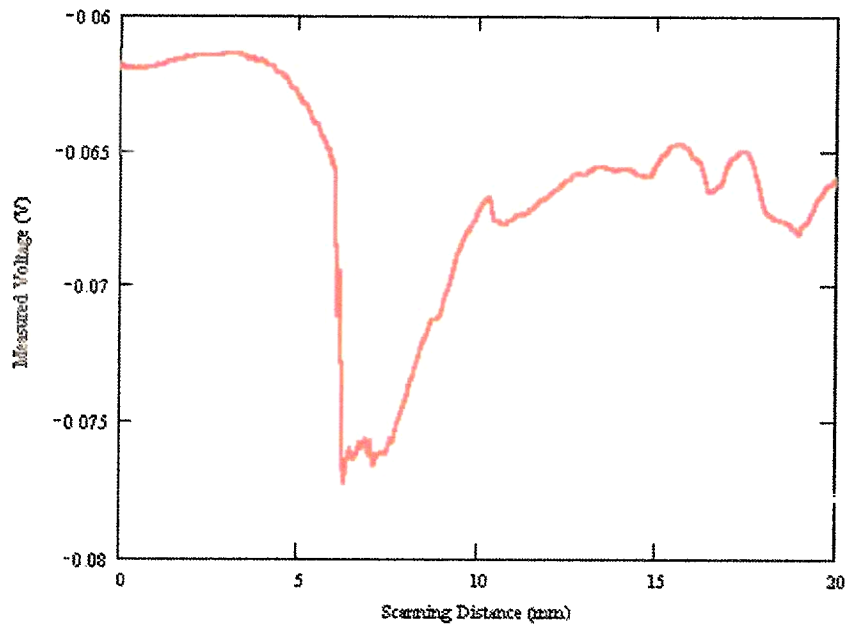


Figure 42. Crack characteristic signal of the first crack on sample PL4295 at 32.15 GHz using coax # 3

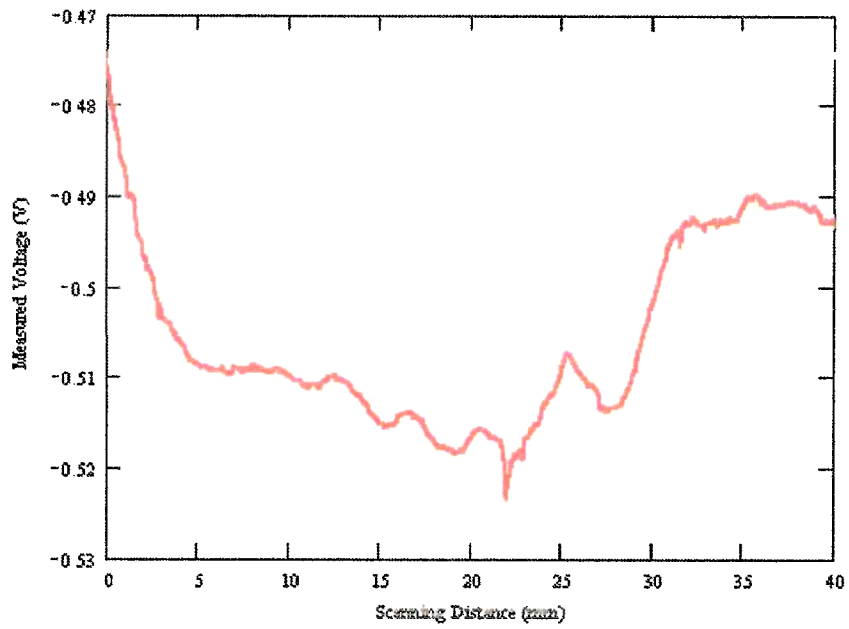


Figure 43. Crack characteristic signal of the second crack on sample PL4295 at 31.4 GHz using coax # 3

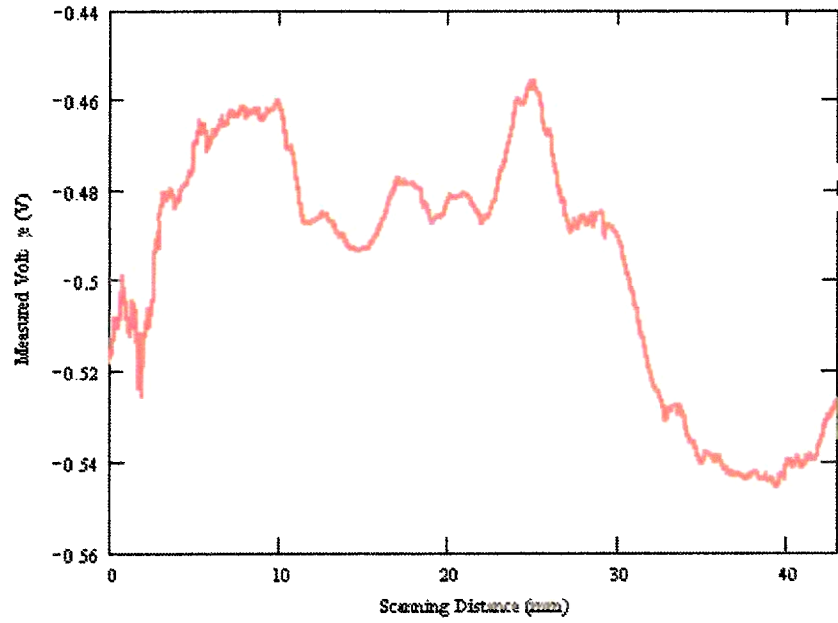


Figure 44 Crack characteristic signal of the second crack on sample PL4295 at 31.6 GHz using coax # 3

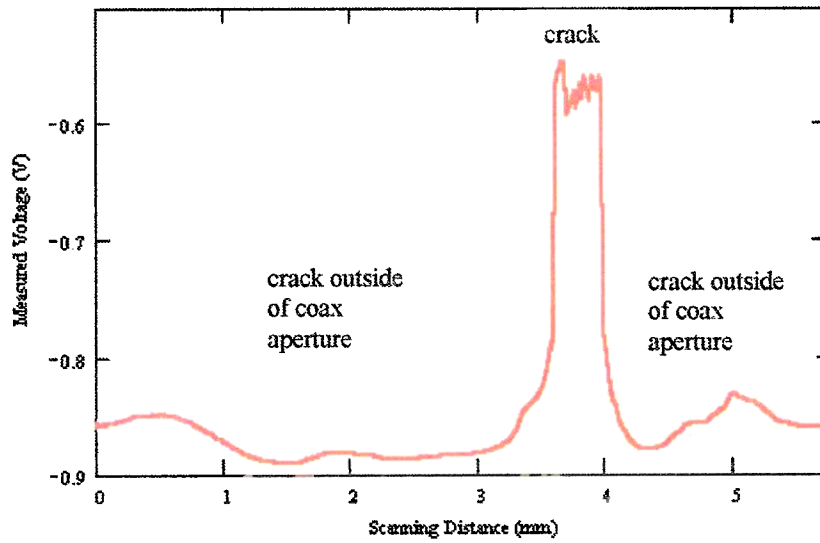


Figure 45 Crack characteristic signal of the first crack on sample PL4296 at 30.75 GHz using coax # 3

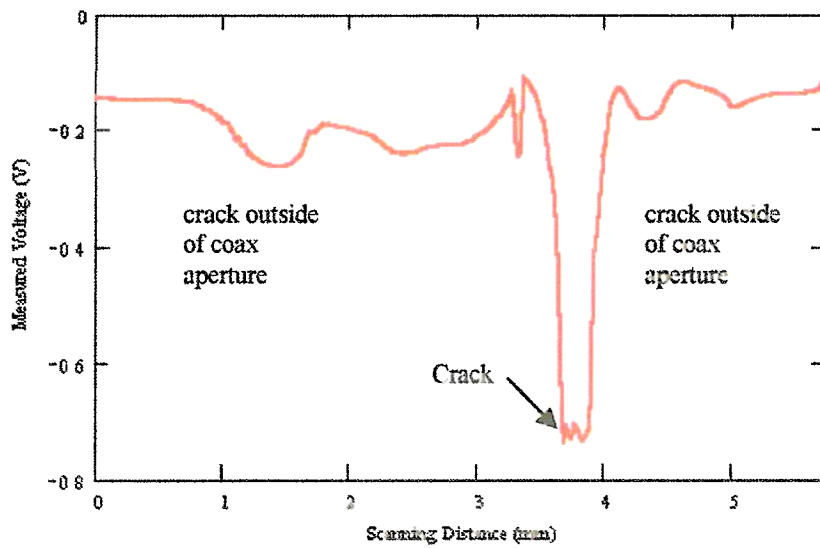


Figure 46: Crack characteristic signal of the first crack on sample PL4296 at 31.1 GHz using coax # 3

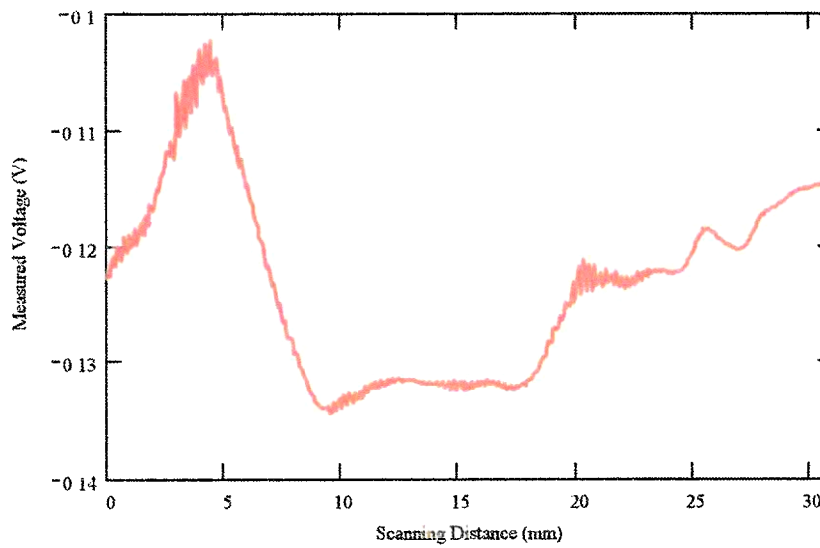


Figure 47: Crack characteristic signal of the second crack on sample PL4296 at 31.1 GHz using coax # 3

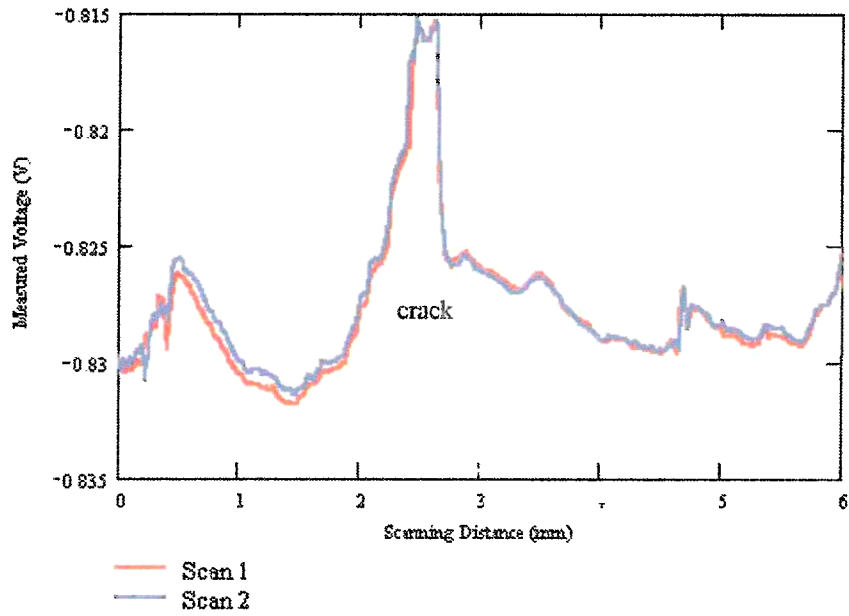


Figure 48. Crack characteristic signal of the first crack on sample T4297 at 35.6 GHz using coax # 2

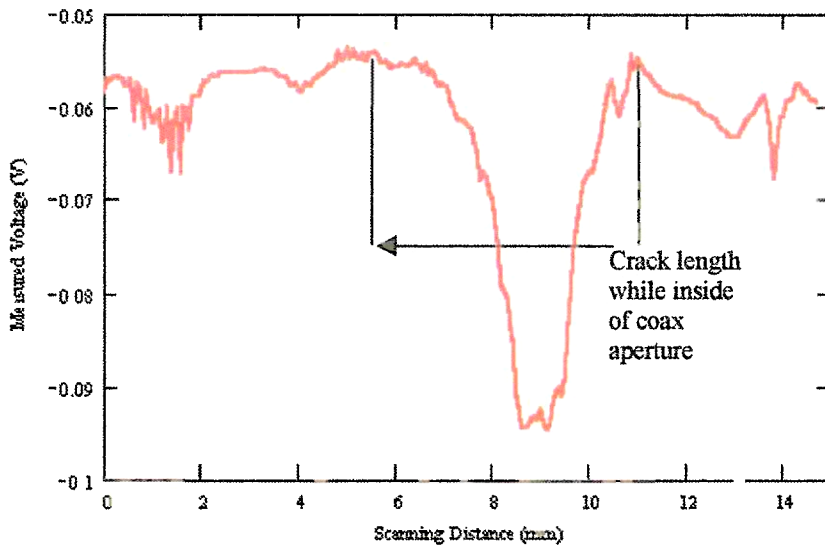


Figure 49: Crack characteristic signal of the second crack on sample T4297 at 32.55 GHz using coax # 3

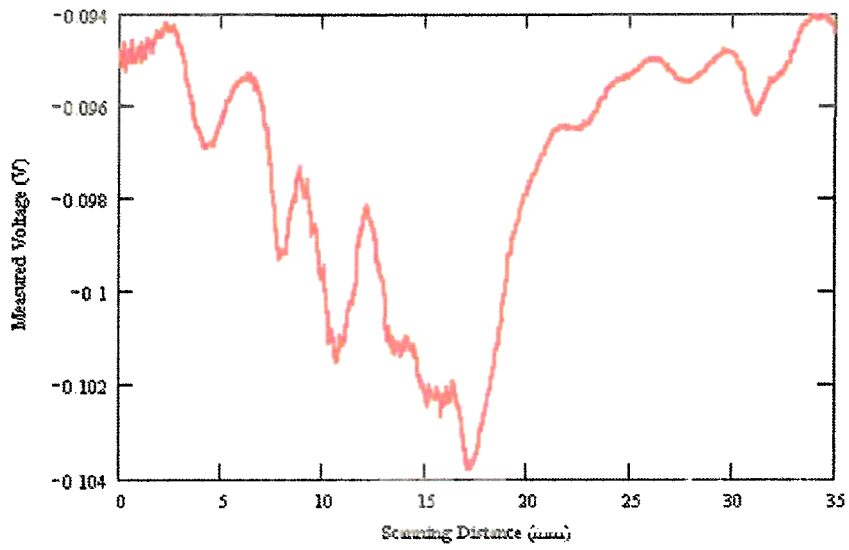


Figure 50 Crack characteristic signal of the first crack on sample T4298 at 30.6 GHz using coax # 3

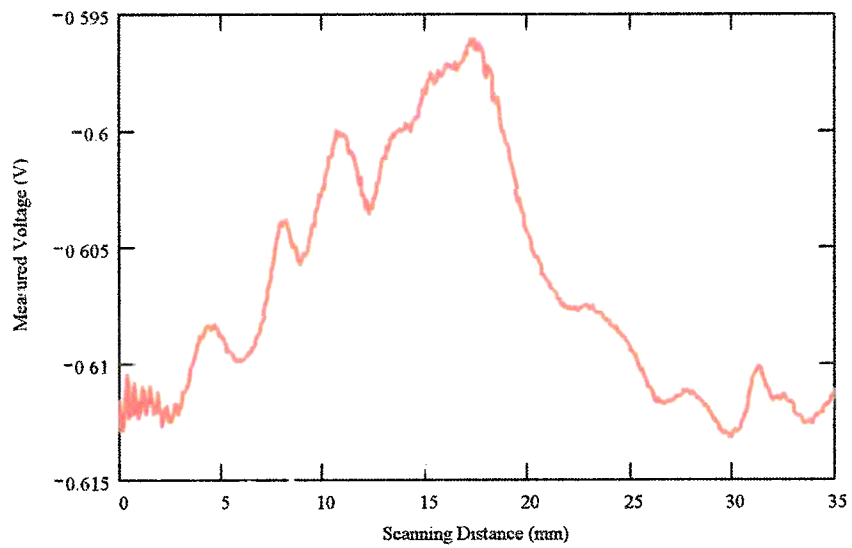


Figure 51 Crack characteristic signal of the first crack on sample T4298 at 31 GHz using coax # 3

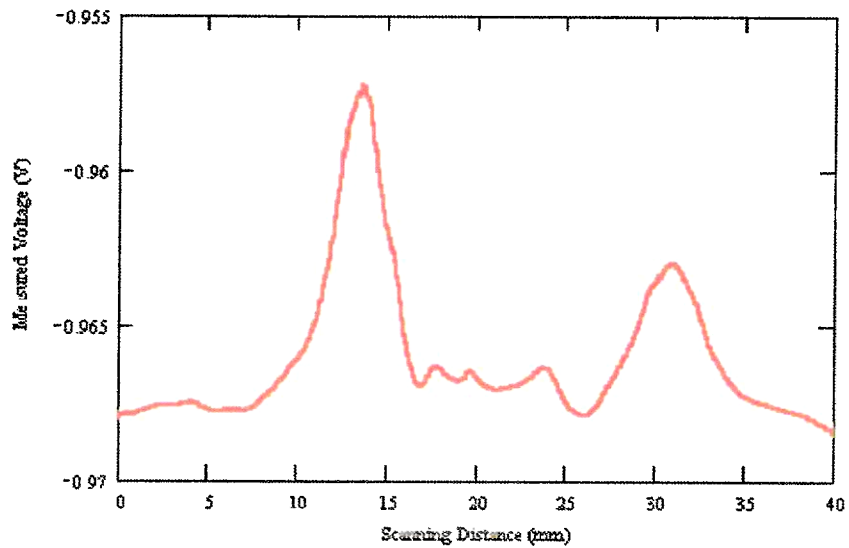


Figure 52 Crack characteristic signal of the second crack on sample T4298 at 30.8 GHz using coax # 3

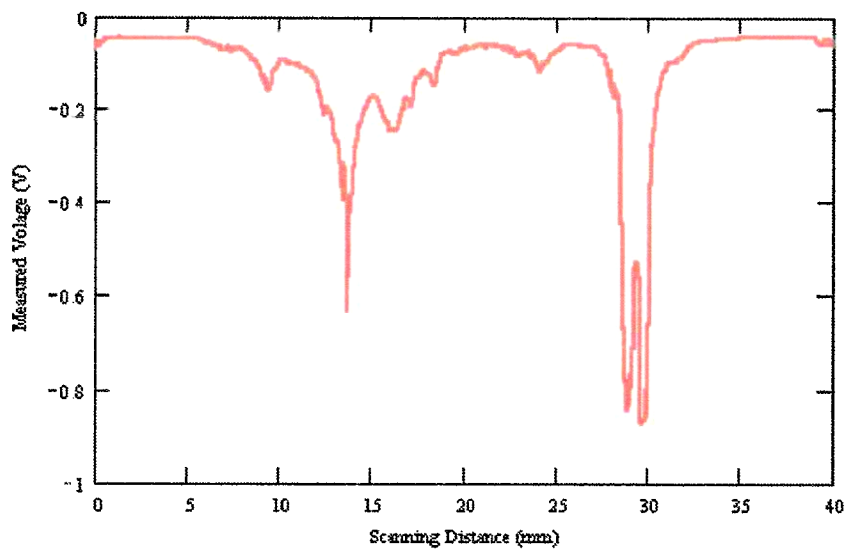


Figure 53 Crack characteristic signal of the second crack on sample T4298 at 31.13 GHz using coax # 3

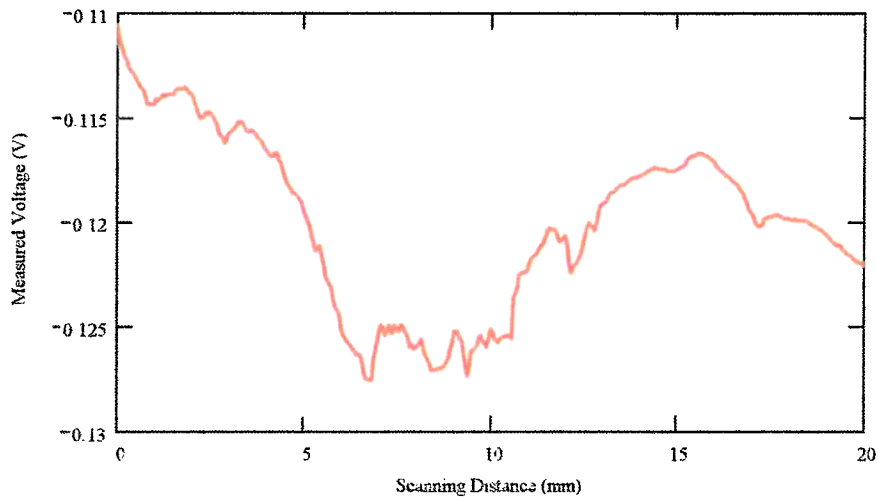


Figure 54 Crack characteristic signal of the first crack on sample PL4295 at 24.8 GHz using coax # 2

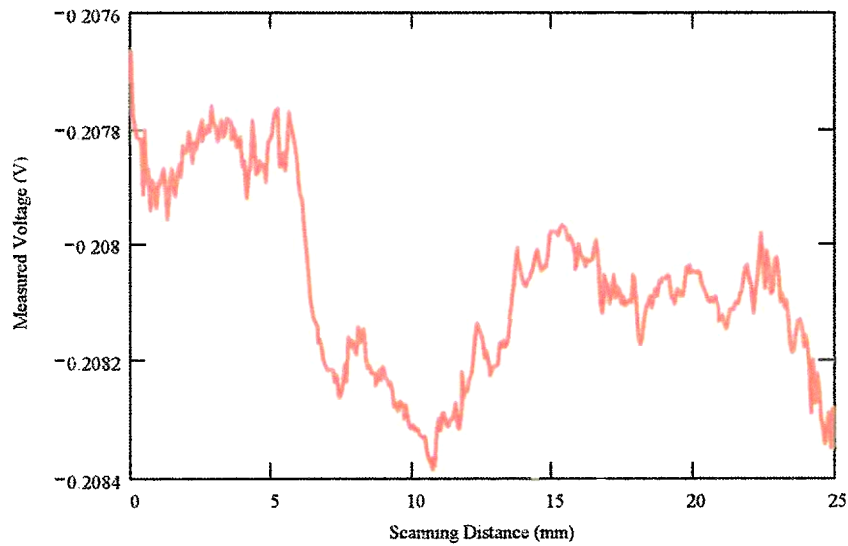


Figure 55 Crack characteristic signal of the second crack on sample PL4295 at 23.66 GHz using coax # 2

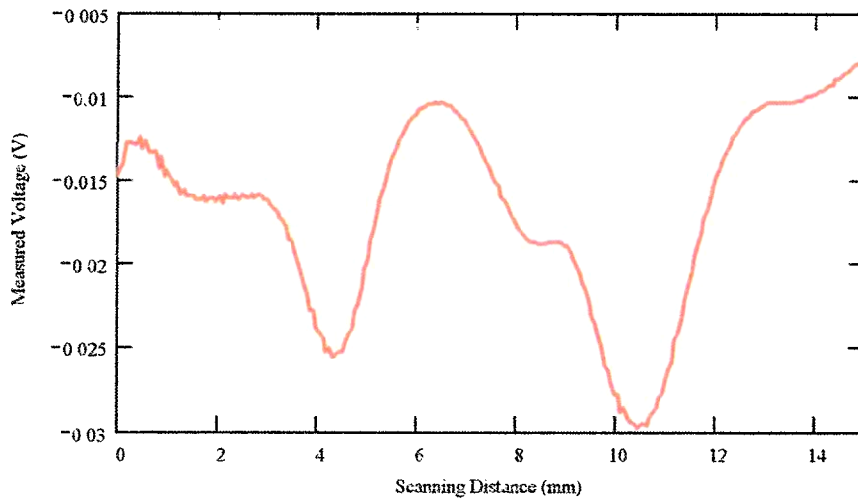


Figure 56 Crack characteristic signal of the first crack on sample PL4296 at 24.08 GHz using coax # 2

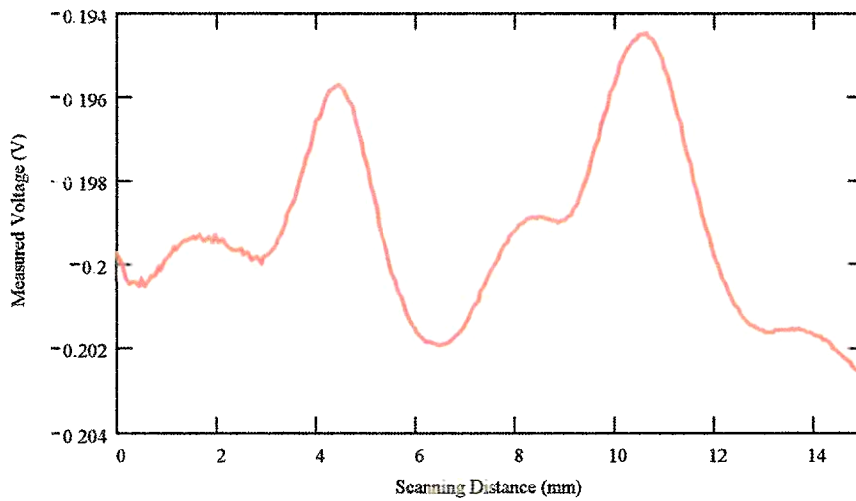


Figure 57 Crack characteristic signal of the first crack on sample PL4296 at 23.44 GHz using coax # 2

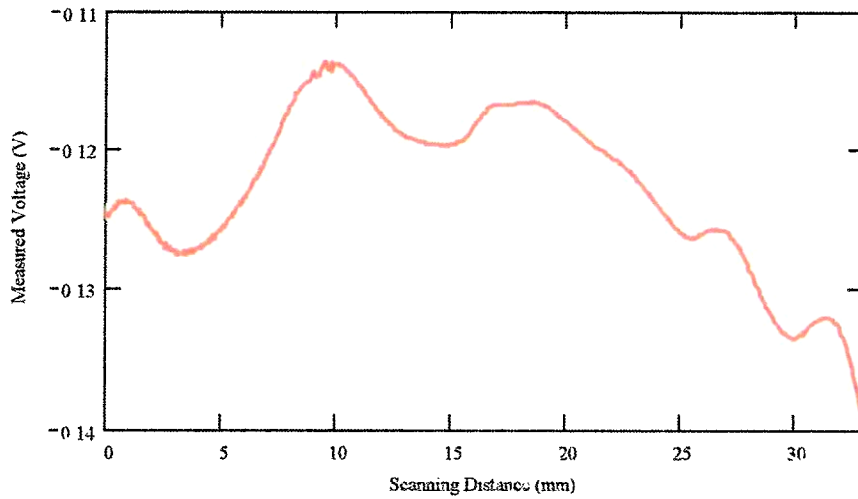


Figure 58 Crack characteristic signal of the second crack on sample PL4296 at 24.4 GHz using coax # 2

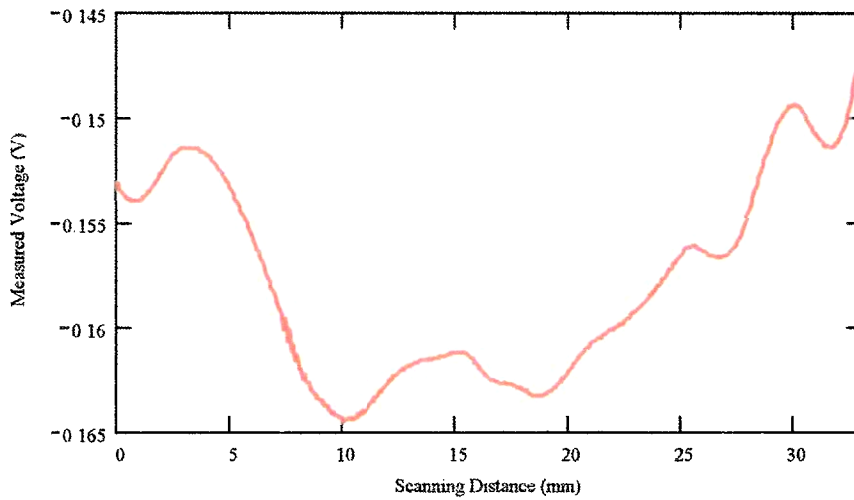


Figure 59 Crack characteristic signal of the second crack on sample PL4296 at 23.8 GHz using coax # 2

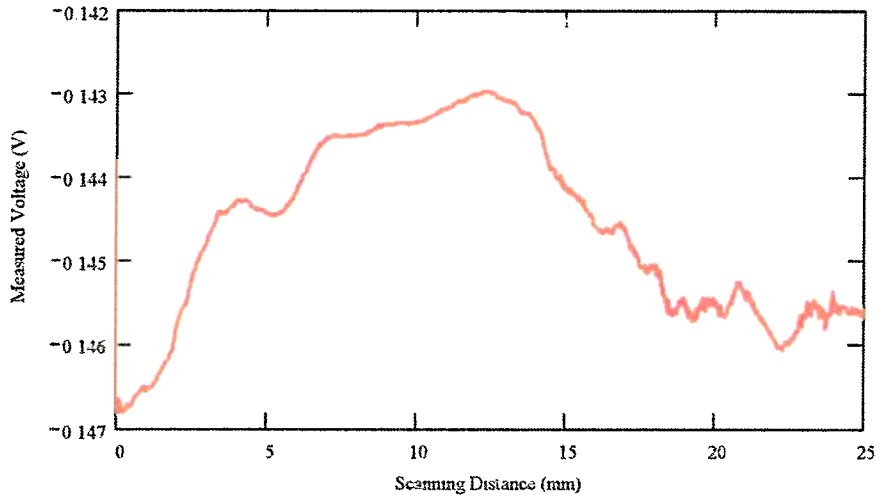


Figure 60 Crack characteristic signal of the second crack on sample T4297 at 23.6 GHz using coax # 2

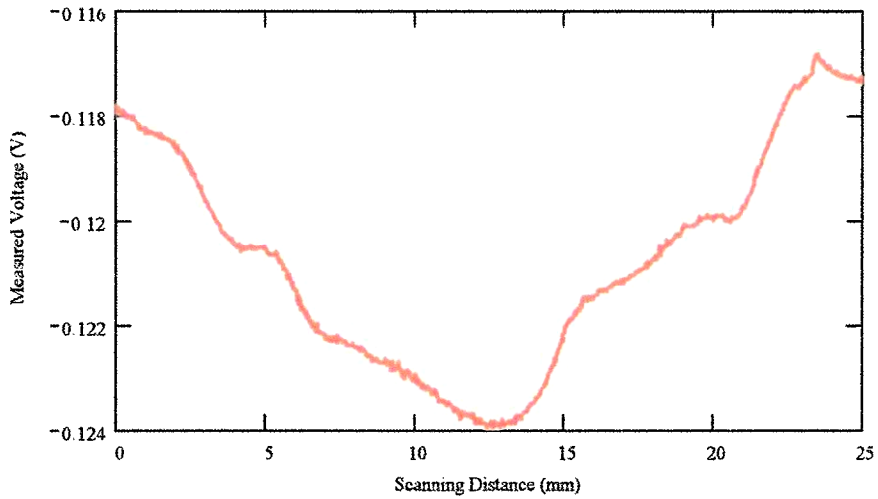


Figure 61 Crack characteristic signal of the second crack on sample T4297 at 22.6 GHz using coax # 2

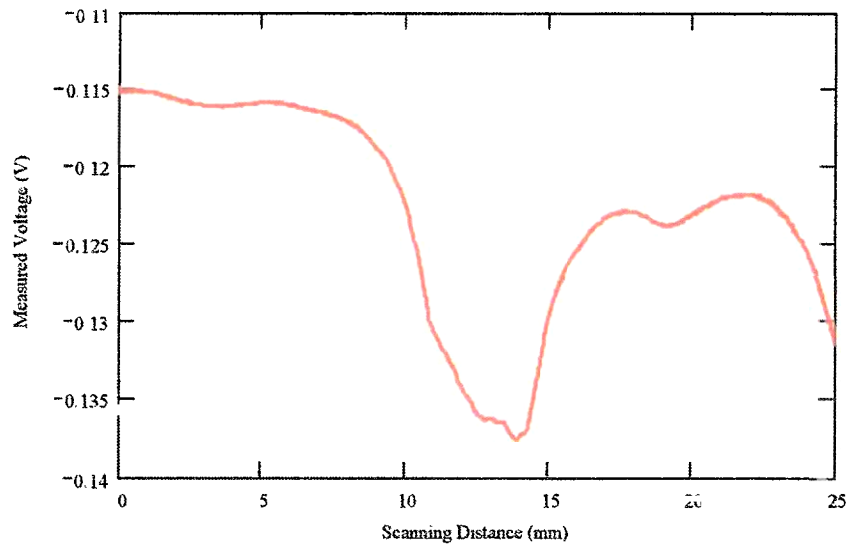


Figure 62 Crack characteristic signal of the first crack on sample T4298 at 24.8 GHz using coax # 2

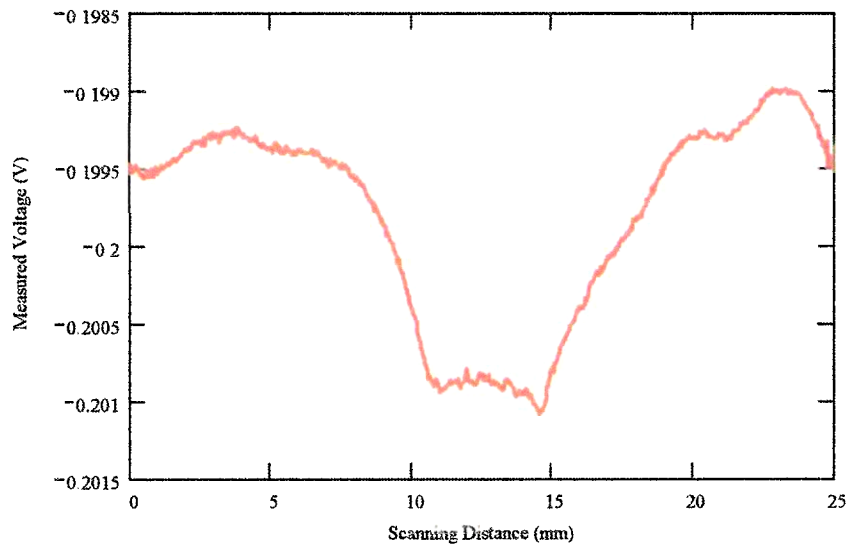


Figure 63 Crack characteristic signal of the first crack on sample T4298 at 23 GHz using coax # 2

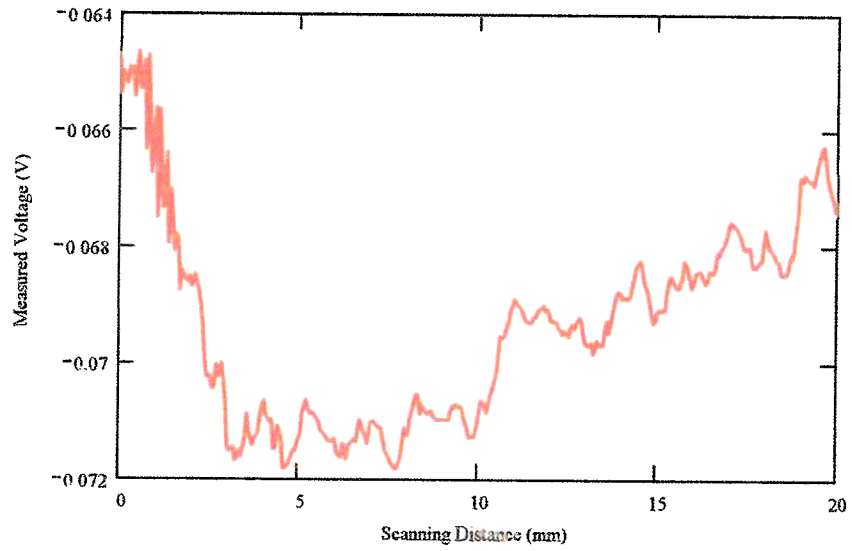


Figure 64 Crack characteristic signal of the first crack on sample PL4295 at 30.16 GHz using coax # 3

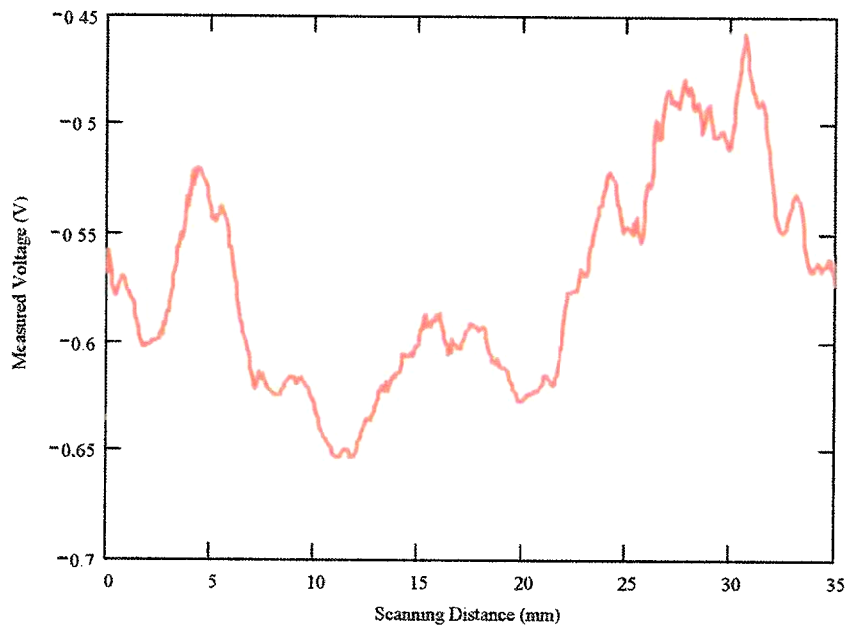


Figure 65 Crack characteristic signal of the second crack on sample PL4295 at 32.0 GHz using coax # 3

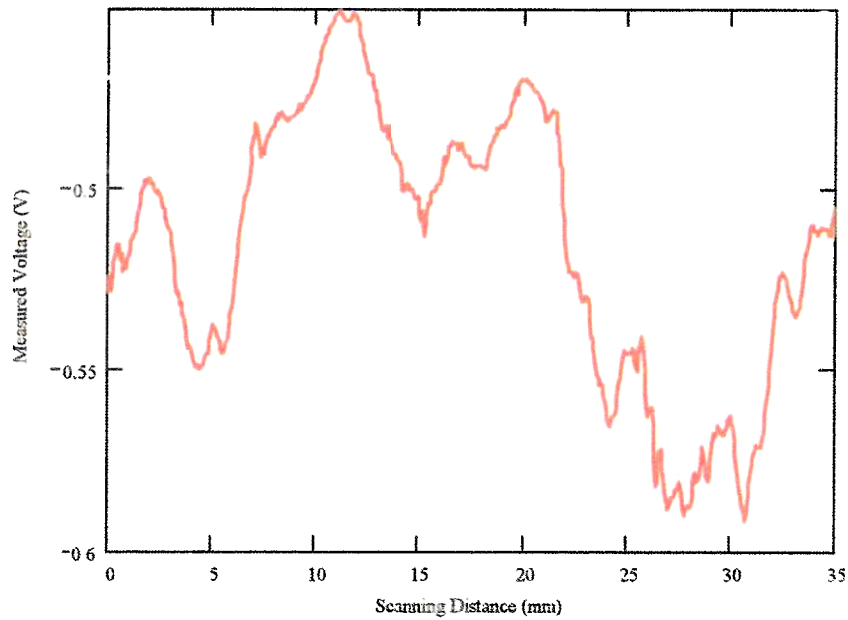


Figure 66 Crack characteristic signal of the second crack on sample PL4295 at 32.7 GHz using coax # 3

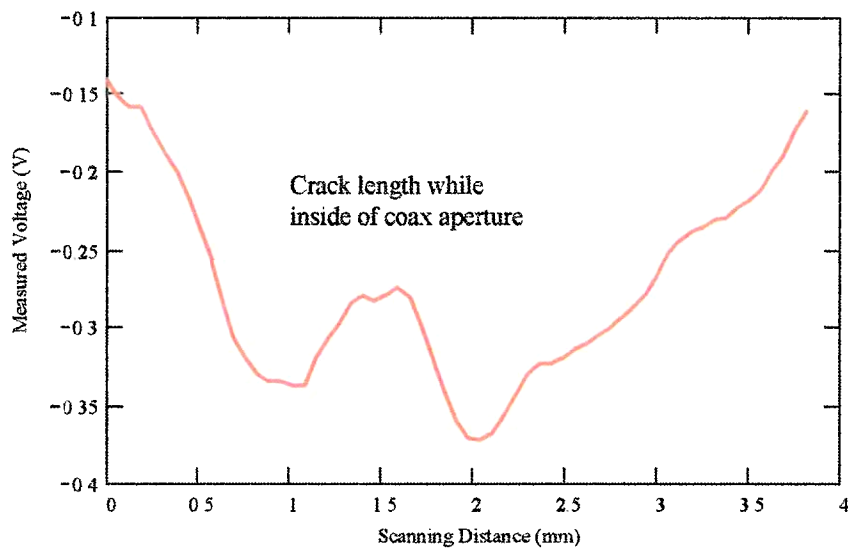


Figure 67: Crack characteristic signal of the first crack on sample PL4296 at 30.6 GHz using coax # 3

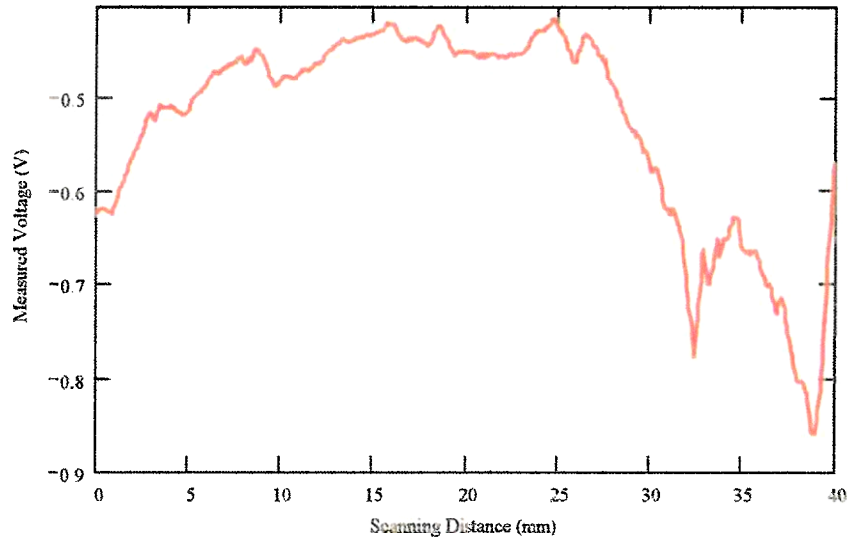


Figure 68 Crack characteristic signal of the second crack on sample PL4296 at 31.8 GHz using coax # 3

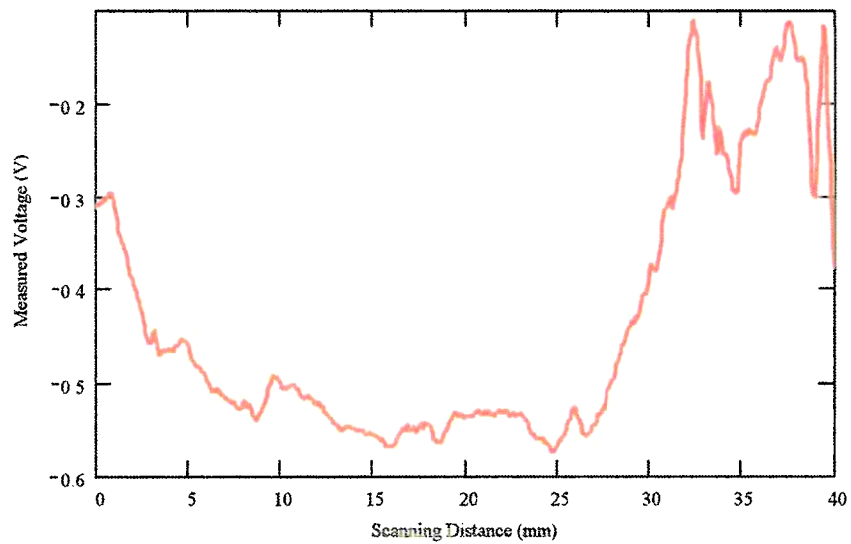


Figure 69 Crack characteristic signal of the second crack on sample PL4296 at 32 GHz using coax # 3

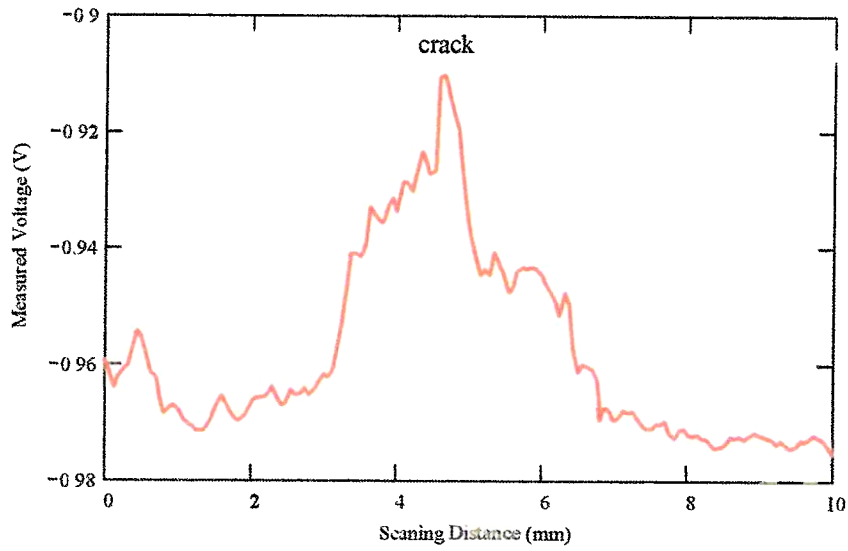


Figure 70 Crack characteristic signal of the first crack on sample T4297 at 31.36 GHz using coax # 3

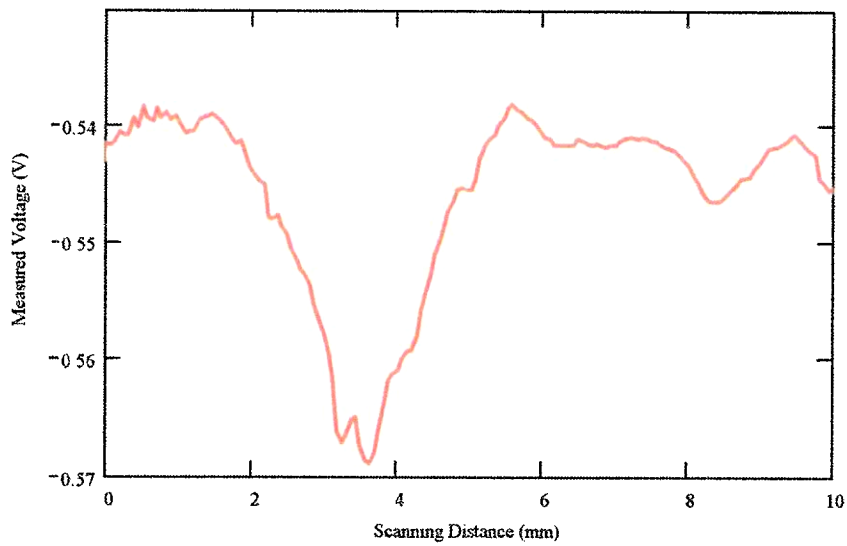


Figure 71 Crack characteristic signal of the second crack on sample T 4297 at 32.26 GHz using coax # 3

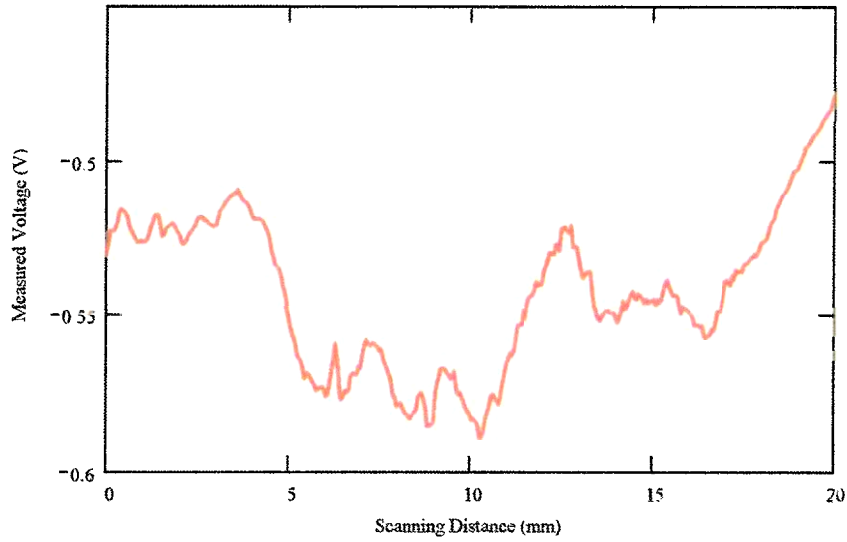


Figure 72 Crack characteristic signal of the first crack on sample T4298 at 31.7 GHz using coax # 3.

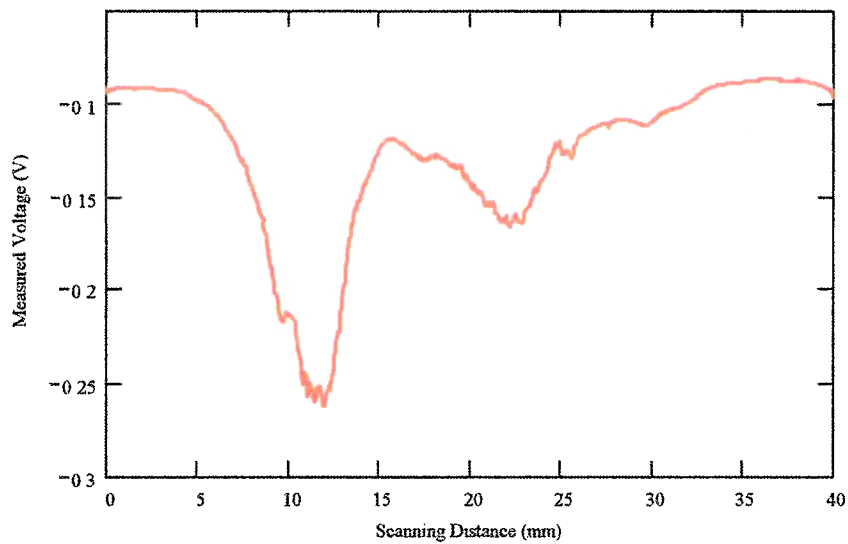


Figure 73 Crack characteristic signal of the second crack on sample T4298 at 31.6 GHz using coax # 3.

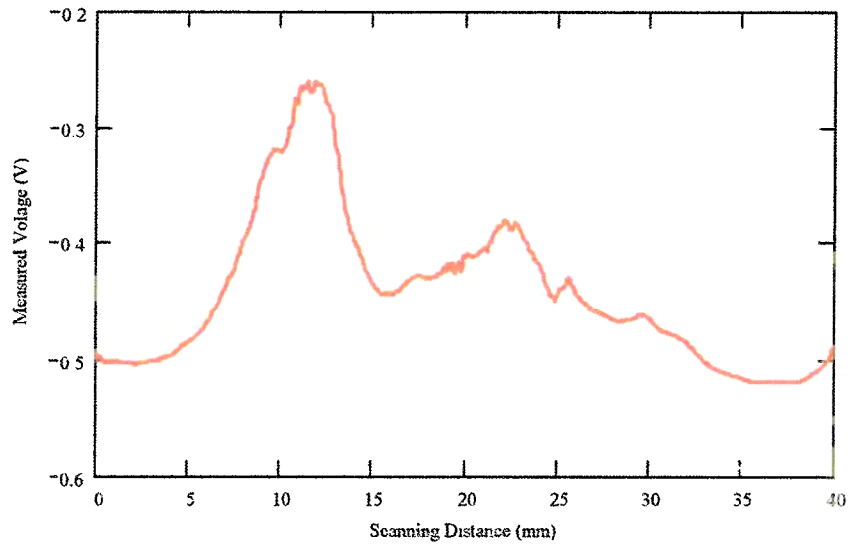


Figure 74 Crack characteristic signal of the second crack on sample T4298 at 32.13 GHz using coax # 3

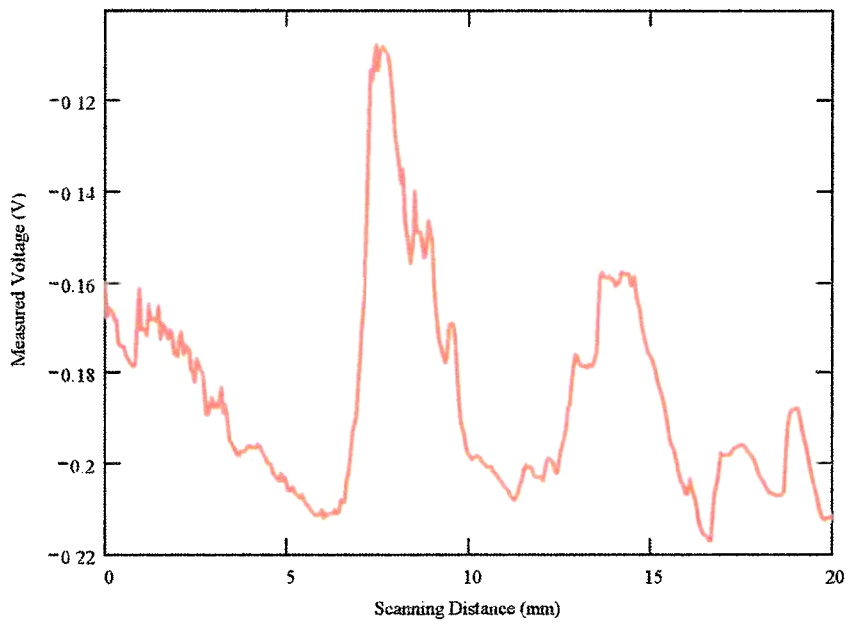


Figure 75 Crack characteristic signal of the first crack on sample PL4295 at 30.6 GHz using coax # 3

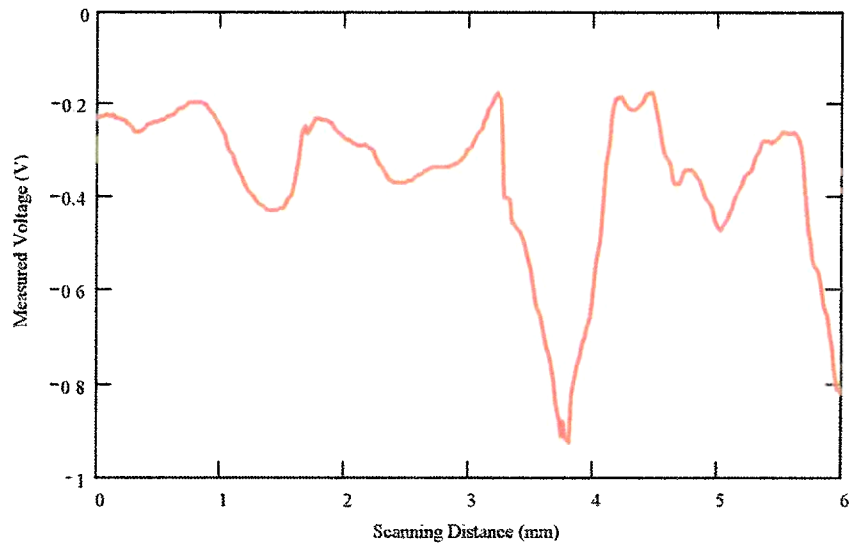


Figure 76 Crack characteristic signal of the first crack on sample PL4296 at 30.6 GHz using coax # 3

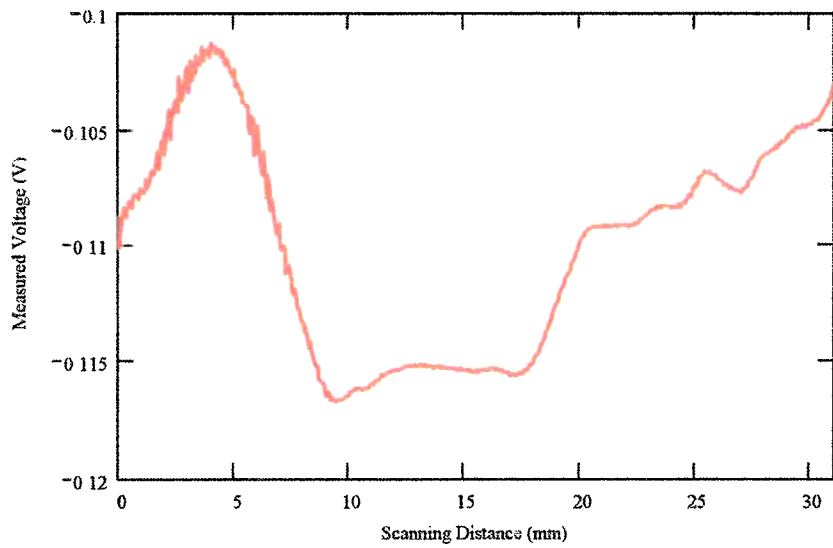


Figure 77 Crack characteristic signal of the second crack on sample PL4296 at 30.6 GHz using coax # 3

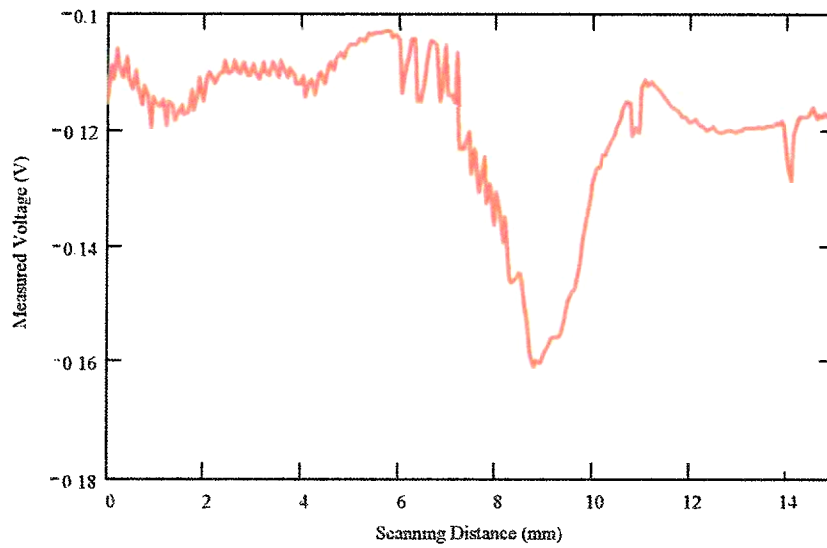


Figure 78 Crack characteristic signal of the second crack on sample T4297 at 30.6 GHz using coax # 3

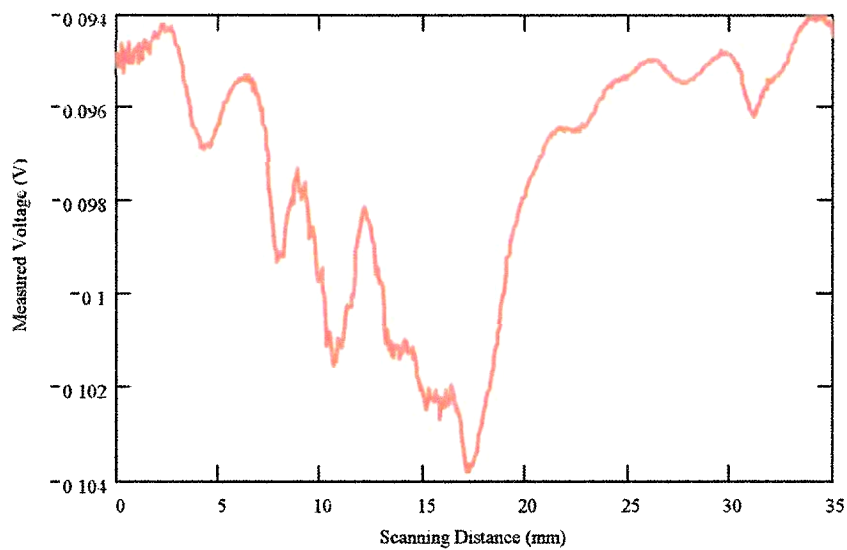


Figure 79: Crack characteristic signal of the first crack on sample T4298 at 30.6 GHz using coax # 3

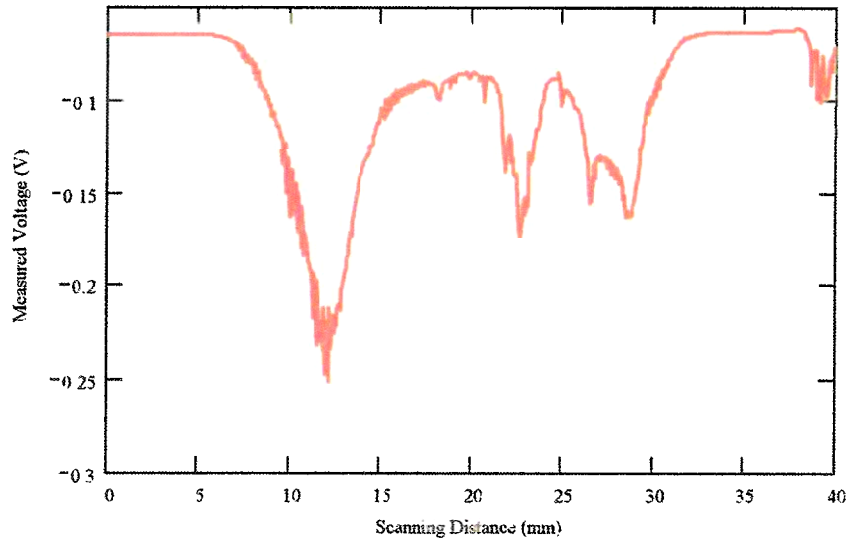


Figure 80 Crack characteristic signal of the second crack on sample T4298 at 30.6 GHz using coax # 3

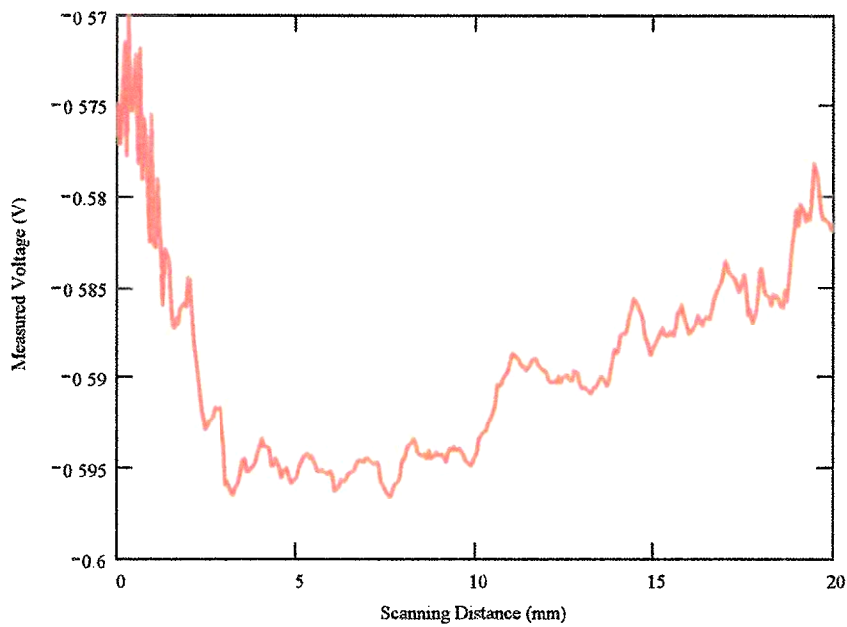


Figure 81 Crack characteristic signal of the first crack on sample PL4295 at 30.6 GHz using coax # 3

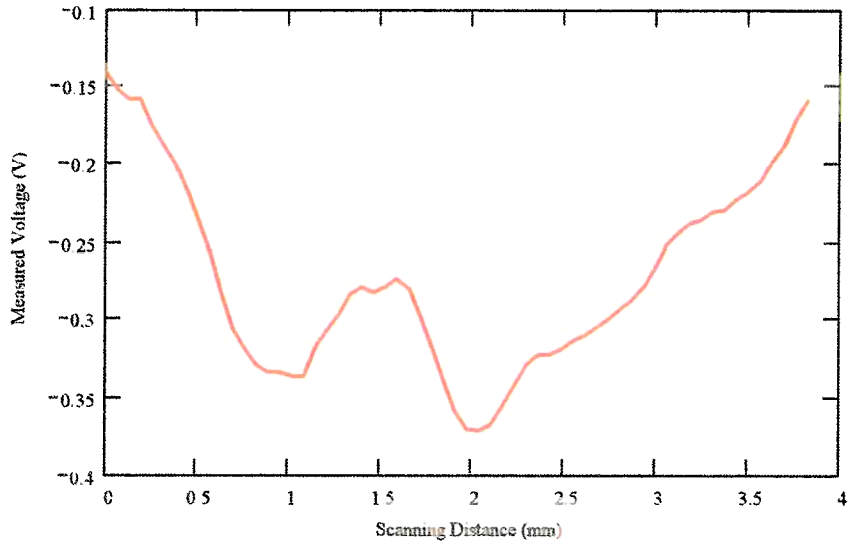


Figure 82: Crack characteristic signal of the first crack on sample PL4296 at 30.6 GHz using coax # 3

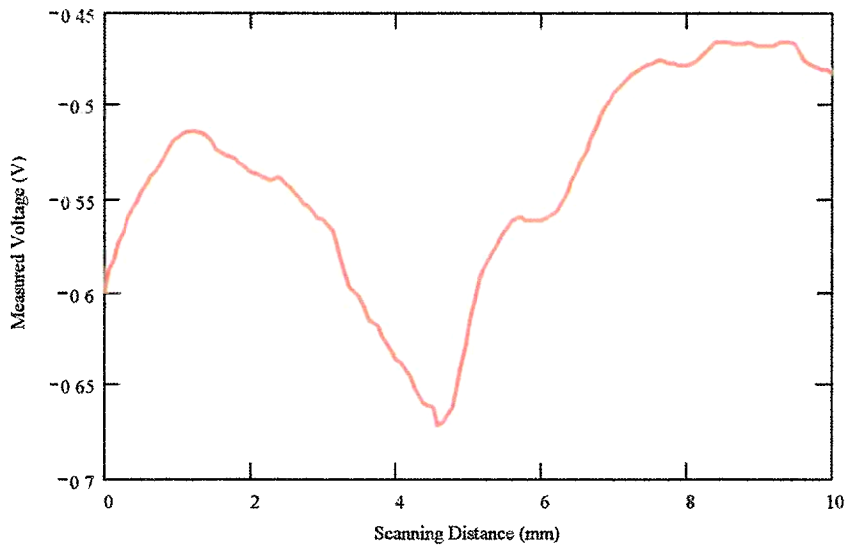


Figure 83: Crack characteristic signal of the first crack on sample T4297 at 30.6 GHz using coax # 3

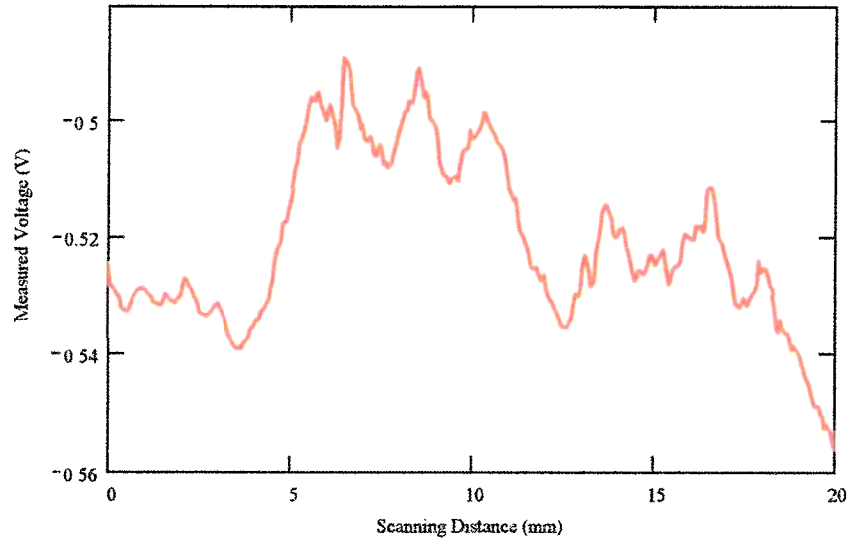
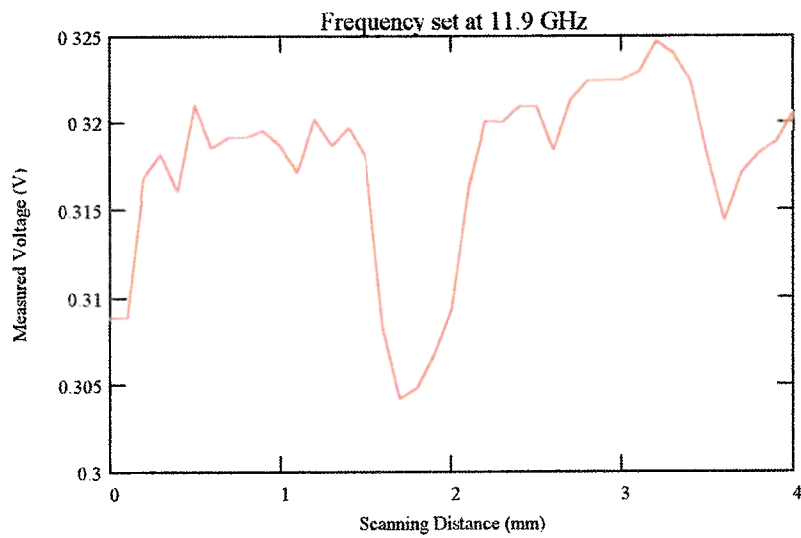


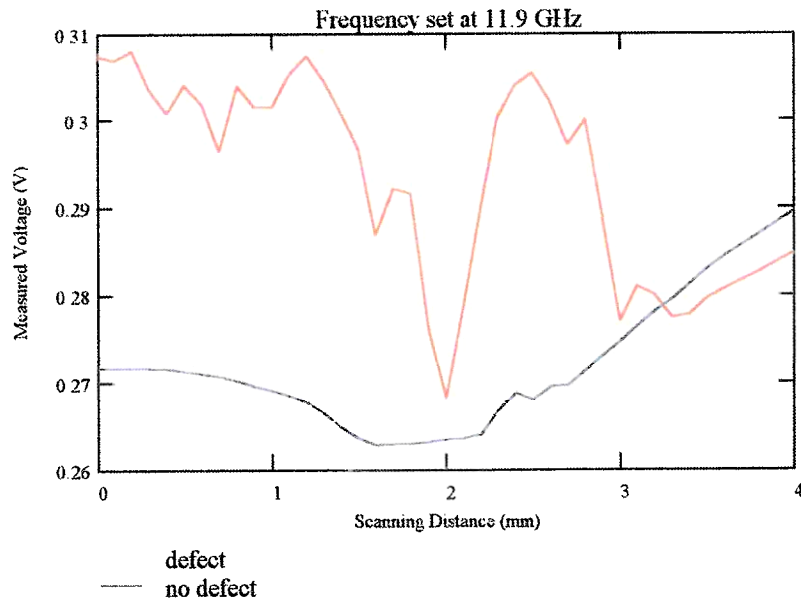
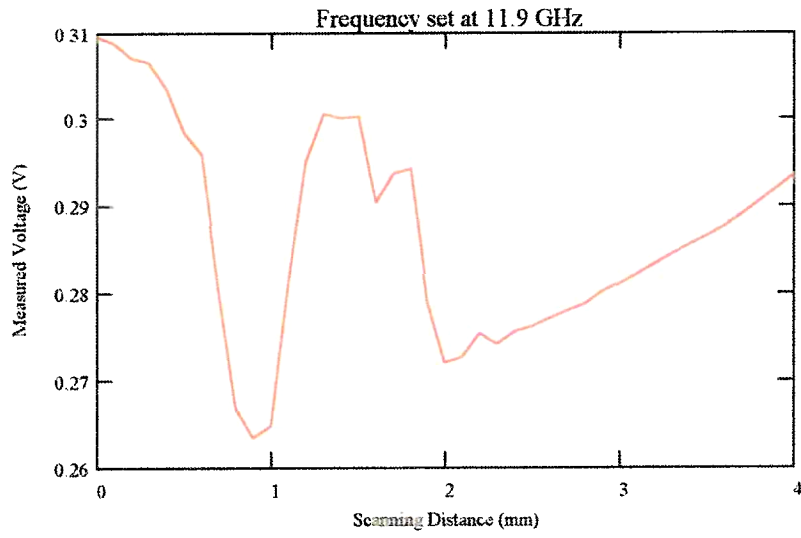
Figure 84 Crack characteristic signal of the first crack on sample T4298 at 30.6 GHz using coax # 3

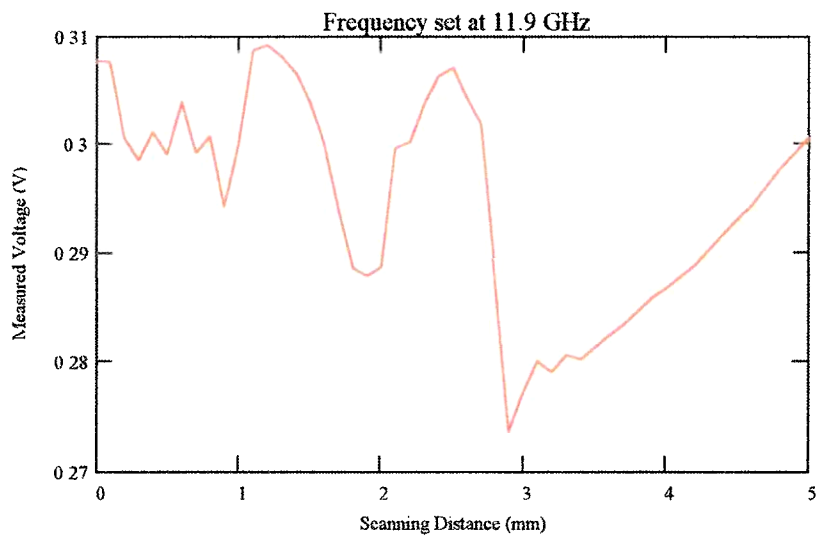
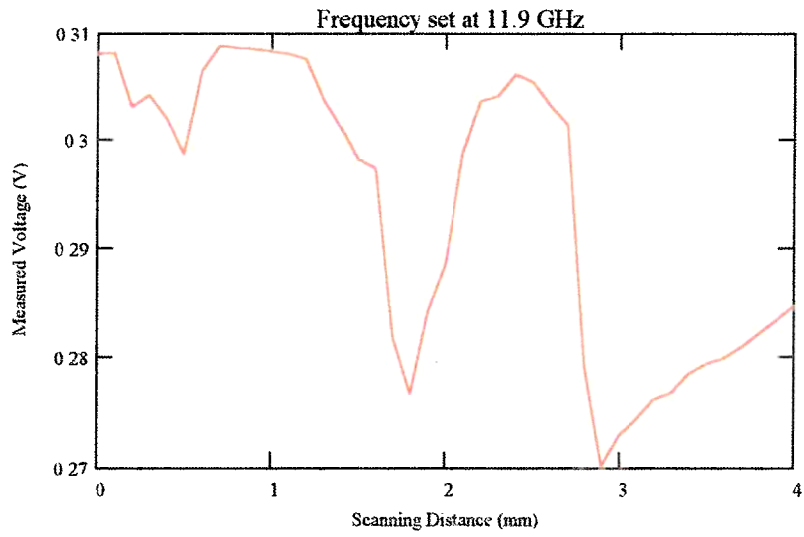
These are the results of the work done on detecting cracks in the welded joints, of the VTRC samples of the pipe, PL1497, PL1498, T1495, and T1496. There are four different types of cracks on these samples, and they are a Toe Indication, Root Indication, Transverse Indication, and a Centerline Indication. The pipe sample has three cracks on the welded joint. The first crack is a Centerline Indication with a length of 10 mm. The Second crack is a Toe Indication with a length of 10 mm. The third crack is a Transverse Indication with a length of 11 mm. Sample PL1497 has two defects/cracks that are on the center of the weld, and both are on the top of the sample. Defect one is a Centreline Indication with a length of 36.8 mm, and defect two is a Transverse Indication with a length of 11 mm. Sample PL1498 also has two defects along the edge of the weld. Defect two is on the bottom of the sample, while defect one is on the top. Defect one is a Toe Indication with a length of 61mm, and defect two is a Root Indication with a length of 24 mm. Sample T1495 has two defects that are on the weld. Defect one is a Centreline Indication with a length of 64 mm, and defect two is a Transverse Indication with a length of 5.8 mm. Sample T1496 also has two defects that run along the edge of the weld. Defect one is a Toe Indication with a length of 71 mm, and defect two is a Root Indication with a length of 34 mm.

I. Pipe Sample
A. Crack #1

Frequency Band: X-band
Orientation: Scan perpendicular to crack length
Scan Resolution: 0.102 mm per step
Scan length: 20 mm
Frequency: Varies

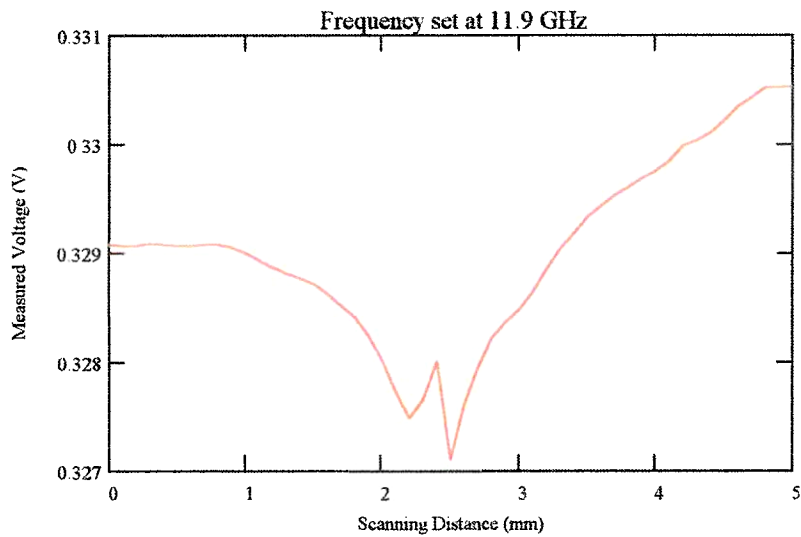


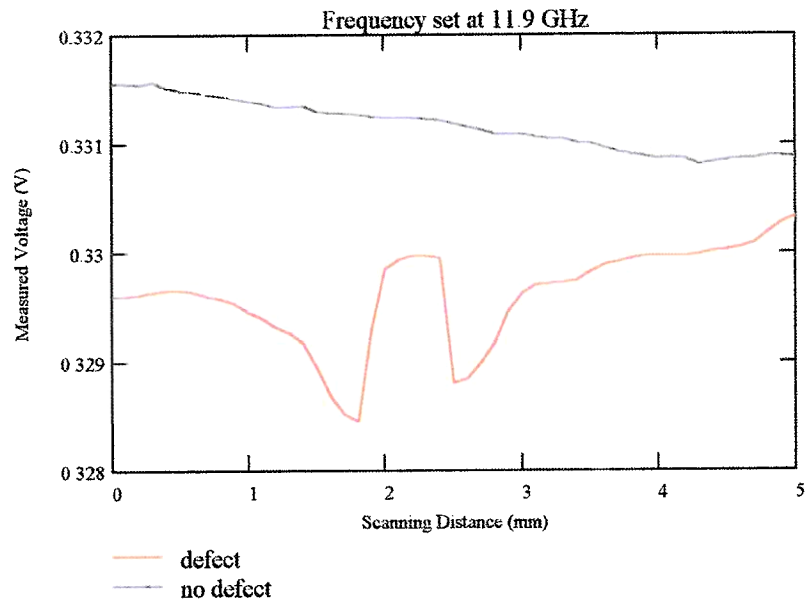
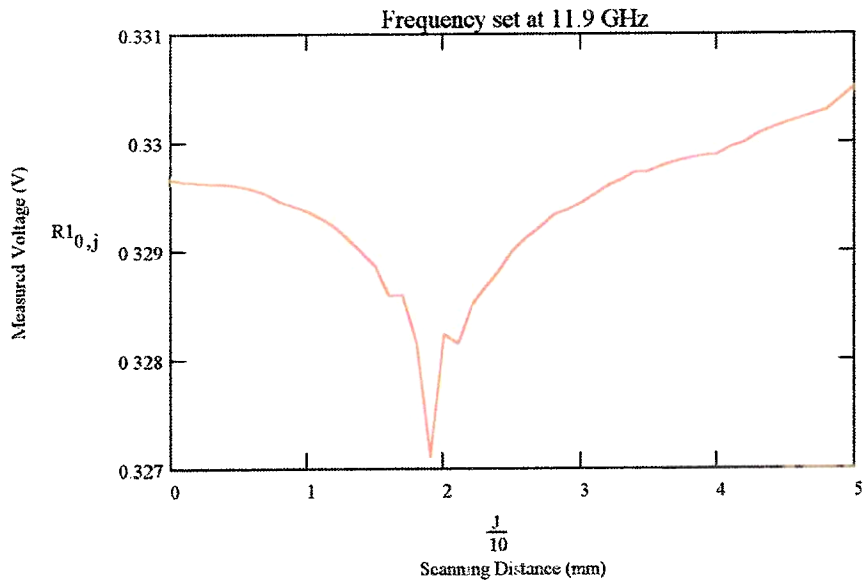


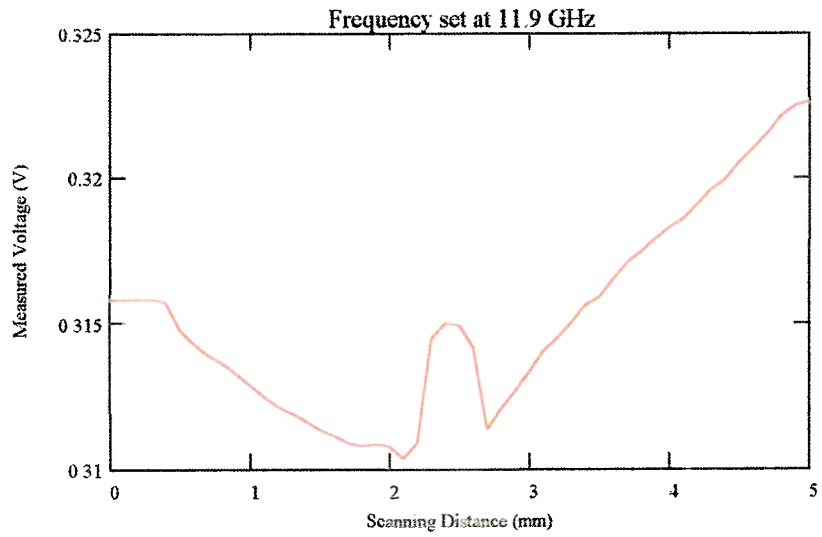
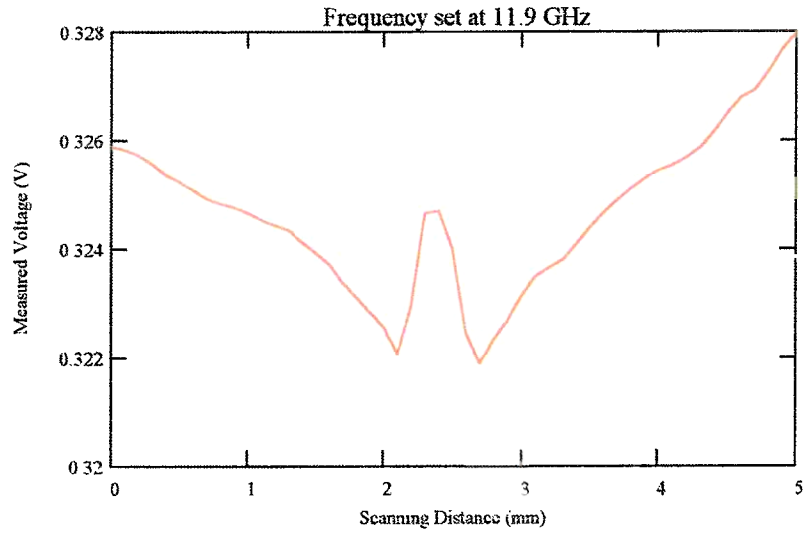


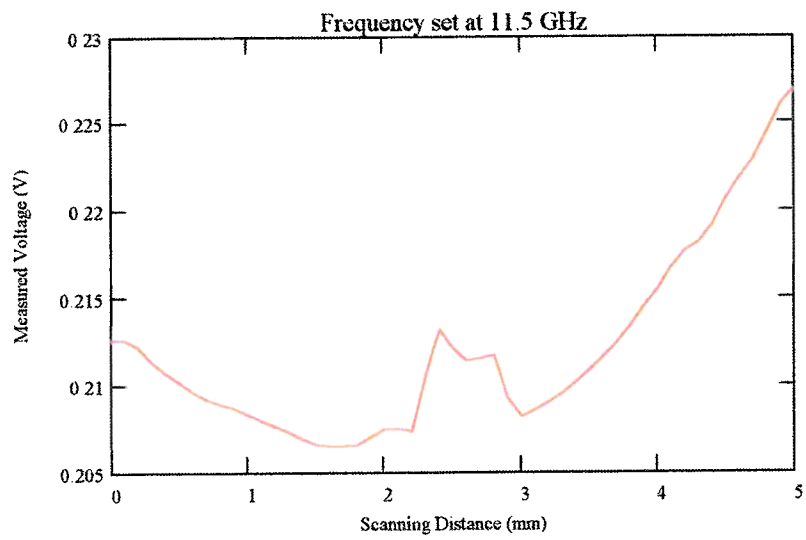
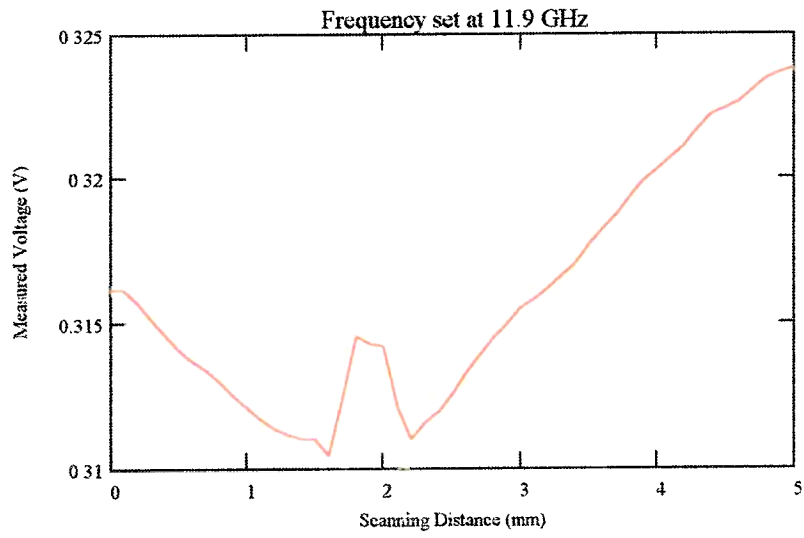
B. Crack #2

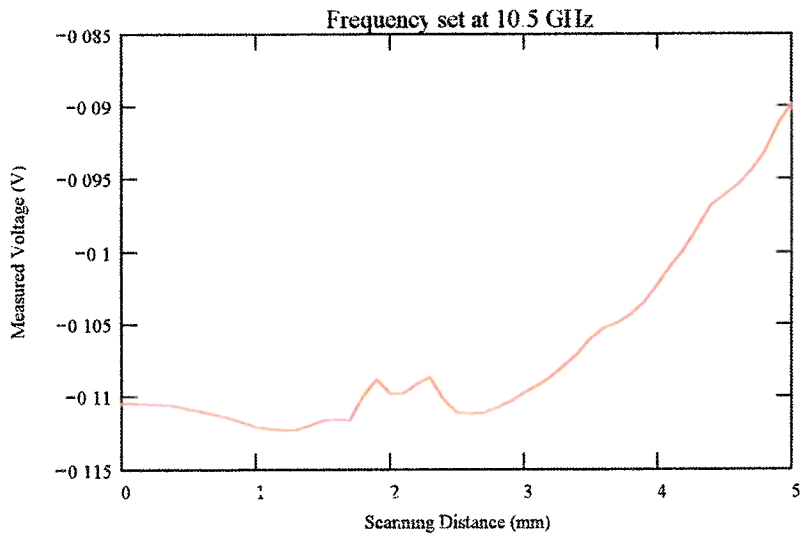
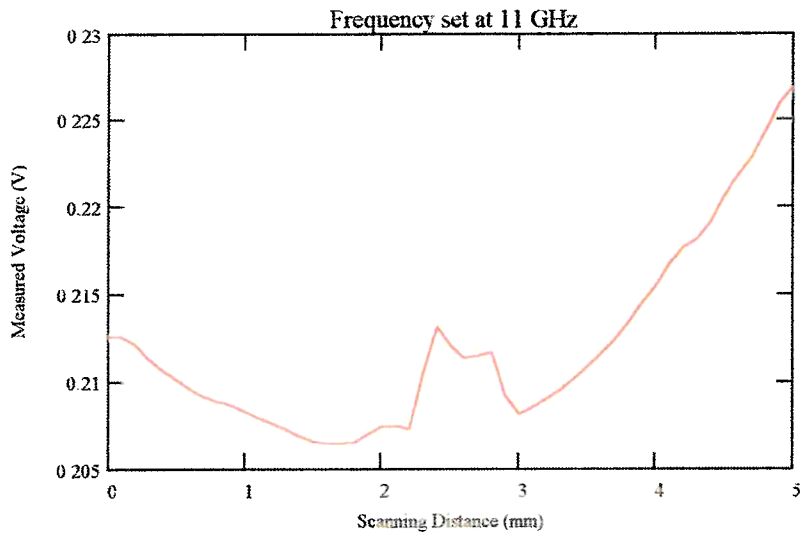
Frequency Band: X-band
Orientation: Scan perpendicular to crack length
Scan Resolution: 0.102 mm per step
Scan length: 20 mm
Frequency: 11.9 GHz

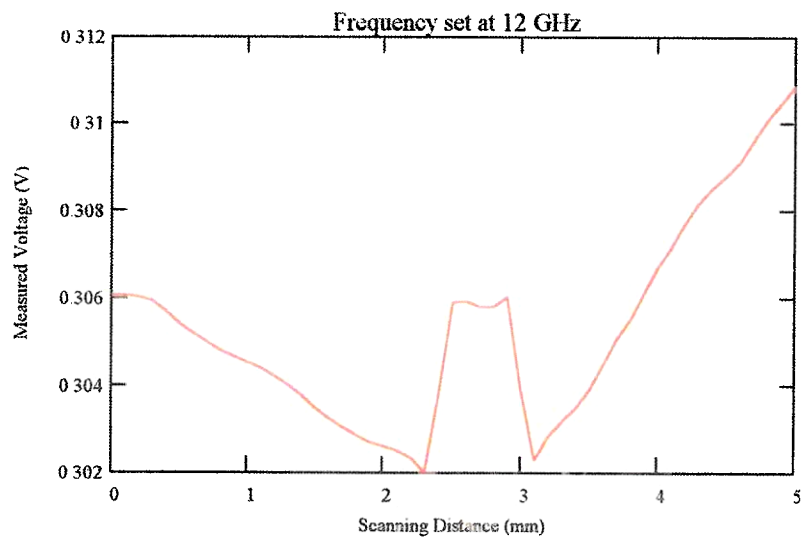
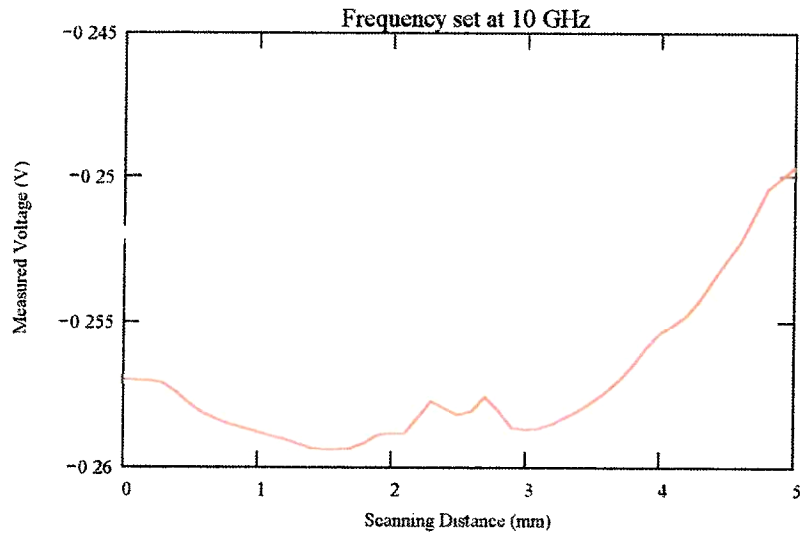


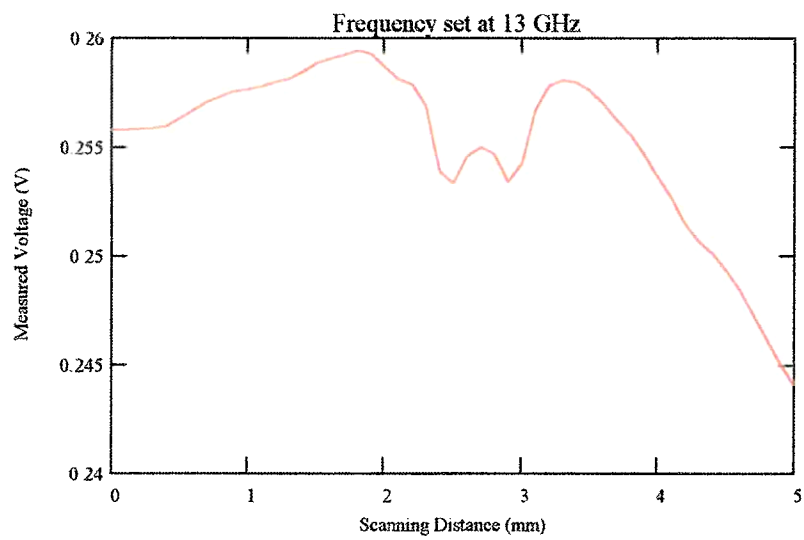
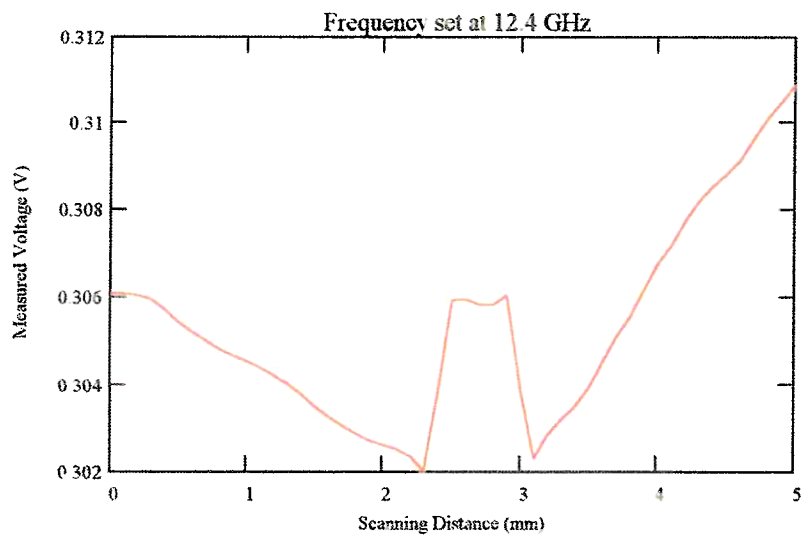


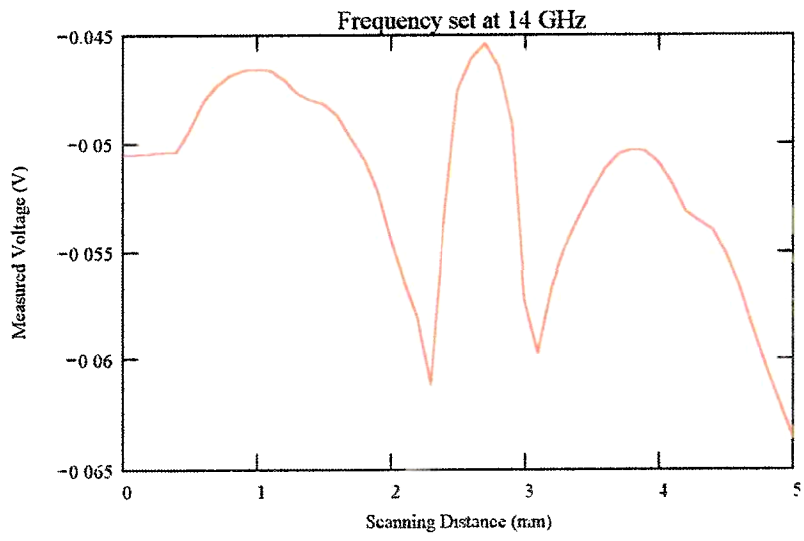






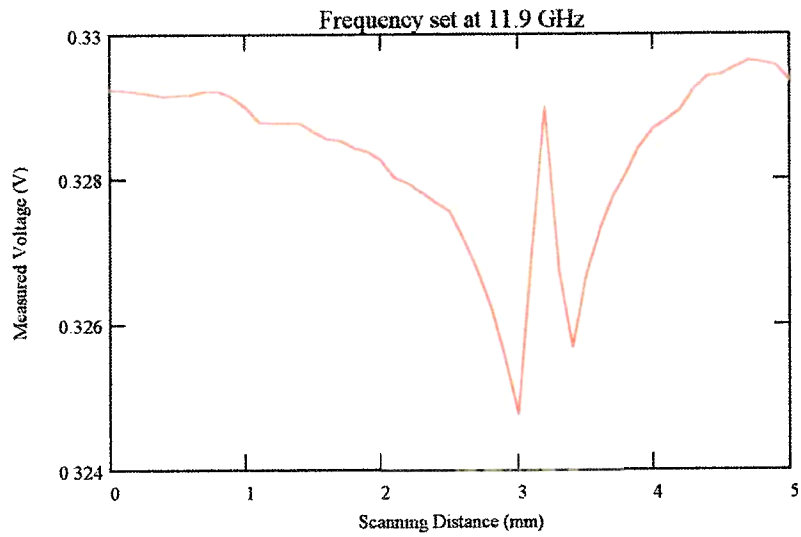


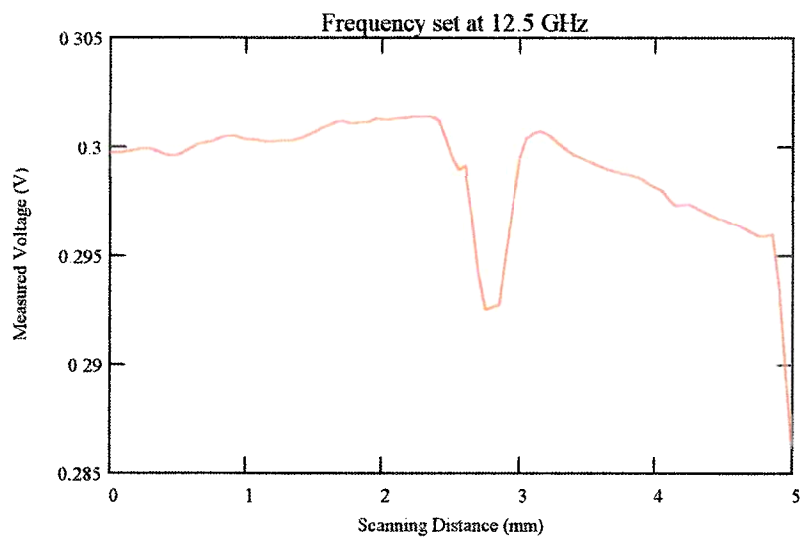
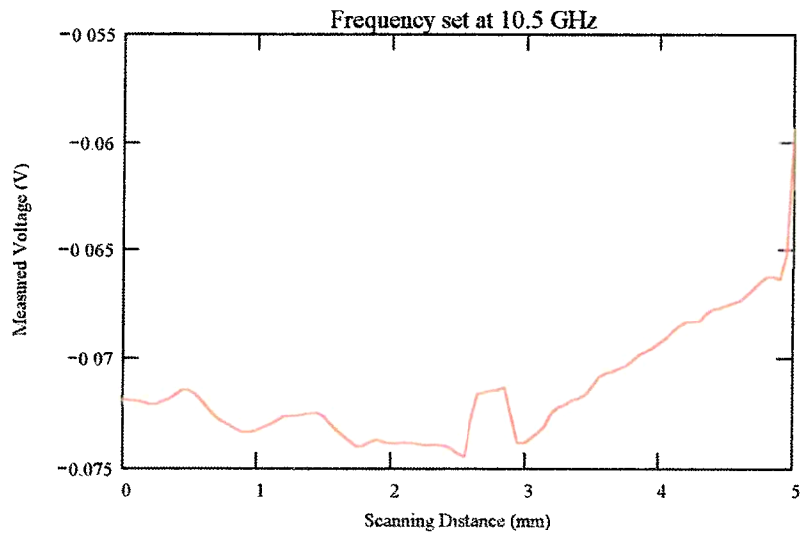


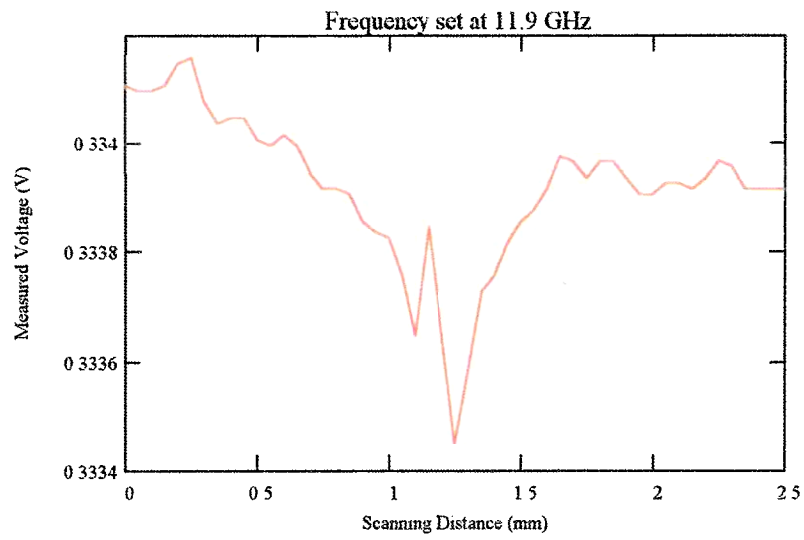
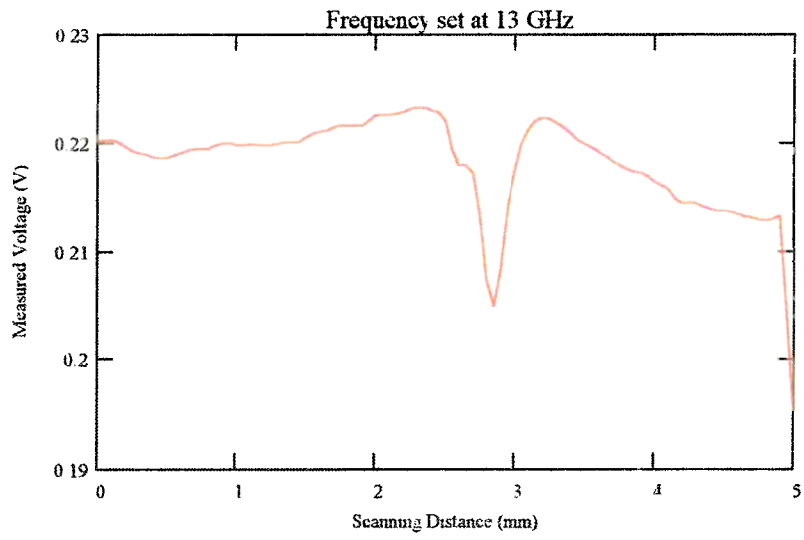


C Crack #

Frequency Band: X-band
Orientation: Scan perpendicular to crack length
Scan Resolution: 0.102 mm per step
Scan length: 20 mm
Frequency: 11.9 GHz







II Sample PL1497

A. Crack #1

This is a Centreline indication crack. The length of the crack is 1.45 in. This crack runs parallel to the welded joint.

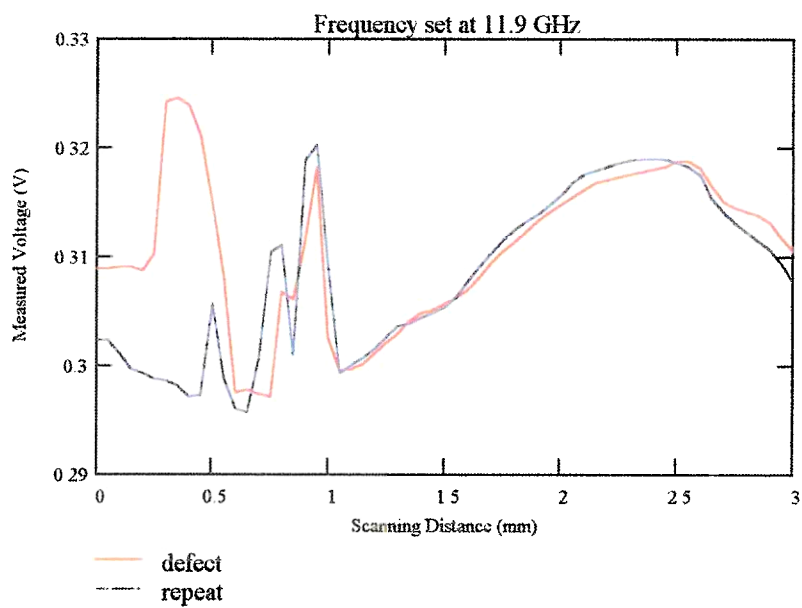
Frequency Band: X-band

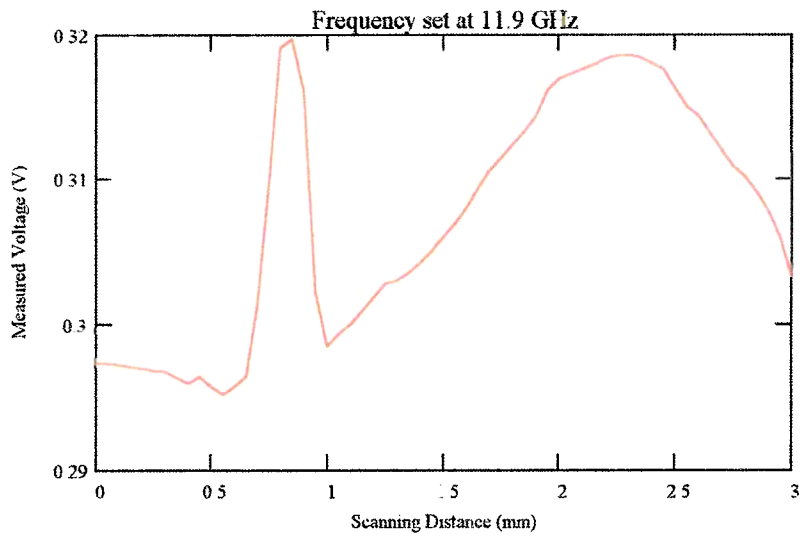
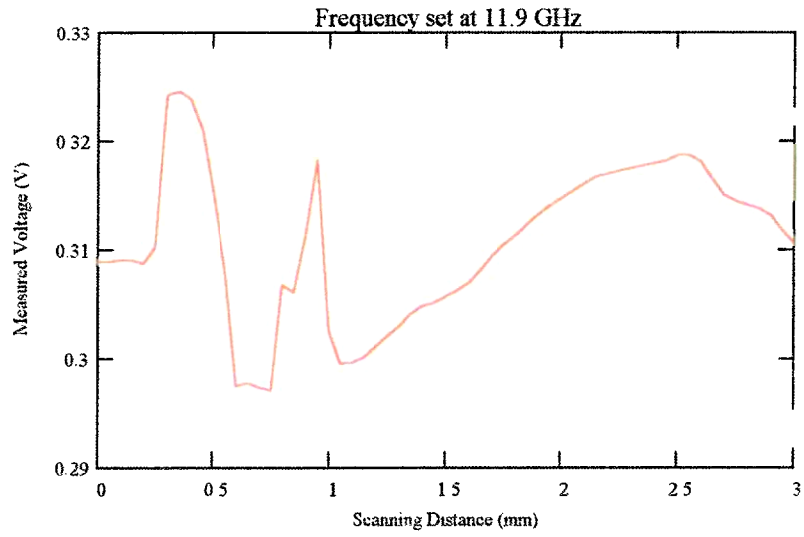
Orientation: Scan perpendicular to crack length.

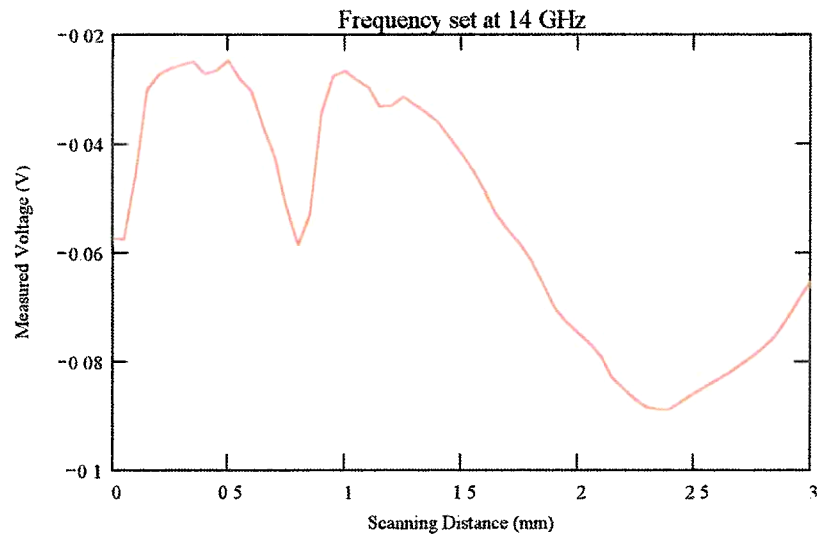
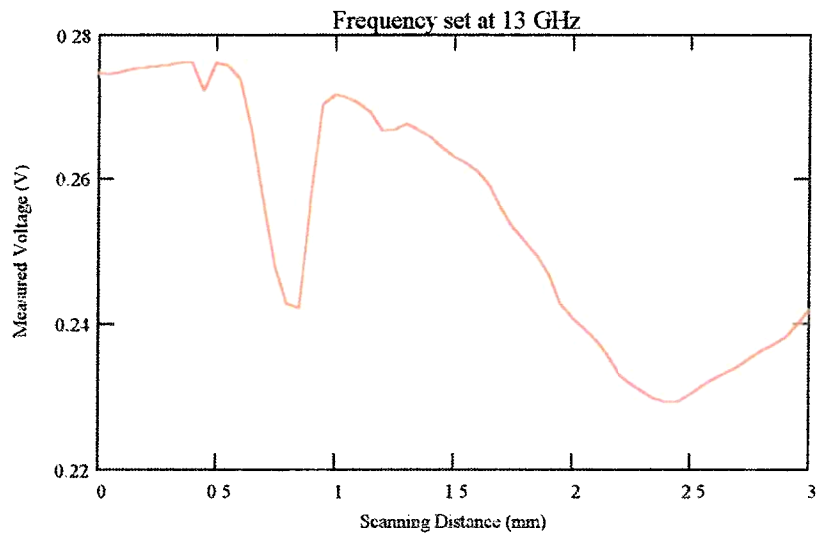
Scan Resolution: 0.102 mm per step

Scan length: 3 mm

Frequency: 11.9 GHz



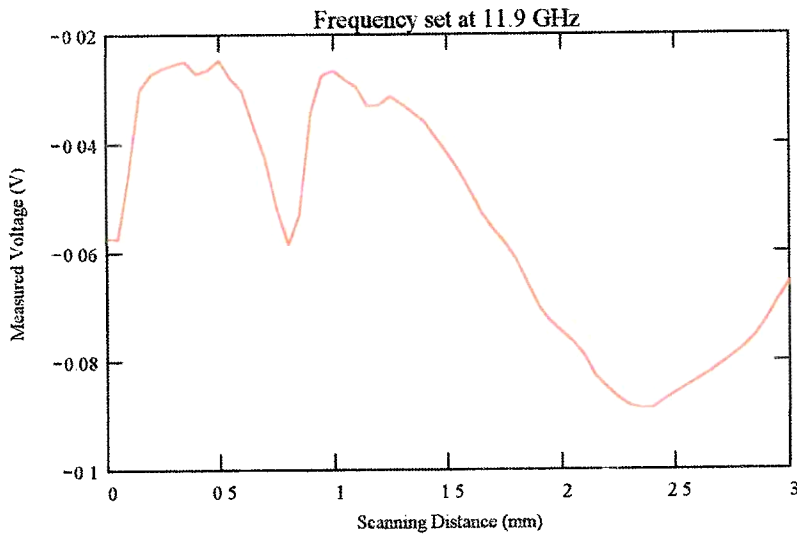


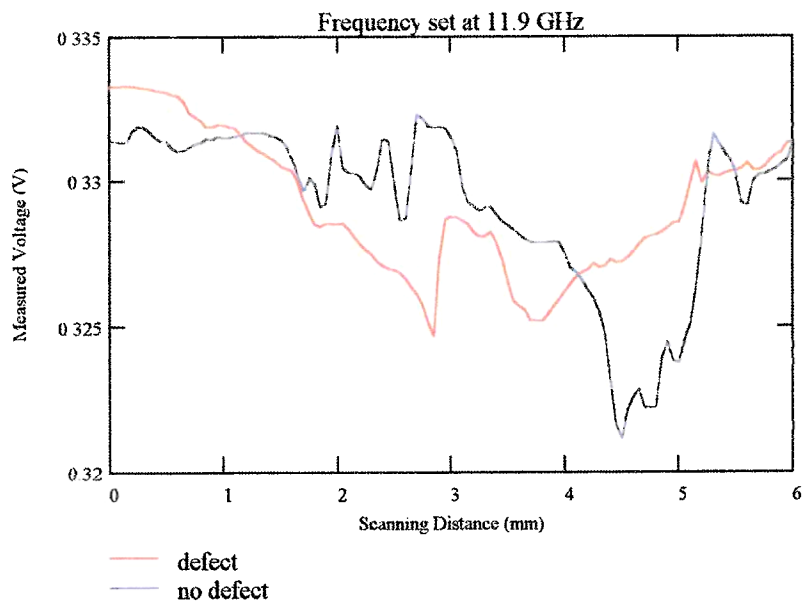
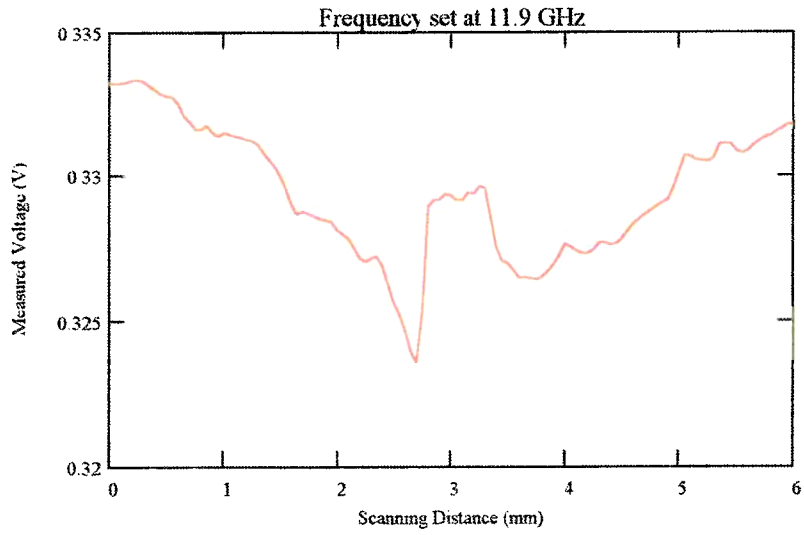


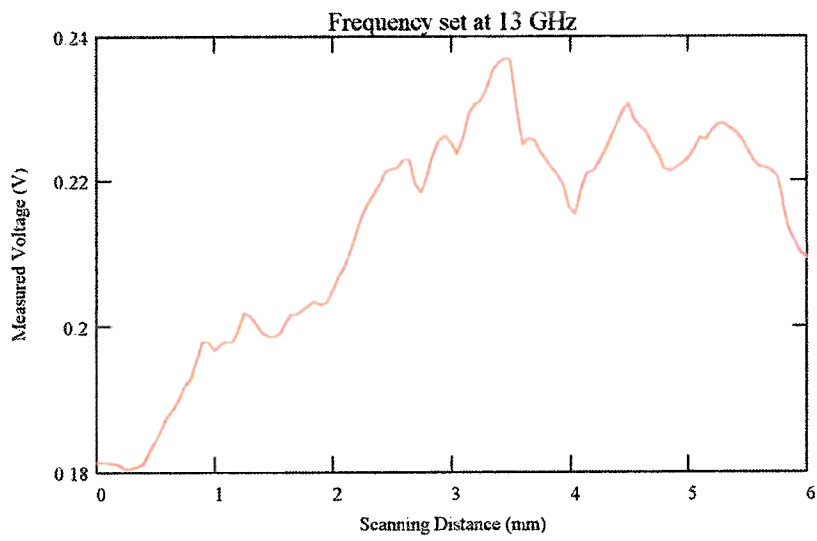
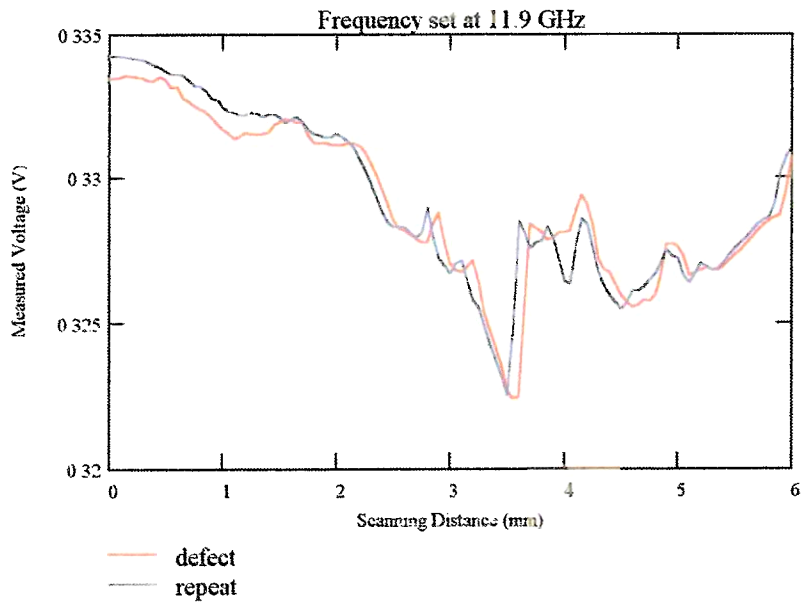
B Crack #2

This is a Transverse indication crack. The length of the crack is 0.43 in. This crack runs perpendicular to the welded joint.

Frequency Band: X-band
Orientation: Scan perpendicular to crack length
Scan Resolution: 0.102 mm per step
Scan length: 6 mm
Frequency: 11.9 GHz







III. Sample T1495

A. Crack #1

This is a Centerline Indication crack. The length of the crack is 2.51 in. This crack runs perpendicular to the welded joint.

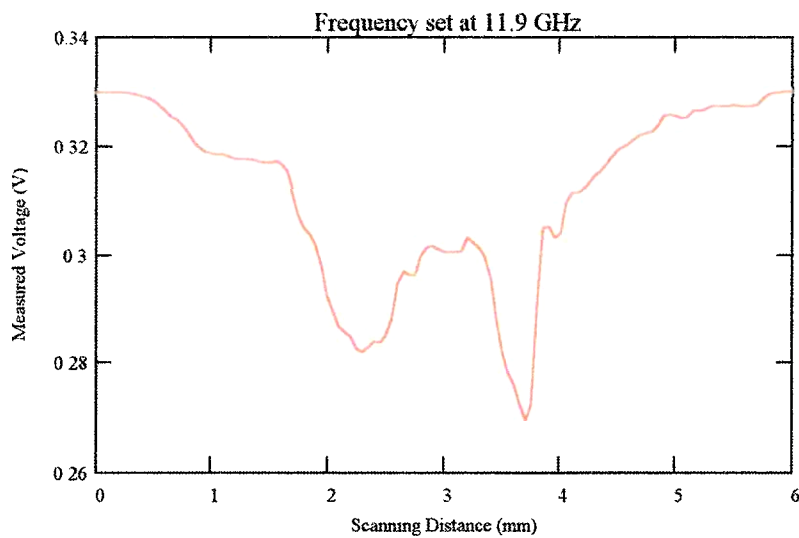
Frequency Band: X-band

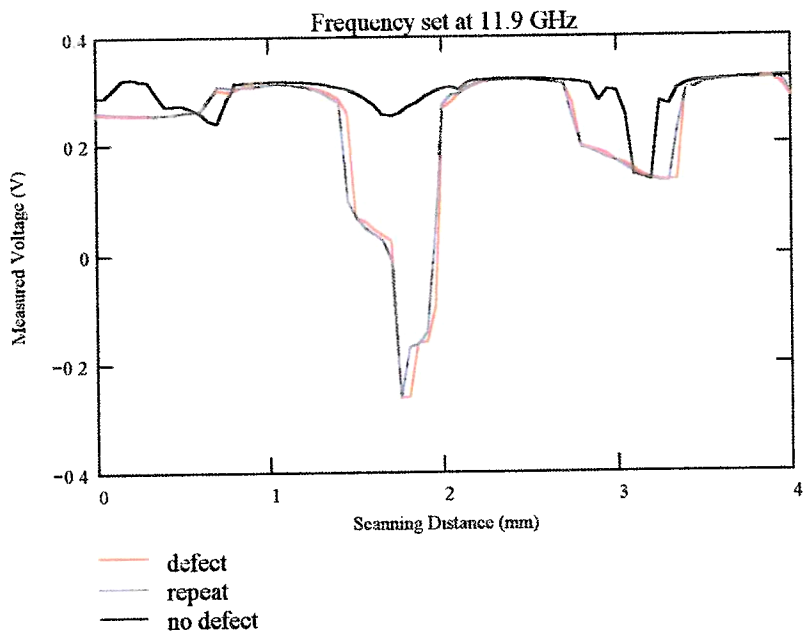
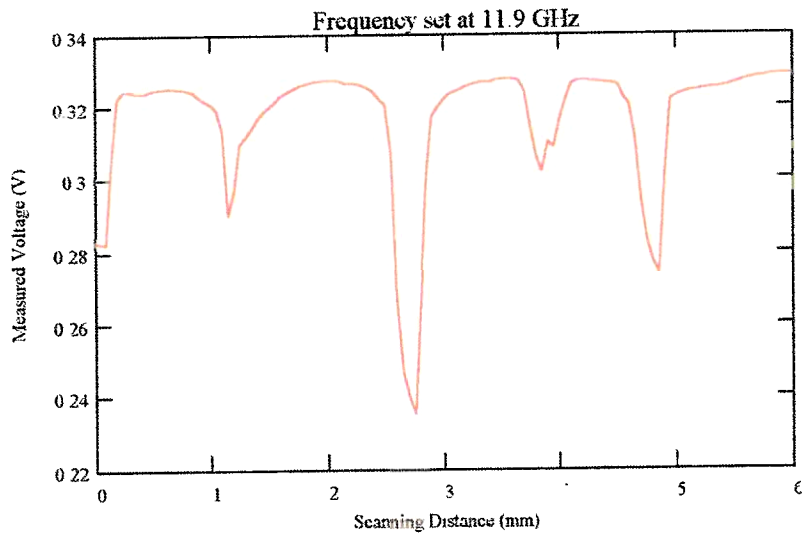
Orientation: Scan perpendicular to crack length.

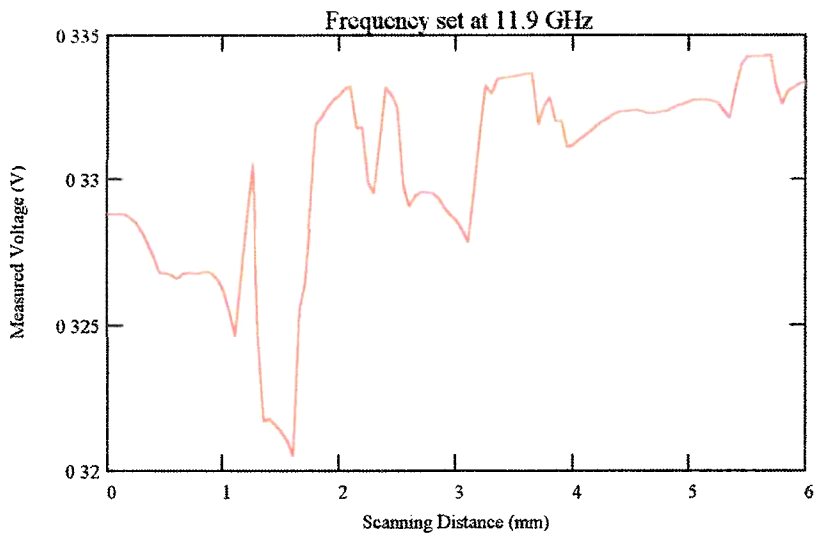
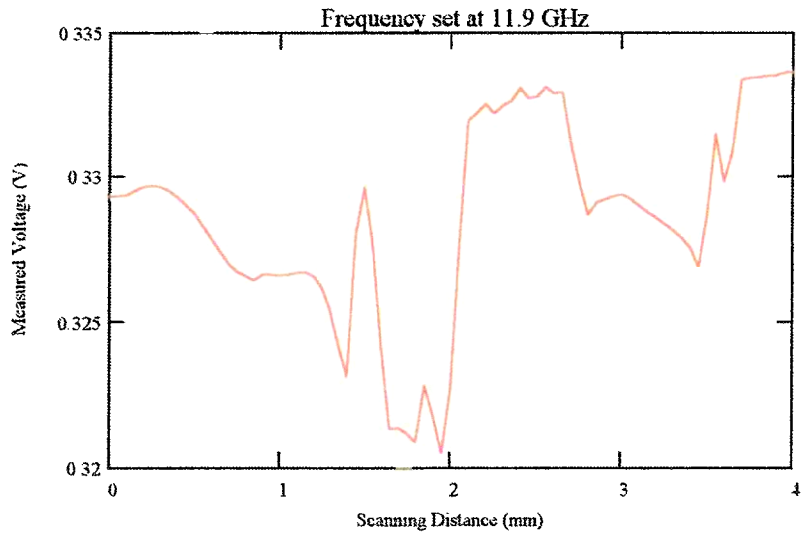
Scan Resolution: 0.102 mm per step

Scan length: 6 mm

Frequency: 11.9 GHz







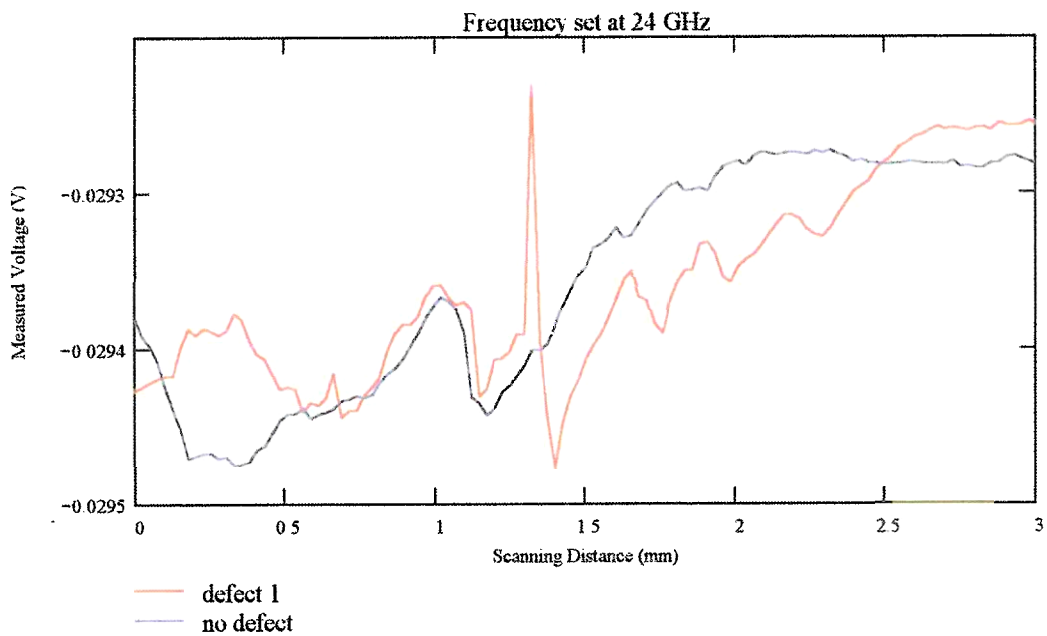
These are the results of the work done on detecting cracks in the welded joints, of the VTRC samples PL1497, PL1498, T1495, and T1496, after they have been rusted. There are four different types of cracks on these samples, and they are a Toe Indication, Root Indication, Transverse Indication, and a Centerline Indication. Sample PL1497 has two defects/cracks that are on the center of the weld, and both are on the top of the sample. Defect one is a Centerline Indication with a length of 36 mm, and defect two is a Transverse Indication with a length of 11 mm. Sample PL1498 also has two defects along the edge of the weld. Defect two is on the bottom of the sample, while defect one is on the top. Defect one is a Toe Indication with a length of 61 mm, and defect two is a Root Indication with a length of 24 mm. Sample T1495 has two defects that are on the weld. Defect one is a Centerline Indication with a length of 64 mm, and defect two is a Transverse Indication with a length of 5.8 mm. Sample T1496 also has two defects that run along the edge of the weld. Defect one is a Toe Indication with a length of 71 mm, and defect two is a Root Indication with a length of 34 mm.

Several measurements at different frequencies were conducted to detect the presence of the cracks on this specimen. There are two different ways to scan a crack, parallel is to scan along the length of the crack and perpendicular is to scan across the length of the crack.

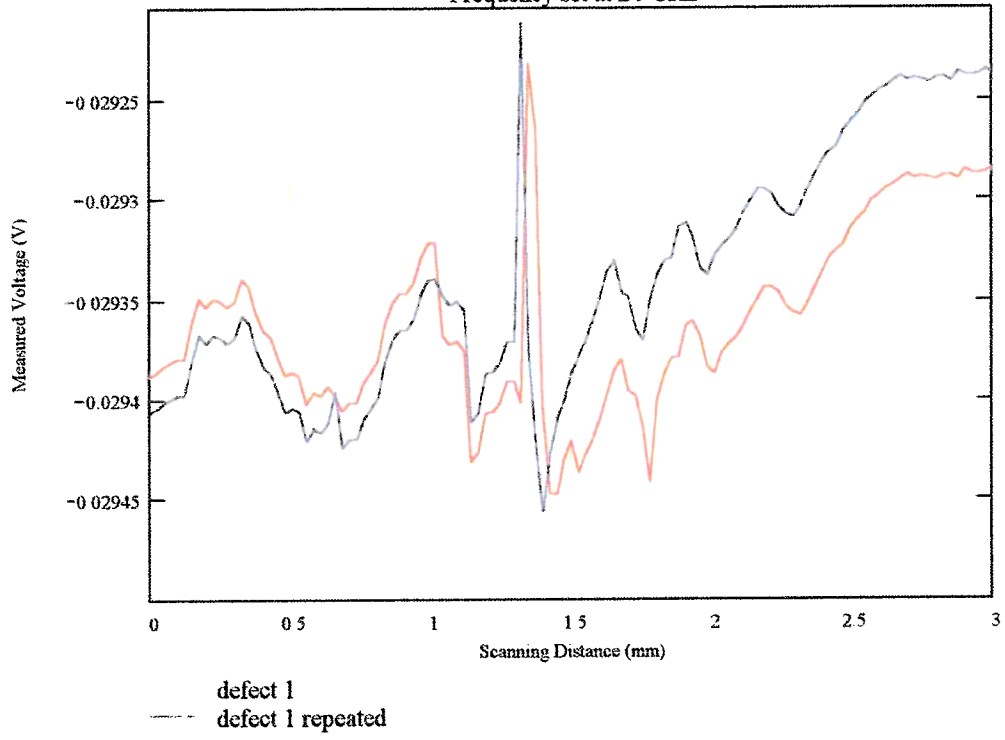
I Sample PL1497 Rusted
A Crack #1

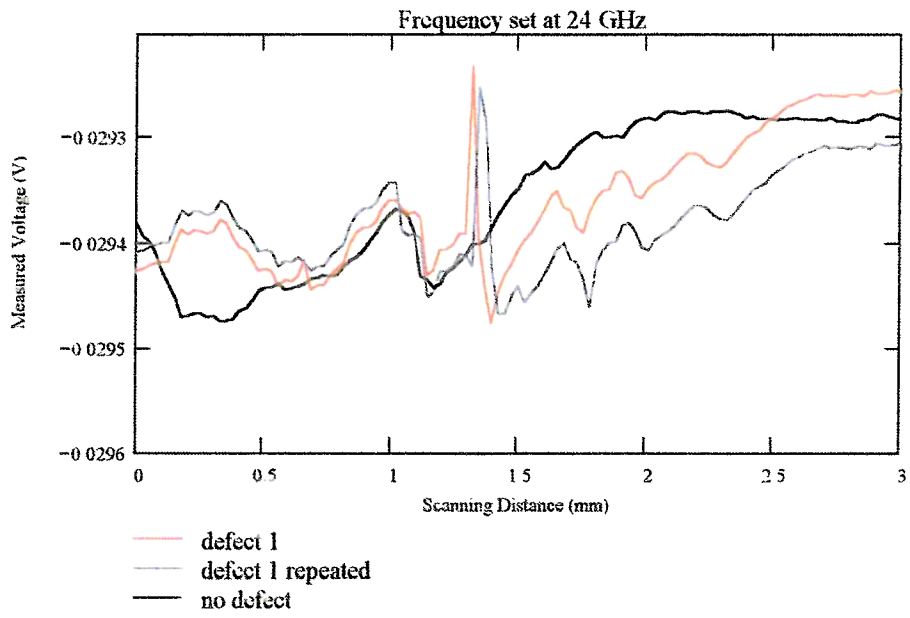
This is a Centreline Indication crack. The length of the crack is 1.45 in. This crack runs parrallel to the welded joint.

Frequency Band: K-band
Orientation: Scan perpendicular to crack length.
Probe: coax no 3
Scan Resolution: 0.0255 mm
Scan length: 3 mm
Frequency: 24 GHz

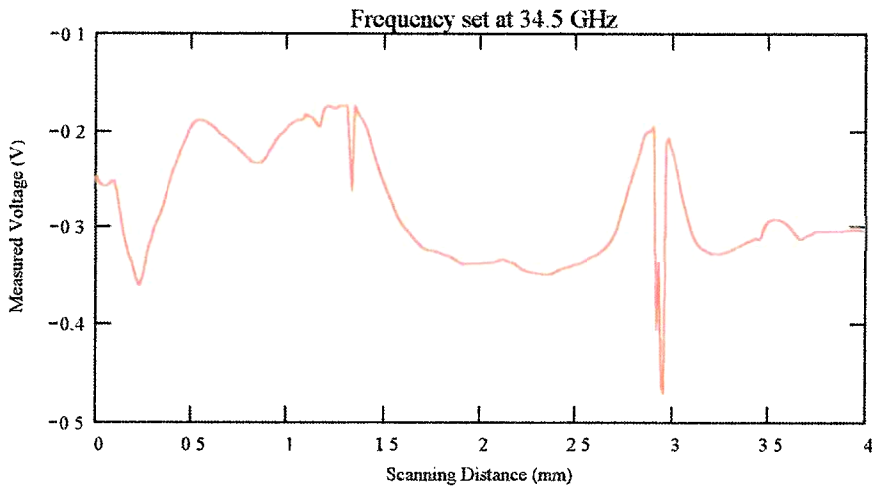


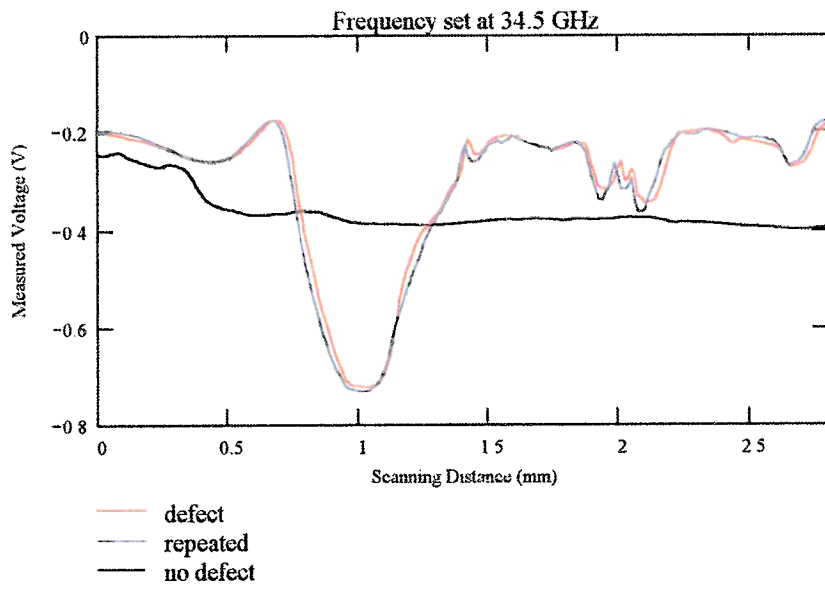
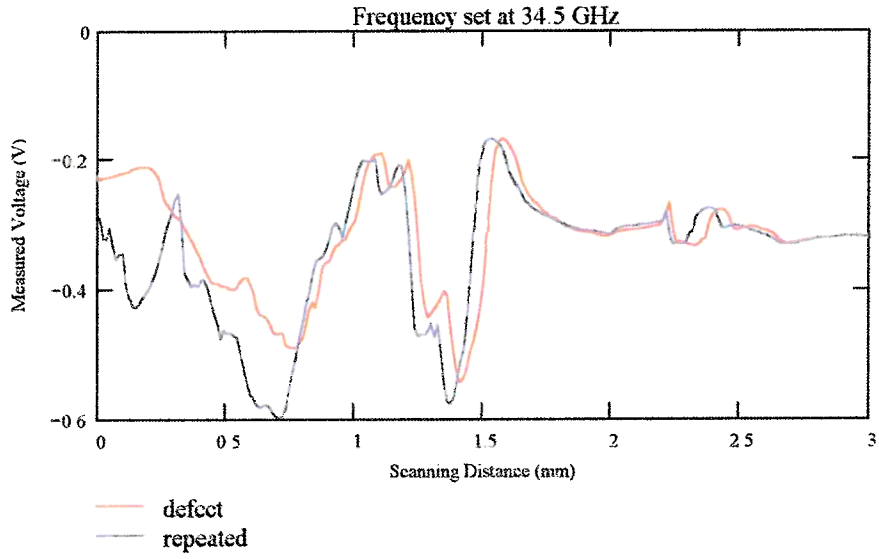
Frequency set at 24 GHz





Frequency Band: Ka-band
Orientation: Scan perpendicular to crack length
Probe: coax no. 3
Scan Resolution: 0.0255 mm
Scan length: 3-4 mm
Frequency: 34.5 GHz

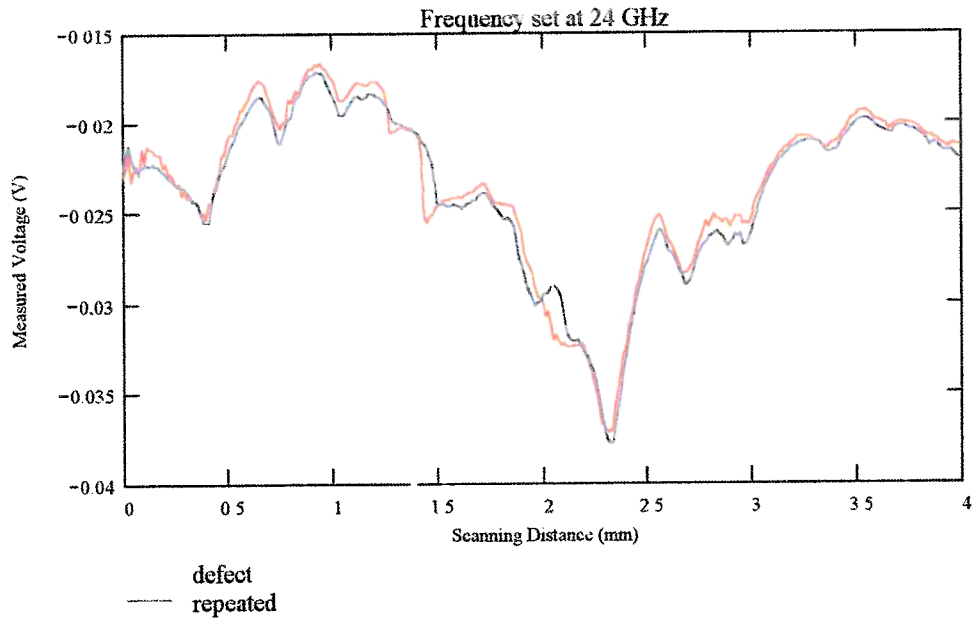


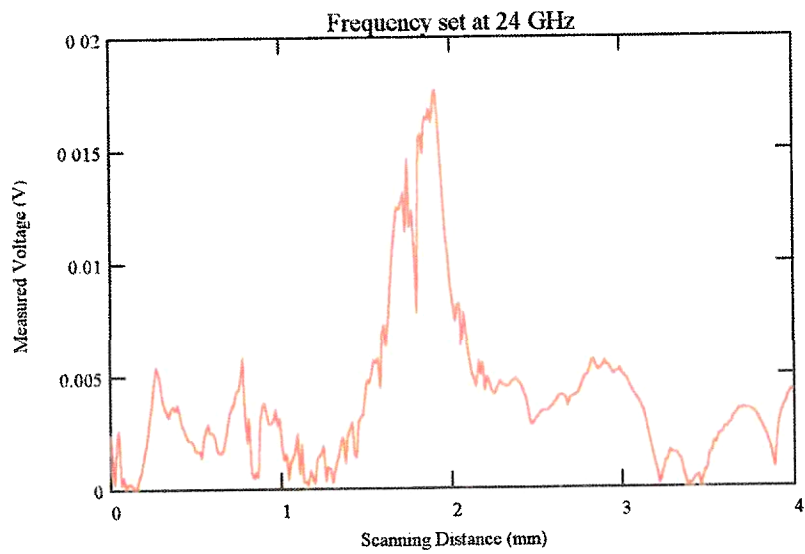
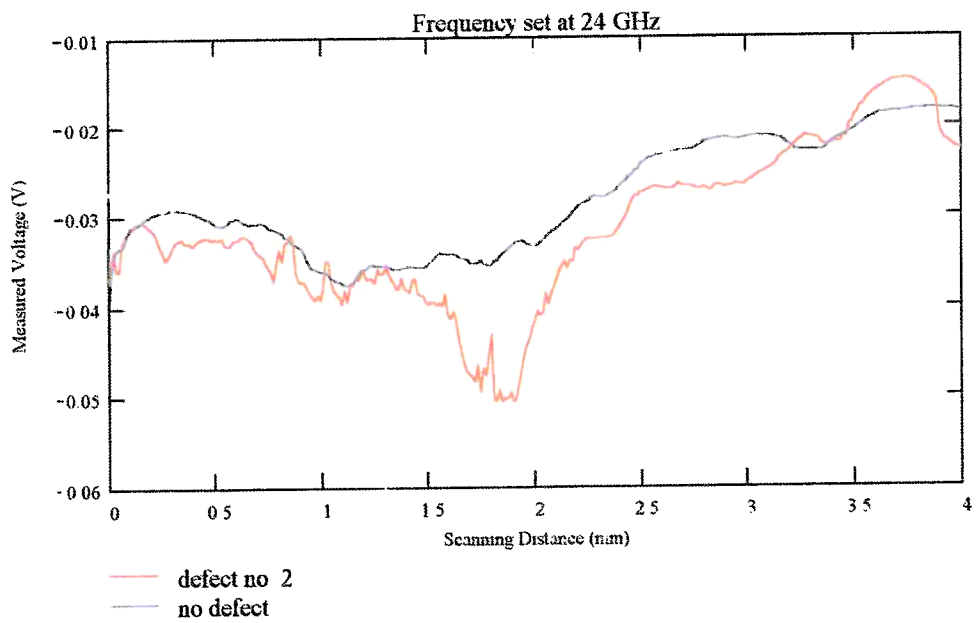


B Crack #2

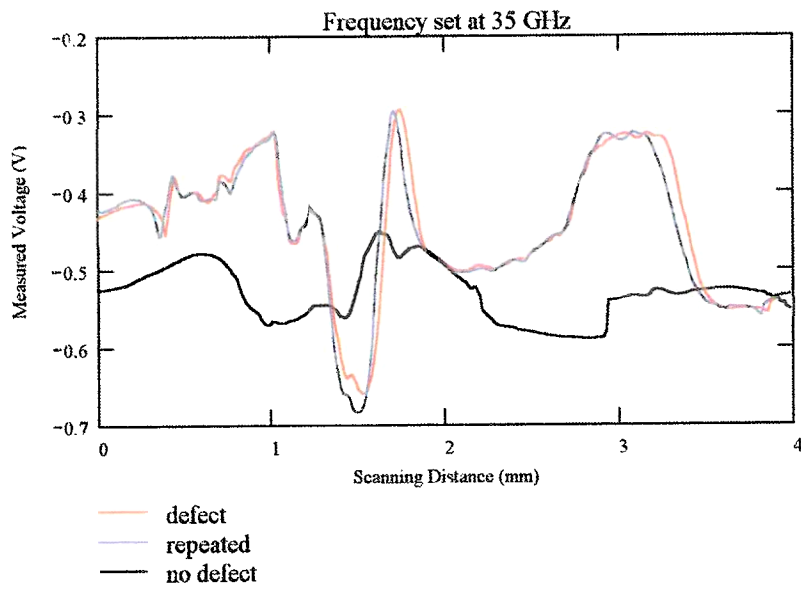
the This is a Transverse Indication crack. The length of
the crack is 0.43 in. This crack runs perpendicular to
the welded joint

Frequency Band: K-band
Orientation: Scan perpendicular to crack length.
Probe: coax no. 3
Scan Resolution: 0.0127 mm
Scan length: 4 mm
Frequency: 24 GHz





Frequency Band: Ka-band
Orientation: Scan perpendicular to crack length
Probe: coax no. 3
Scan Resolution: 0.0127 mm
Scan length: 4 mm
Frequency: 35 GHz

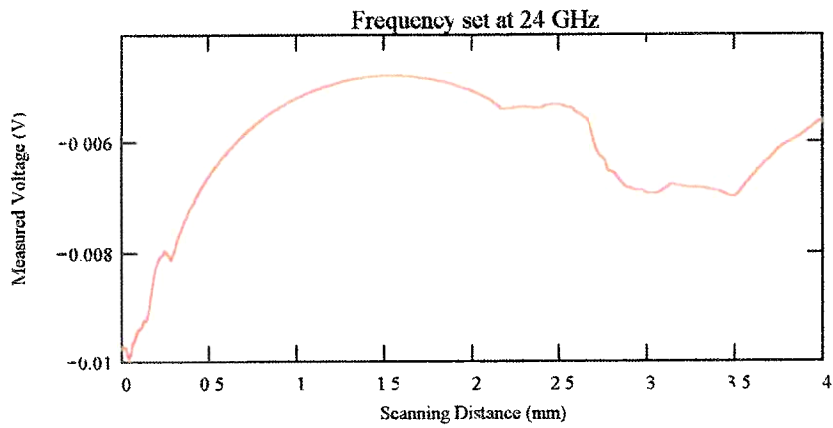


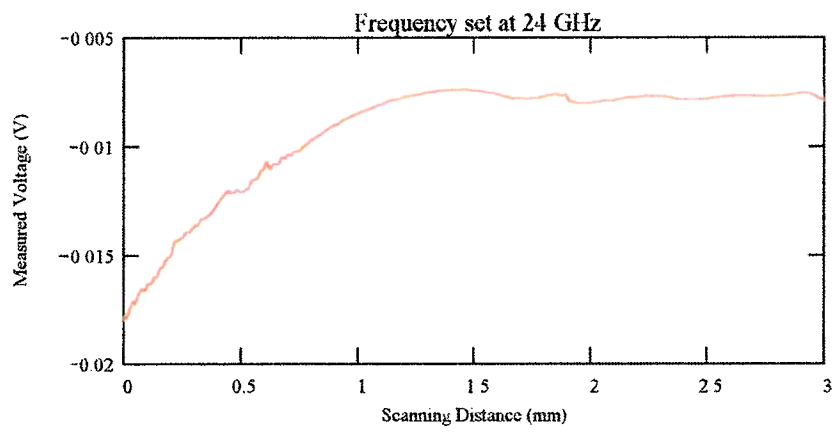
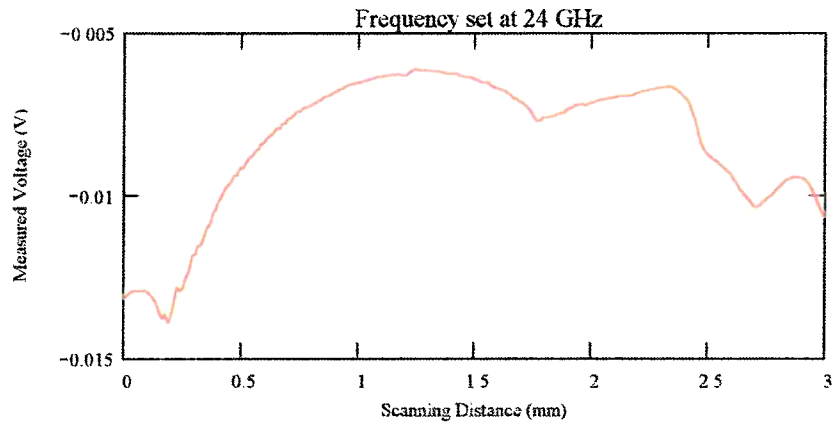
II Sample PL1498

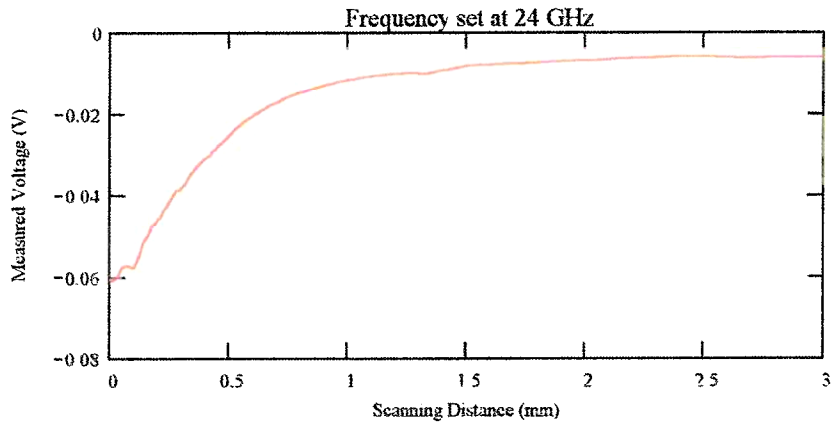
A. Crack #1

This is a Toe Indication crack. The length of the crack is 2.40 in. This crack runs parallel to the welded joint

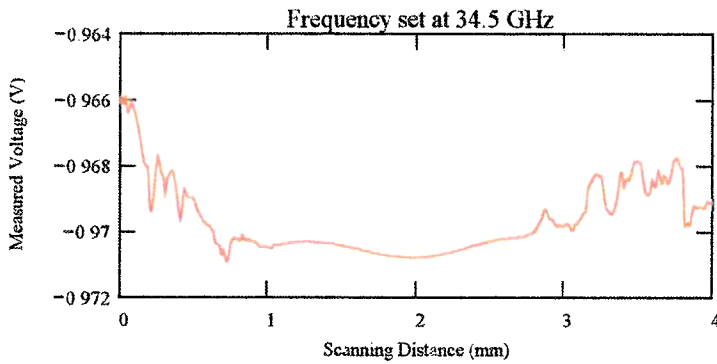
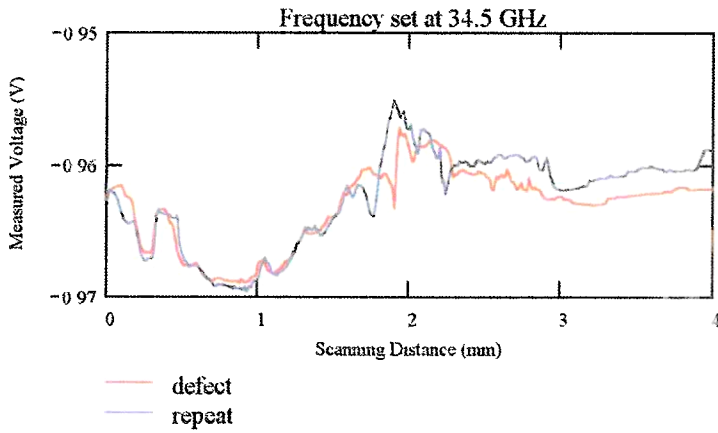
Frequency Band: K-band
Orientation: Scan perpendicular to crack length
Probe: coax no. 3
Scan Resolution: 0.0127 mm
Scan length: 3 mm
Frequency: 24 GHz







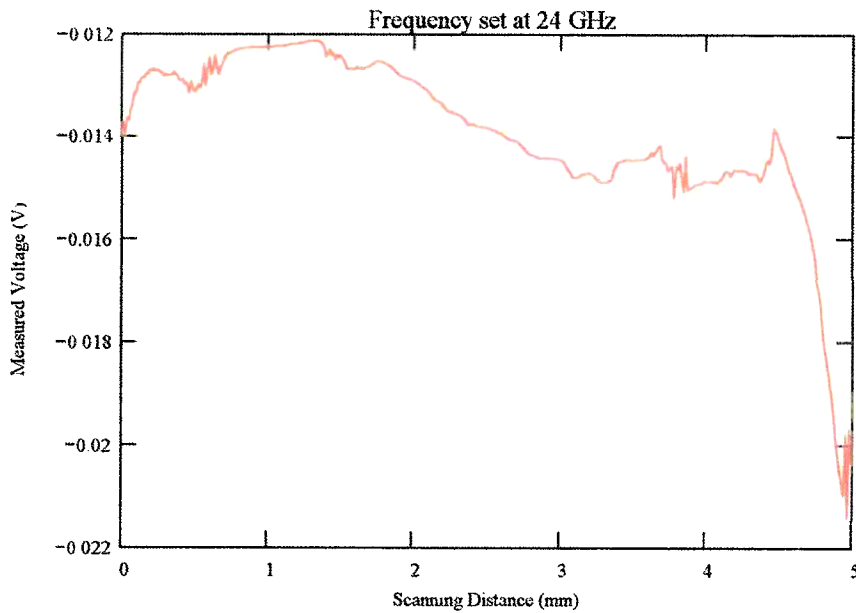
Frequency Band: Ka-band
Orientation: Scan perpendicular to crack length.
Probe: coax no. 3
Scan Resolution: 0.0127 mm
Scan length: 4 mm
Frequency: 34.5 GHz

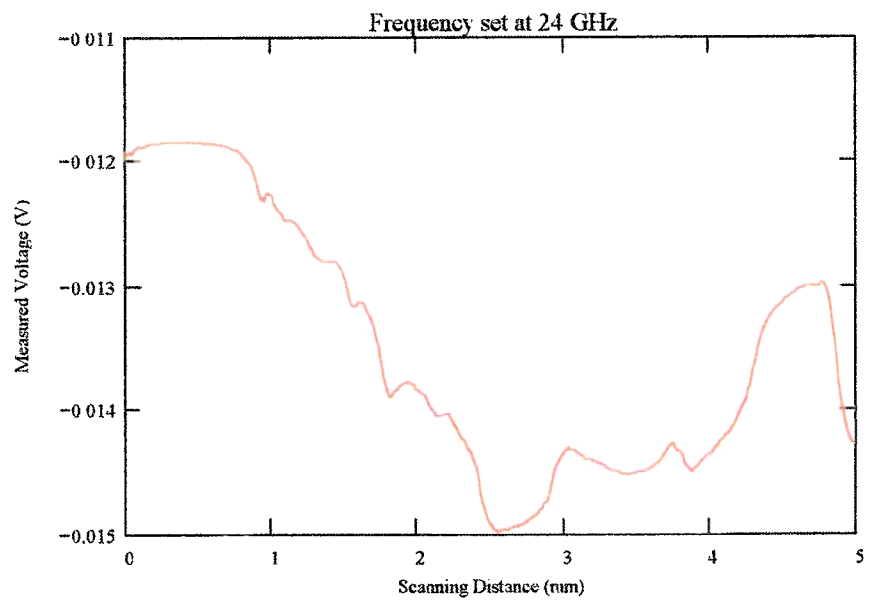
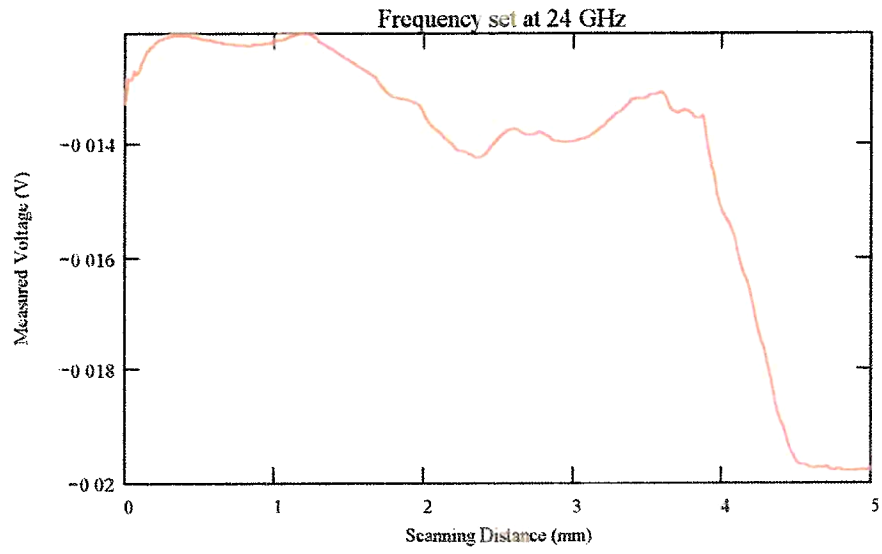


B Crack #2

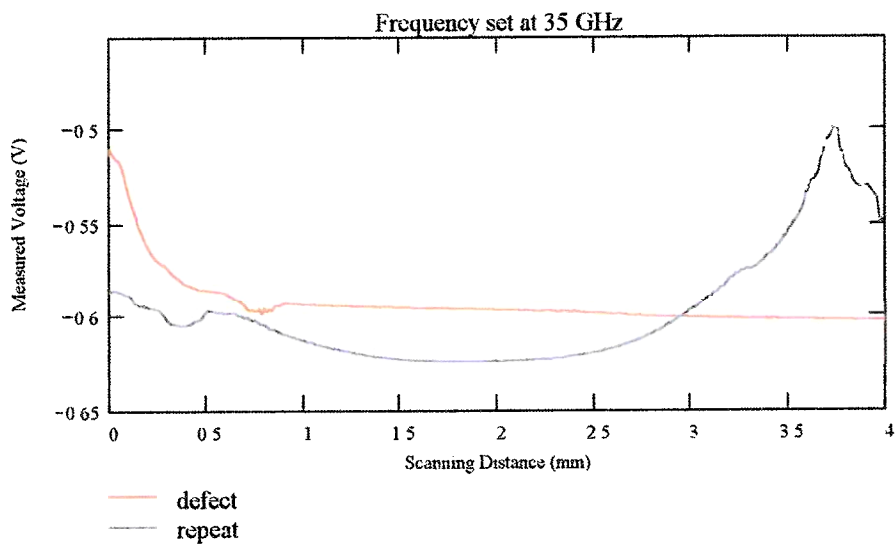
This is a Root Indication crack. The length of the crack is 0.94 in. This crack runs parallel to the welded joint.

Frequency Band: K-band
Orientation: Scan perpendicular to crack length.
Probe: coax no. 1
Scan Resolution: 0.0127 mm
Scan length: 5 mm
Frequency: 24 GHz





Frequency Band: Ka-band
Orientation: Scan perpendicular to crack length.
Probe: coax no. 3
Scan Resolution: 0.0127 mm
Scan length: 4 mm
Frequency: 35 GHz

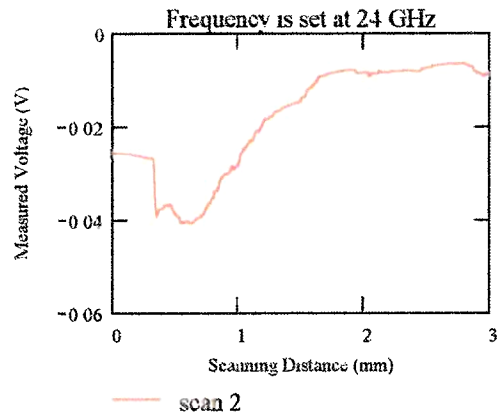
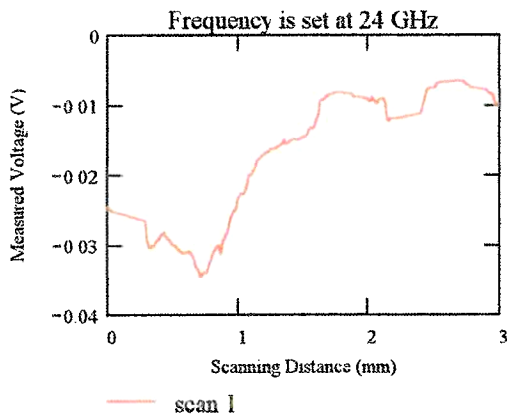


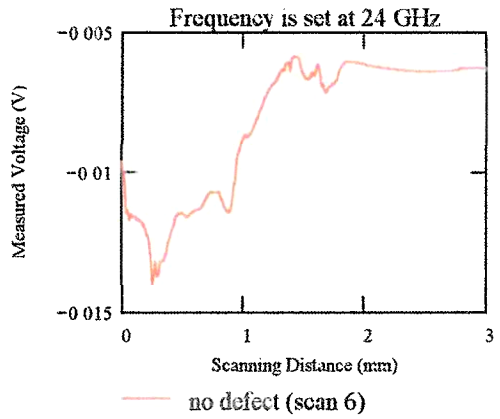
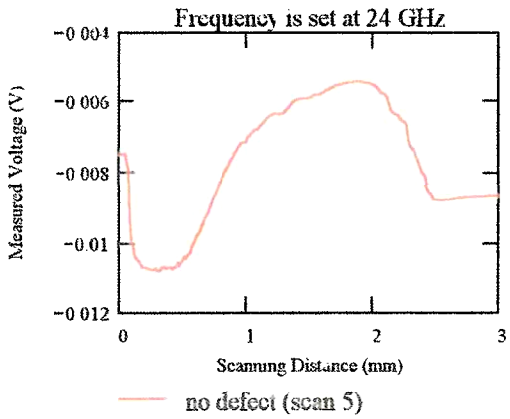
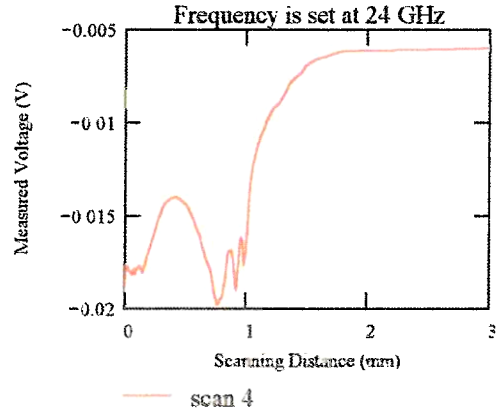
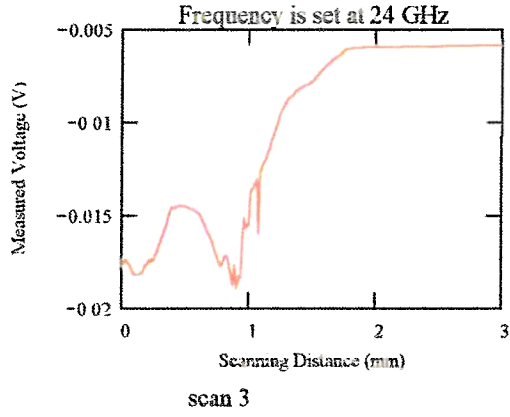
III. Sample T1495 Rusted

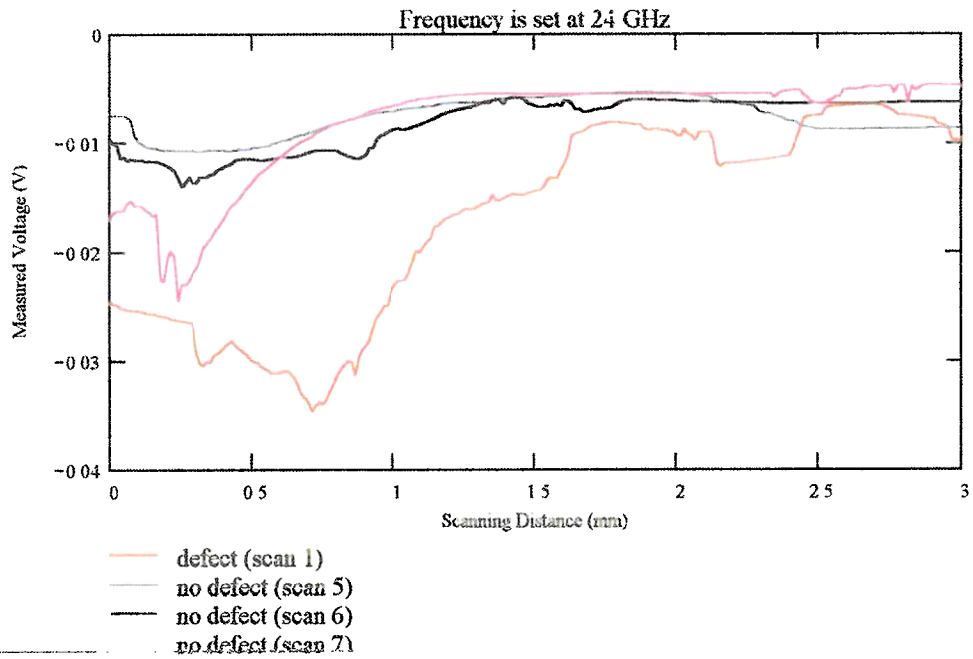
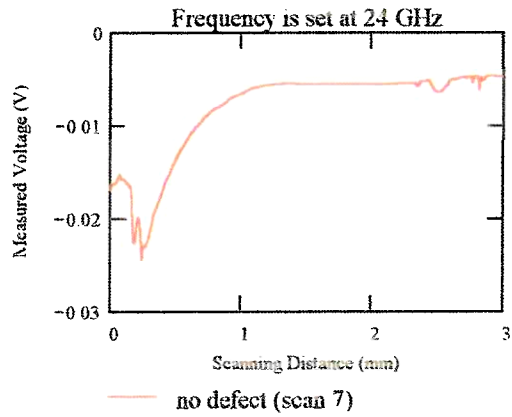
A. Crack #1

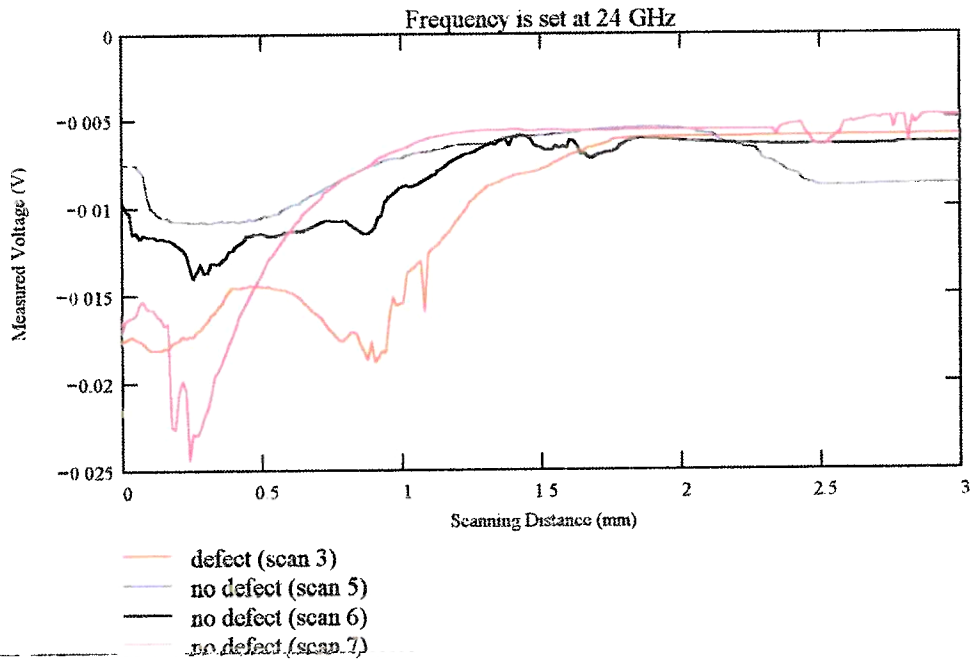
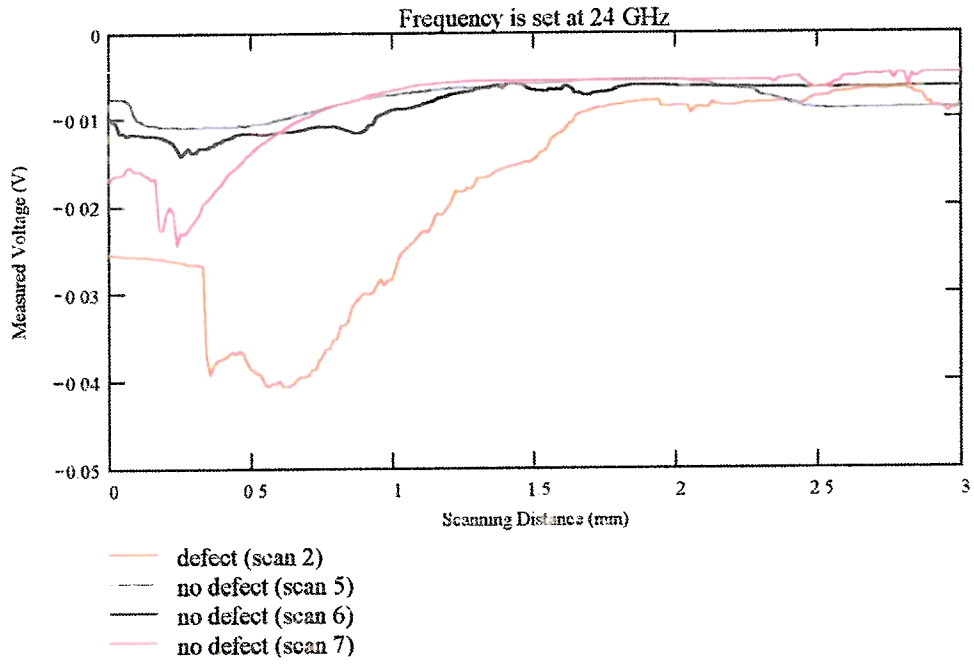
This is a Centerline Indication crack. The length of the crack is 2.51 in. This crack runs perpendicular to the welded joint.

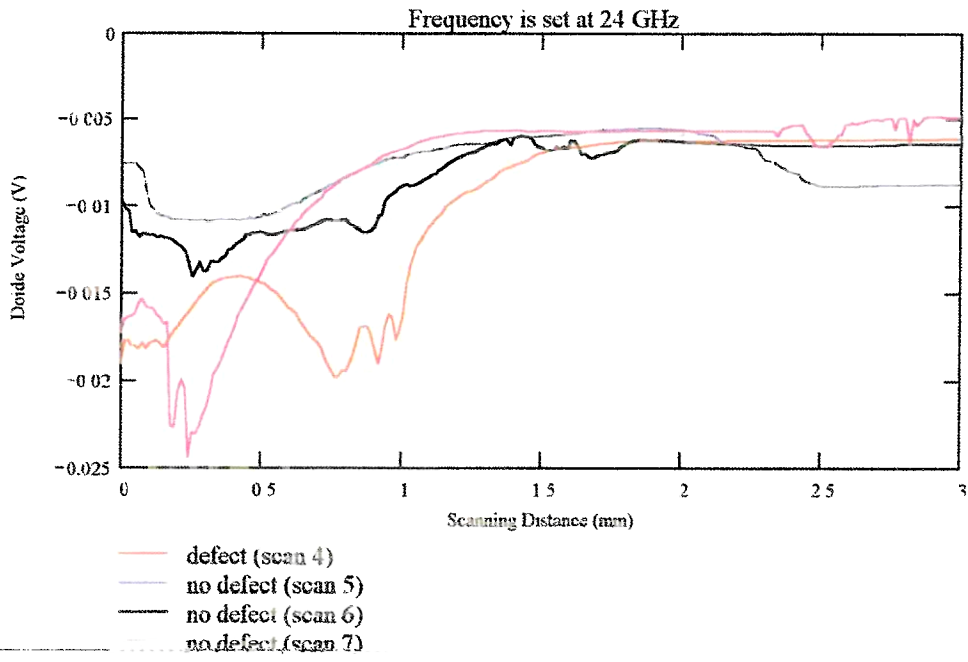
Frequency Band: K-band
Orientation: Scan perpendicular to crack length
Probe: coax no. 3
Scan Resolution: 0.0127 mm per step
Scan length: 3 mm
Frequency: 24



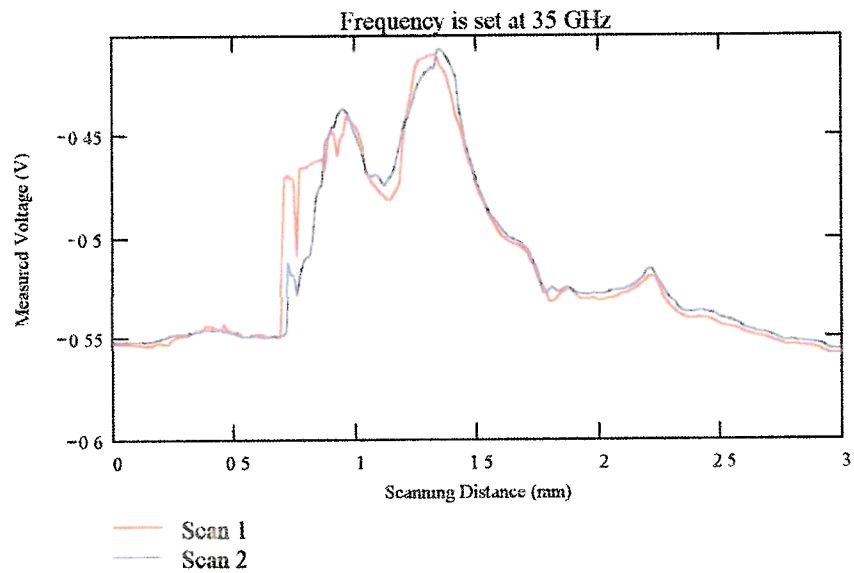








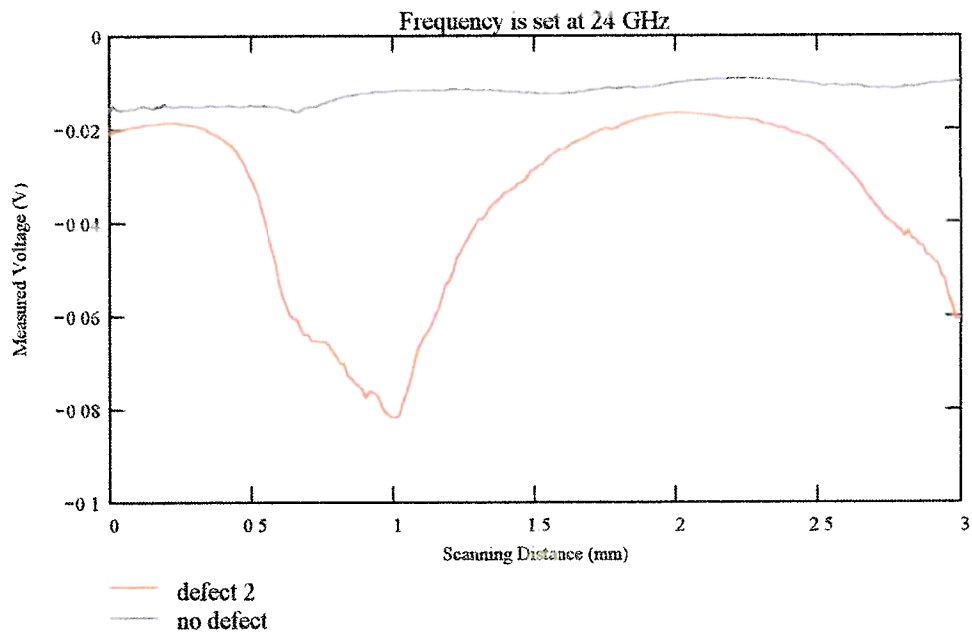
Frequency Band: Ka-band
Orientation: Scan parrallel to crack length
Probe: coax no. 3
Scan Resolution: 0.0127 mm per step
Scan length: 3 mm
Frequency: 35 GHz



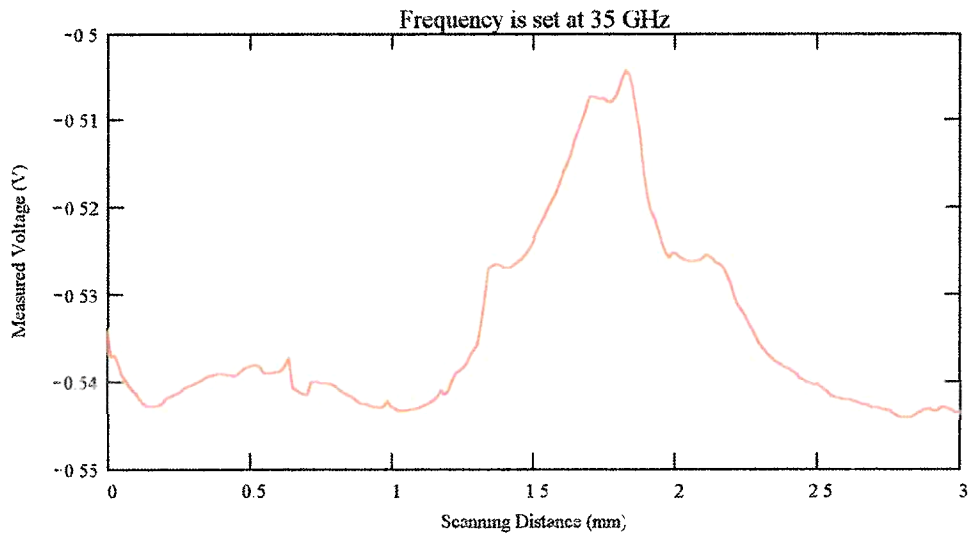
B Crack #2

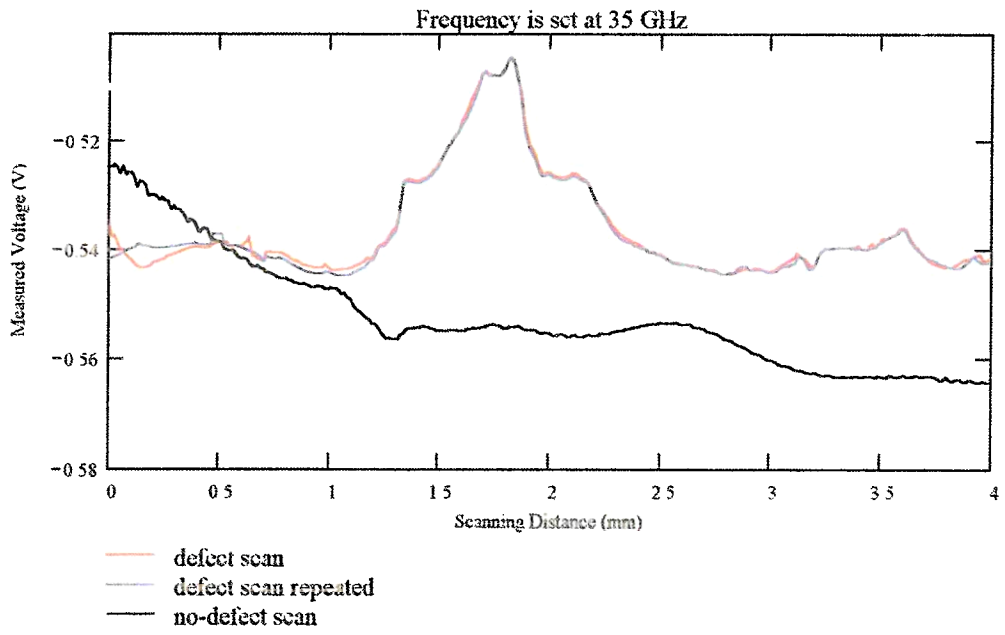
This is a Transverse Indication crack. The length of the crack is 0.23 in. This crack runs perpendicular to the welded joint

Frequency Band: K-band
Orientation: Scan perpendicular to crack length
Probe: coax no. 3
Scan Resolution: 0.0127 mm per step
Scan length: 3 mm
Frequency: 24



Frequency Band: Ka-band
Orientation: Scan perpendicular to crack length.
Probe: coax no. 3
Scan Resolution: 0.0127 mm per step
Scan length: 3-4 mm
Frequency: 35





IV. Sample T4296 Rusted

A. Crack #1

This is a Toe Indication crack. The length of the crack is 2.87 in. This crack runs parallel to the welded joint.

Frequency Band: K-band

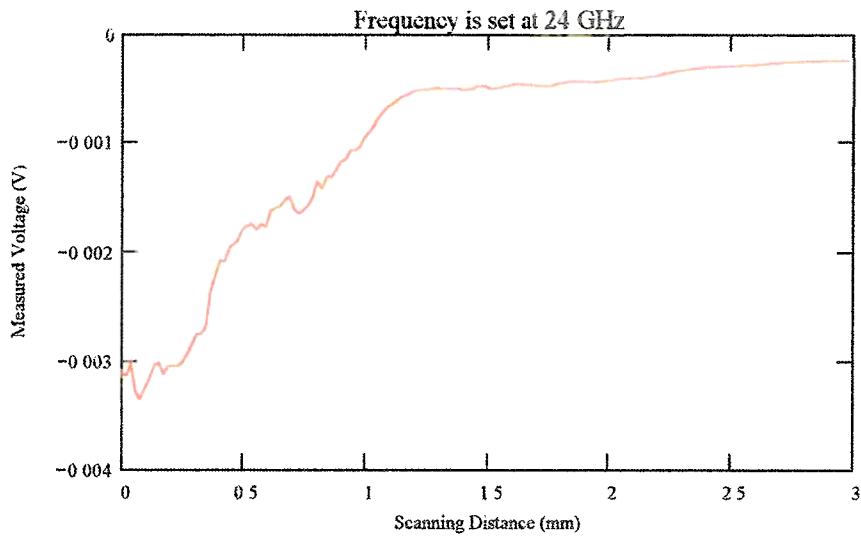
Orientation: Scan perpendicular to crack length.

Probe: coax no 3

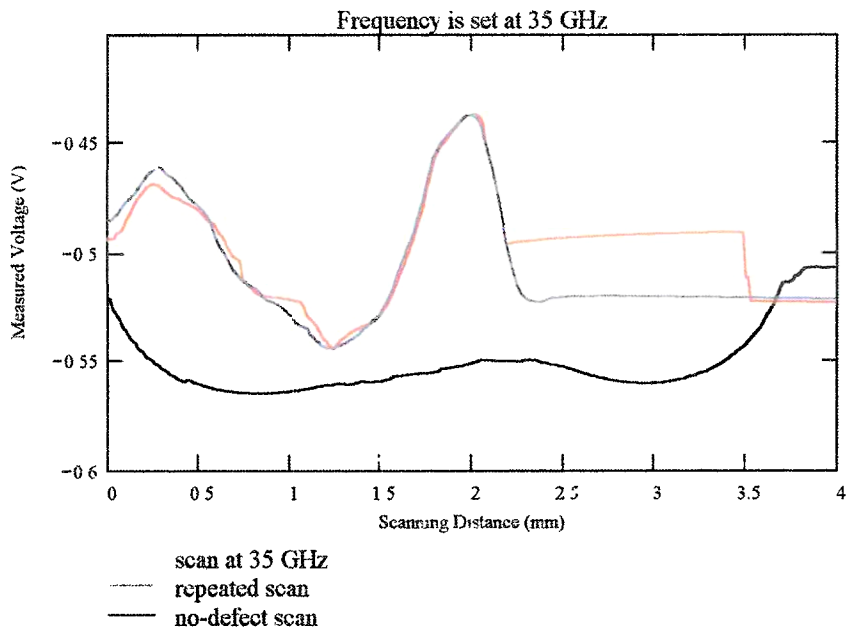
Scan Resolution: 0.0197 mm per step

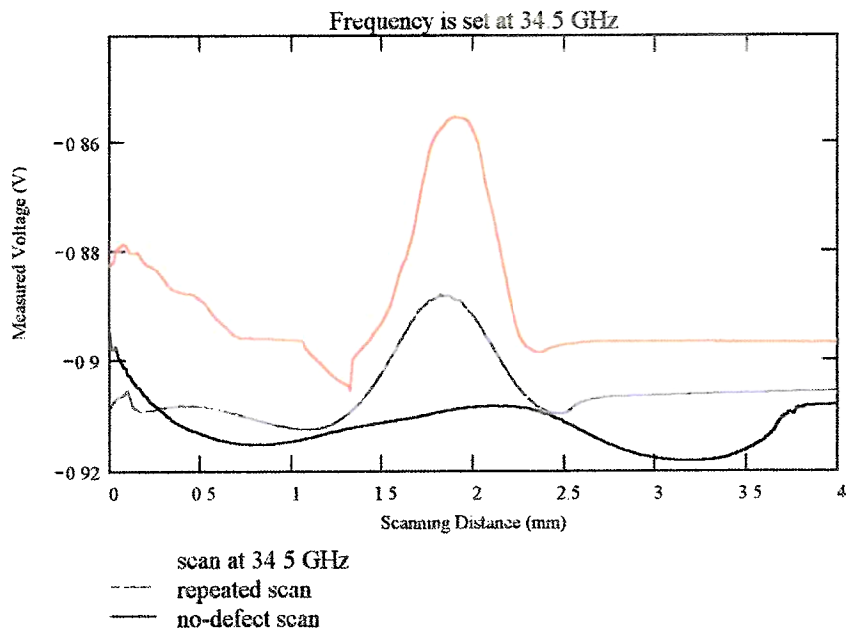
Scan length: 3 mm

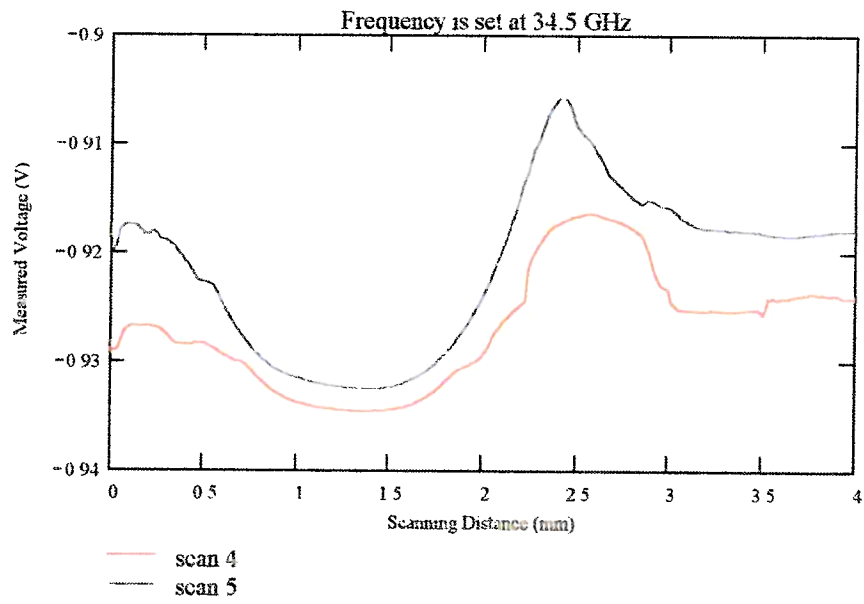
Frequency: 24



Frequency Band: Ka-band
Orientation: Scan perpendicular to crack length
Probe: coax no 3
Scan Resolution: 0.0127 mm per step
Scan length: 4 mm
Frequency: varies







These are the results of the work done on detecting cracks in the welded joints, of the VTRC samples PL4295, PL4296, T4297, and T4298. There are four different types of cracks on these samples, and they are a Toe Indication, Root Indication, Transverse Indication, and a Centerline Indication. Sample PL4295 has two defects/cracks along the edge of the weld. Defect two is on the bottom of the sample, while defect one is on the top. Defect one is a Toe Indication with a length of 12 mm, and defect two is a Root Indication with a length of 20 mm. Sample PL4296 also has two defects that are on the weld, and both are on the top of the sample. Defect one is a Transverse Indication with a length of 13 mm, and defect two is a Centreline Indication with a length of 21 mm. Sample T4298 has two defects/cracks along the edge of the weld. Defect one is a Root Indication with a length of 12 mm, and defect two is a Toe Indication with a length of 26 mm. Sample T4297 also has two defects on the weld. Defect one is a Transverse Indication with a length of 13 mm, and defect two is a Centreline Indication with a length of 8 mm.

These cracks were detected using K-band and Ka-band setups. The setups contain a mechanically tuned gun oscillator connected to an isolator, which in turn is connected to a piece of waveguide that is terminated by a waveguide to coax adapter. The coaxial lines at the end of the adapter were changed, these will be shown below. A diode detector is inserted at the middle of the waveguide (perpendicular to the a-dimension of the waveguide) to probe the standing wave pattern for variations due to the presence of a crack. The diode detector produces a dc voltage that is related to the properties of the standing waves inside the waveguide.

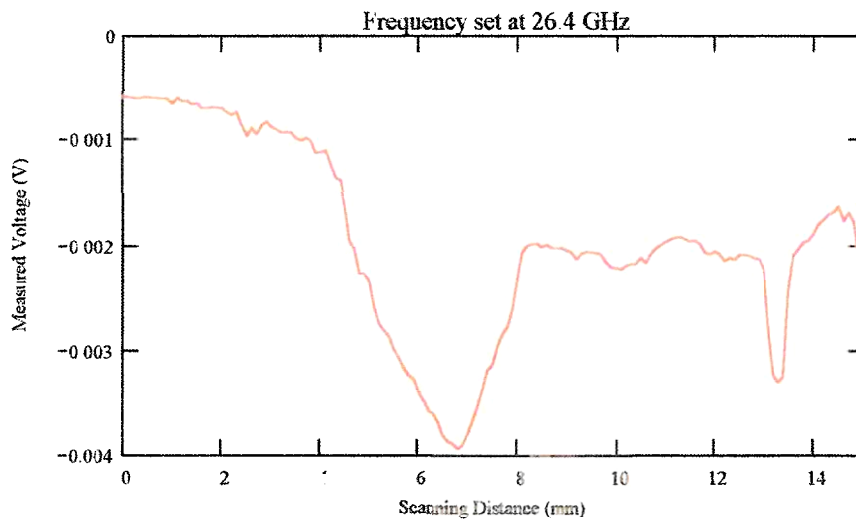
Several measurements at different frequencies were conducted to detect the presence of the cracks on this specimen. there are two different ways to scan a crack, parallel is to scan along the length of the crack and perpendicular is to scan across the length of the crack.

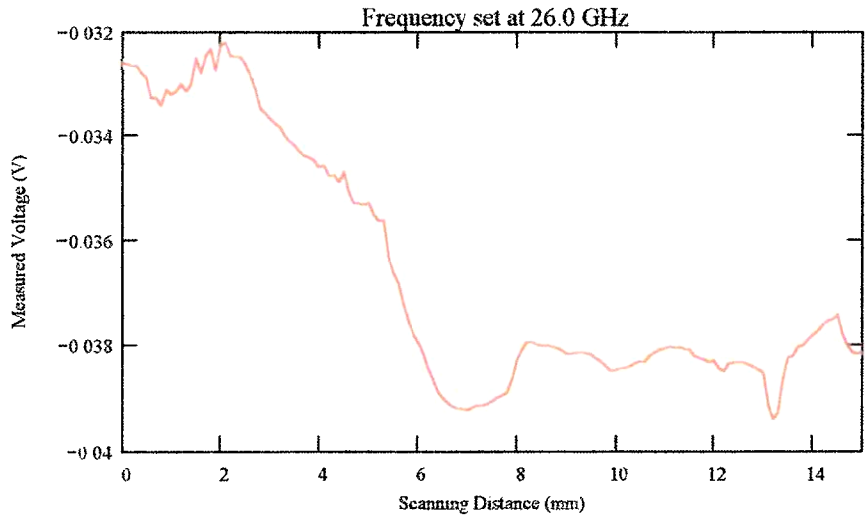
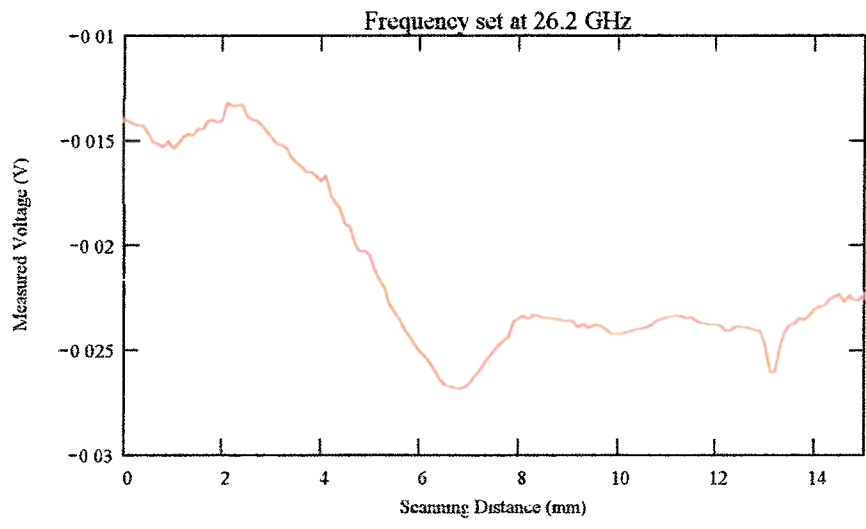
I Sample PL4295

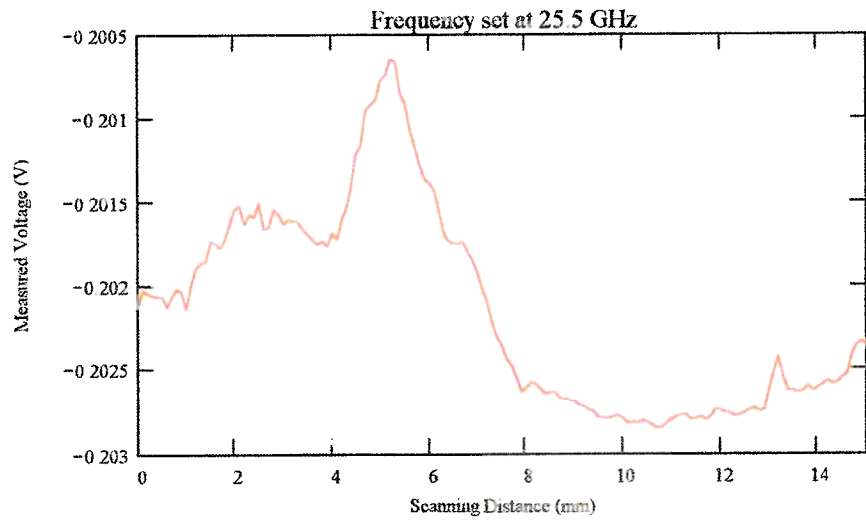
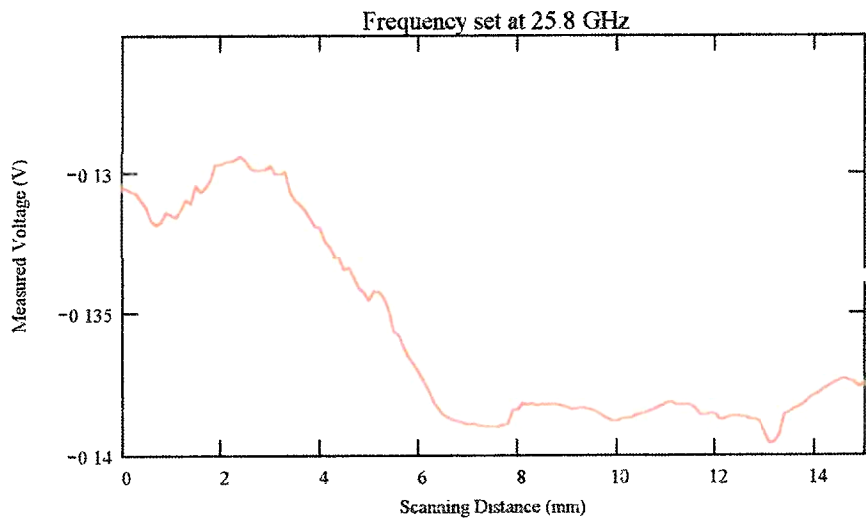
A. Crack #1

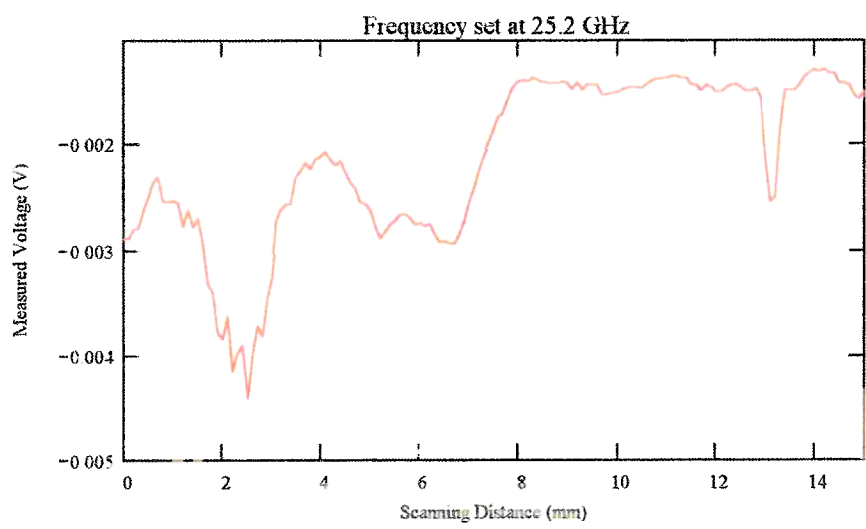
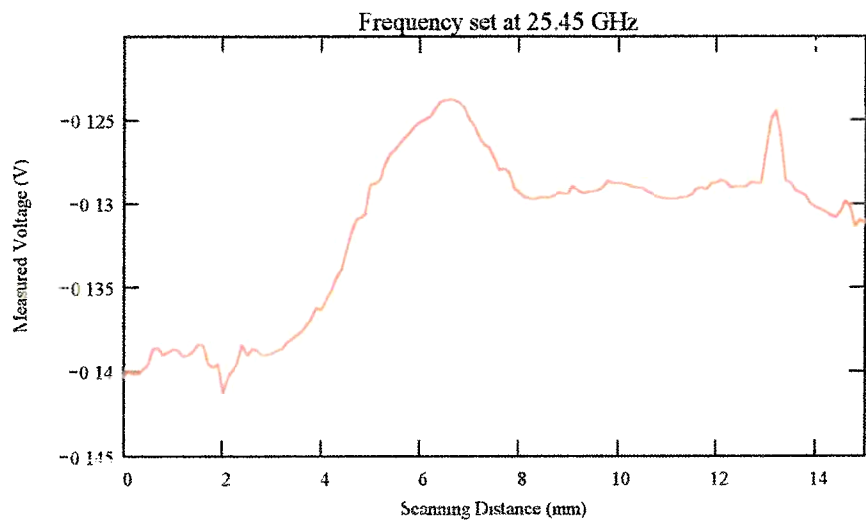
This is a Toe Indication crack. The length of the crack is 12 mm. This crack runs parallel to the welded joint.

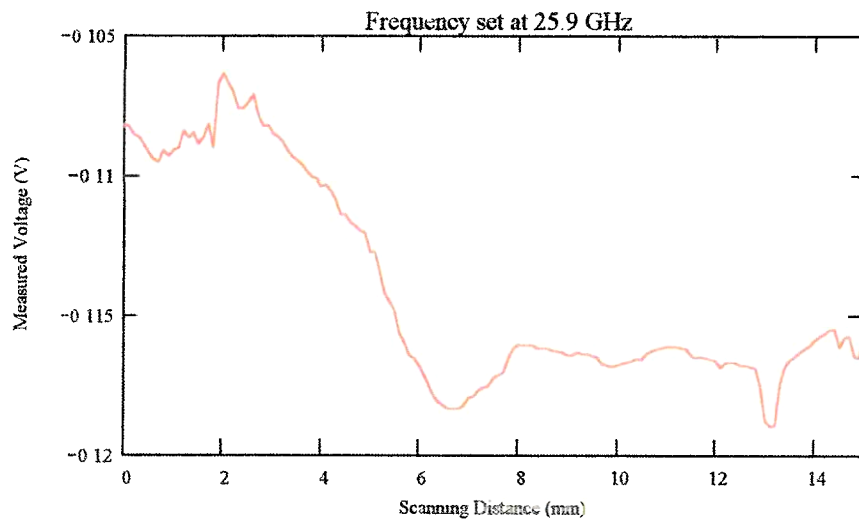
Frequency Band: K-band
Orientation: Scan parallel to crack length.
Probe: Coax no. 3
Scan Resolution: 0.064 mm per step
Scan length: 20 mm
Frequency: Varies



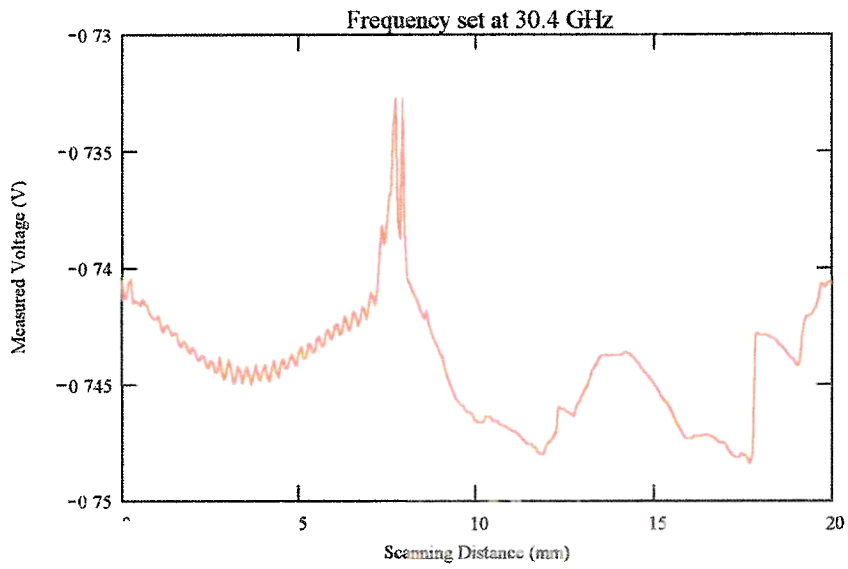


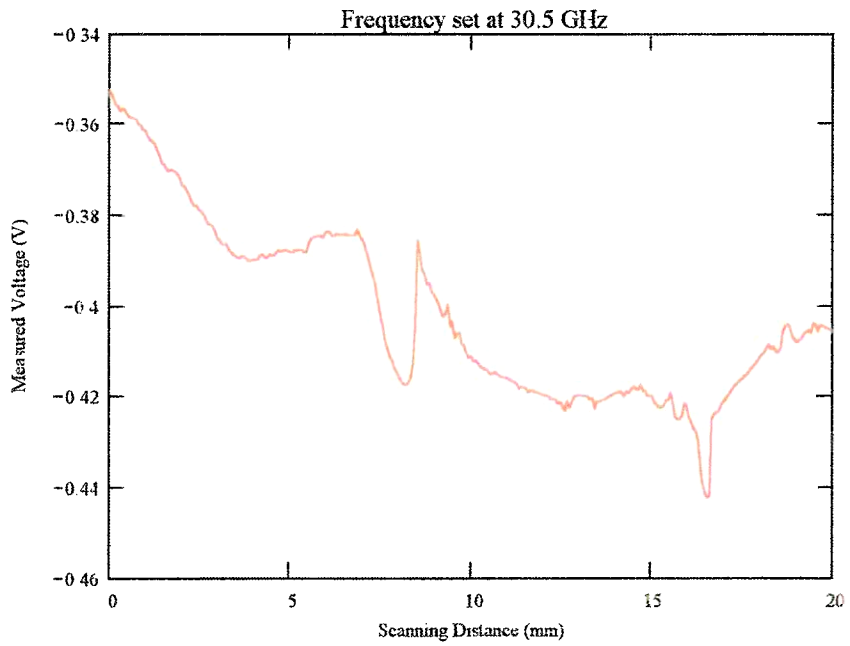
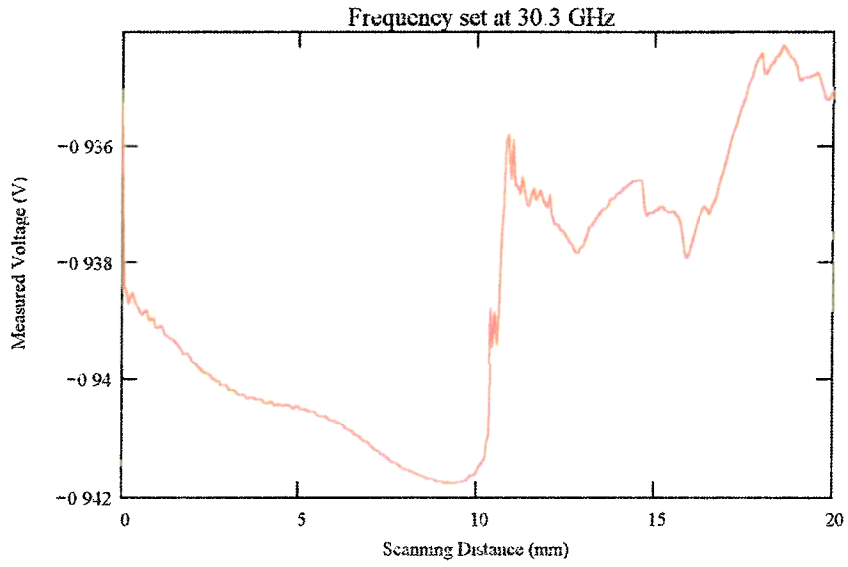


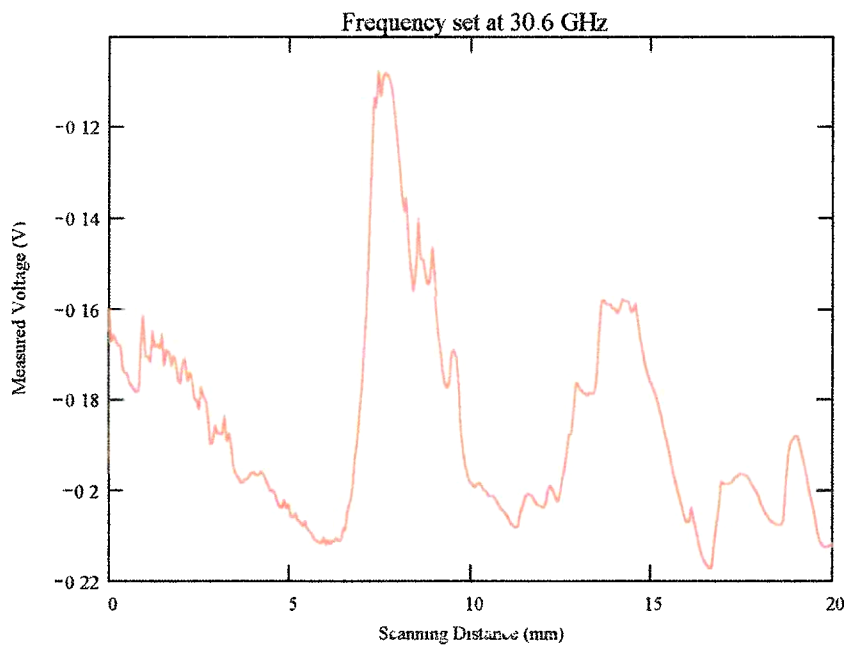
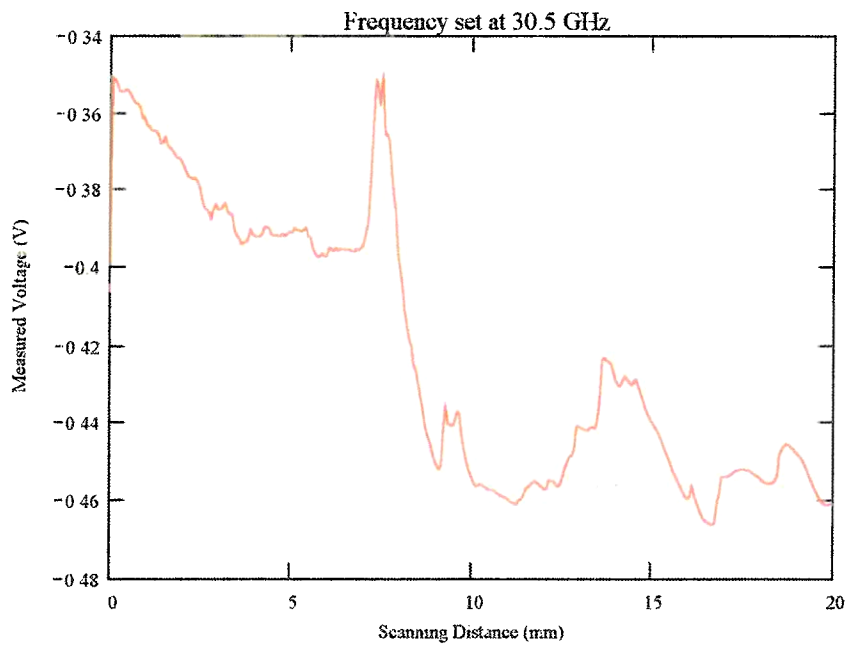


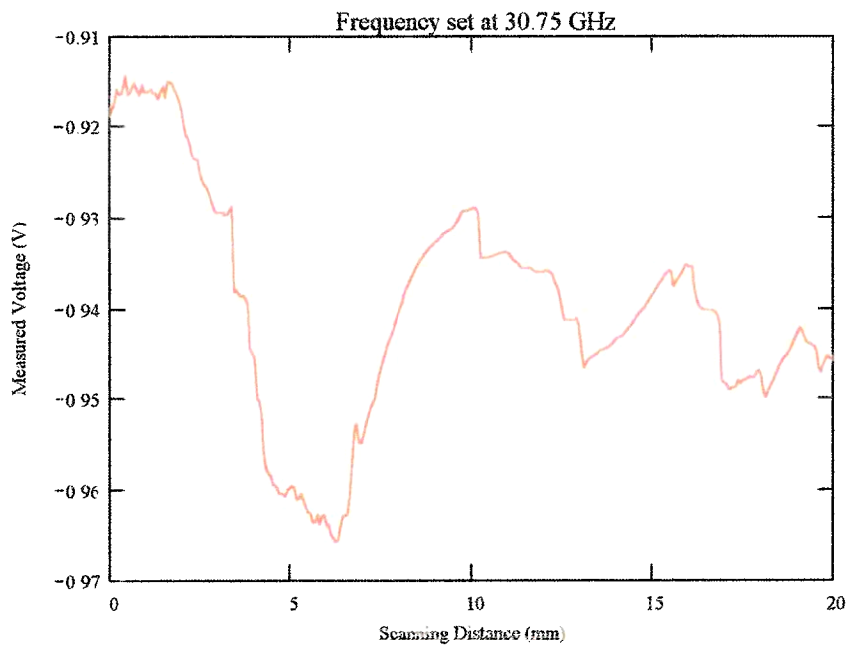
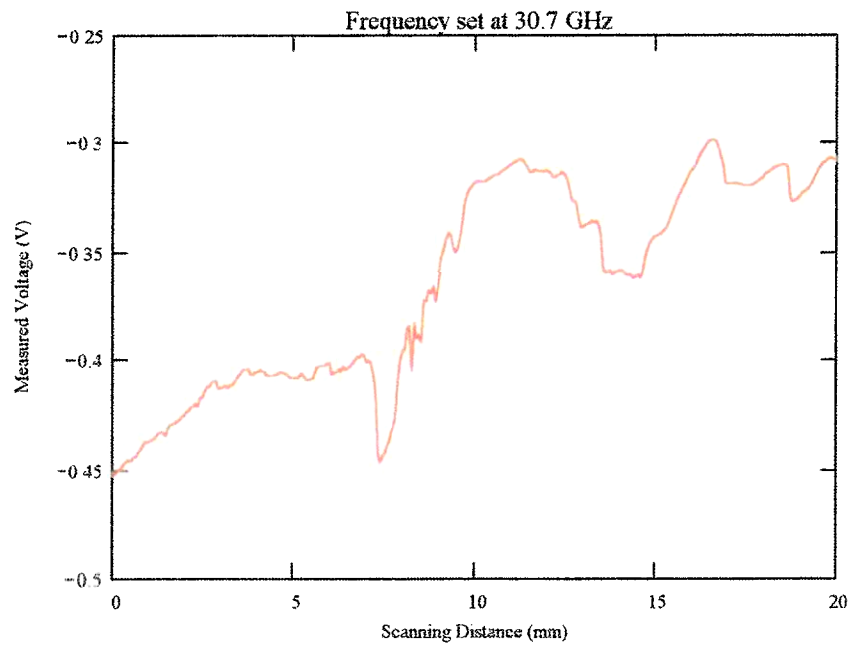


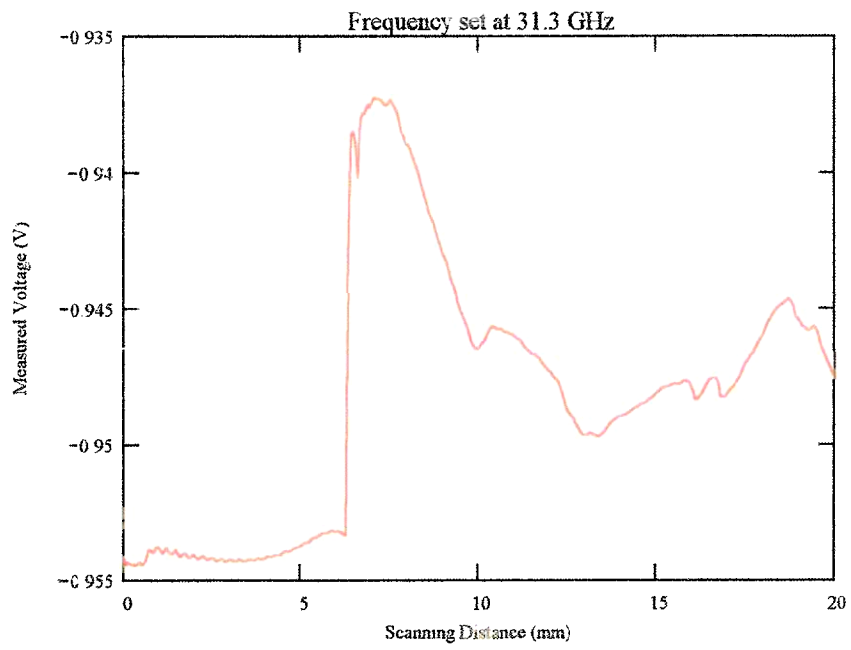
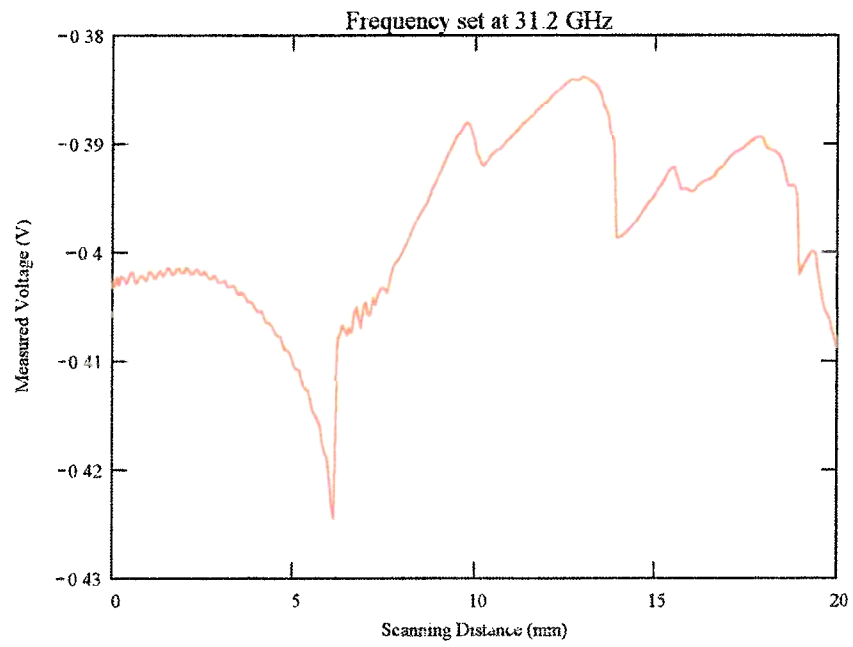
Frequency Band: Ka-band
Orientation: Scan parrallel to crack length.
Probe: Coax no 3
Scan Resolution: 0.064 mm per step
Scan length: 20 mm
Frequency: Varies

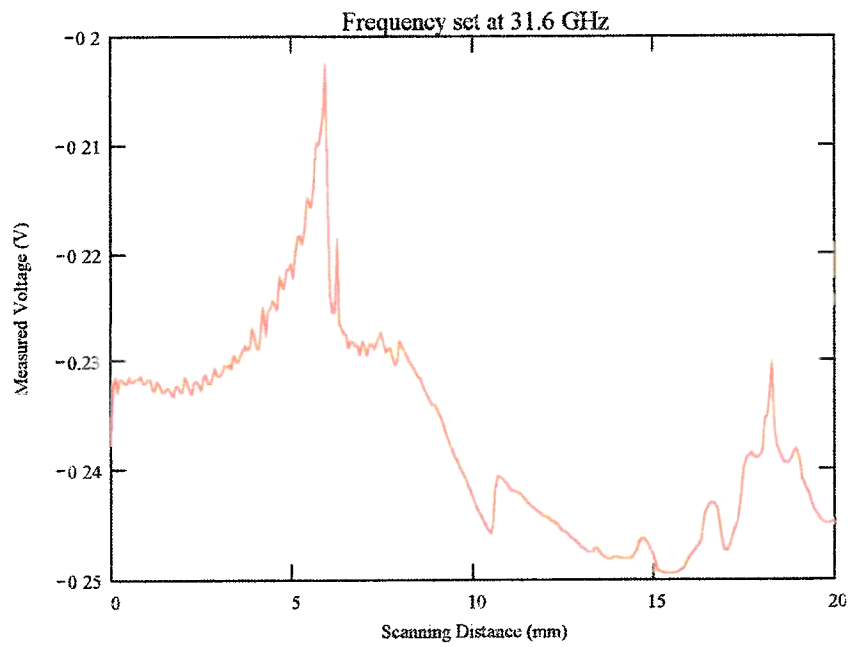
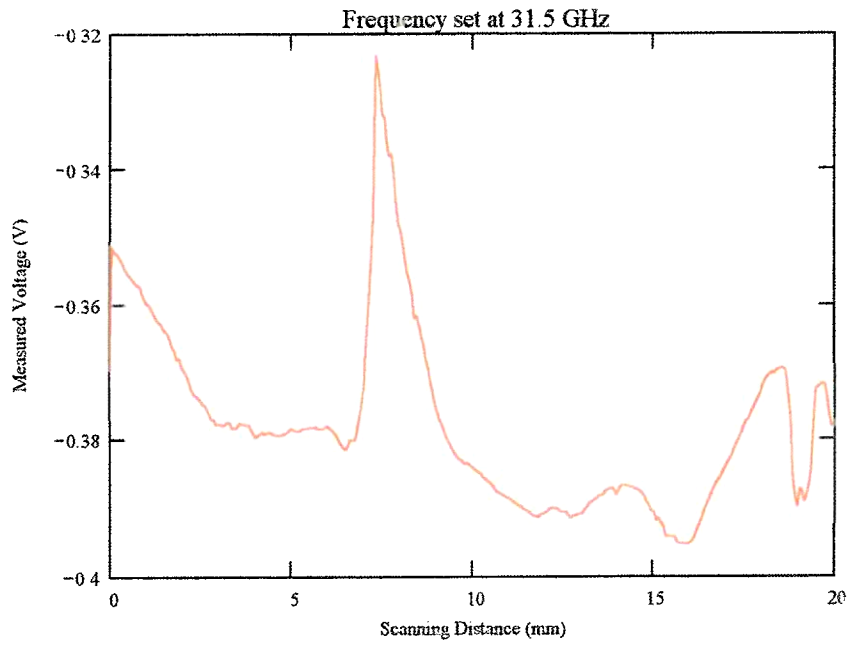


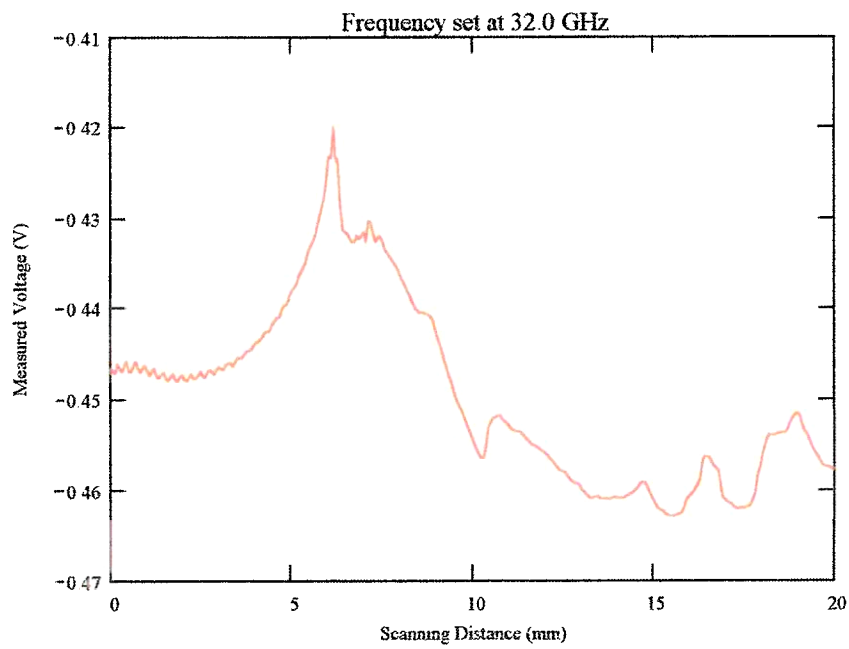
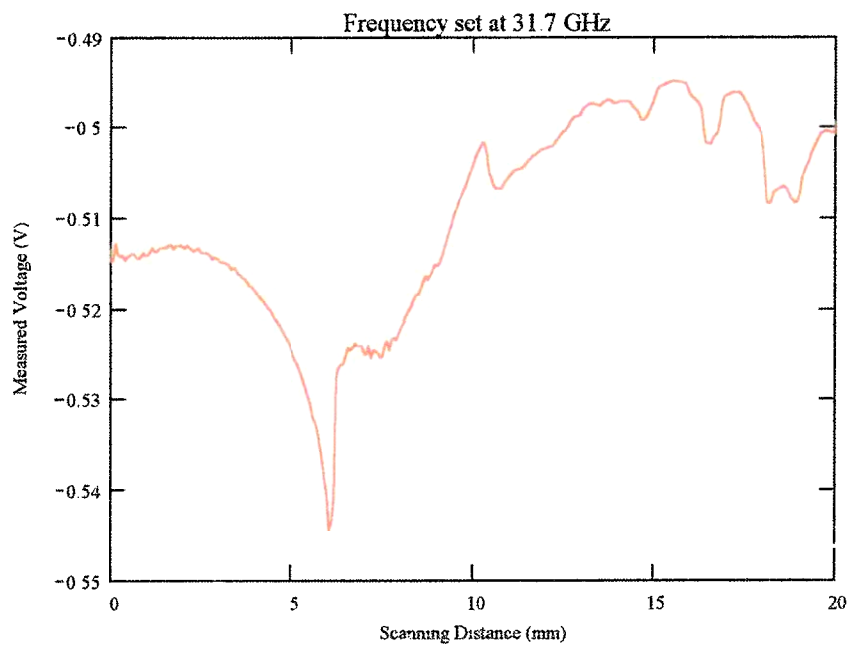


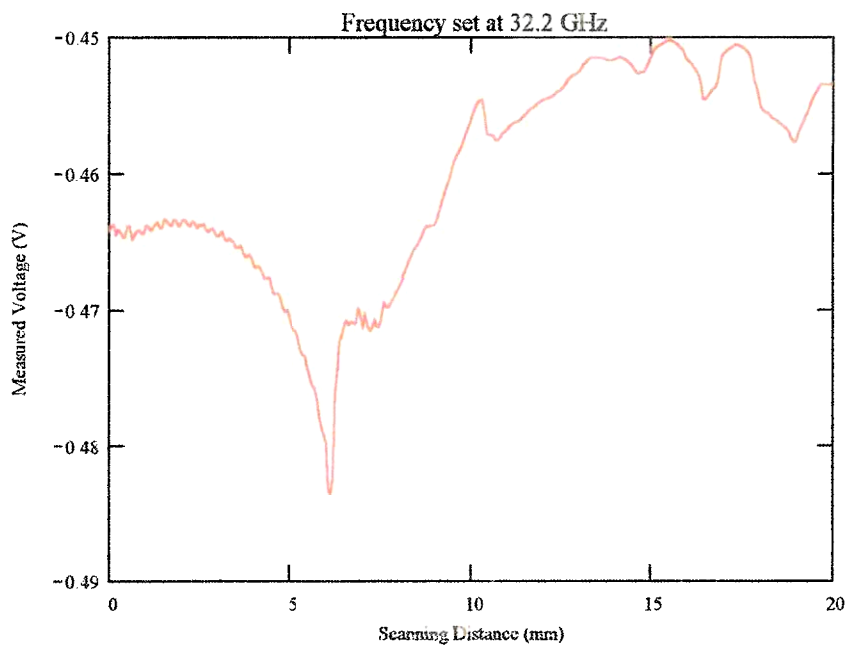
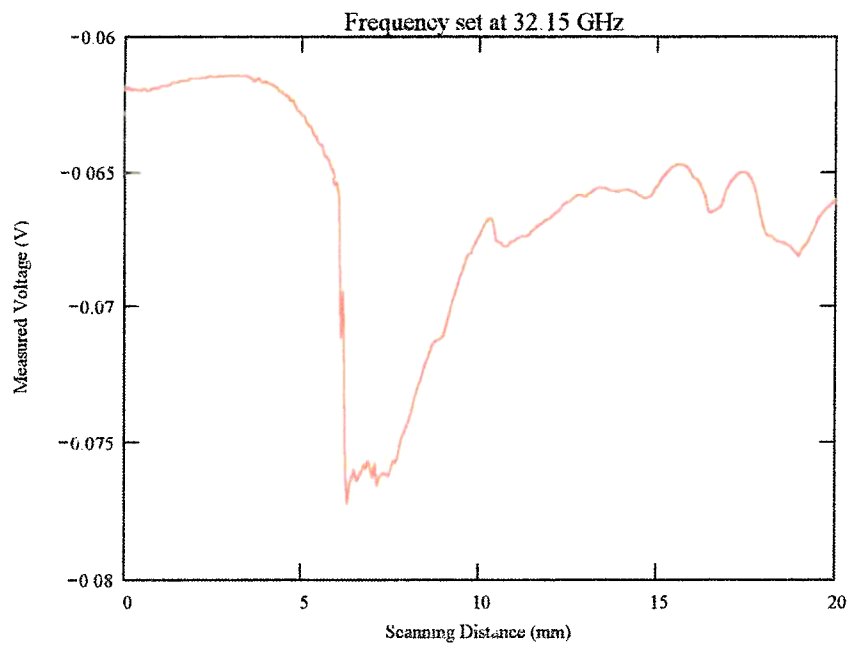








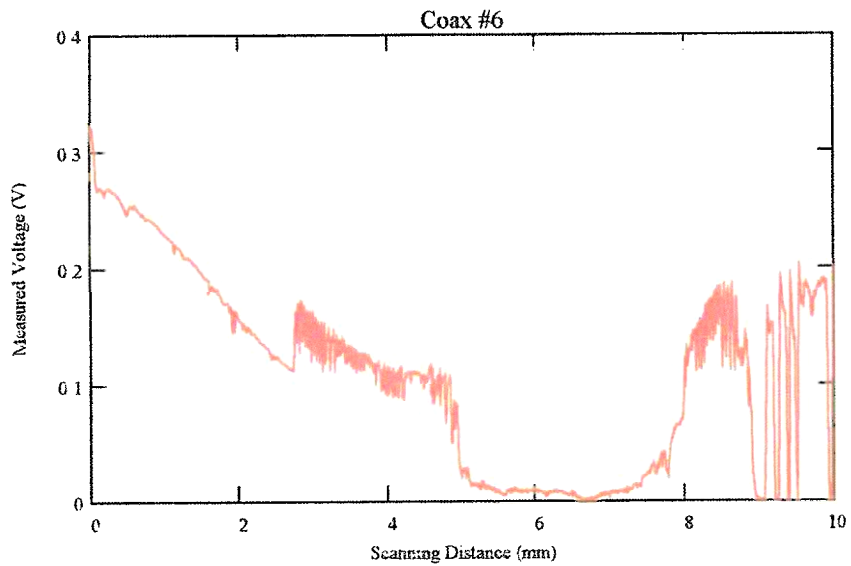


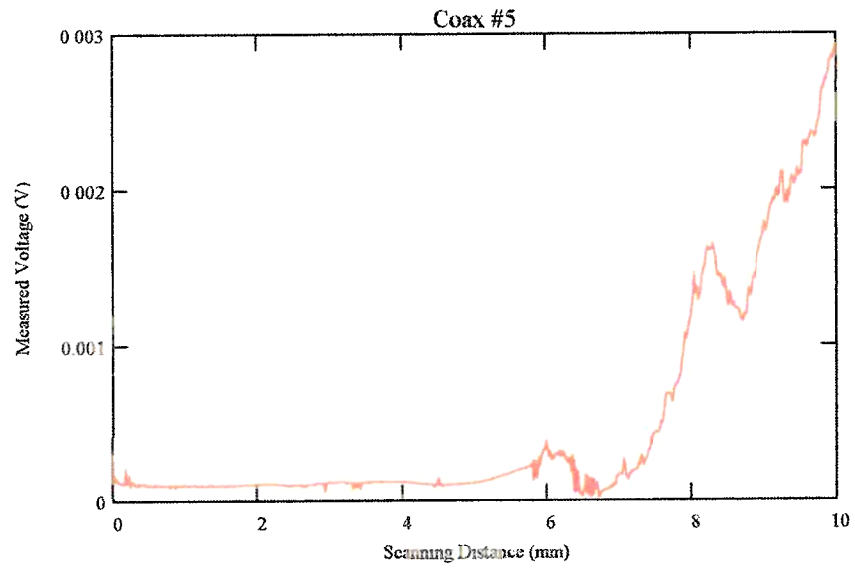
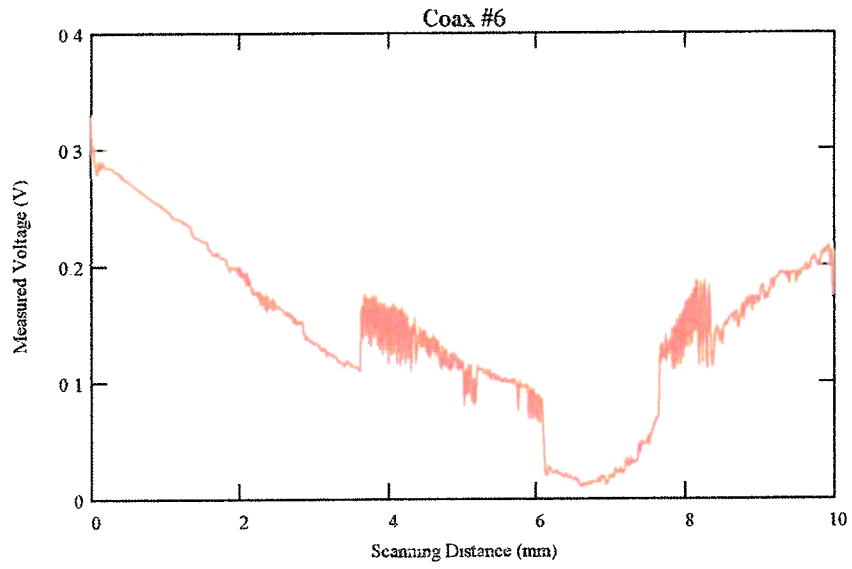


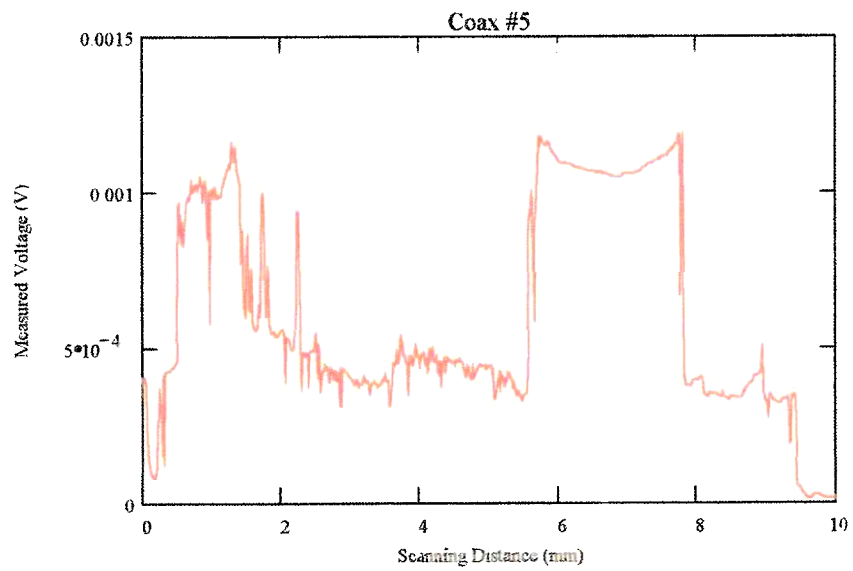
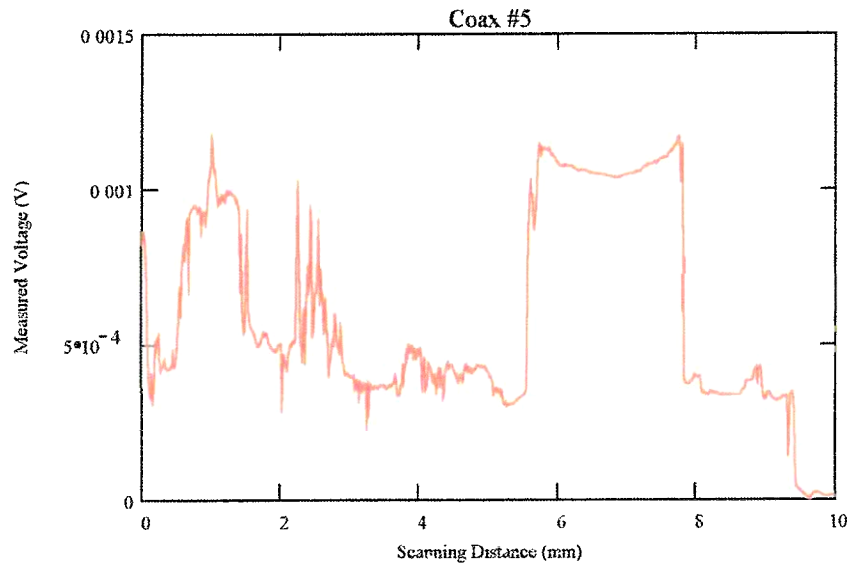
B Crack #2

This is a Root Indication crack. The length of the crack is 24 mm. This crack runs parallel to the welded joint.

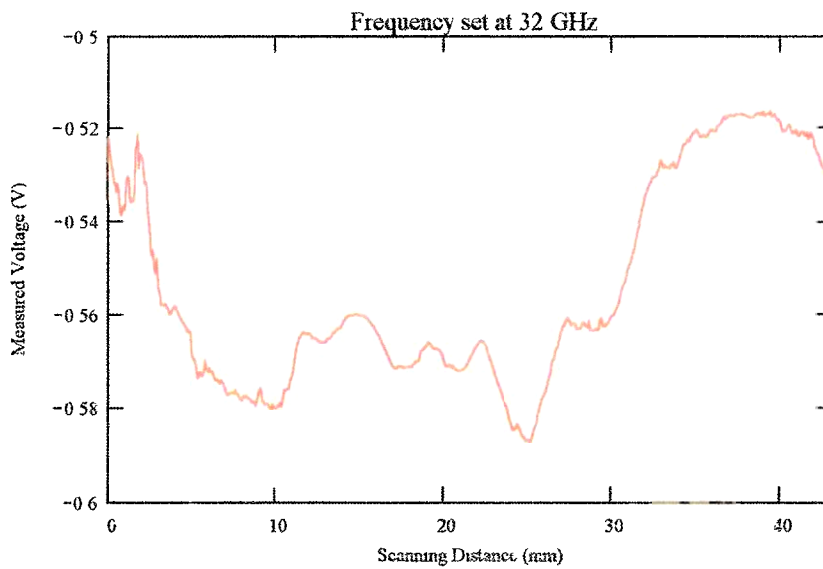
Frequency Band: K-band
Orientation: Scan parallel to crack length
Probe: Coax no. 6, Coax no. 5
Scan Resolution: 0.127 mm per step
Scan length: 10 mm
Frequency: 24 GHz

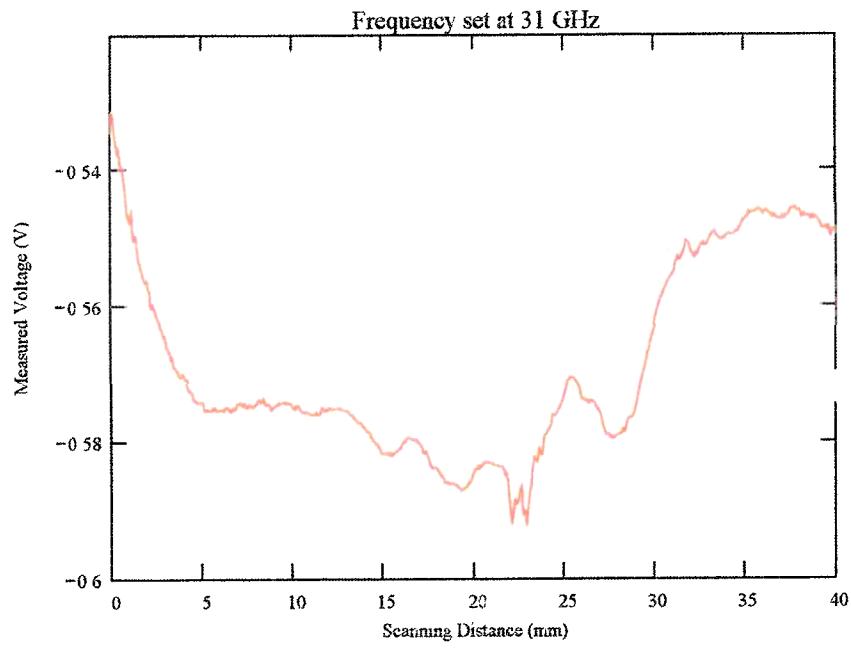
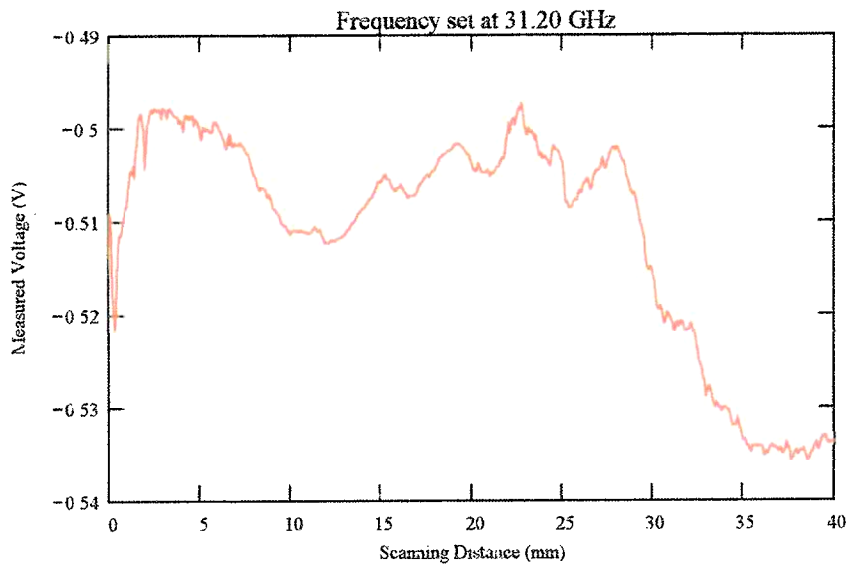


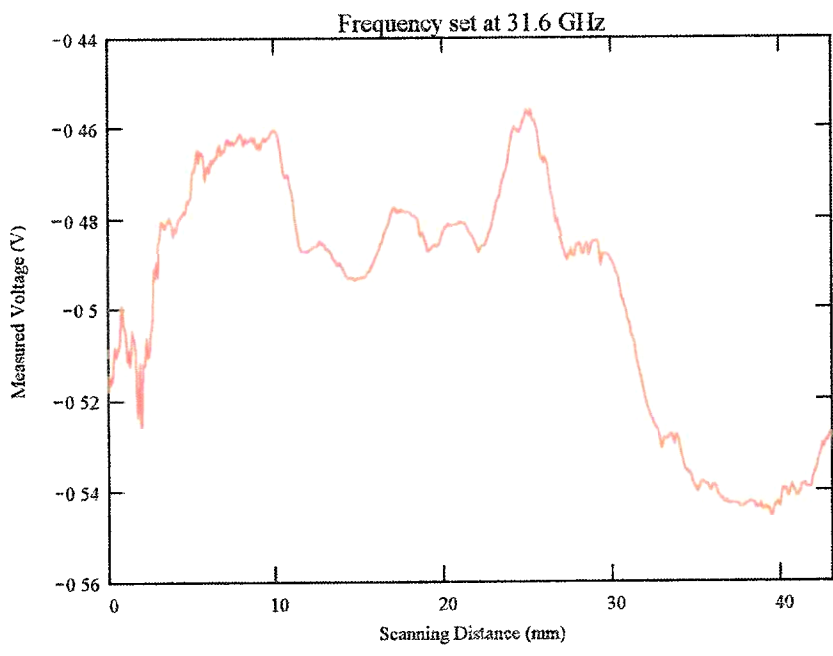
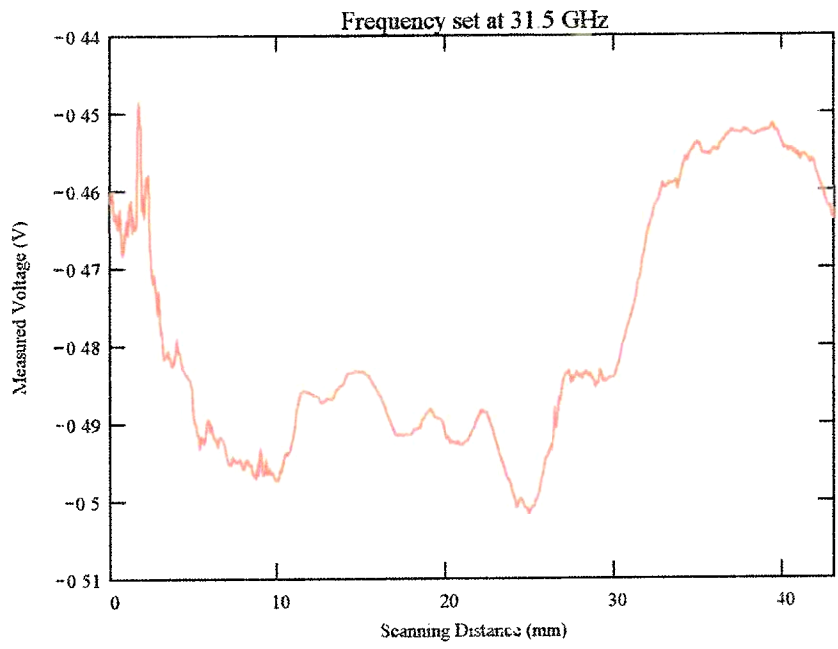


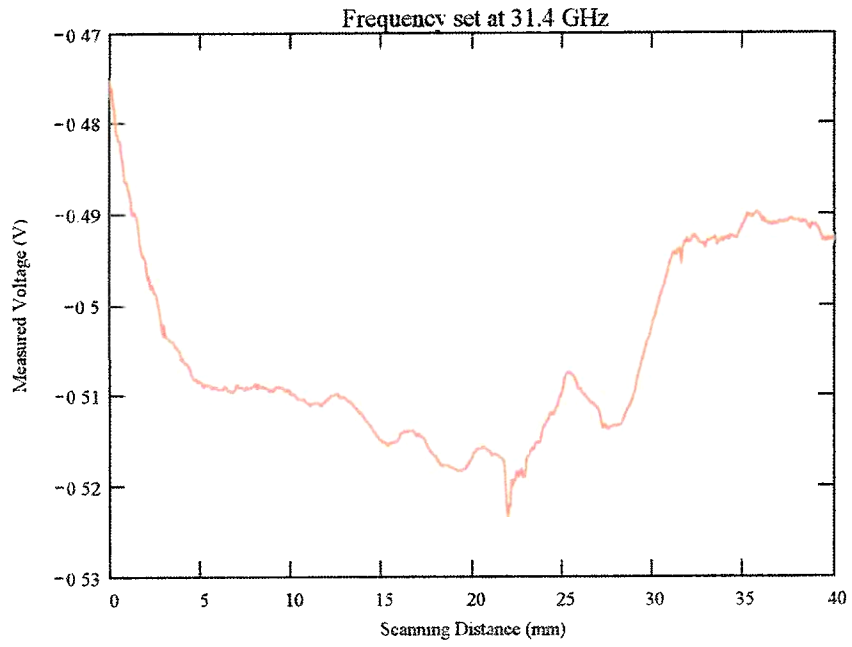


Frequency Band: Ka-band
Orientation: Scan parallel to crack length.
Probe: Coax no. 3
Scan Resolution: 0.064 mm per step
Scan length: 40 mm and 43 mm
Frequency: Varies







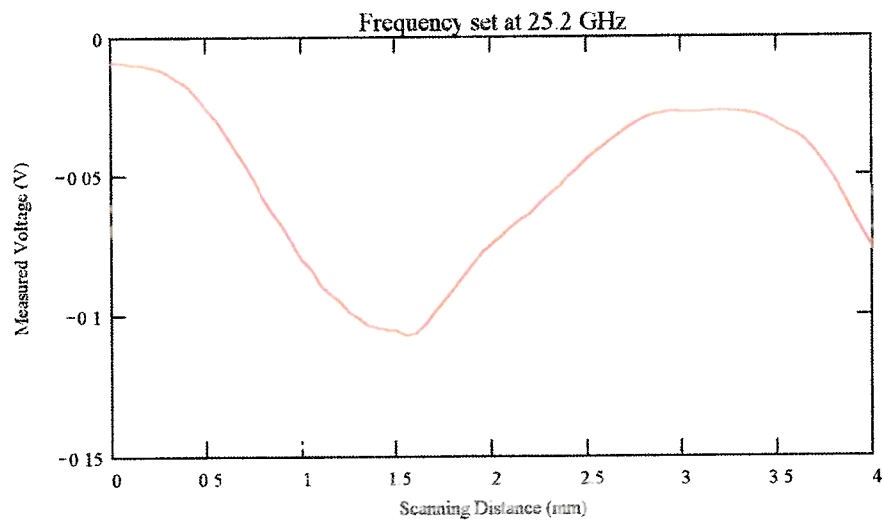


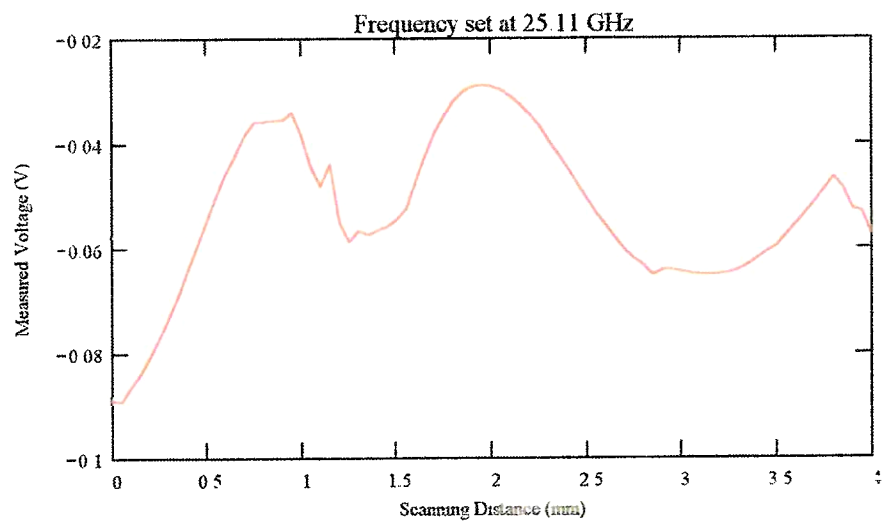
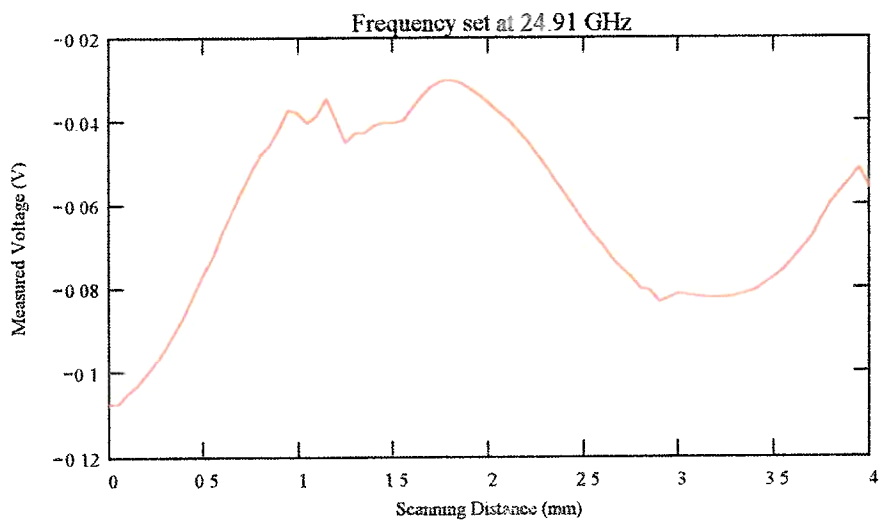
II Sample PL4296

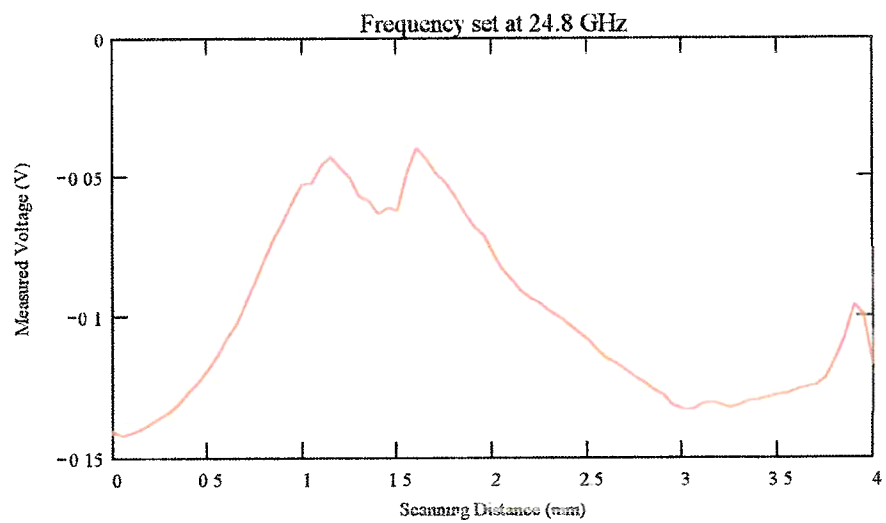
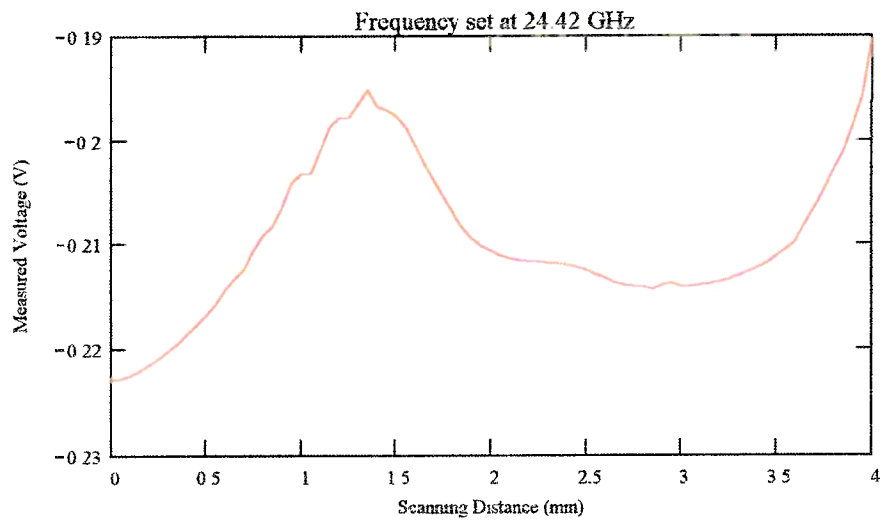
A. Crack #1

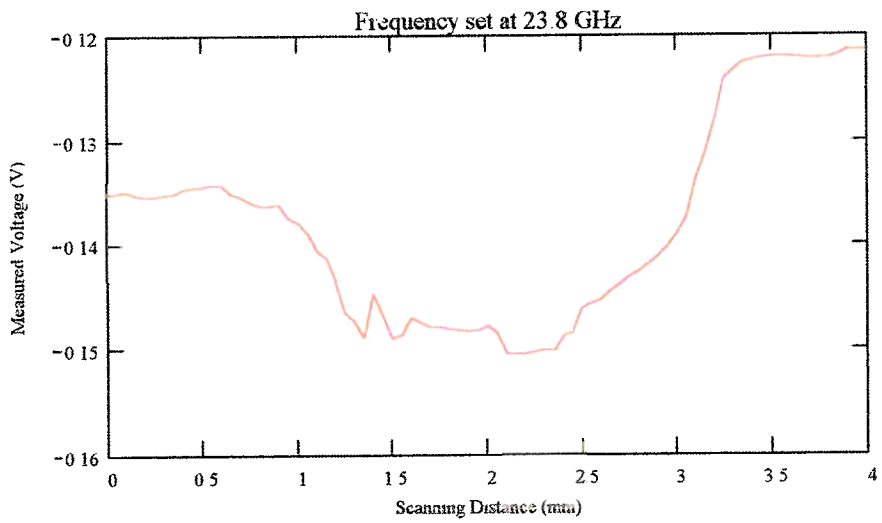
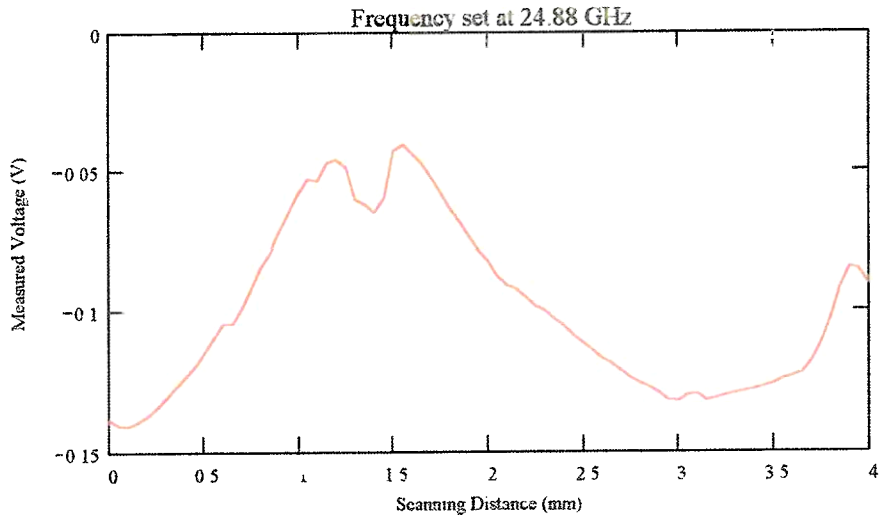
This is a Transverse Indication crack. The length of the crack is 13 mm. This crack runs perpendicular to the welded joint.

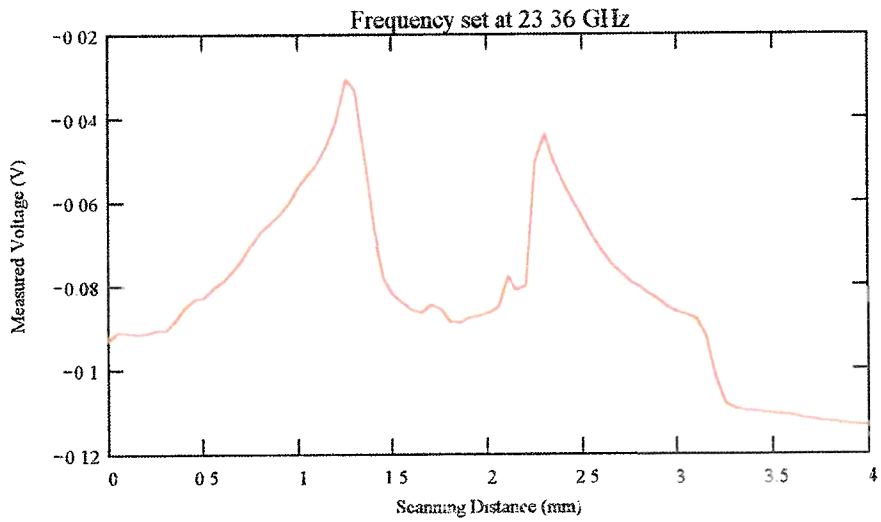
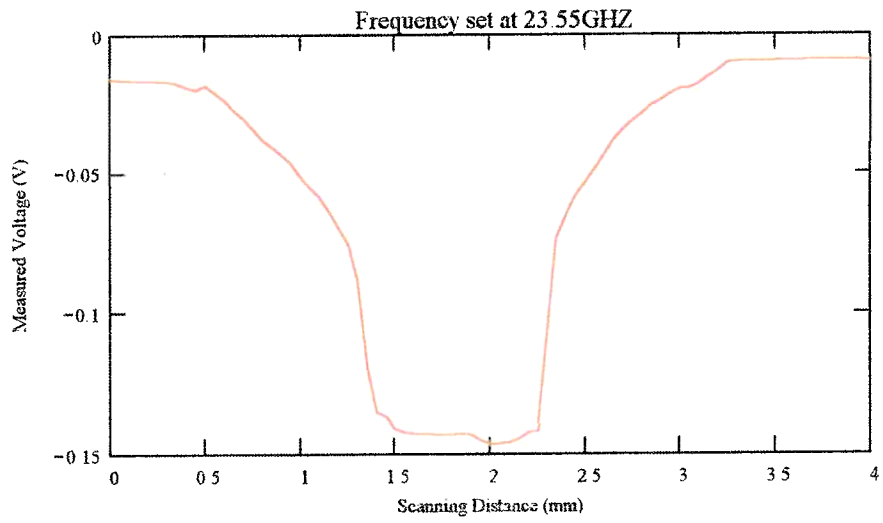
Frequency Band: K-band
Orientation: Scan perpendicular to crack length
Probe: coax no 2
Scan Resolution: .05 mm per step
Scan length: 4 mm
Frequency: Varies

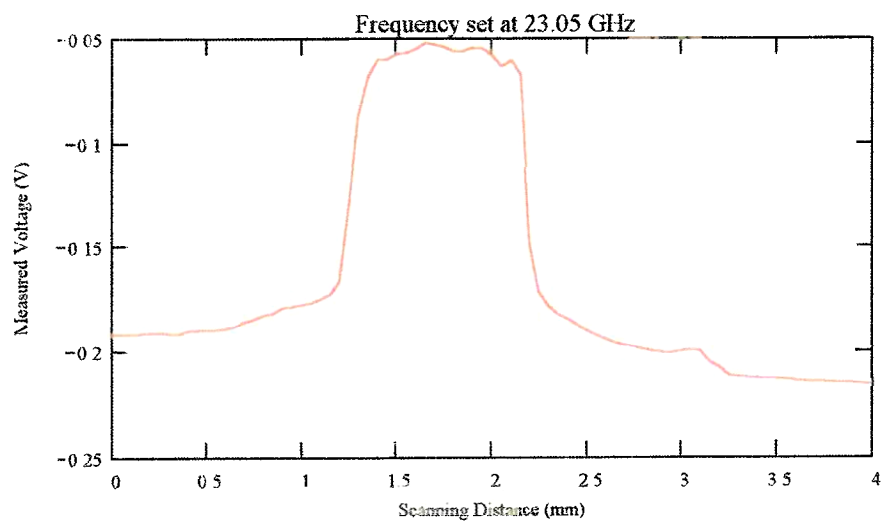




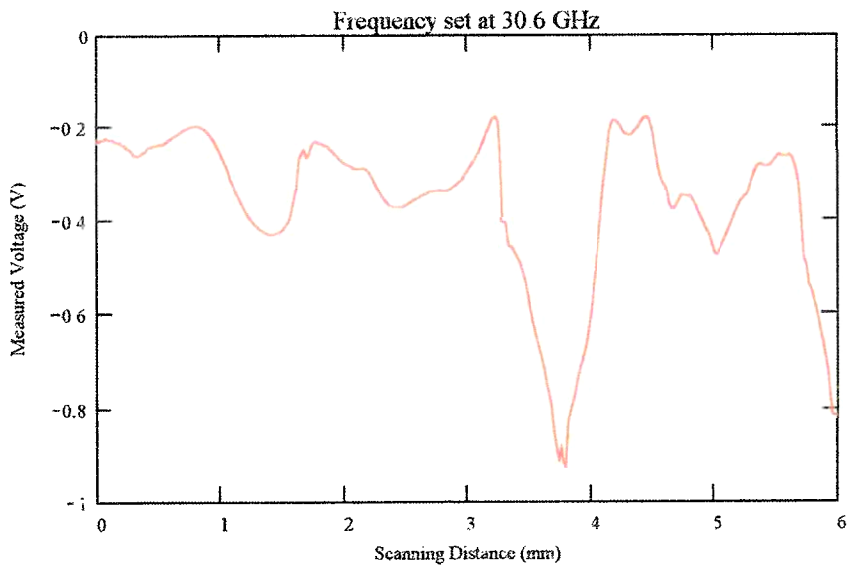


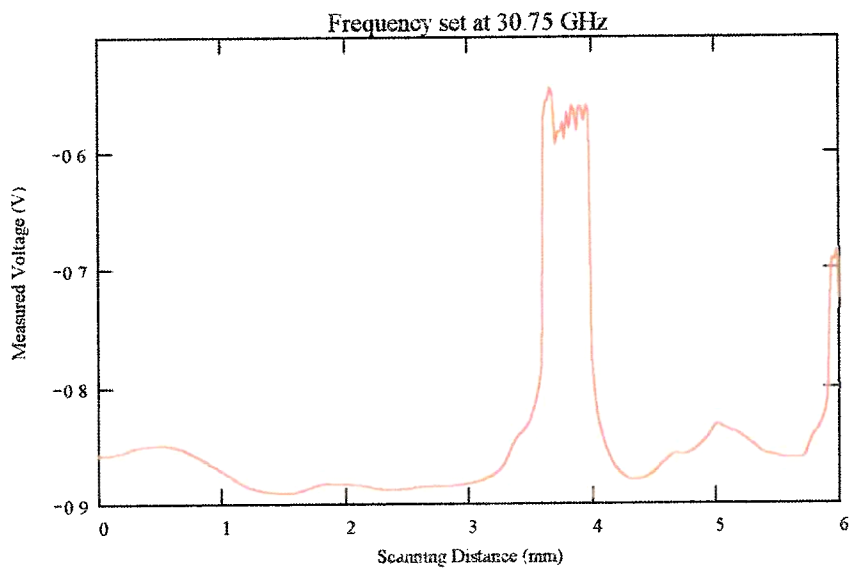
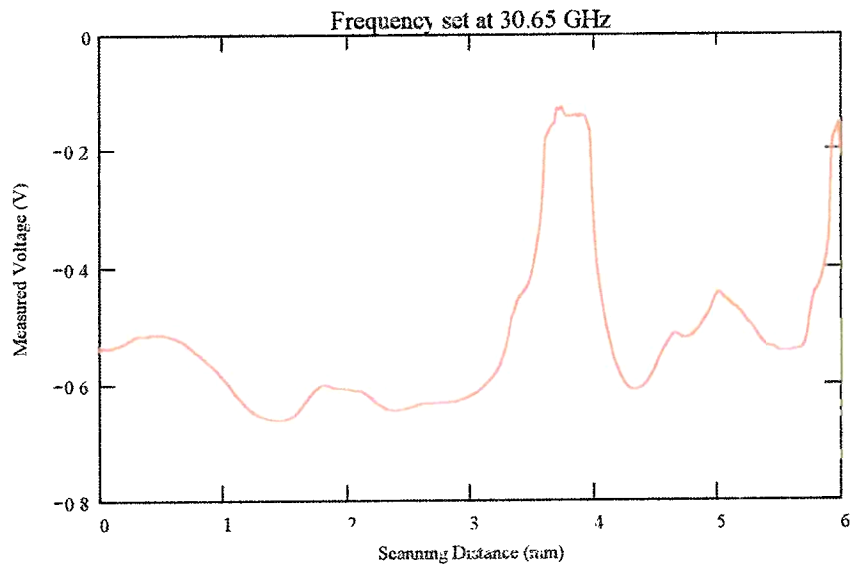


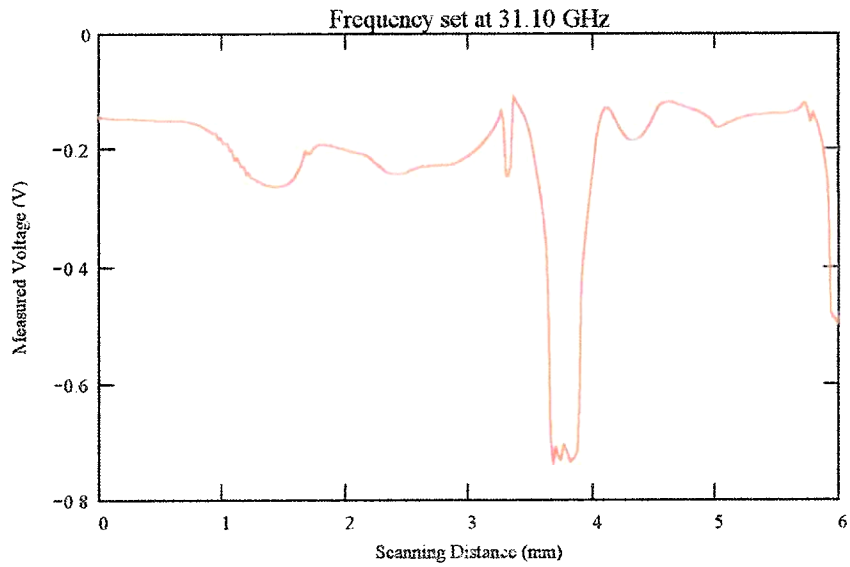
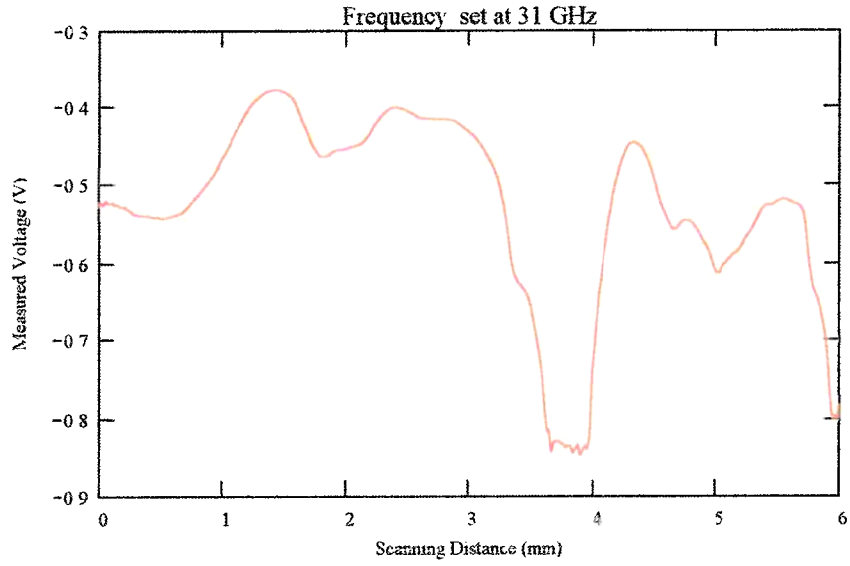


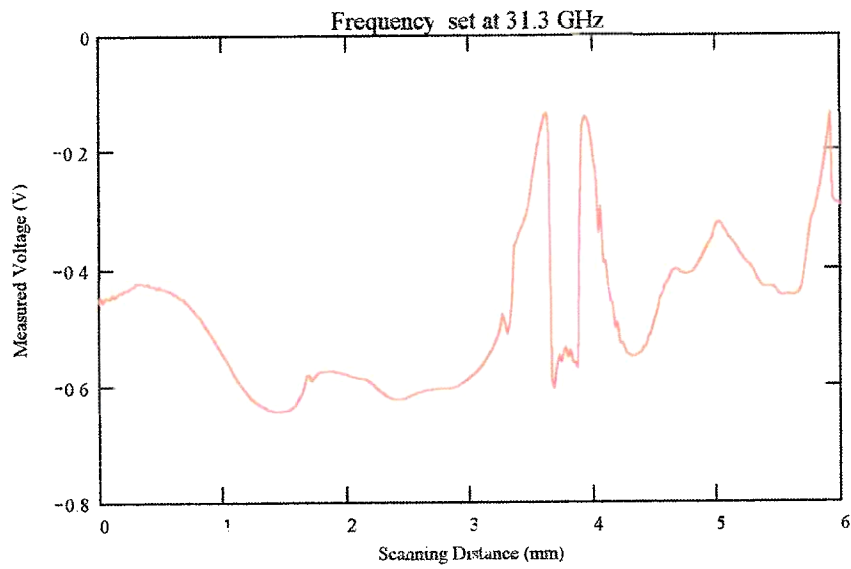
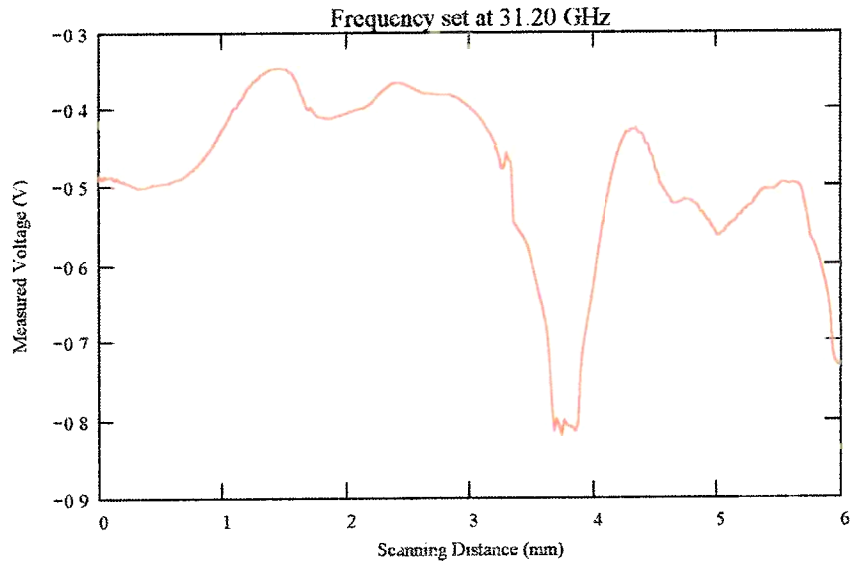


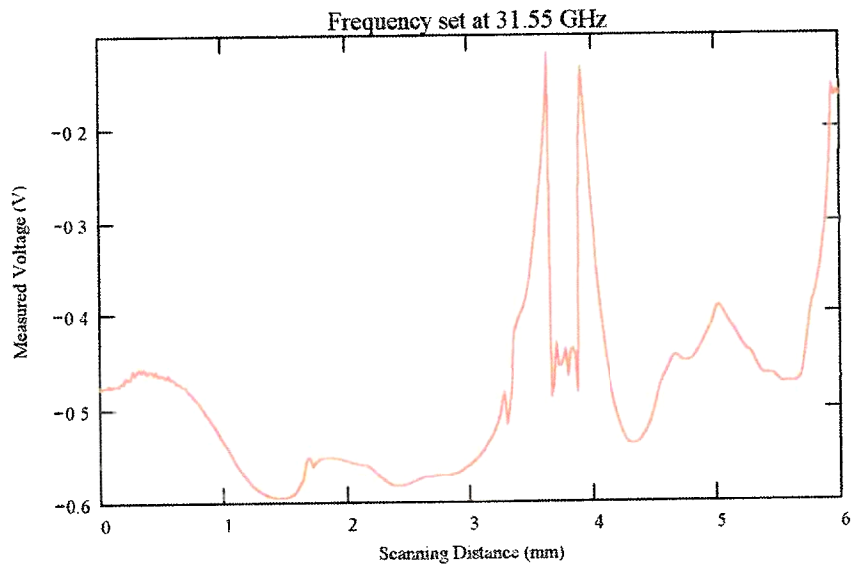
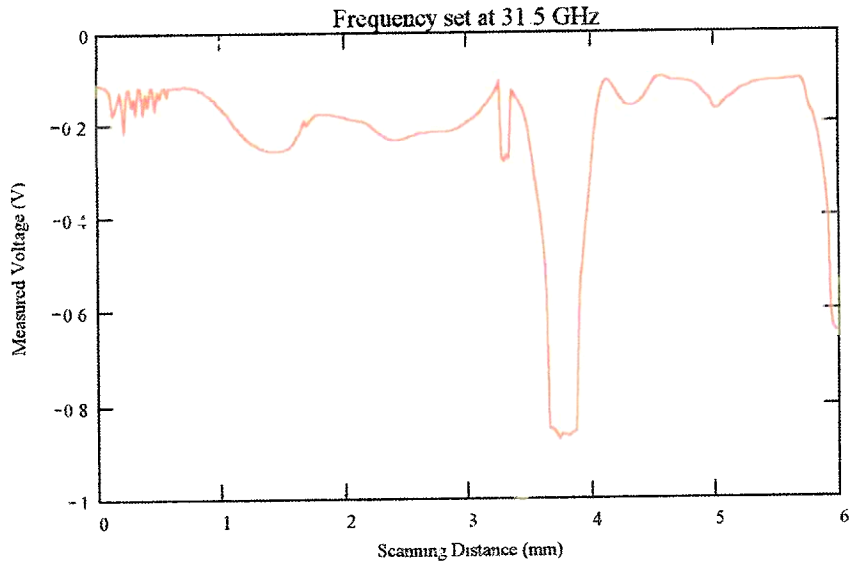
Frequency Band: Ka-band
Orientation: Scan perpendicular to crack length
Probe: coax no 3
Scan Resolution: 0.019 mm per step
Scan length: 6 mm
Frequency: Varies

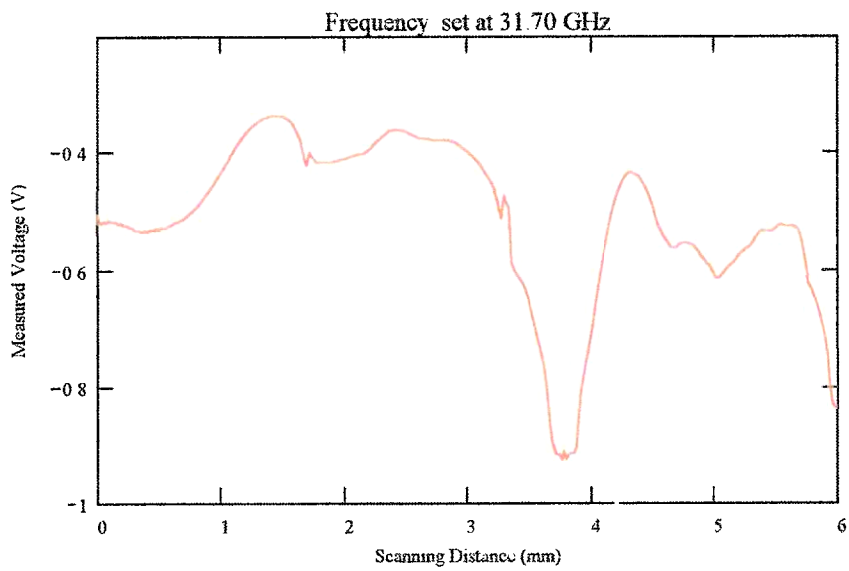
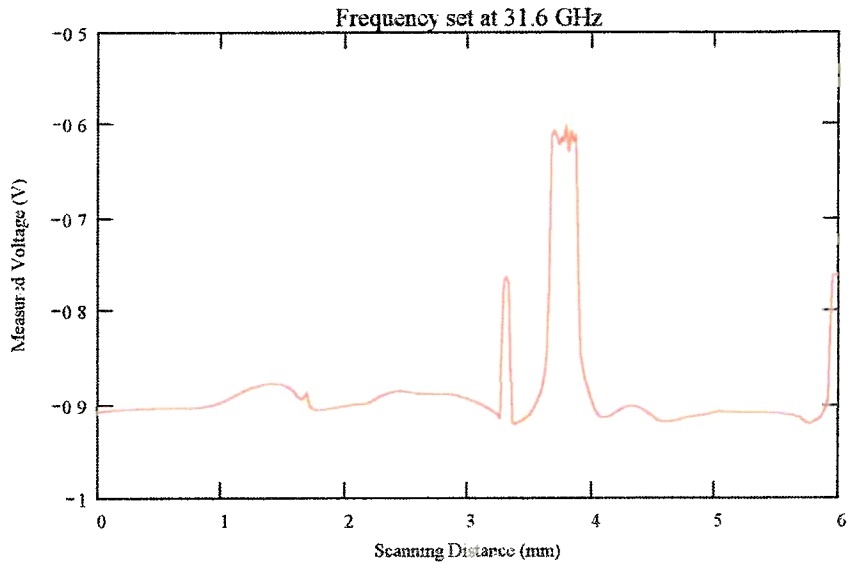


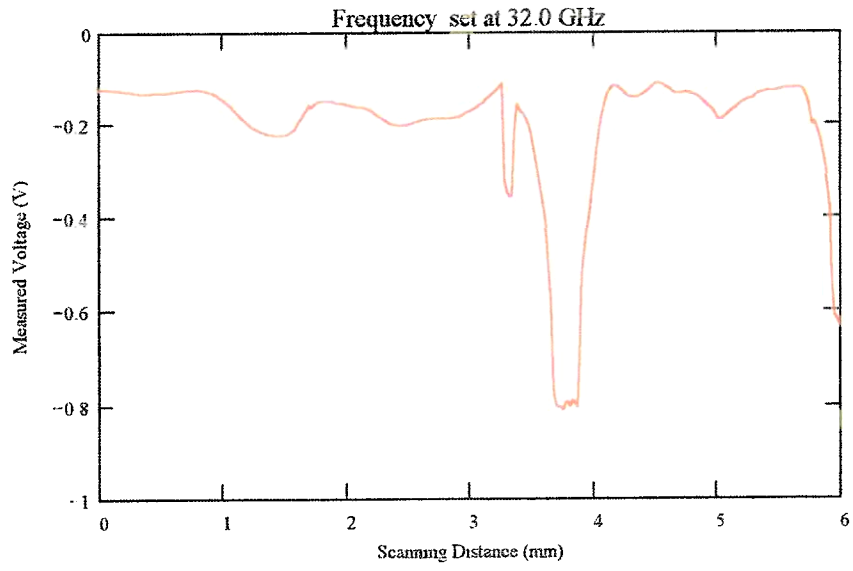








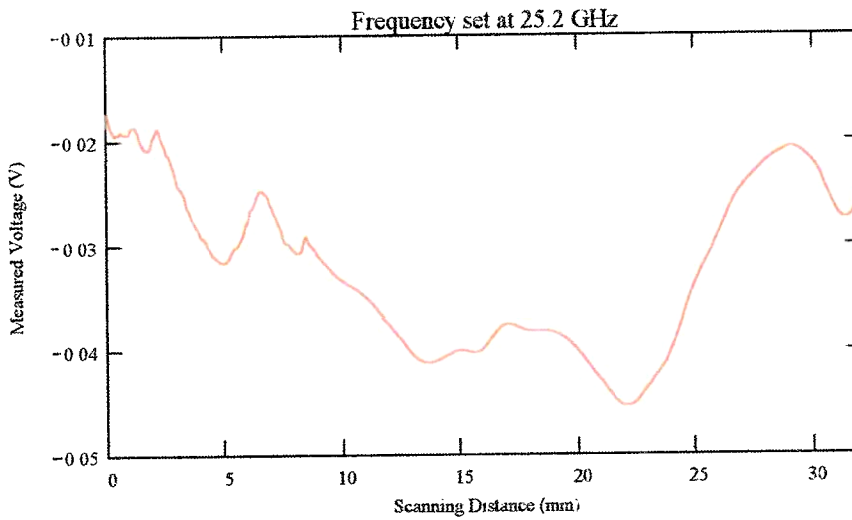


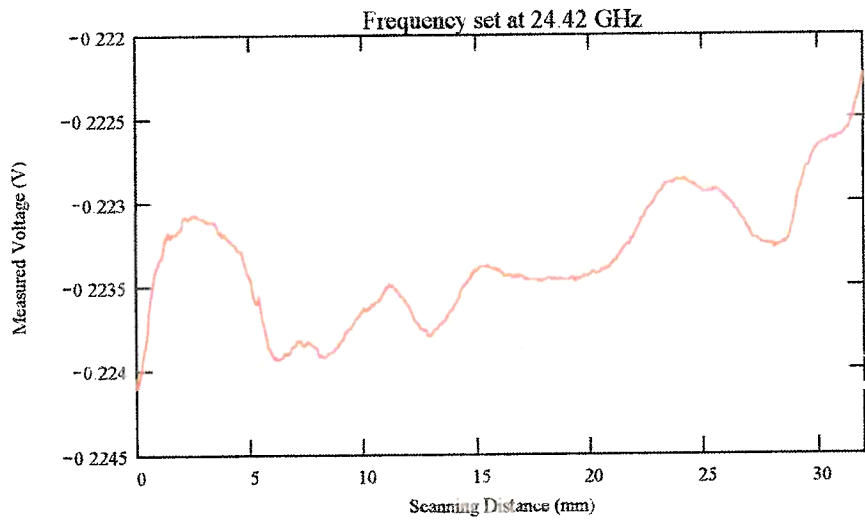
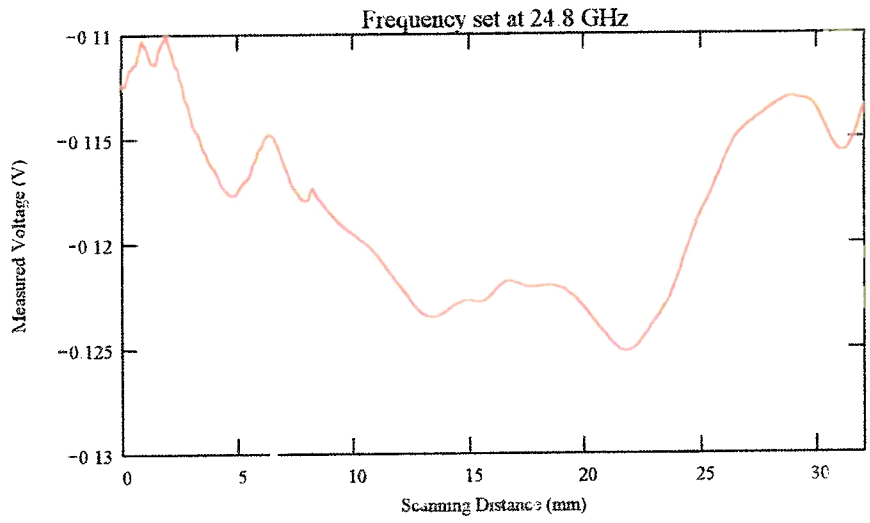


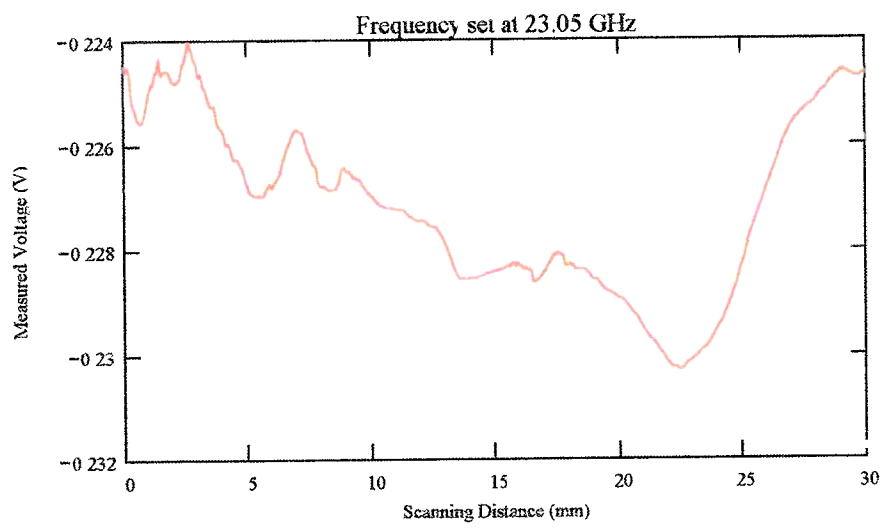
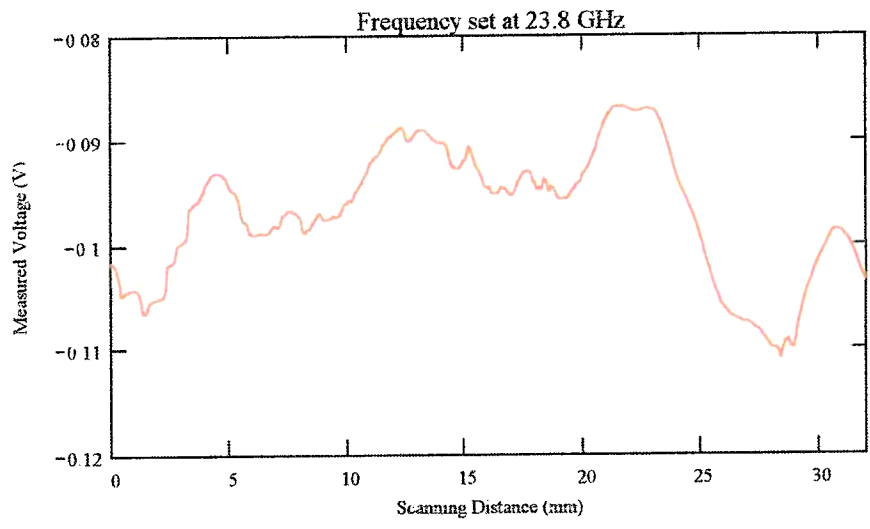
B. Crack #2

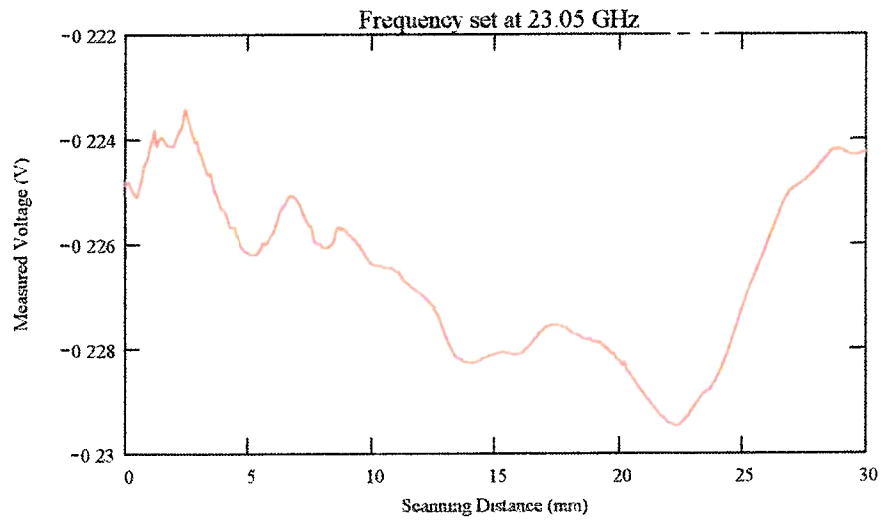
This is a Centreline Indication crack. The length of the crack is 15 mm. This crack runs parallel to the welded joint.

Frequency Band: K-band
Orientation: Scan parallel to crack length
Probe: coax no.2
Scan Resolution: .05 mm per step
Scan length: 32 mm
Frequency: Varies

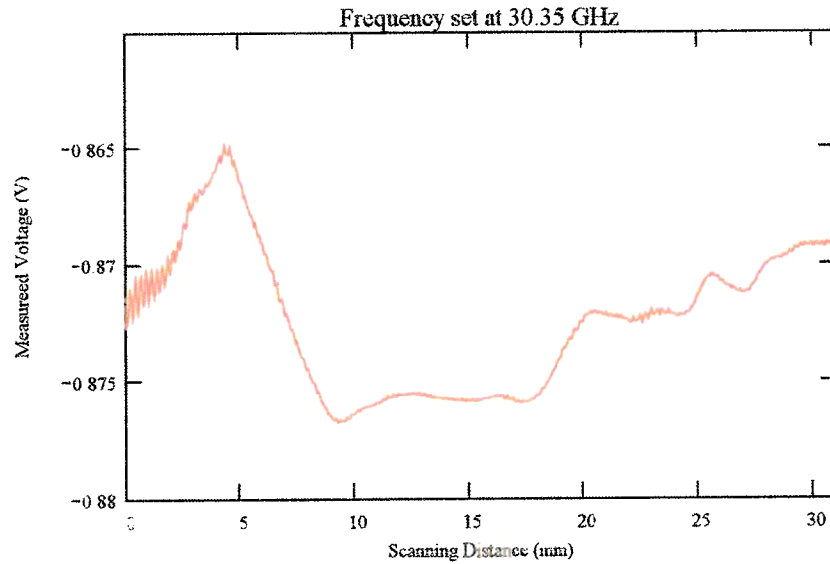


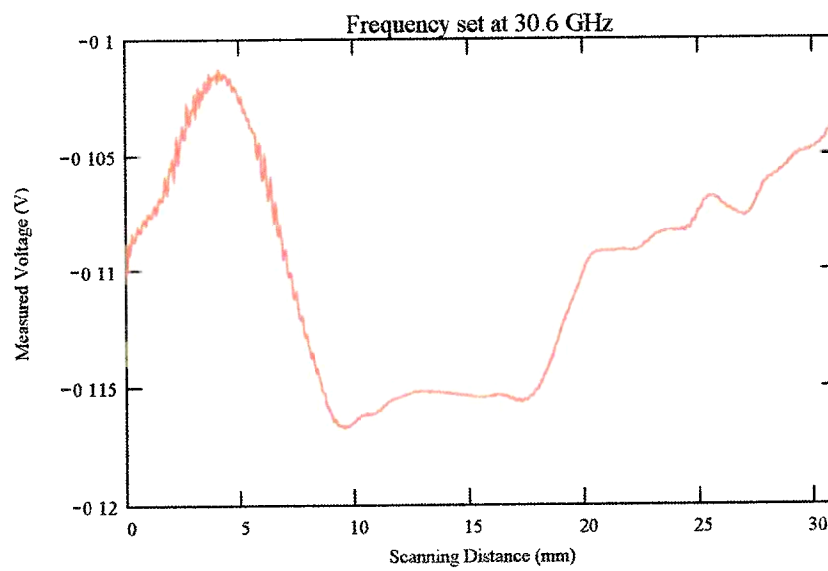
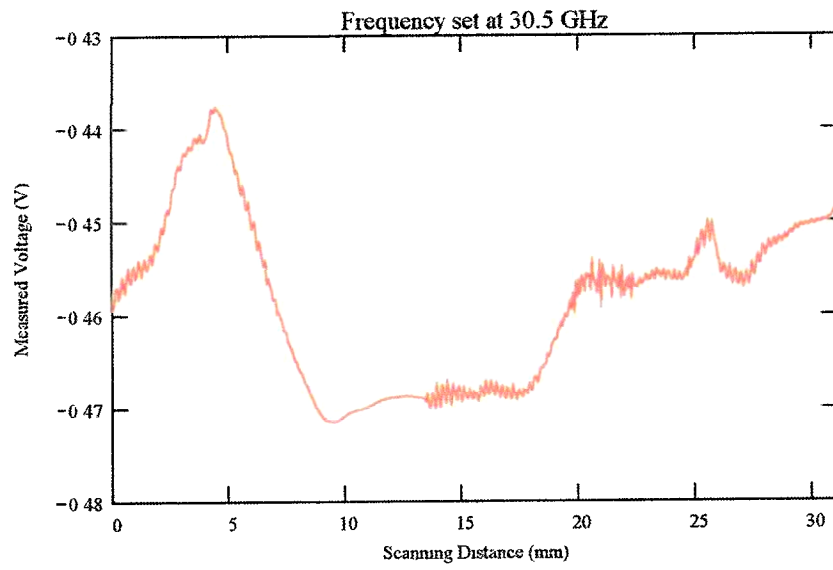


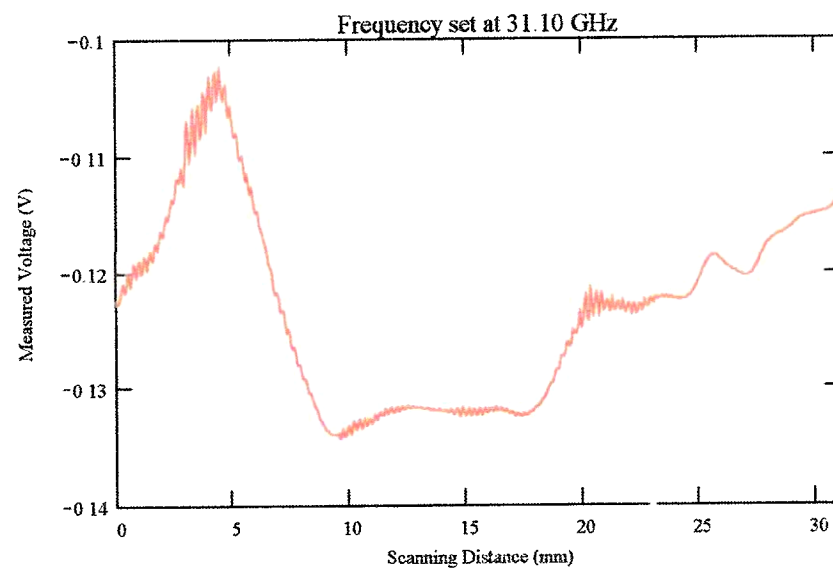
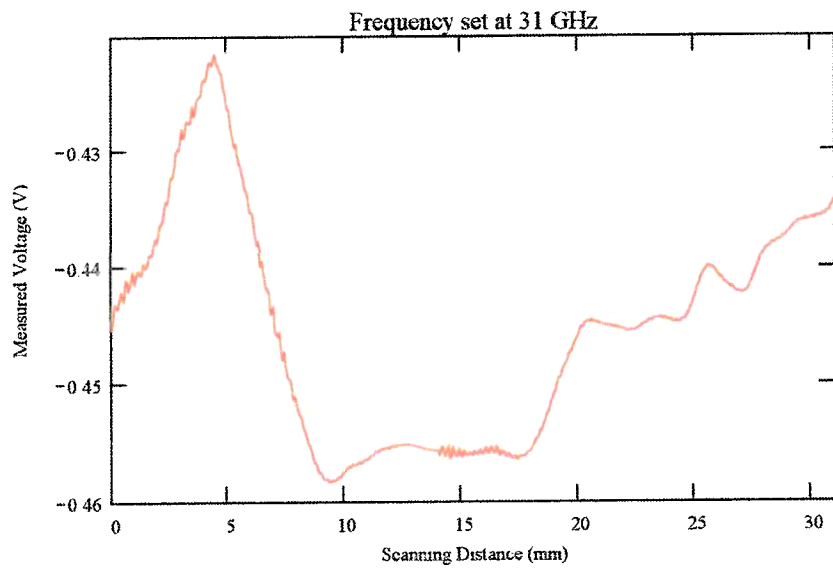


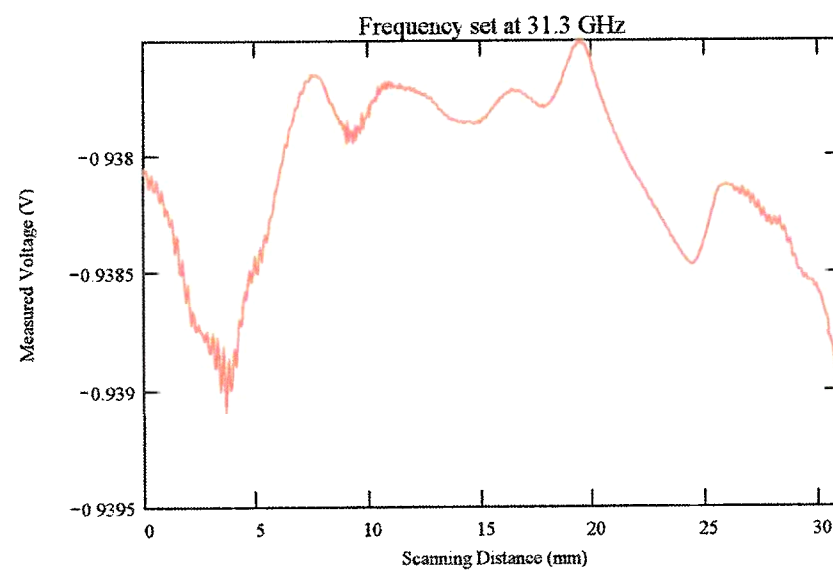
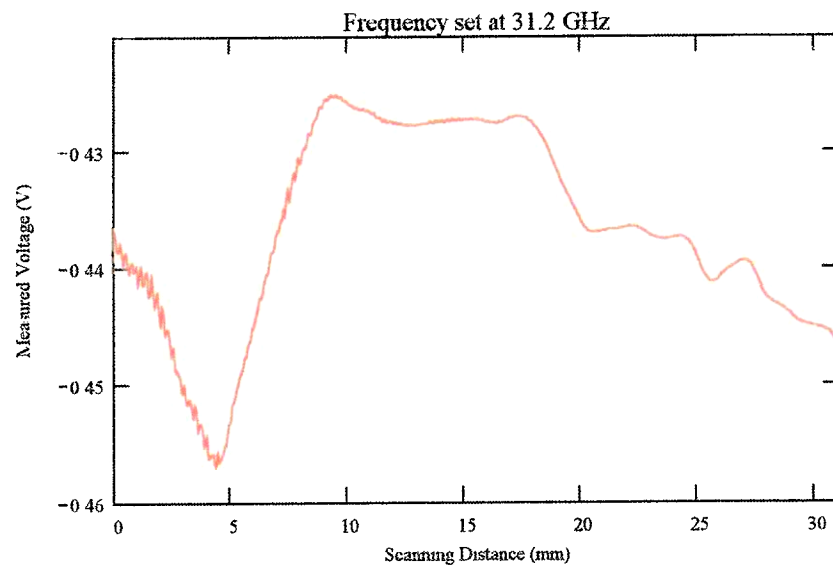


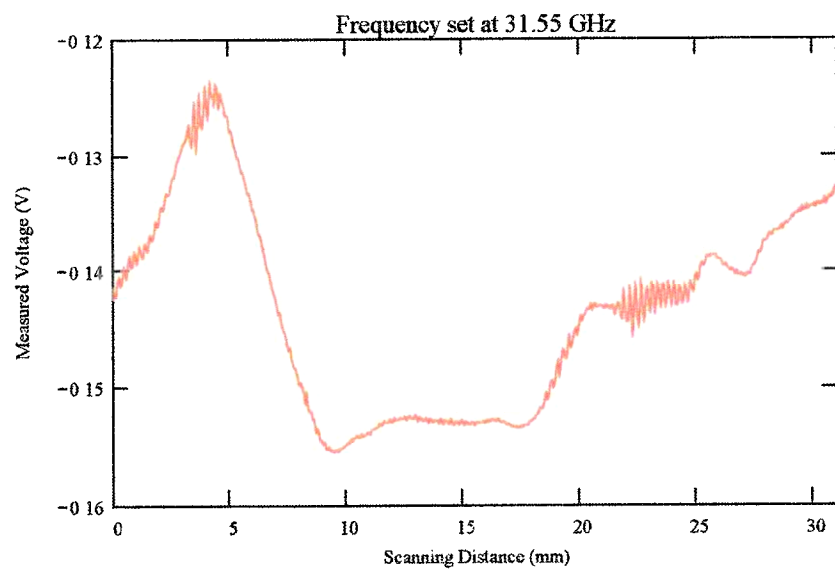
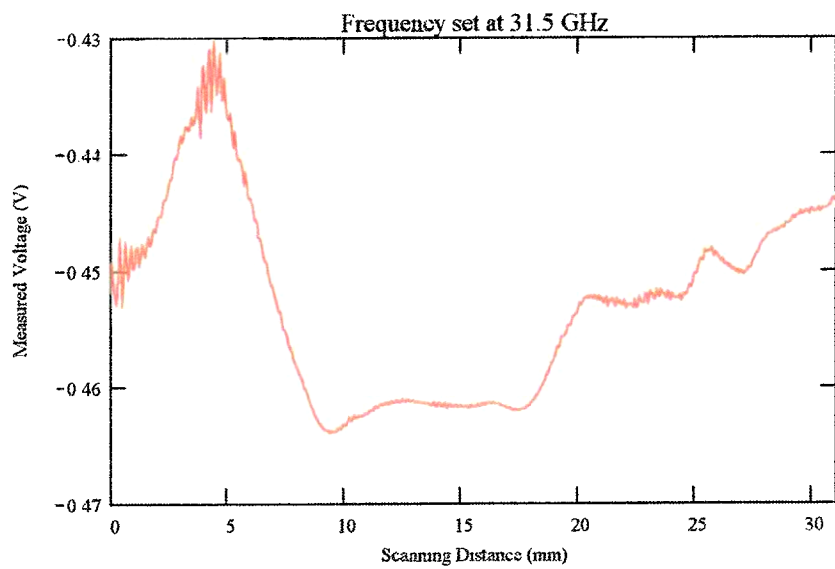
Frequency Band: Ka-band
Orientation: Scan parrallel to crack length
Probe: coax no 3
Scan Resolution: 0.019 mm per step
Scan length: 6 mm
Frequency: Varies

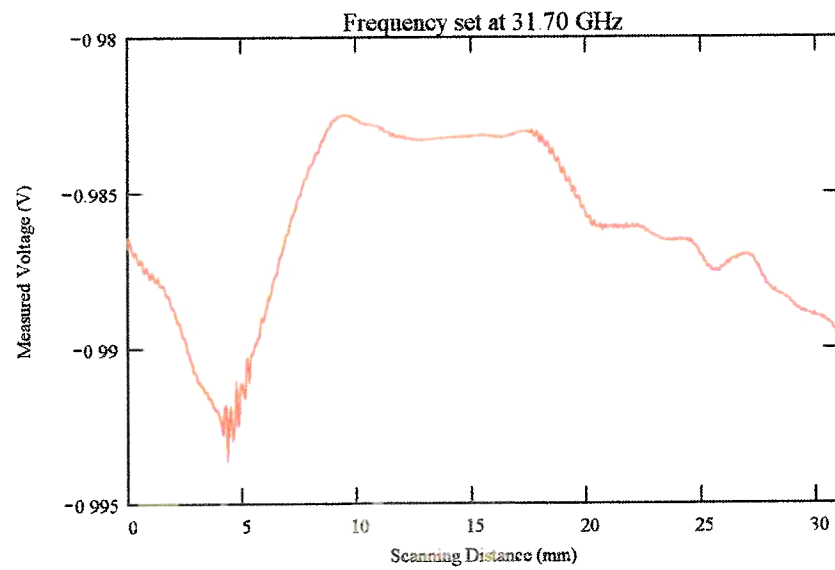
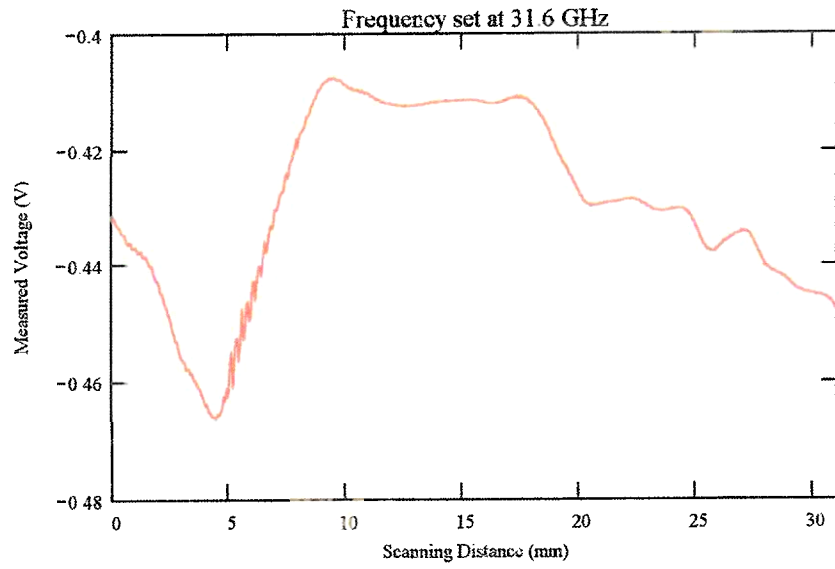


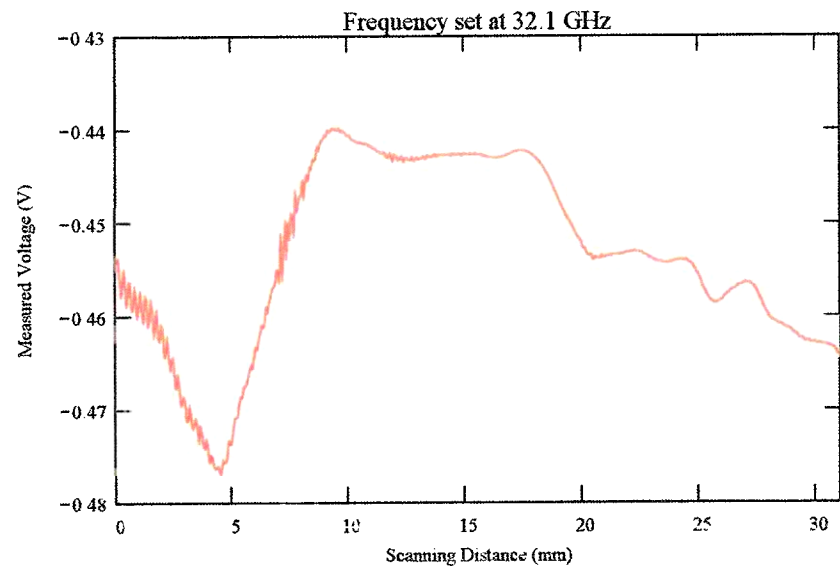
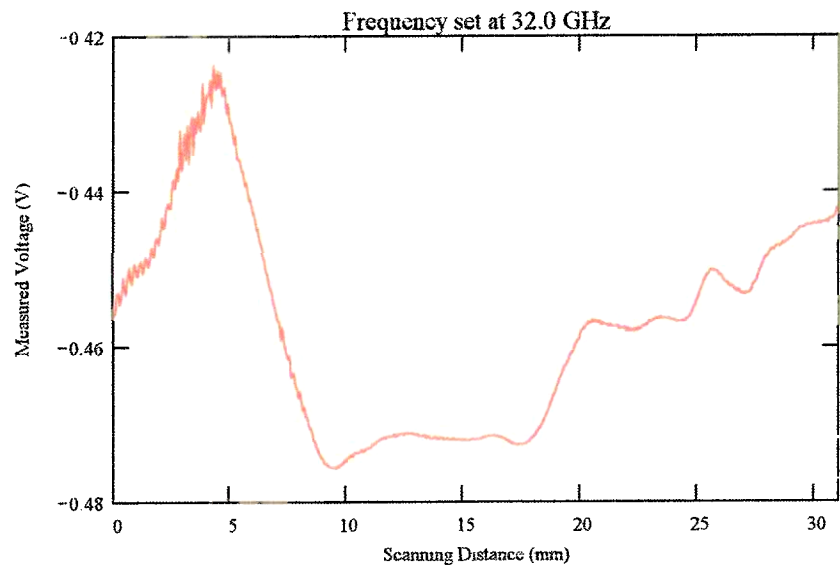


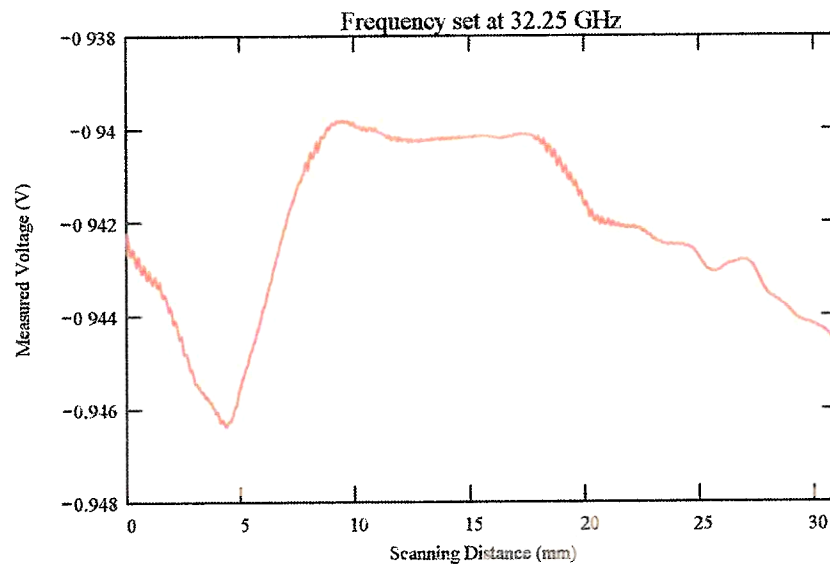
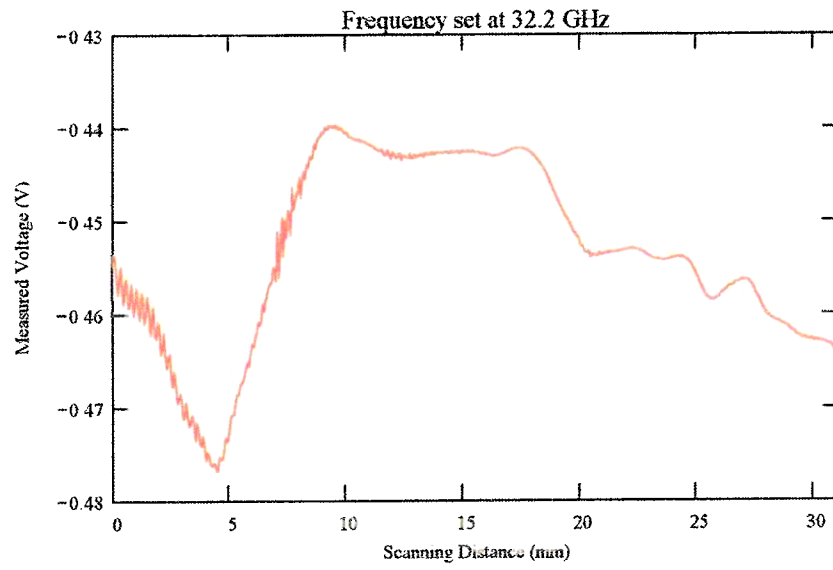


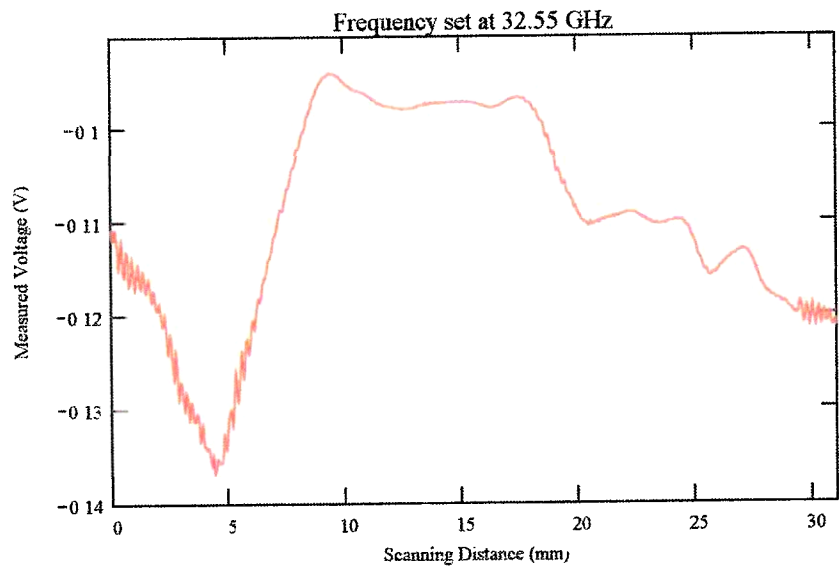
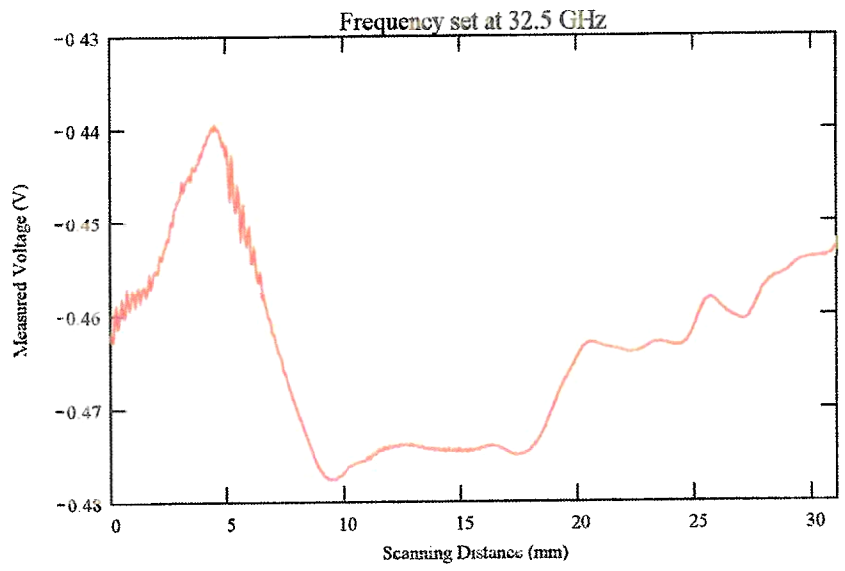


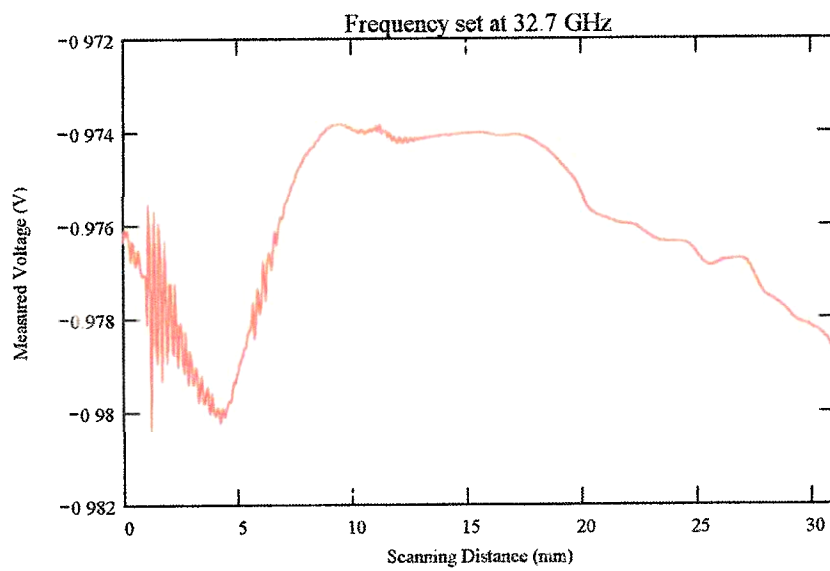
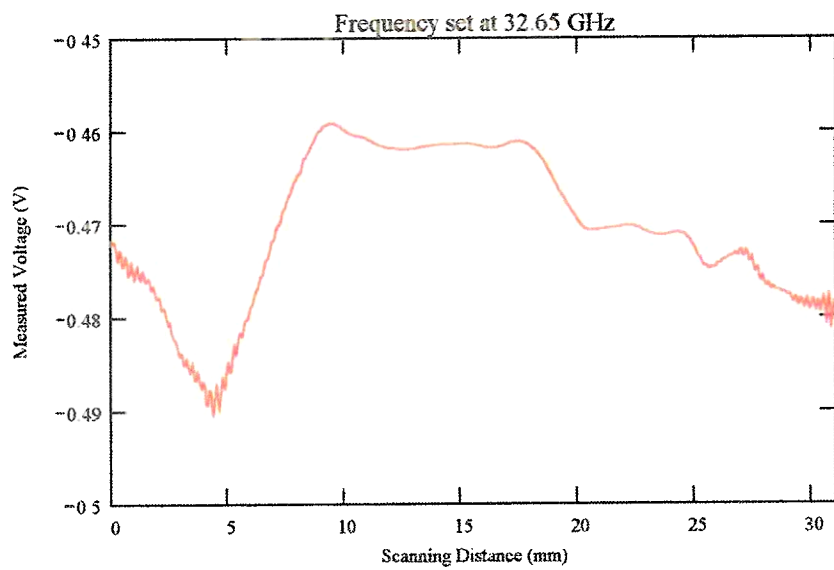


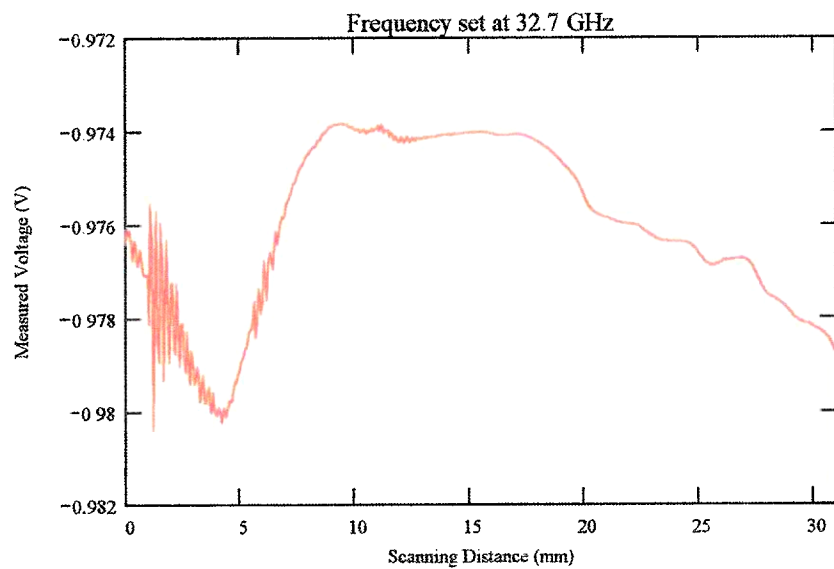
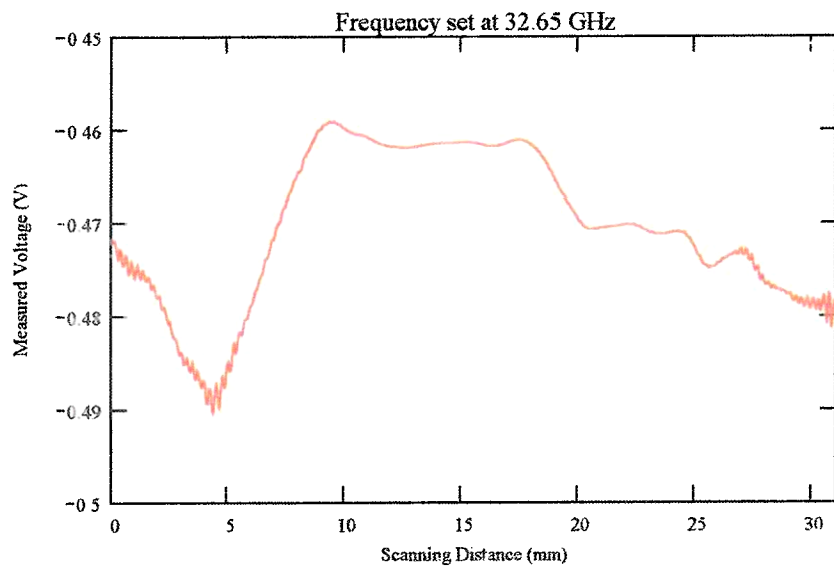


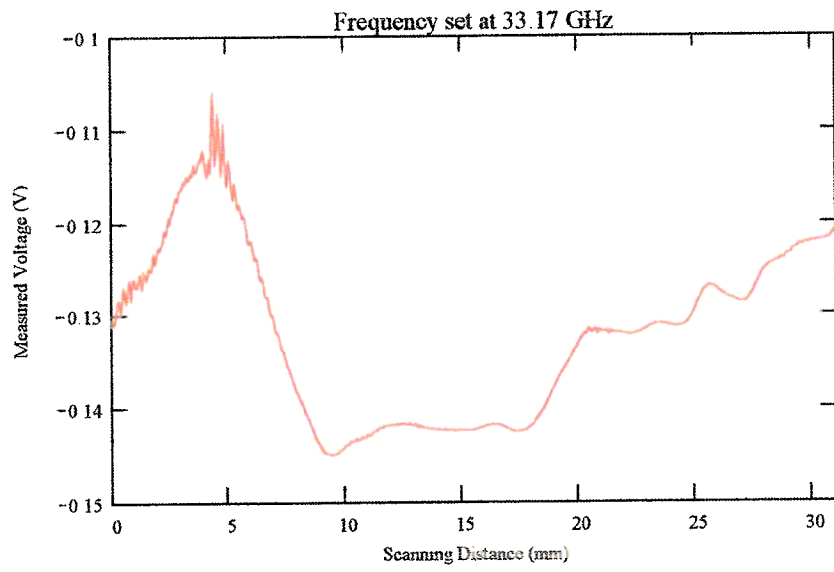
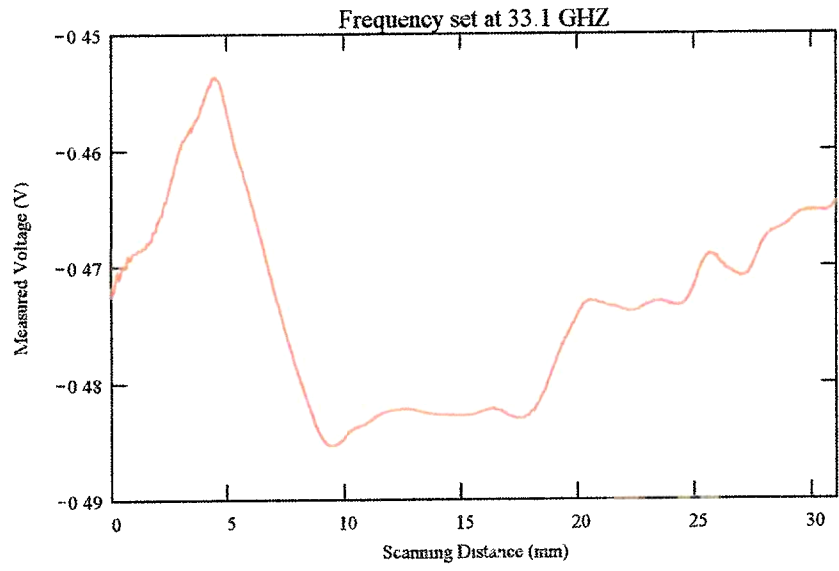


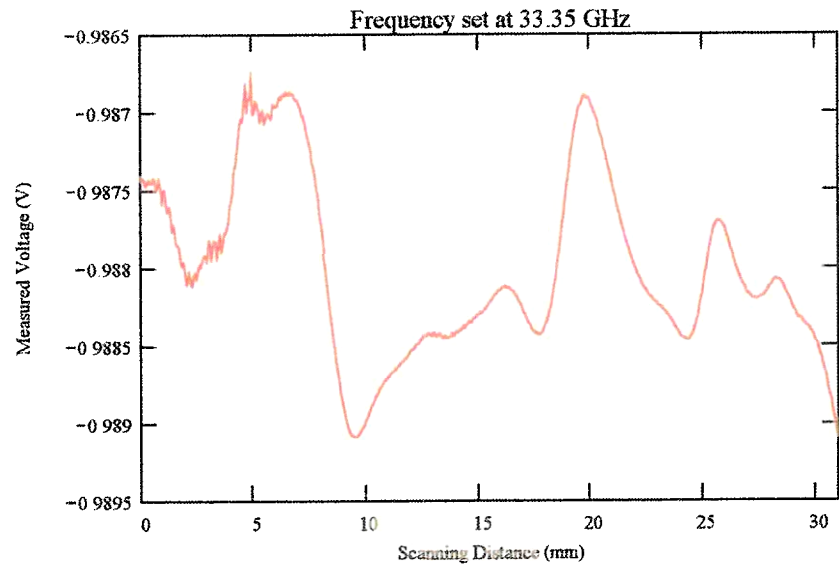
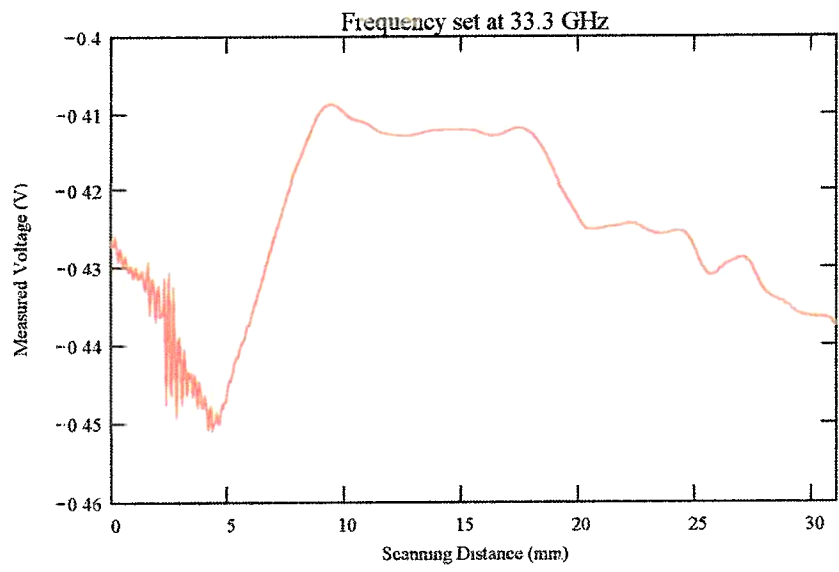


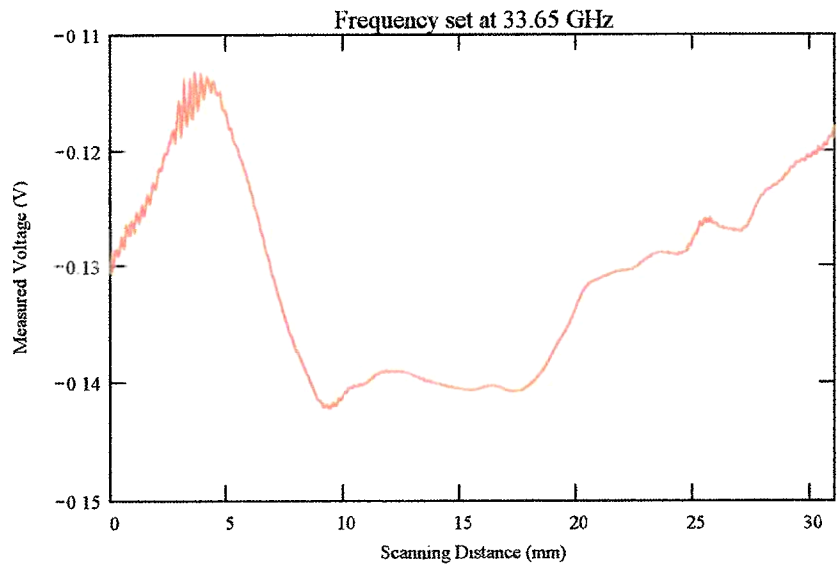
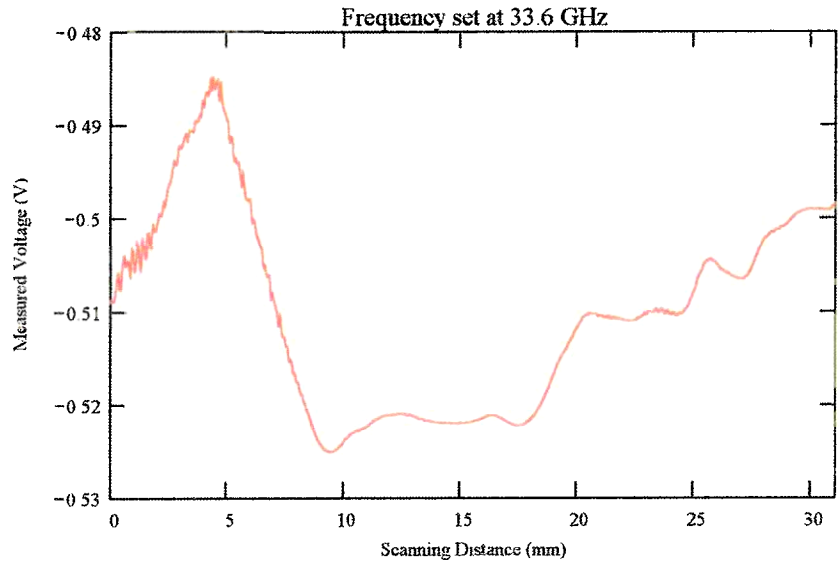


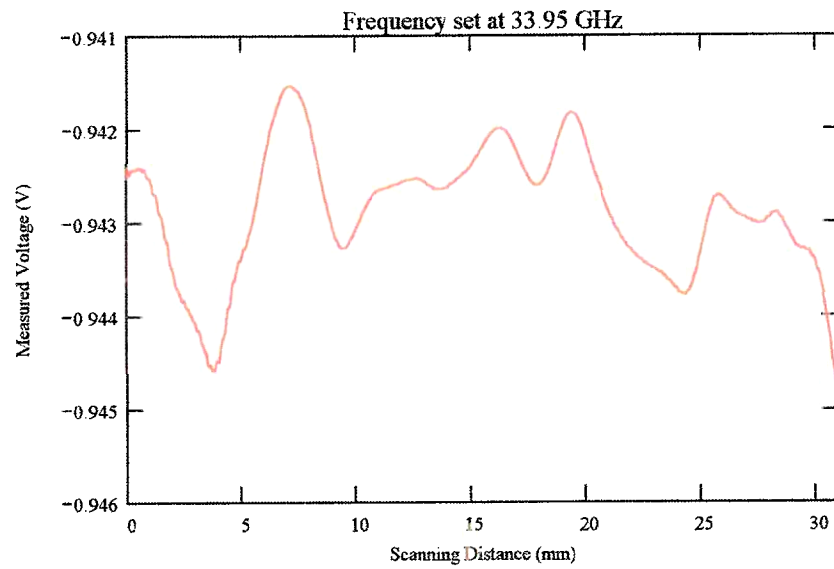
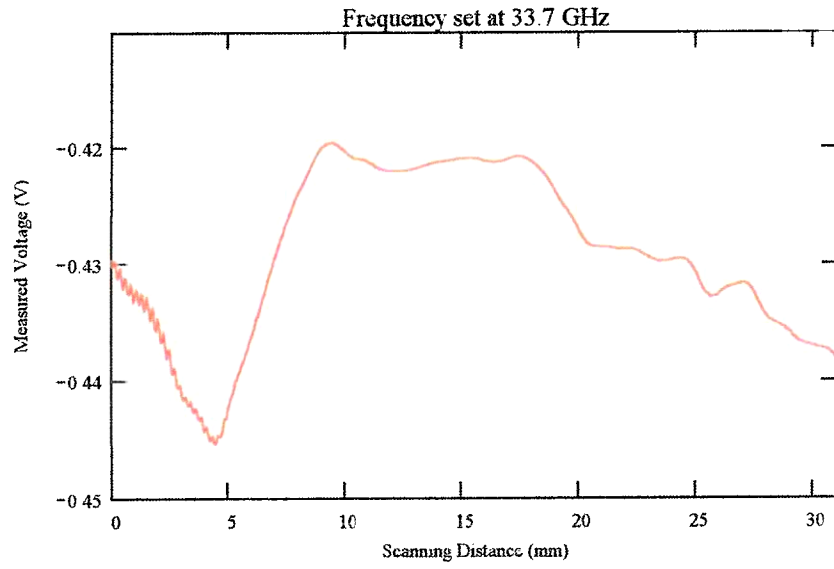


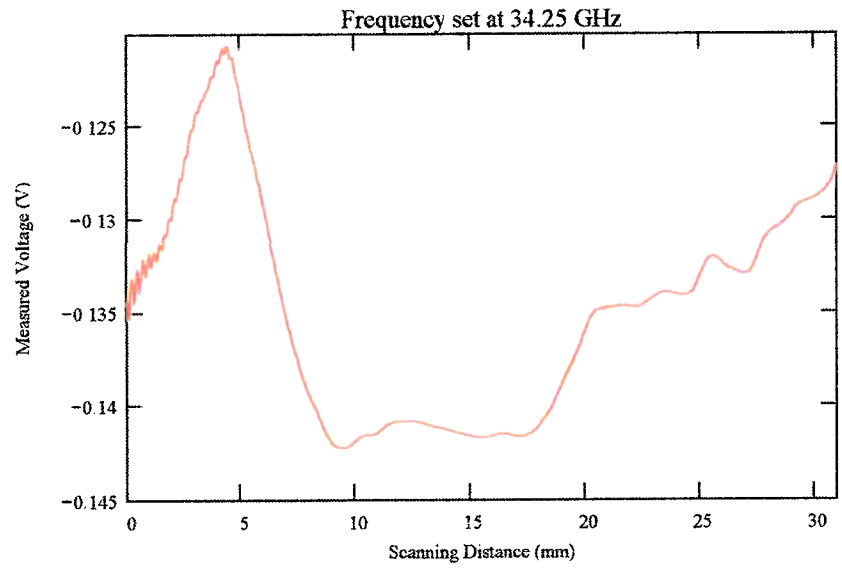
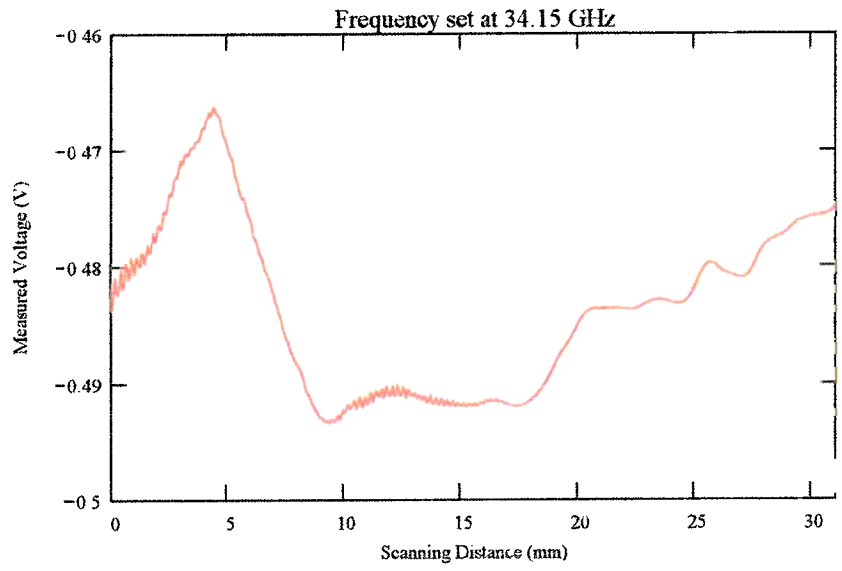


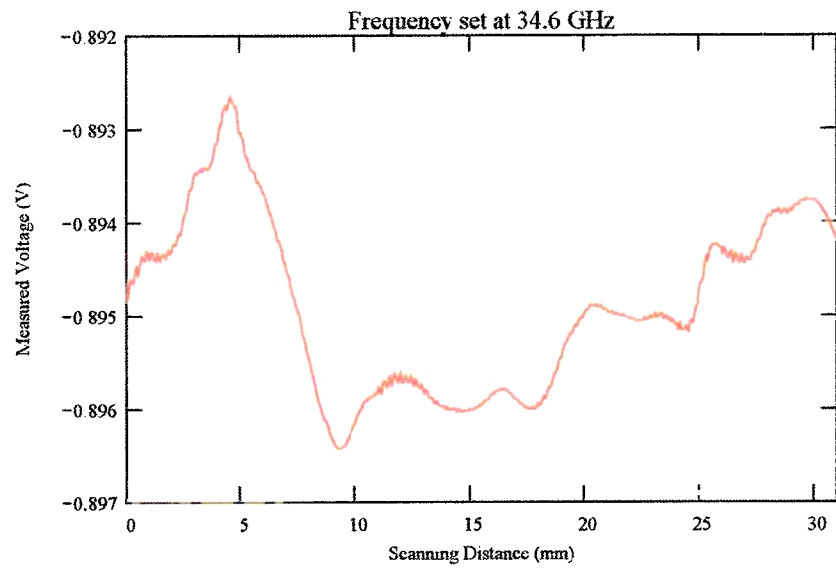
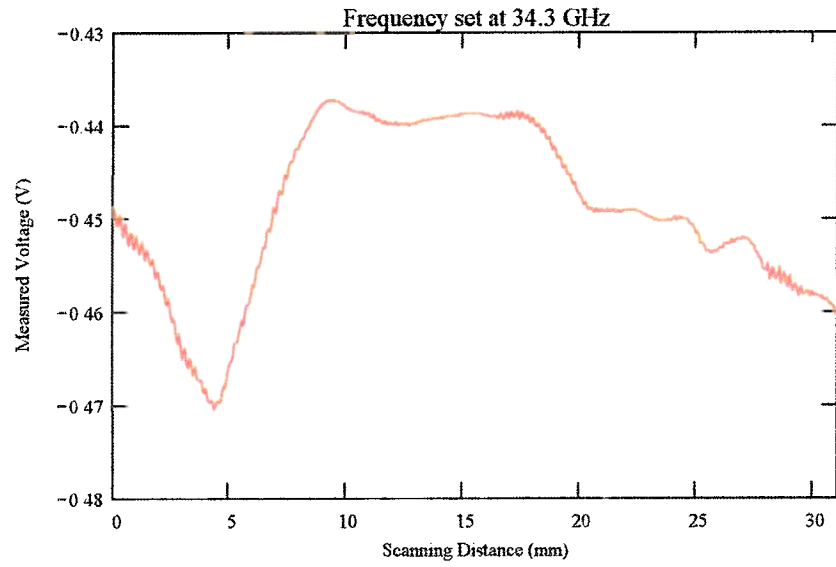


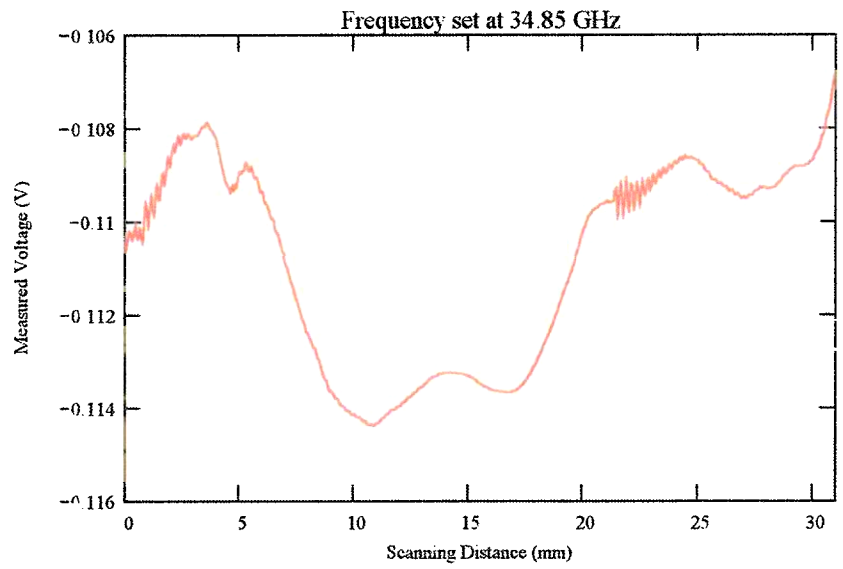
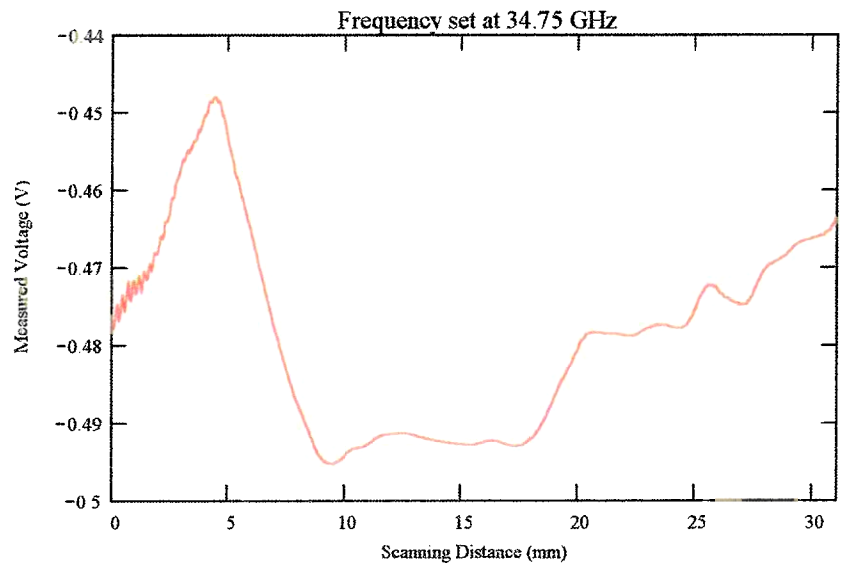


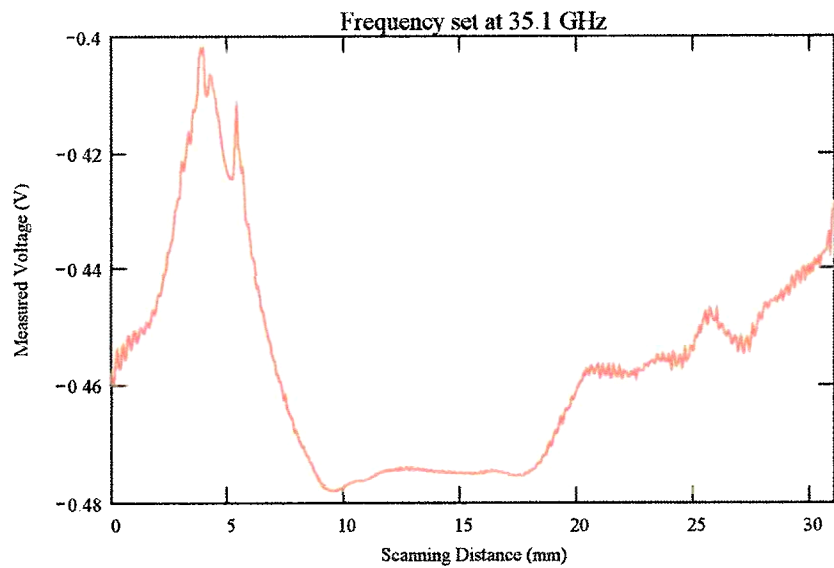
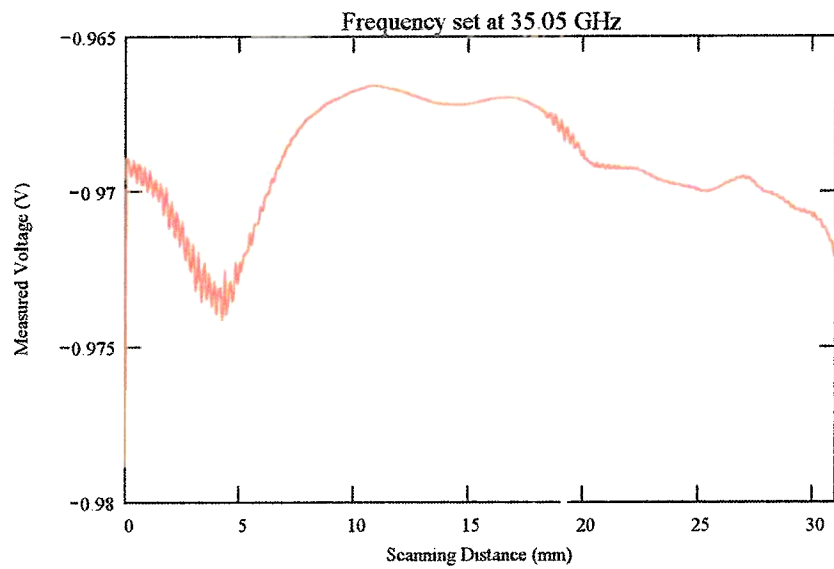


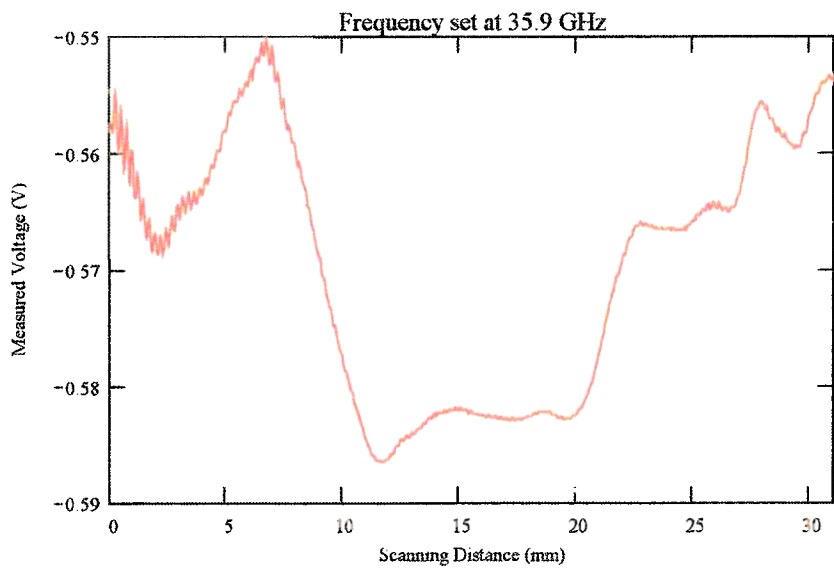
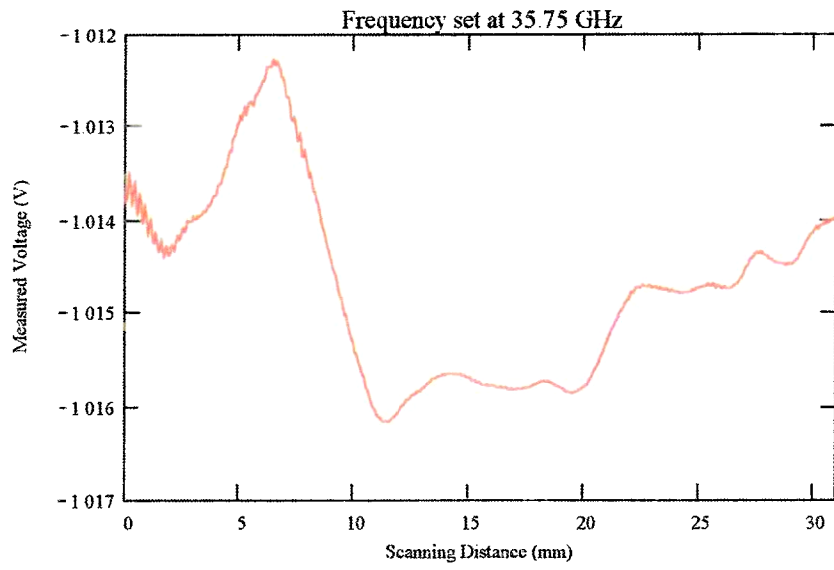


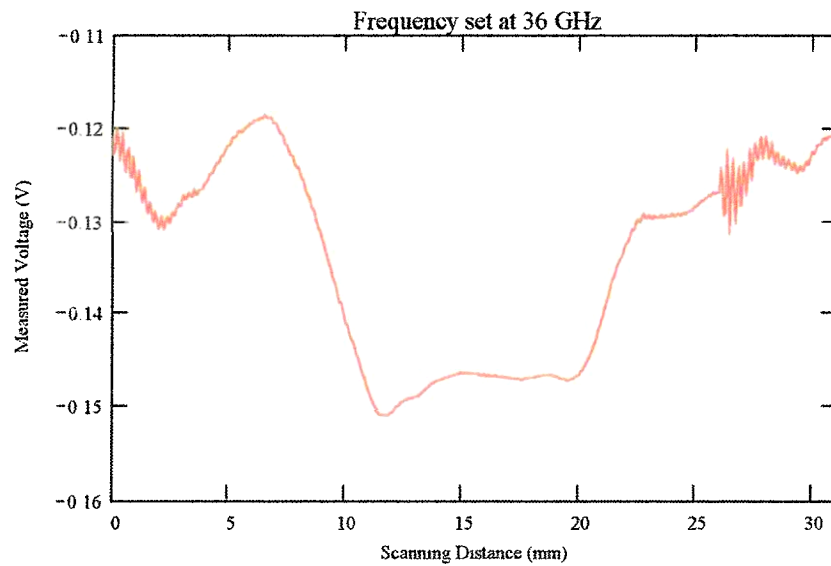










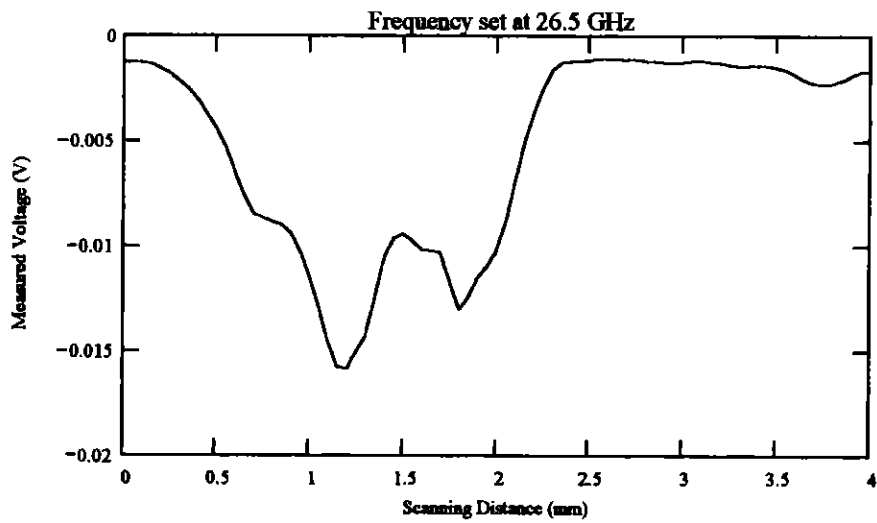


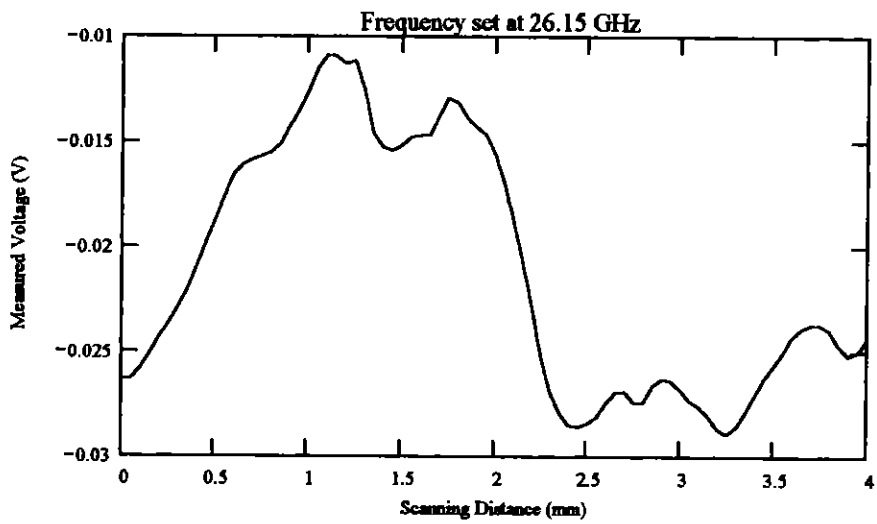
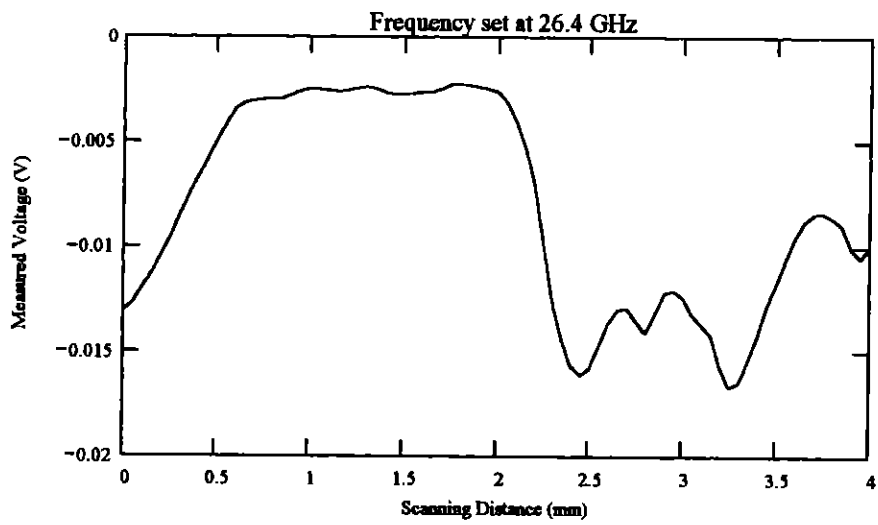
III. Sample T4297

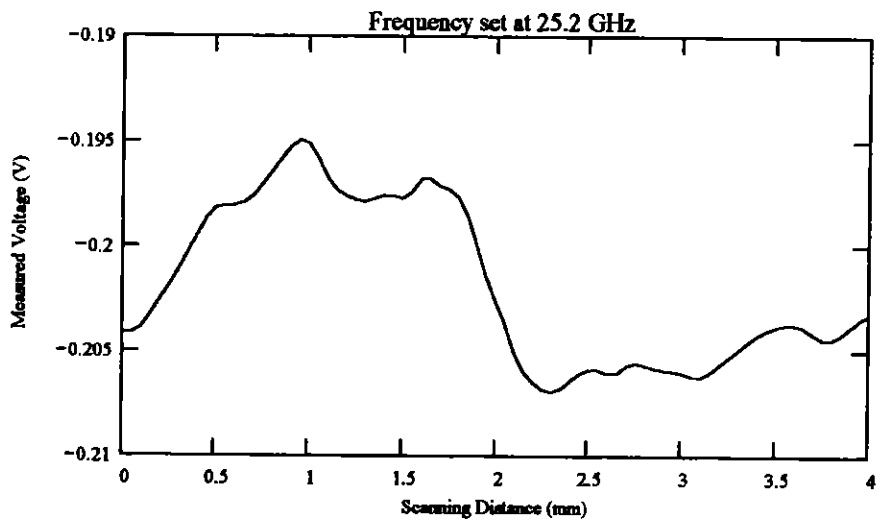
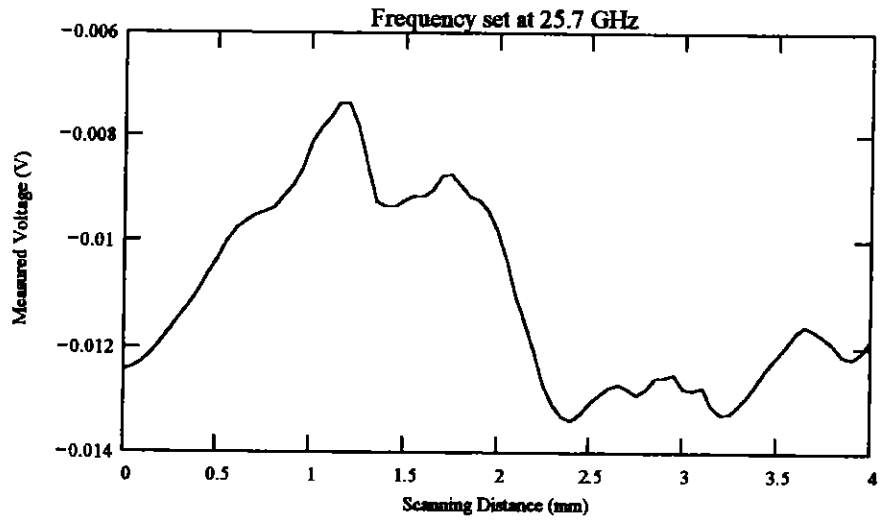
A. Crack #1

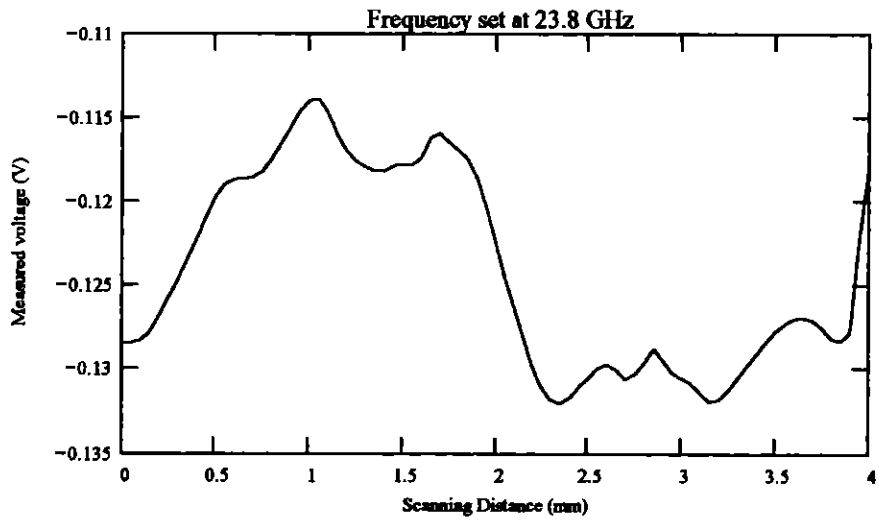
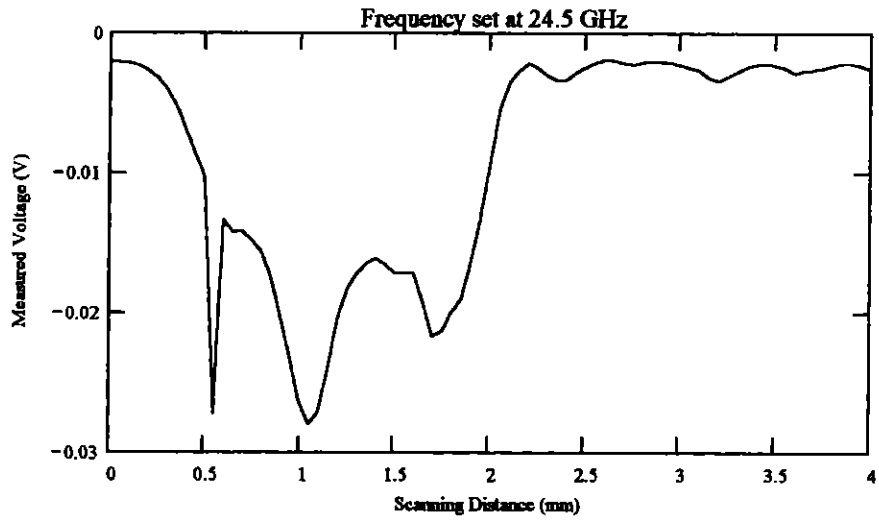
the This is a Transverse Indication crack. The length of
the crack is 11 mm. This crack runs perpendicular to
the welded joint.

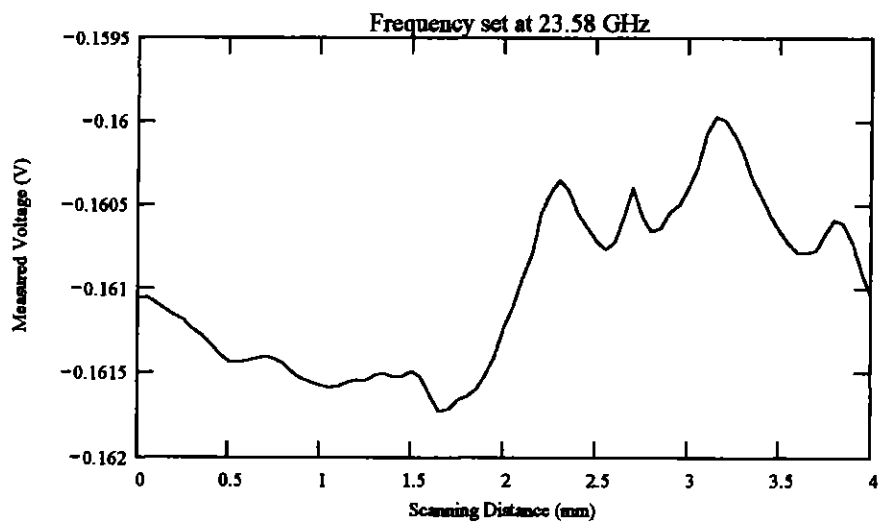
Frequency Band: K-band
Orientation: Scan perpendicular to crack length.
Probe: Coax no. 2
Scan Resolution: .05 mm per step
Scan length: 4 mm
Frequency: Varies



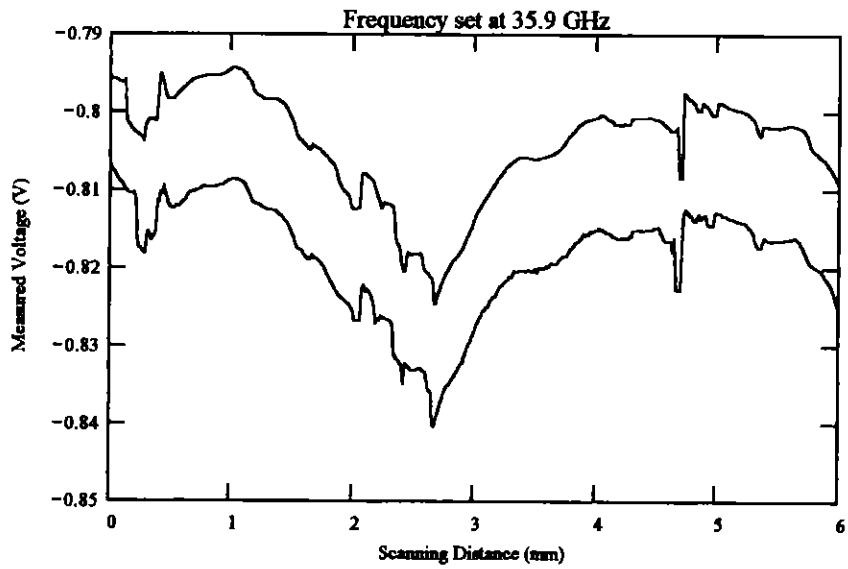


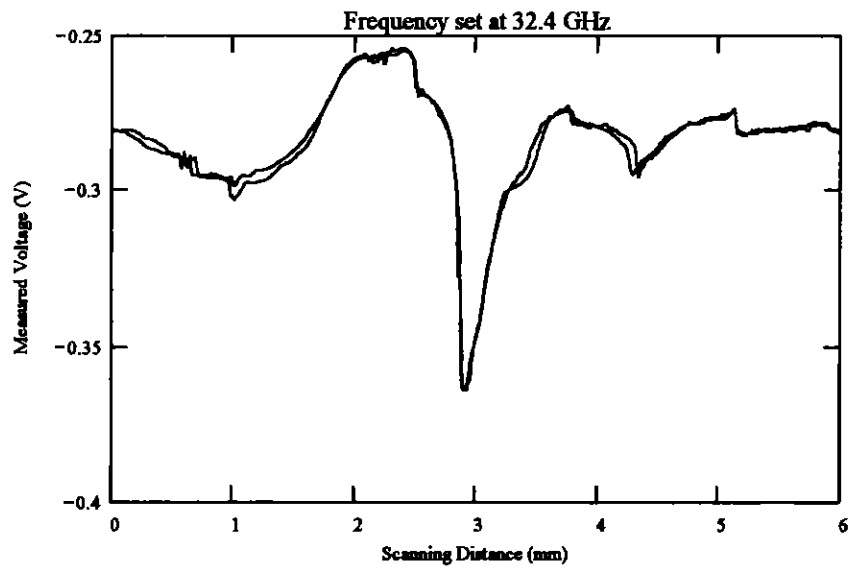
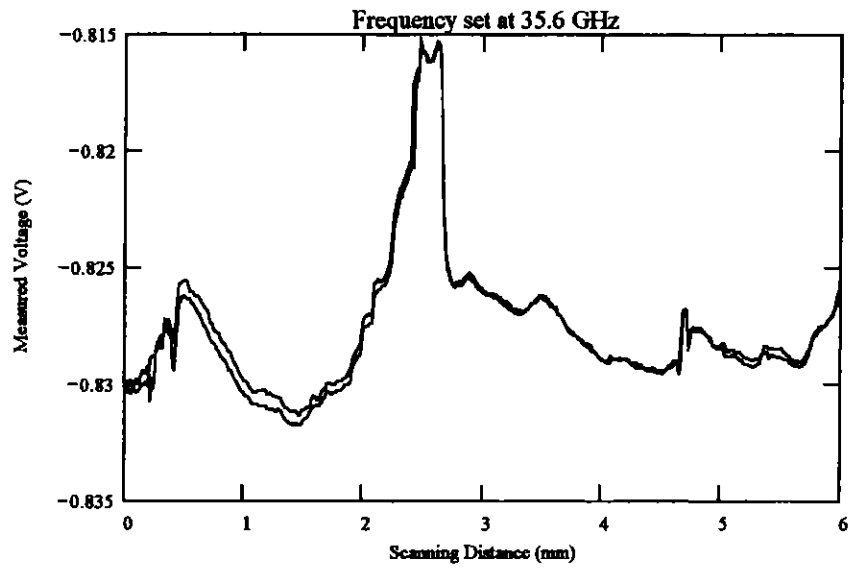


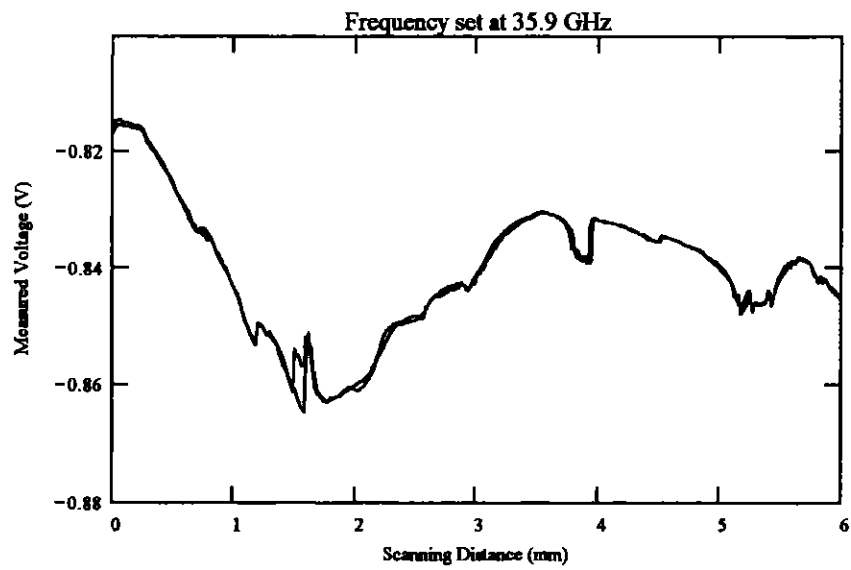
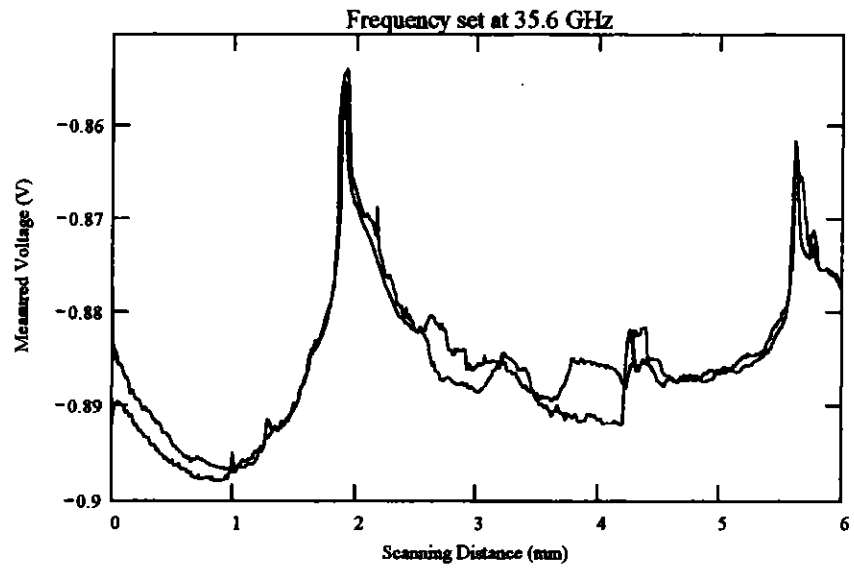


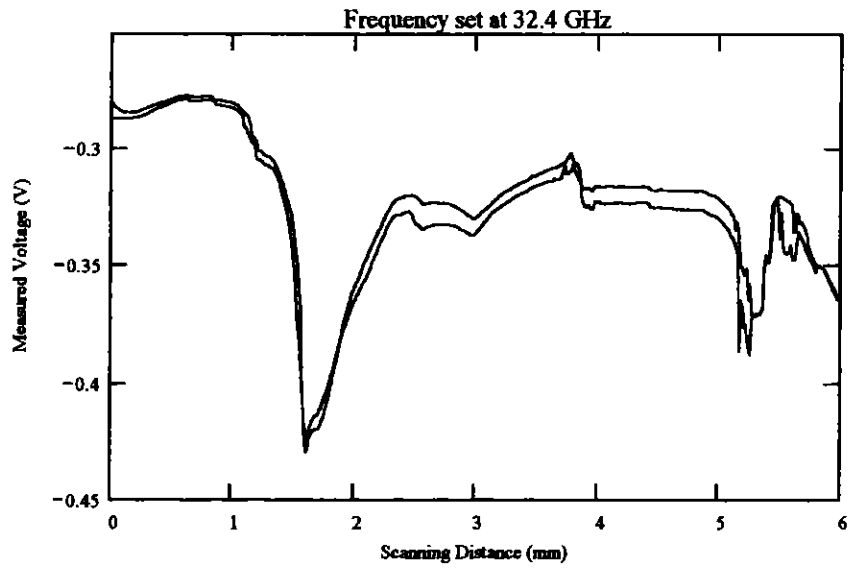


Frequency Band: Ka-band
Orientation: Scan perpendicular to crack length.
Probe: Coax no. 2
Scan Resolution: 0.0125 mm per step
Scan length: 6 mm
Frequency: Varies





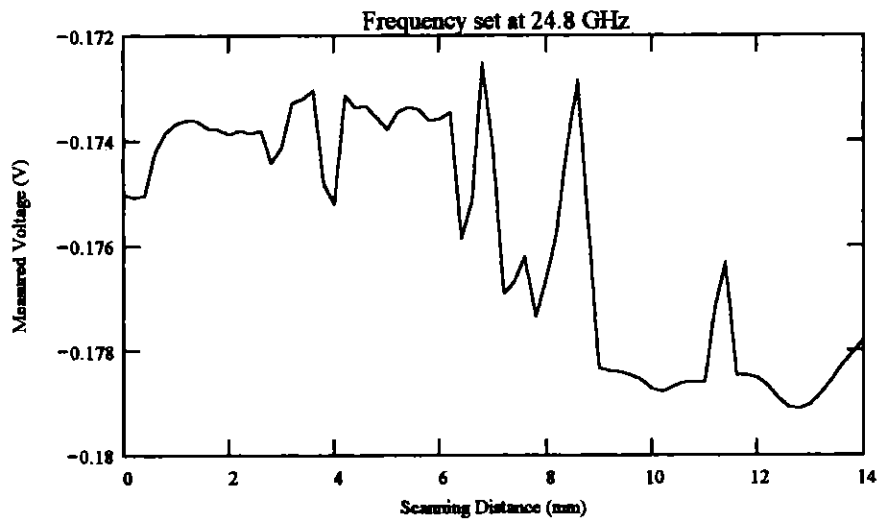


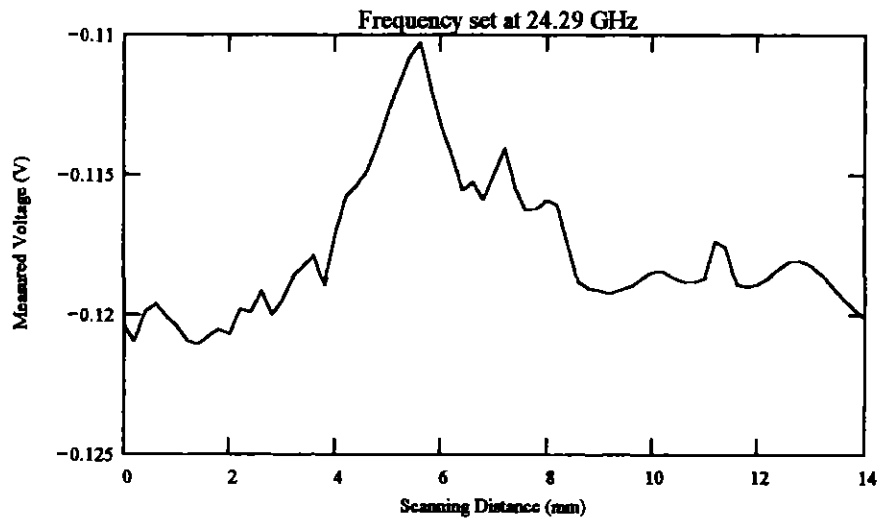
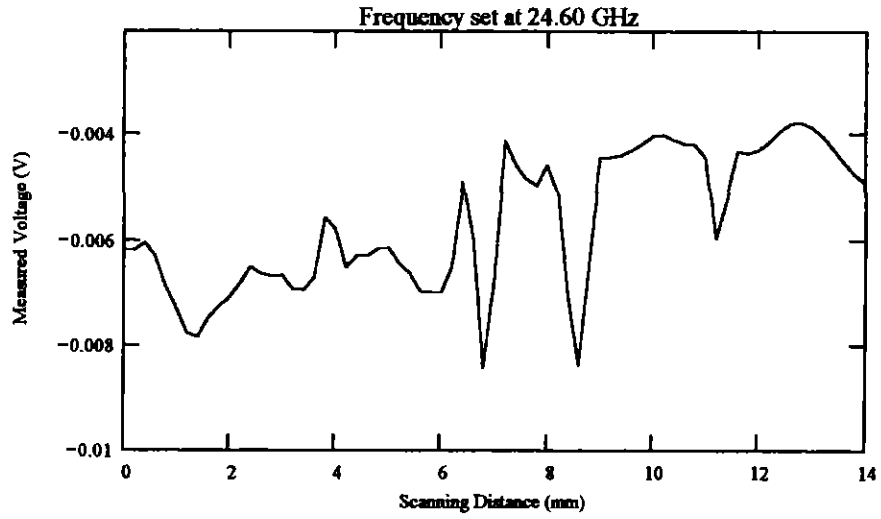


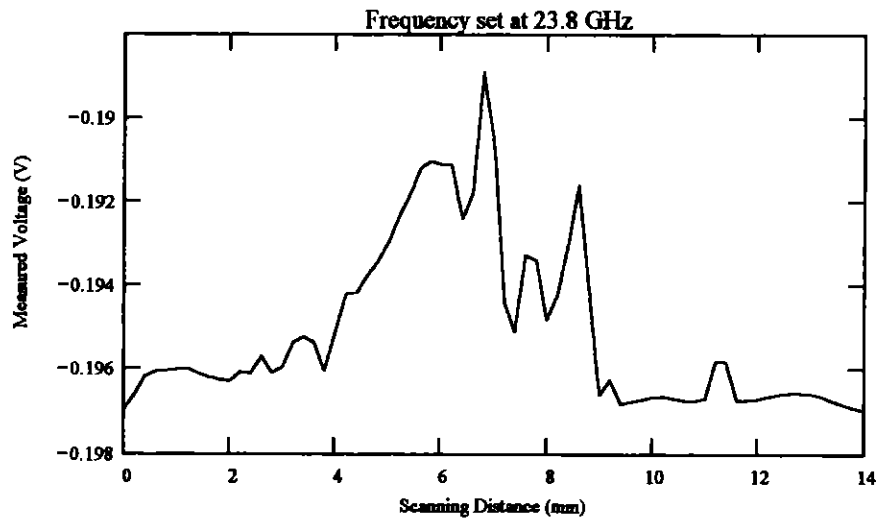
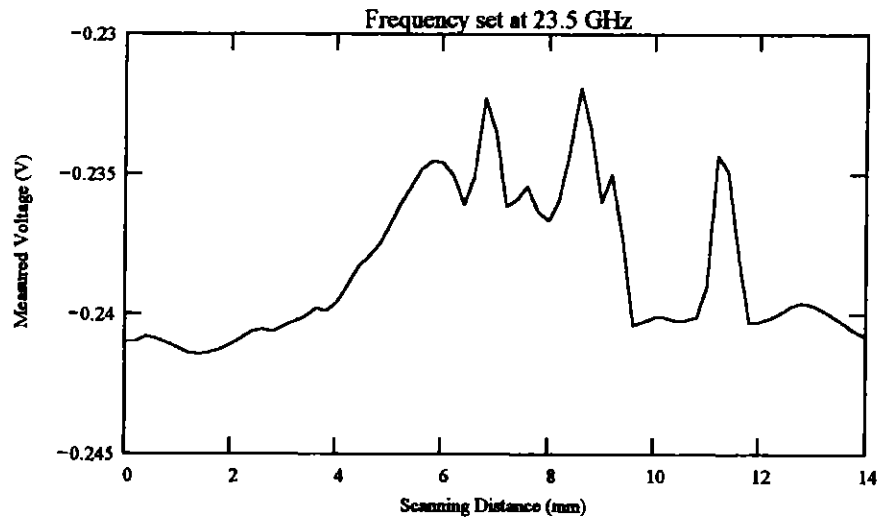
B. Crack #2

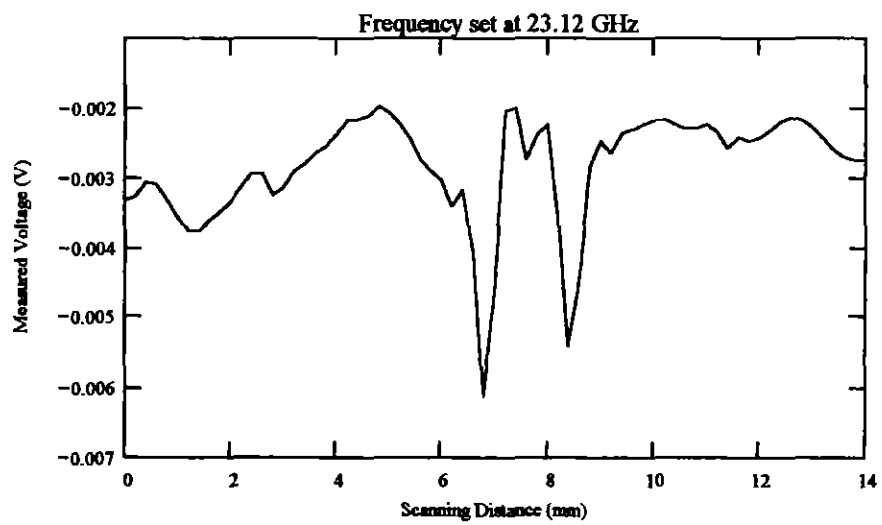
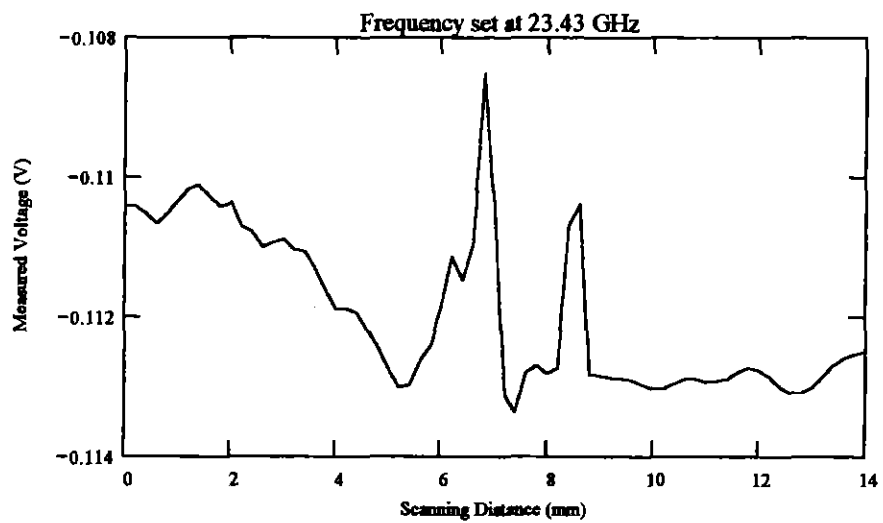
This is a Centreline Indication crack. The length of the crack is 15 mm. This crack runs parallel to the welded joint.

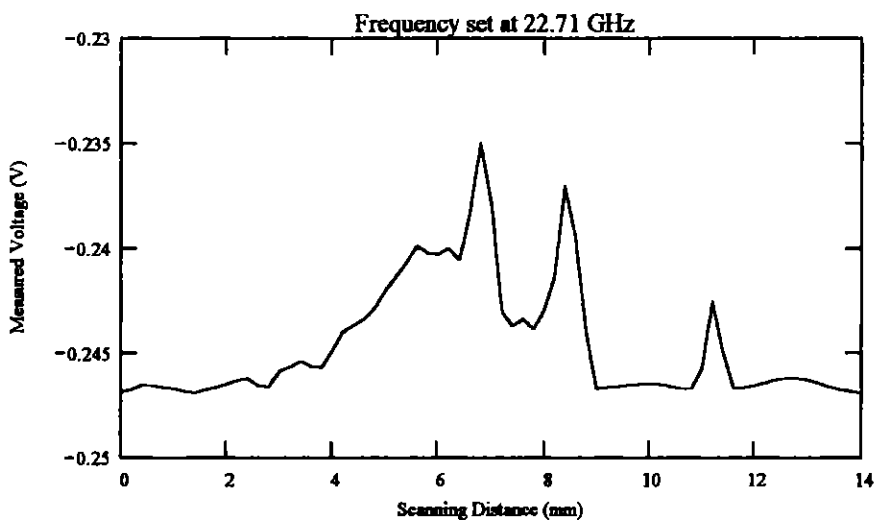
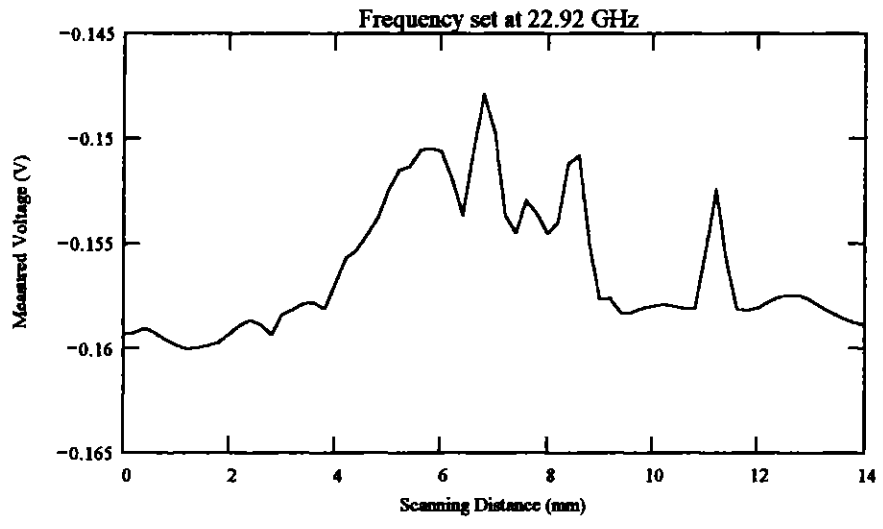
Frequency Band: K-band
Orientation: Scan parallel to crack length.
Probe: Coax no. 2
Scan Resolution: .2 mm per step
Scan length: 14 mm
Frequency: varies



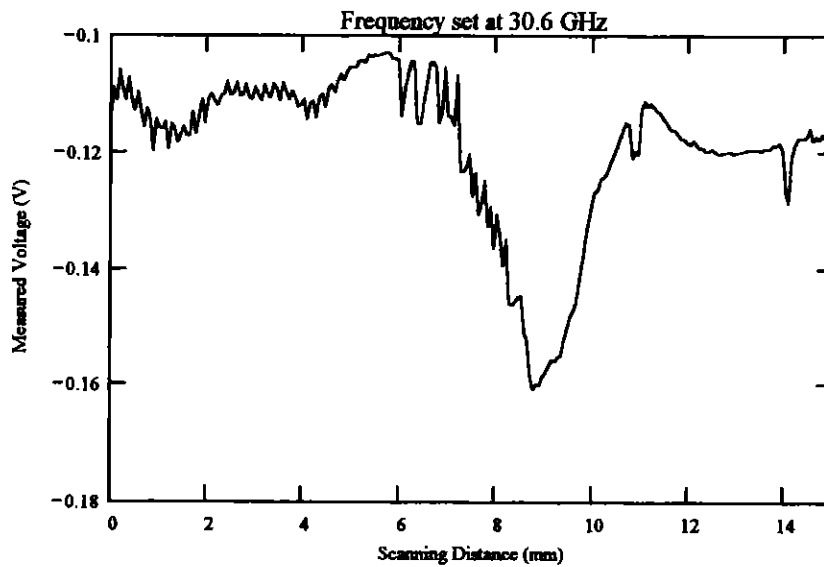


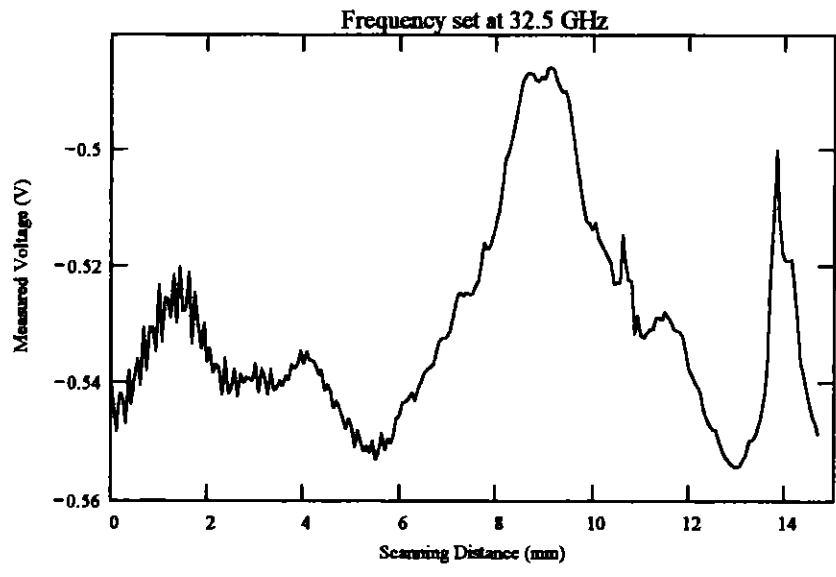
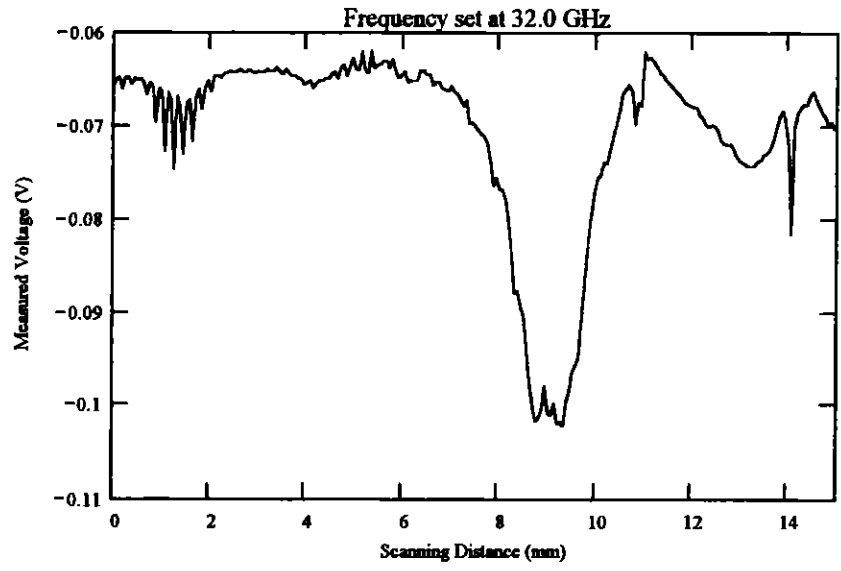


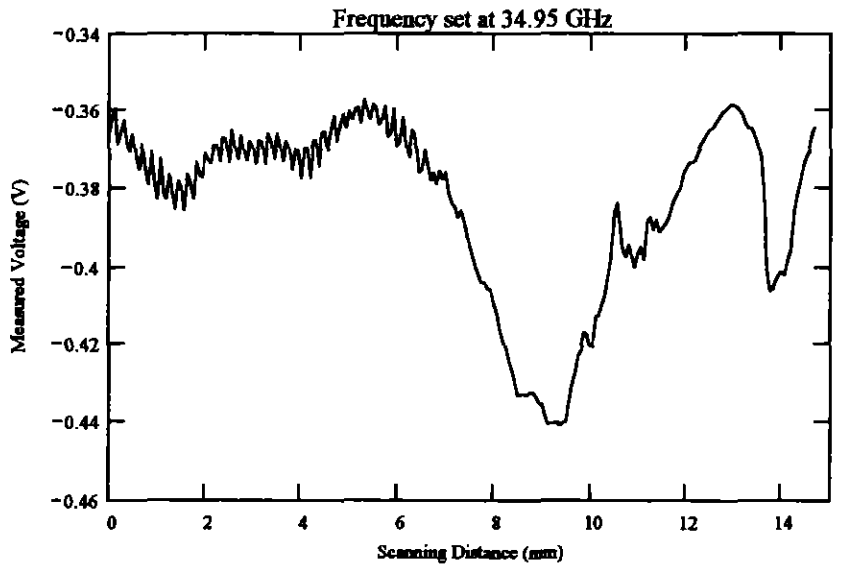
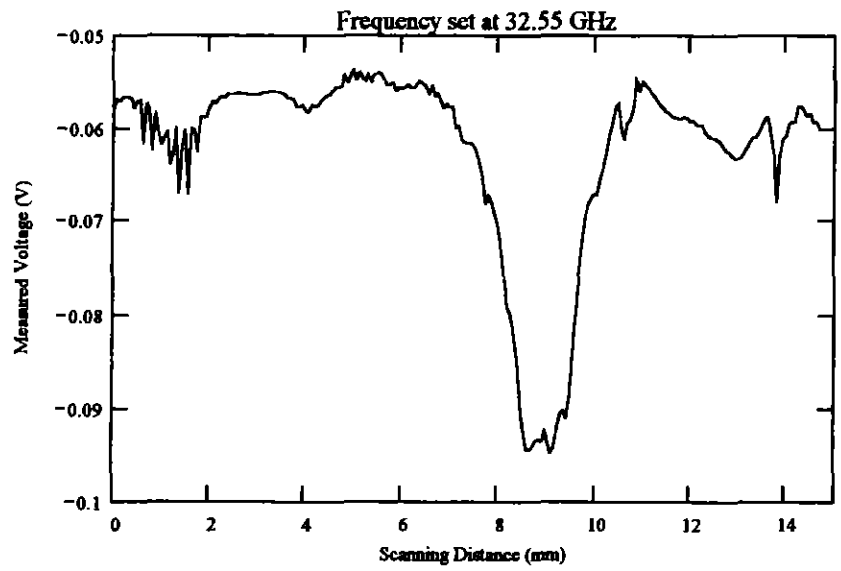


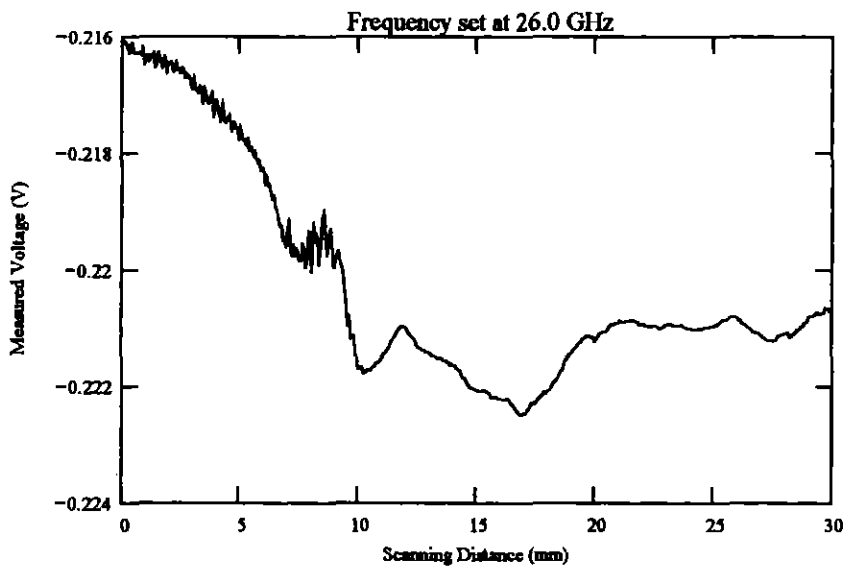
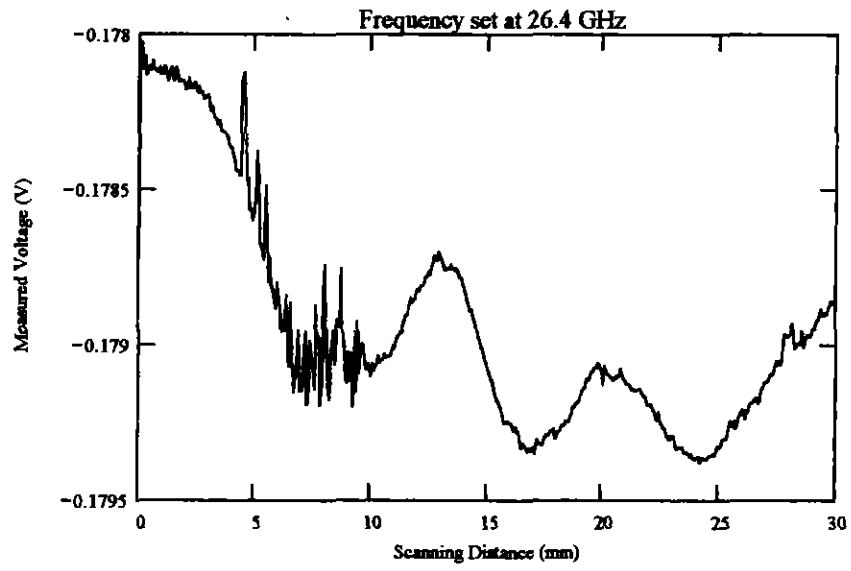


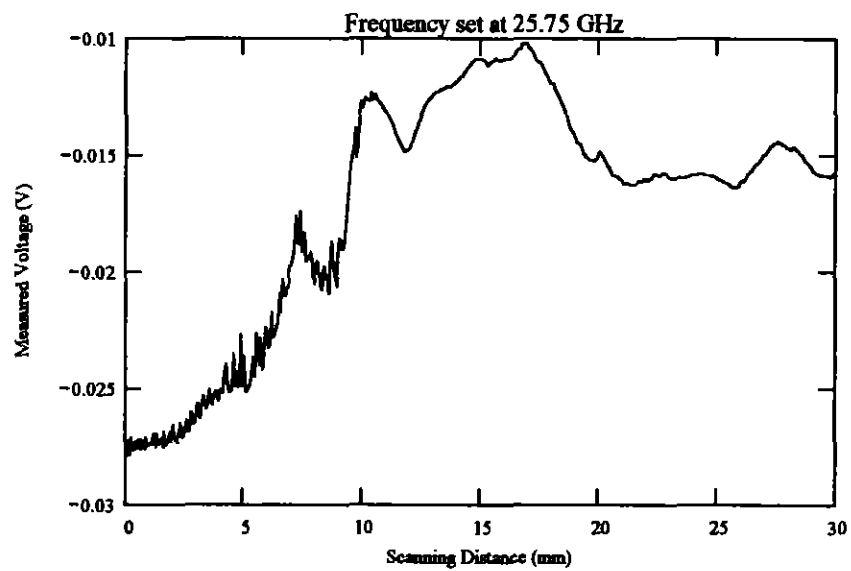
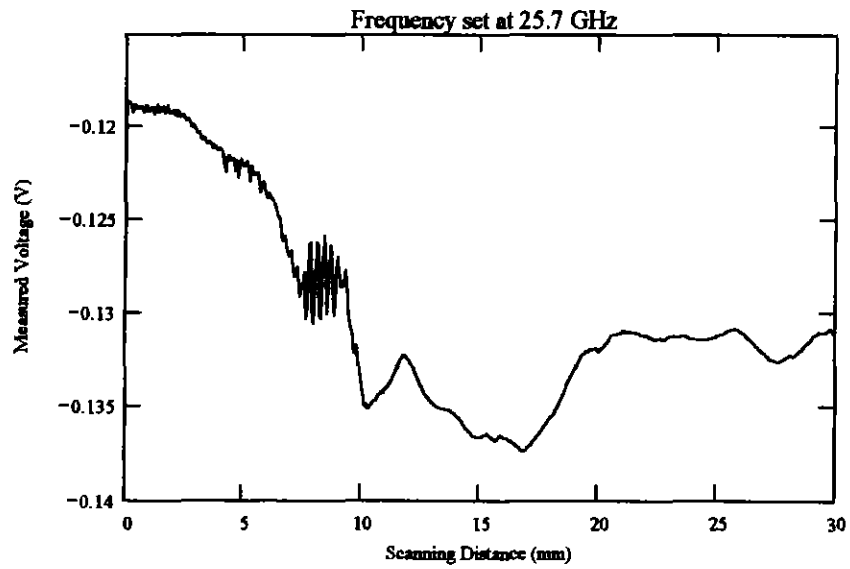
Frequency Band: Ka-band
Orientation: Scan parallel to crack length.
Probe: Coax no. 3
Scan Resolution: 0.064 mm per step
Scan length: 15 mm
Frequency: Varies

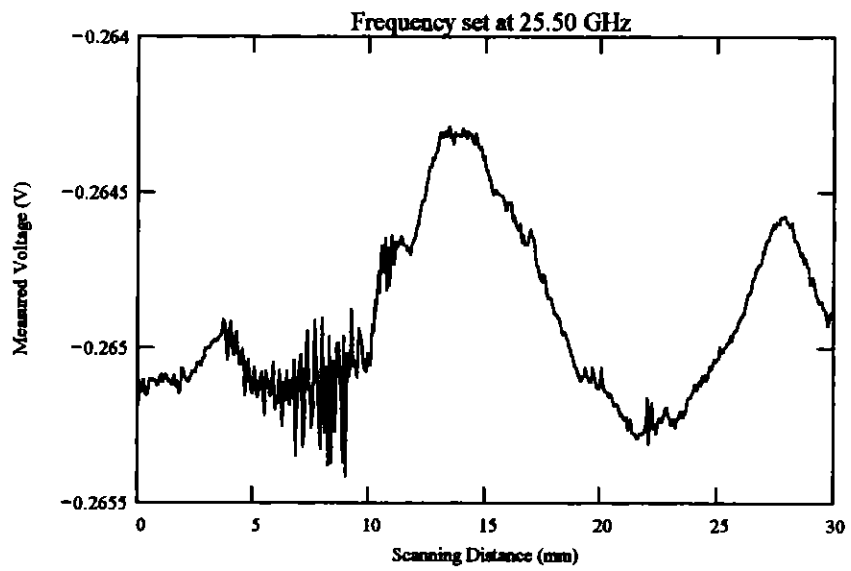
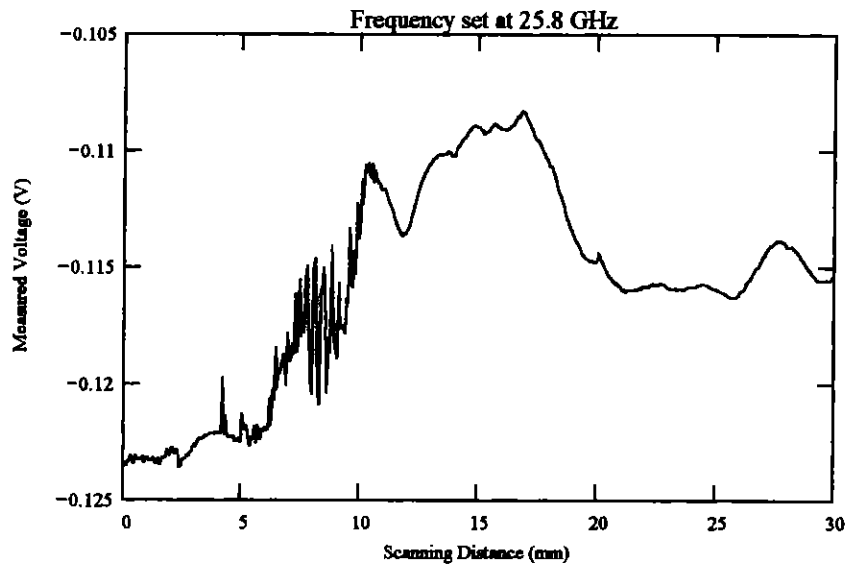


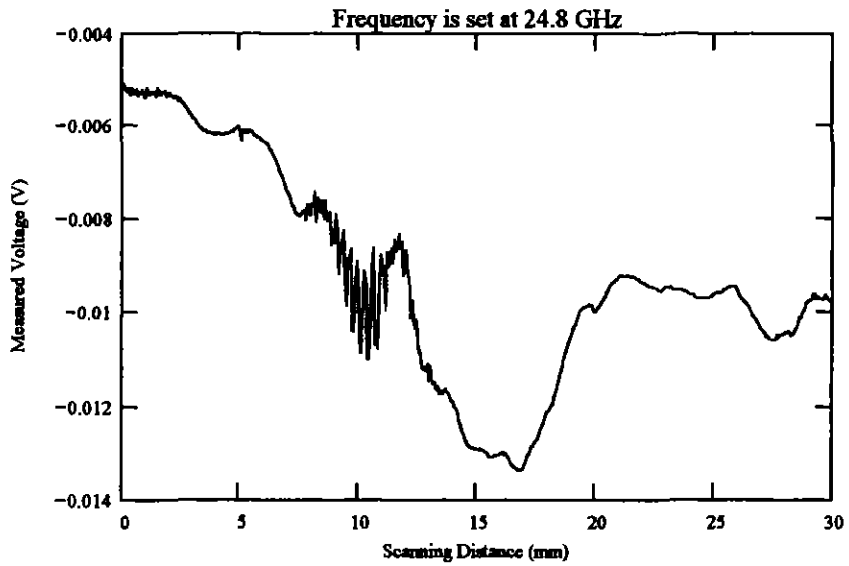
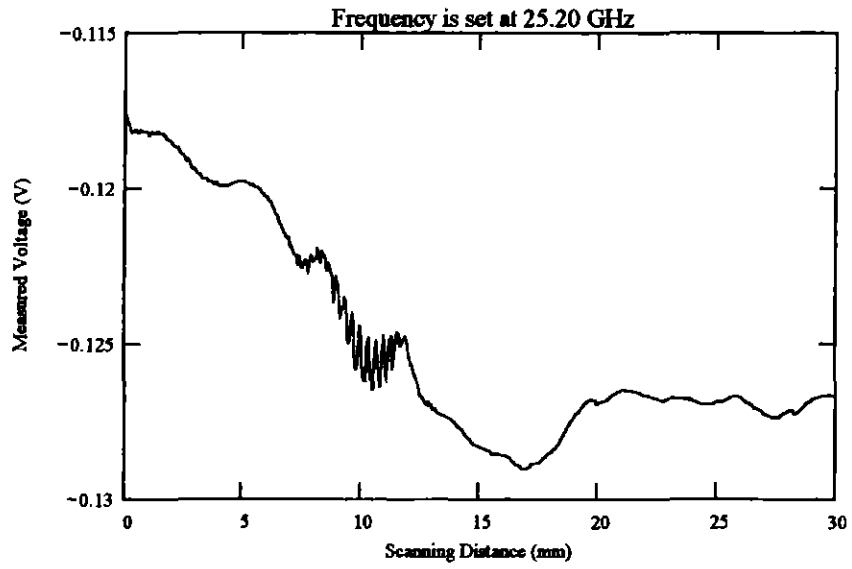


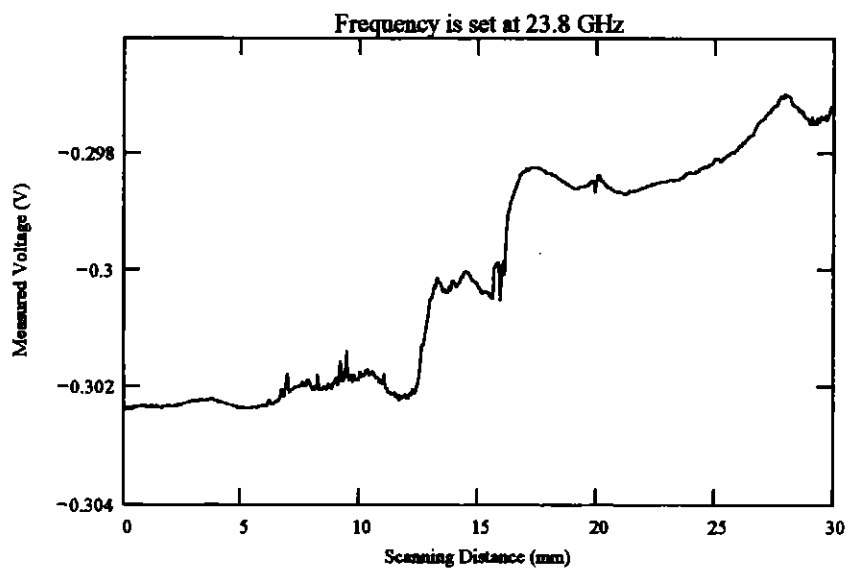
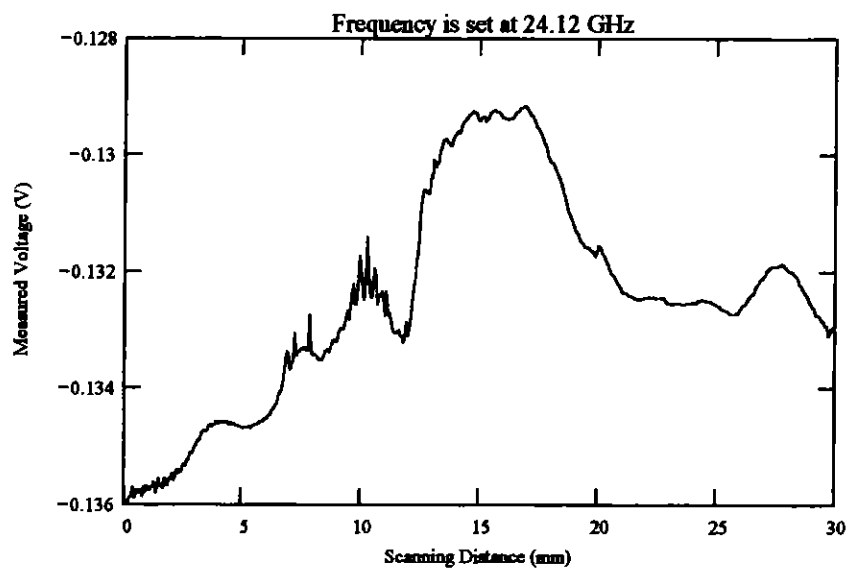


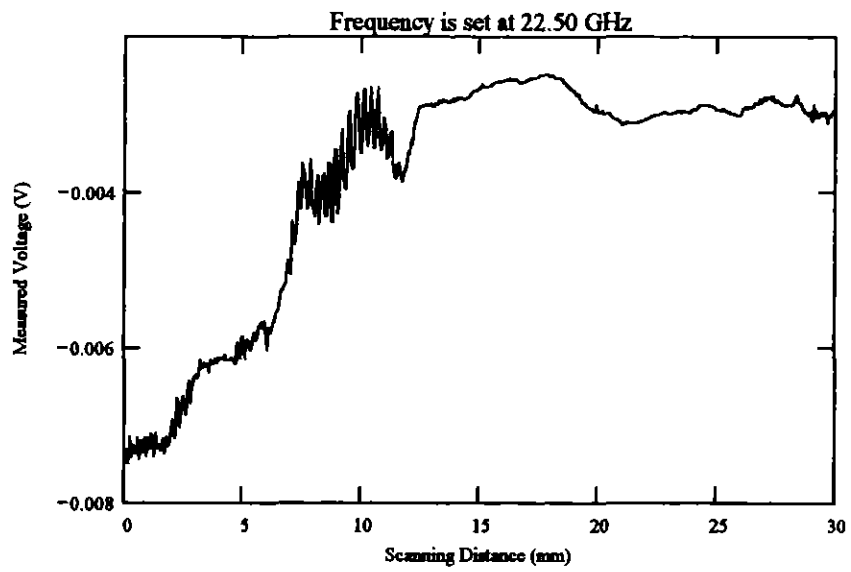
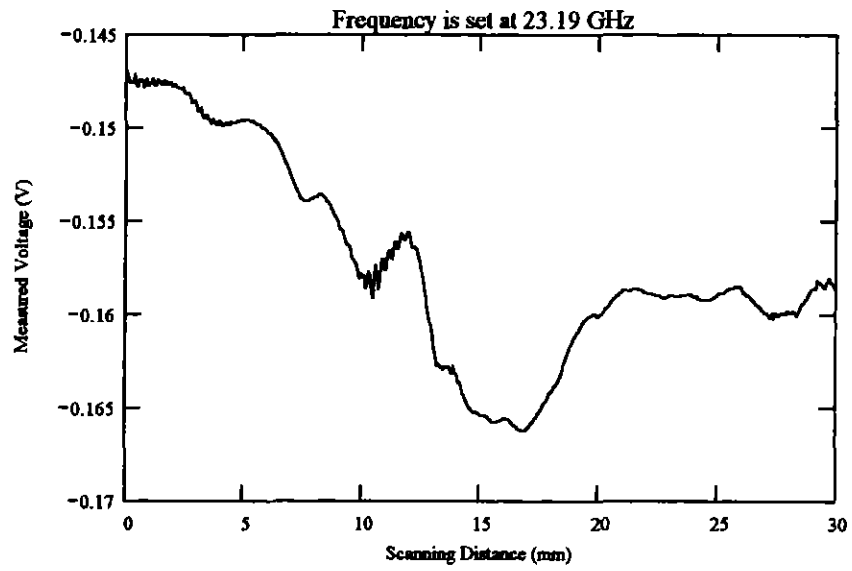




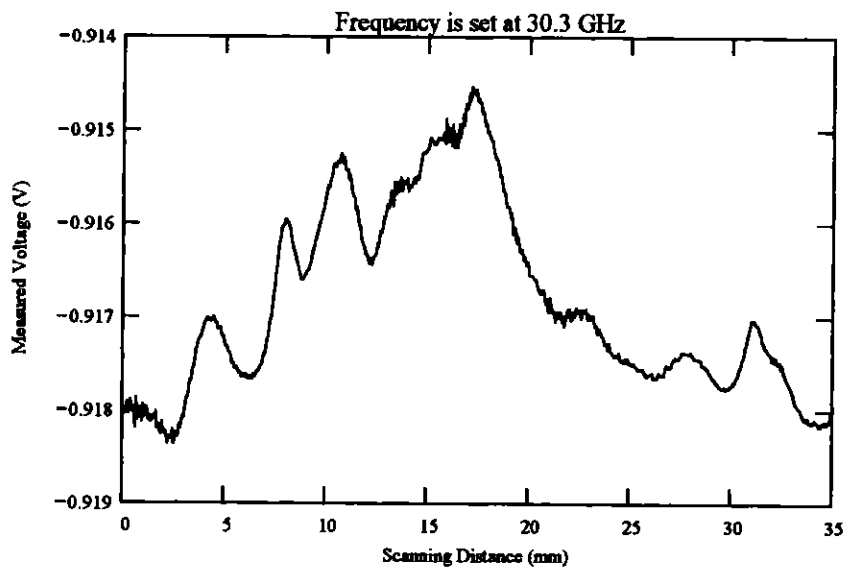


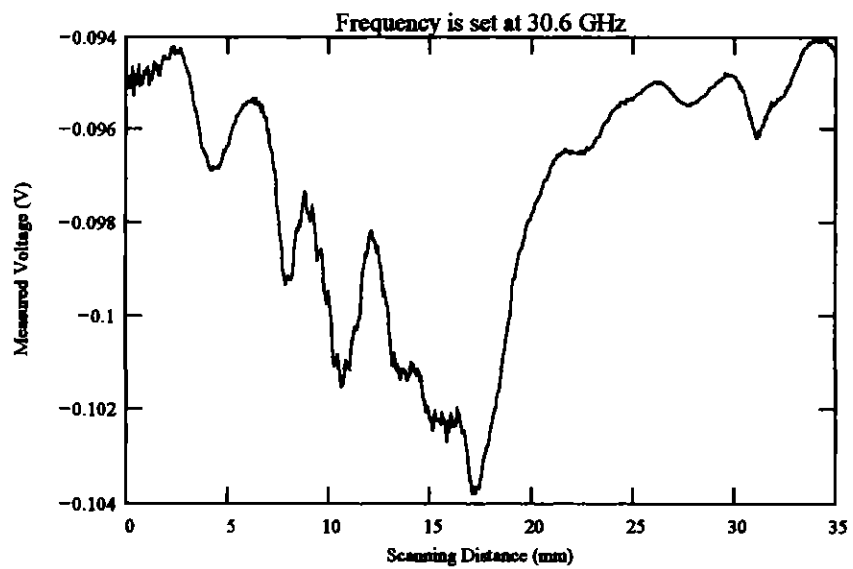
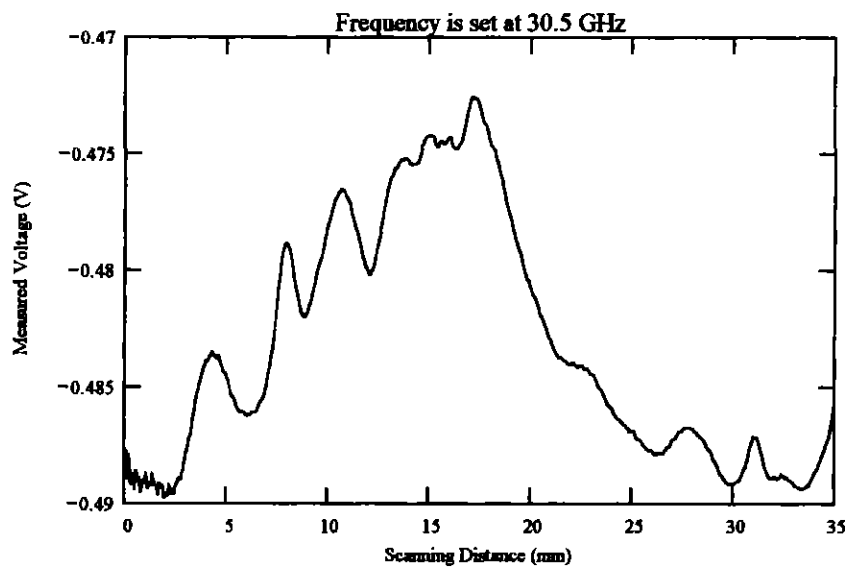


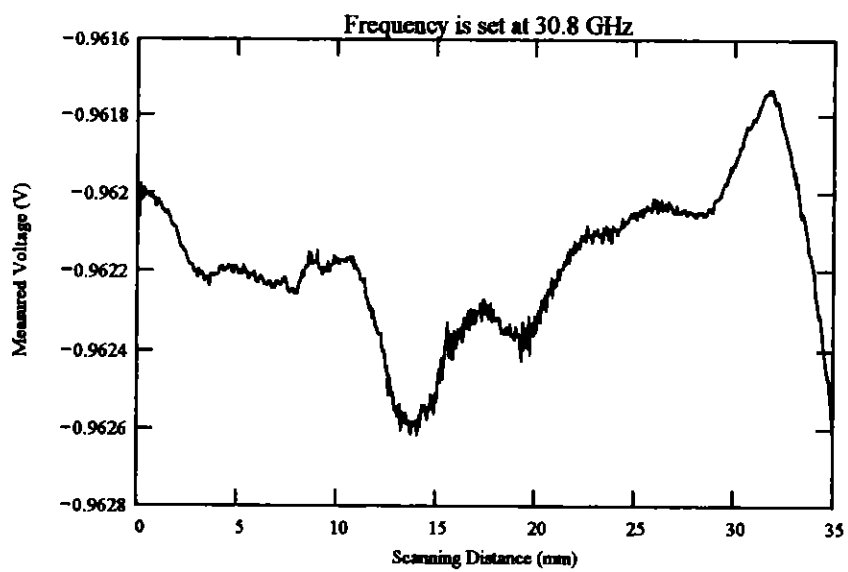
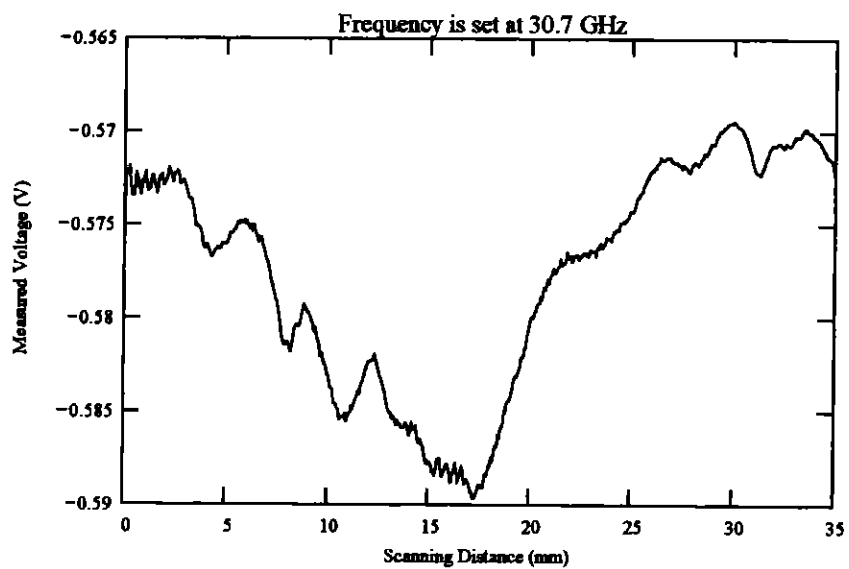


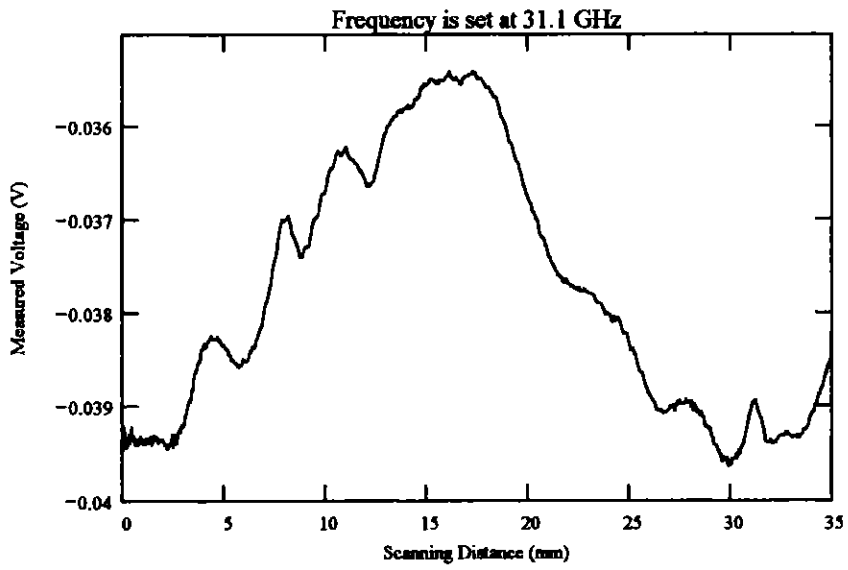
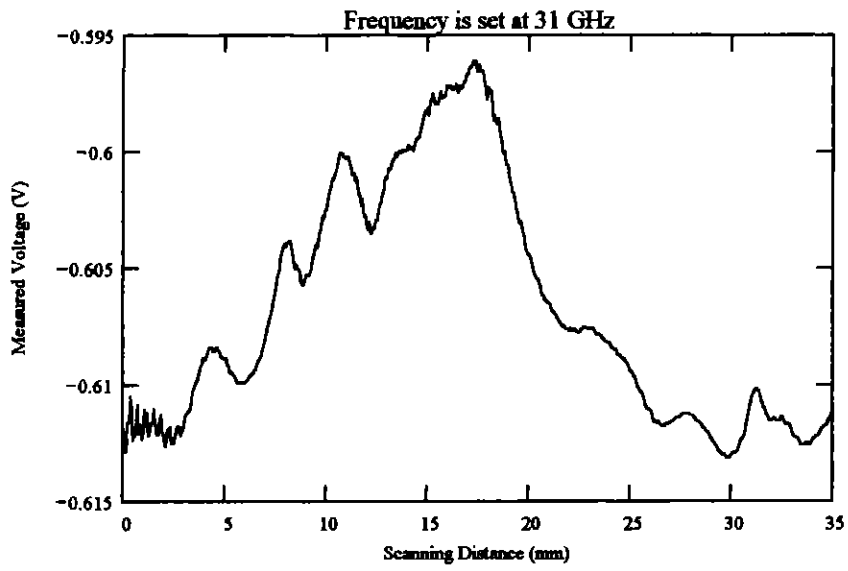


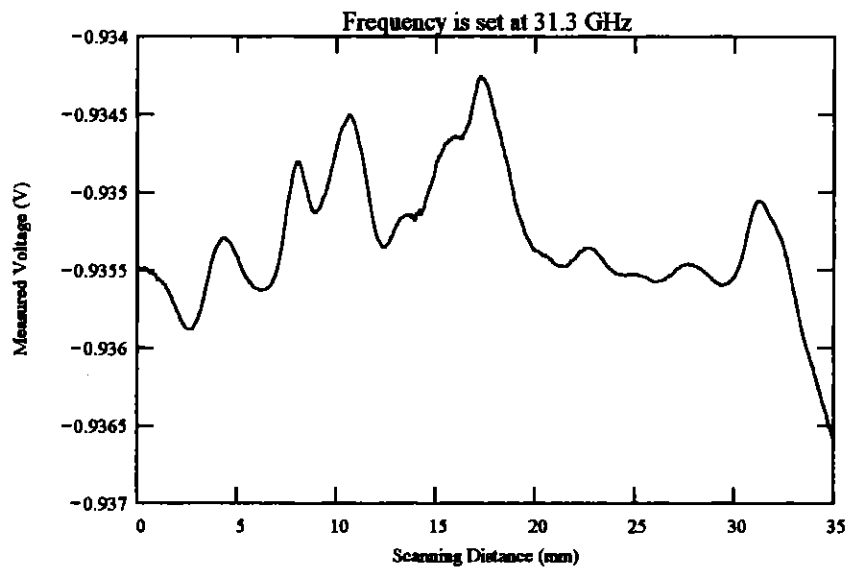
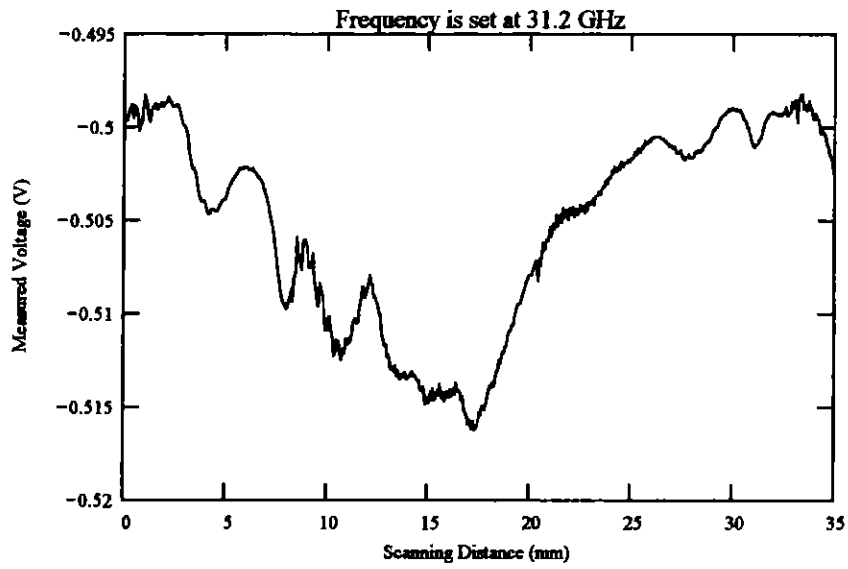
Frequency Band: Ka-band
Orientation: Scan parallel to crack length.
Probe: Coax no. 3
Scan Resolution: 0.064 mm per step
Scan length: 35 mm
Frequency: Varies

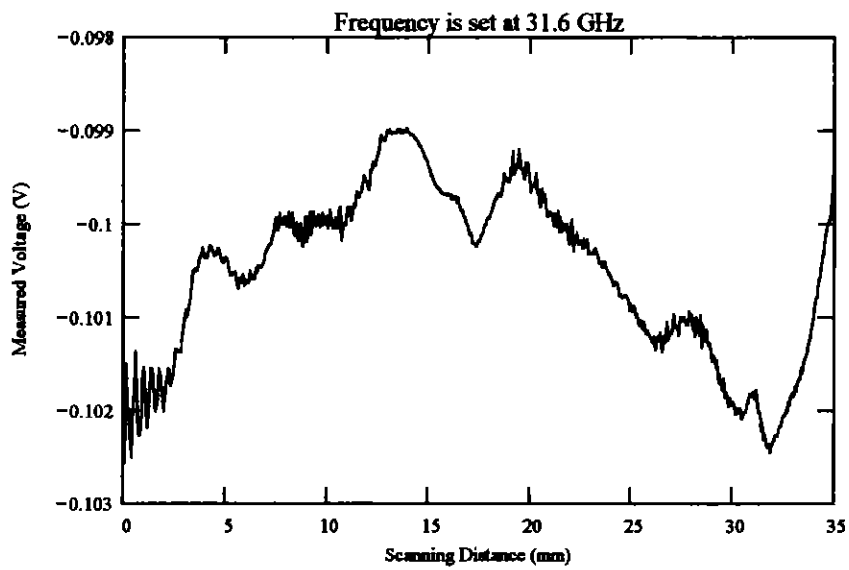
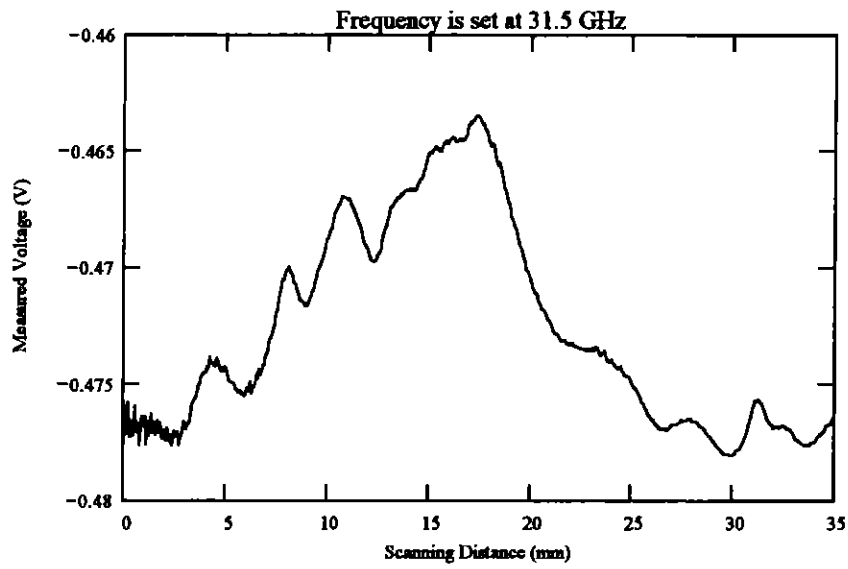


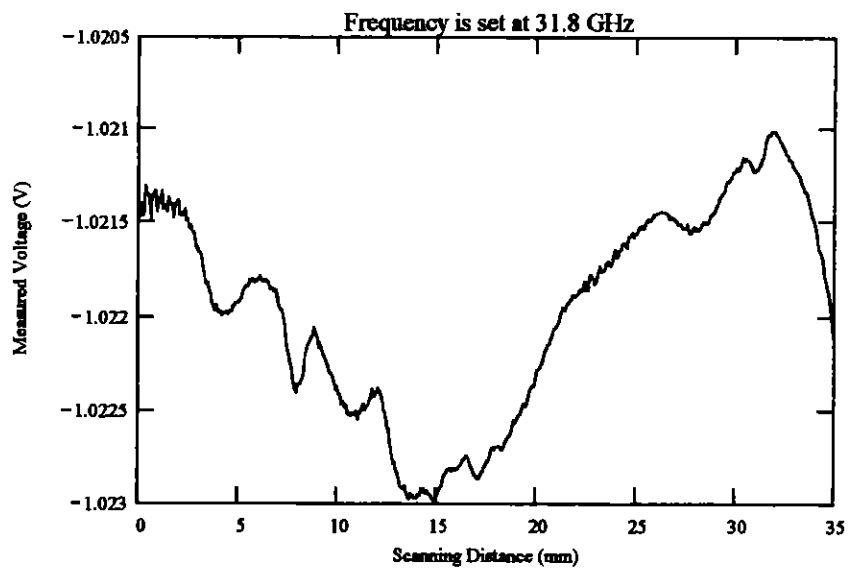
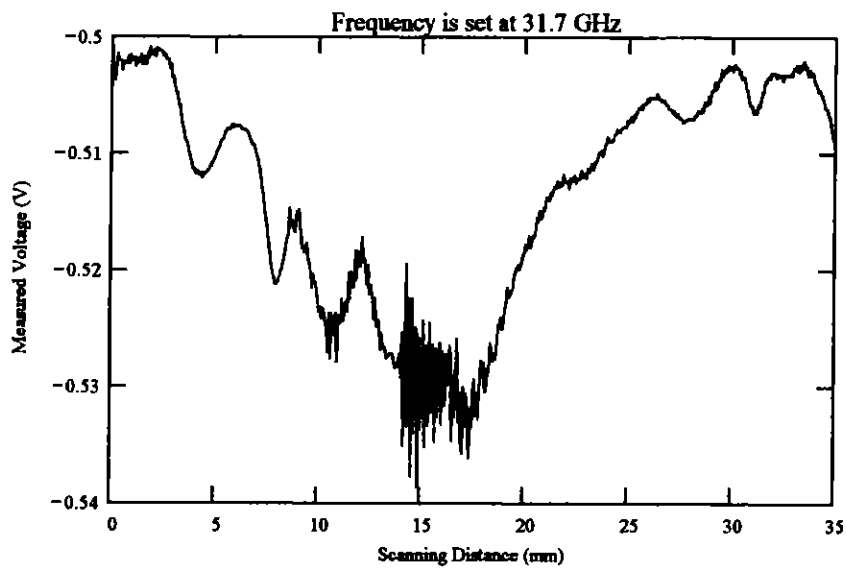


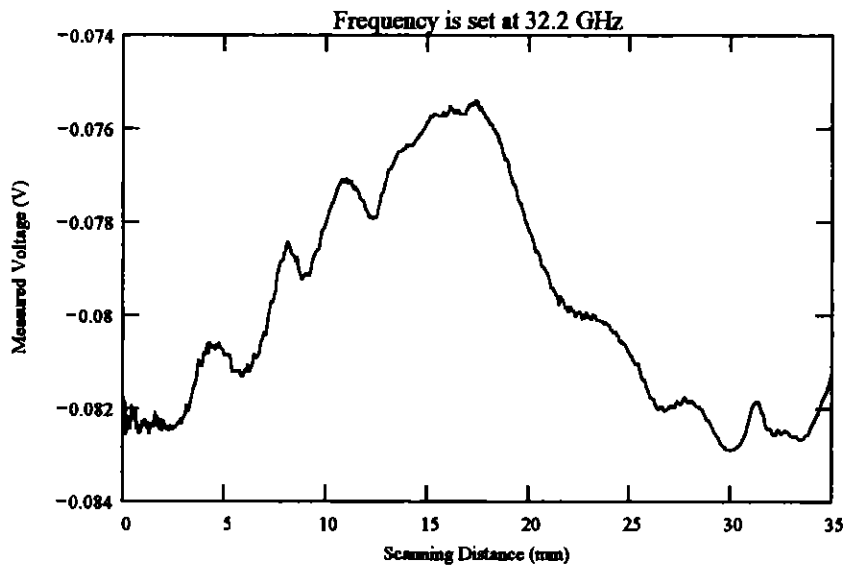
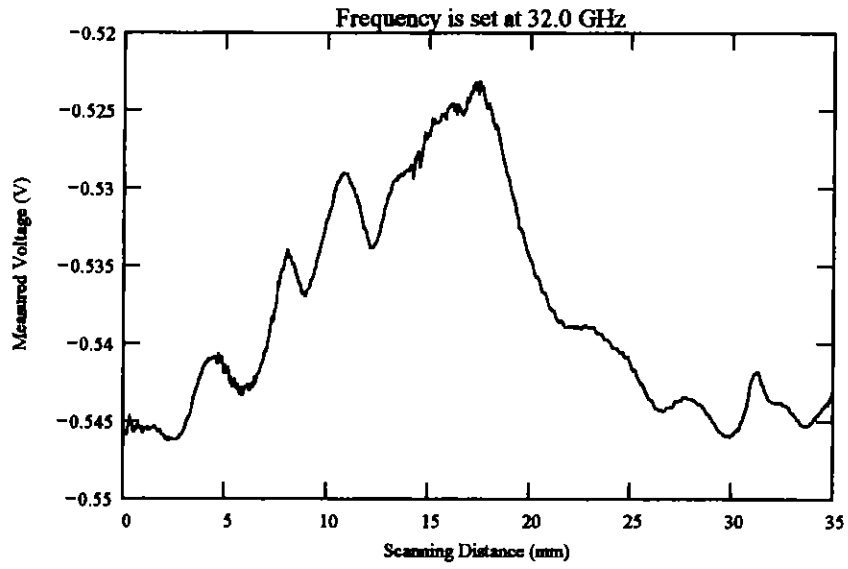


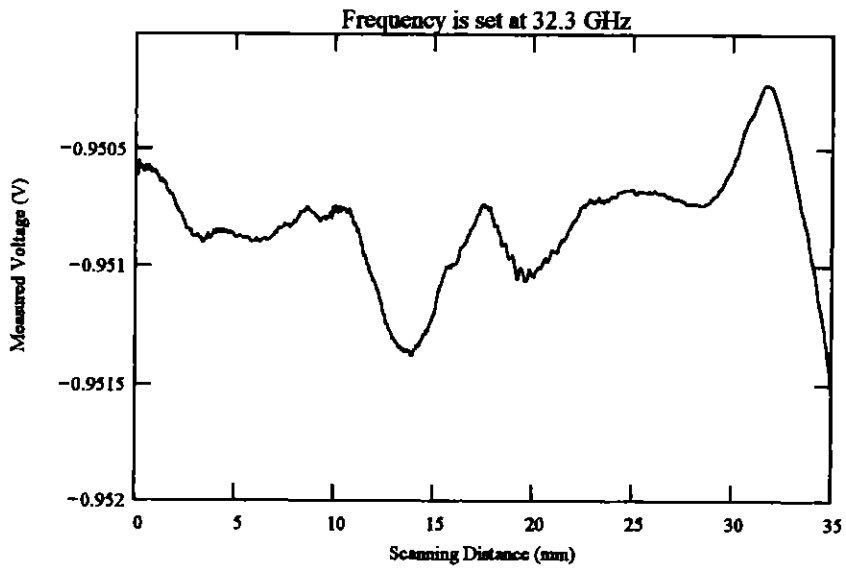
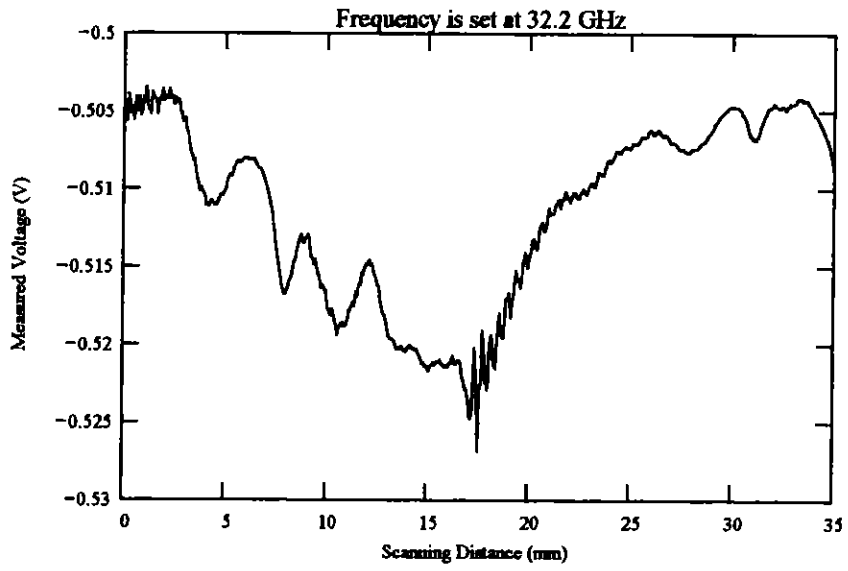


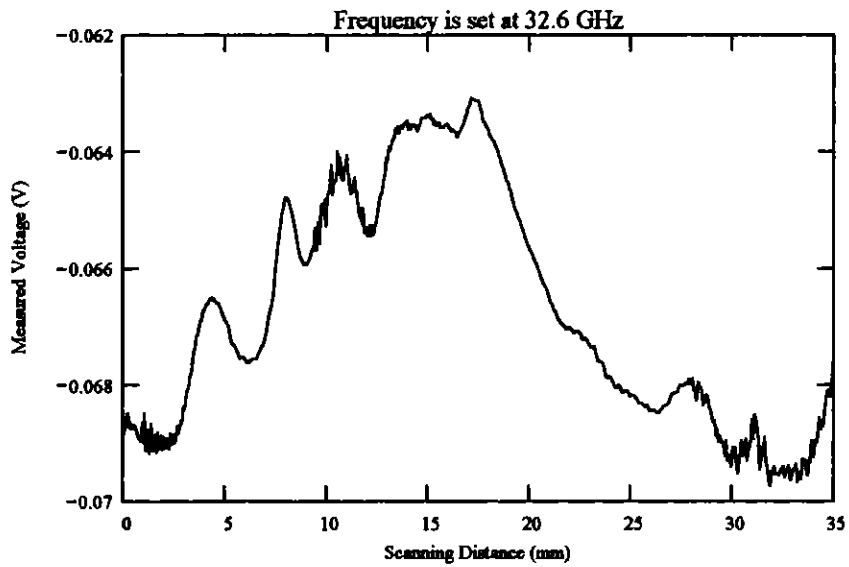
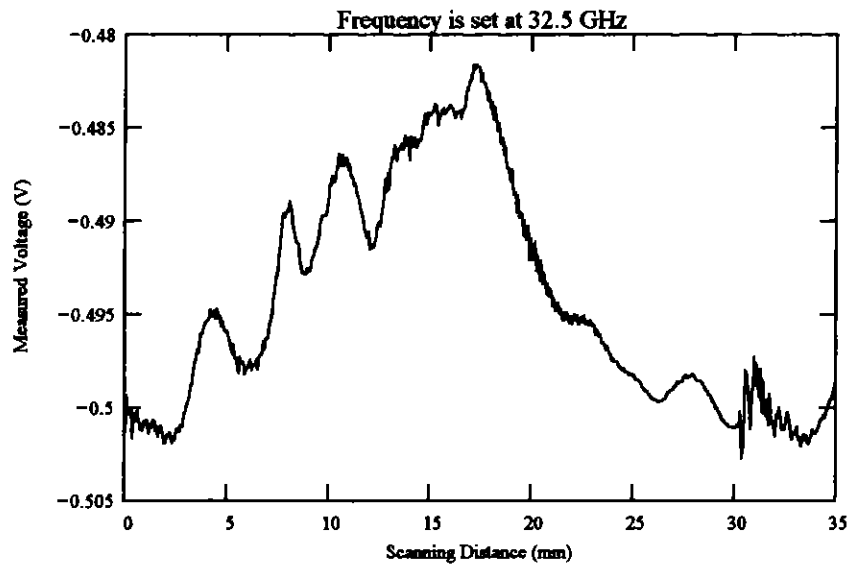


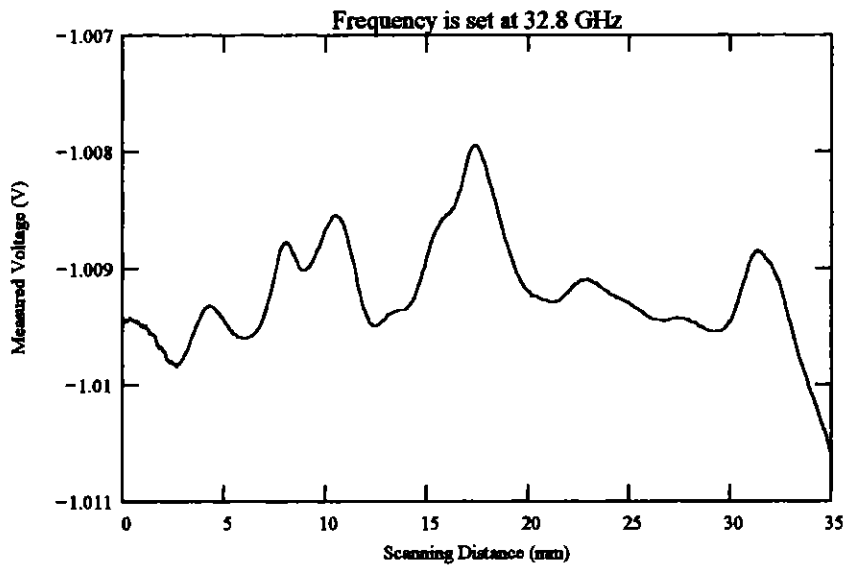
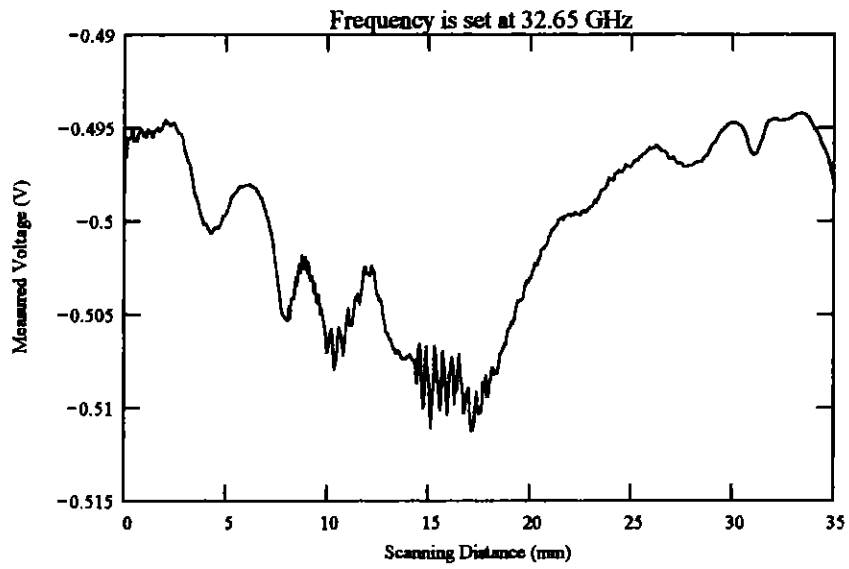


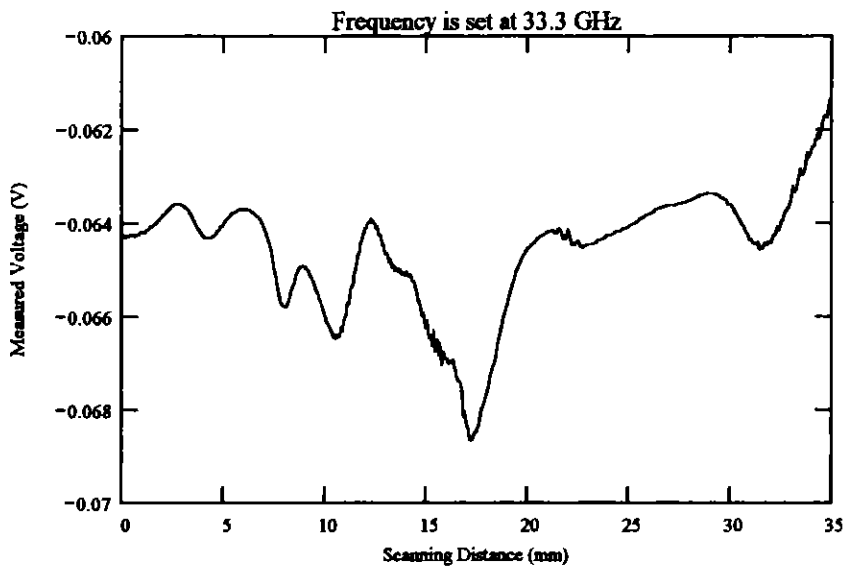
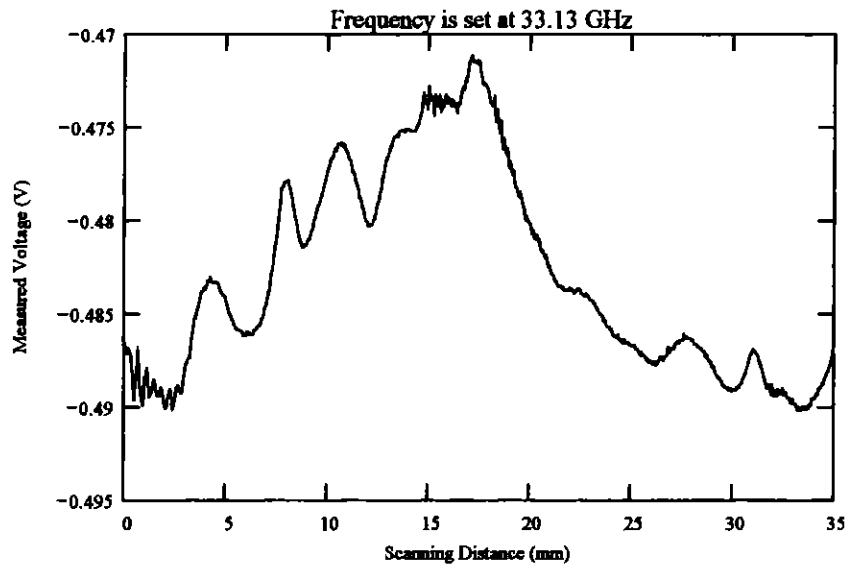


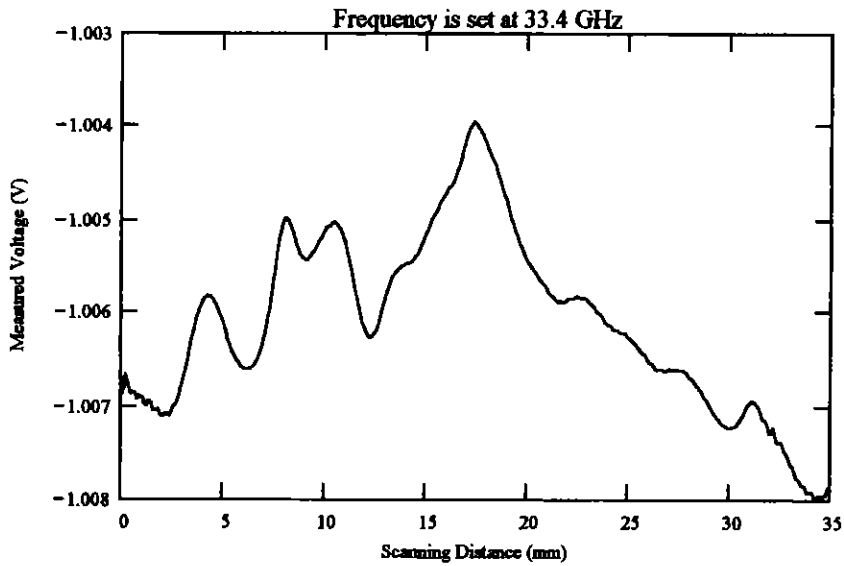
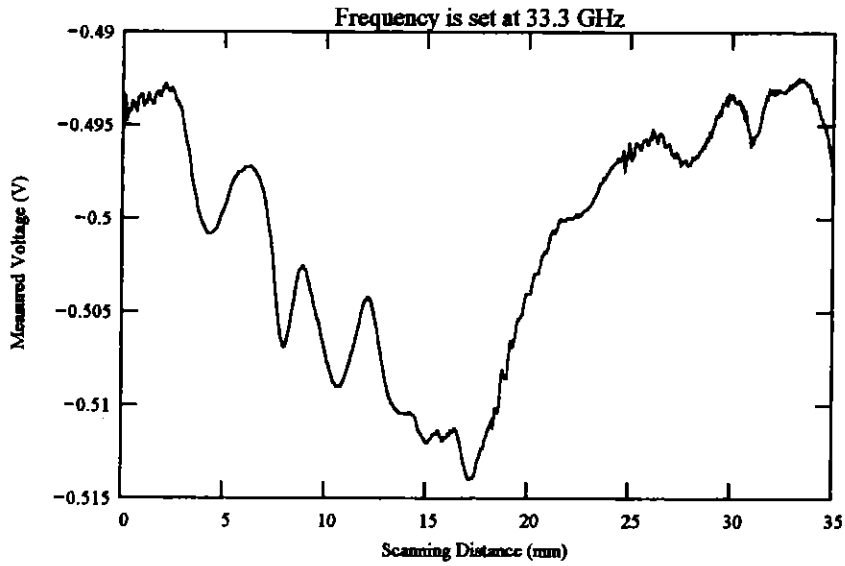


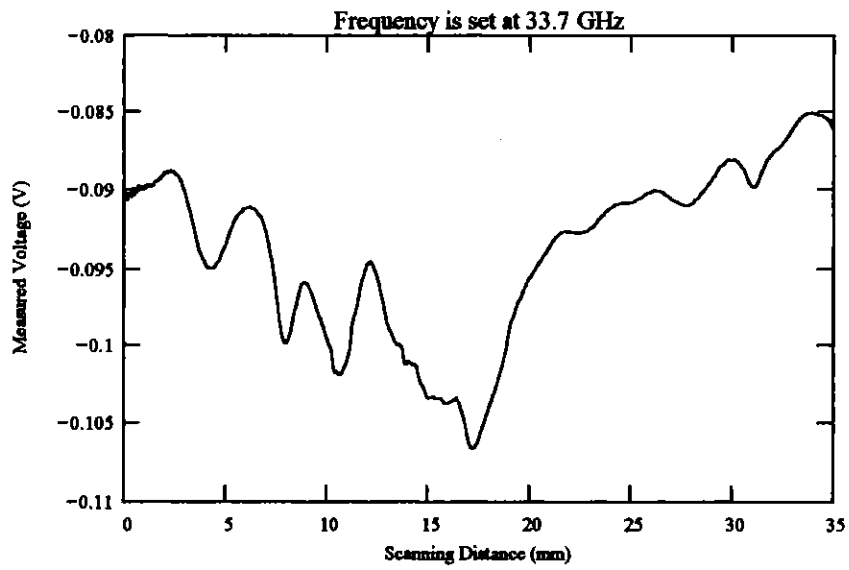
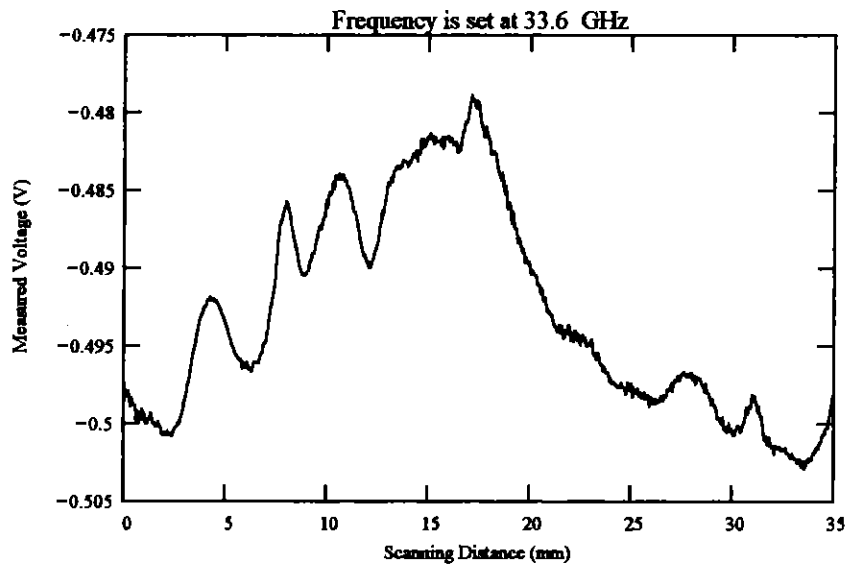


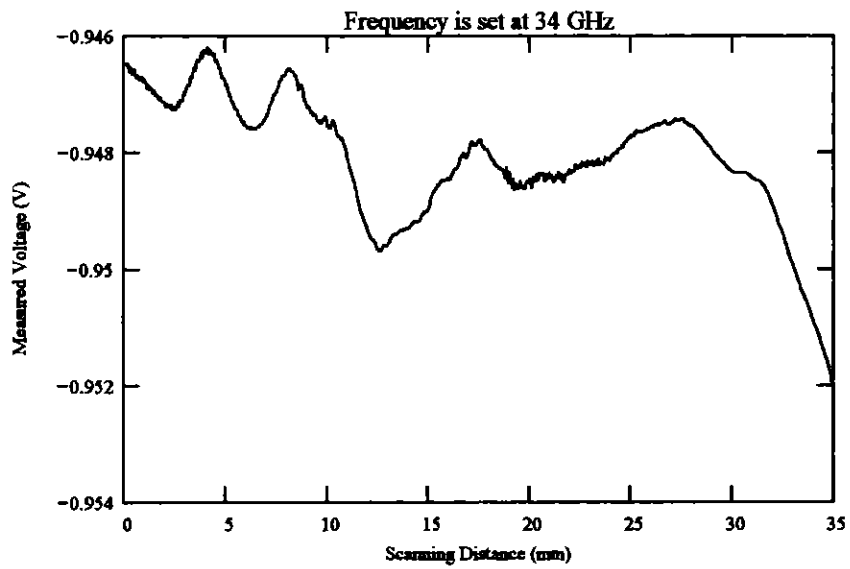
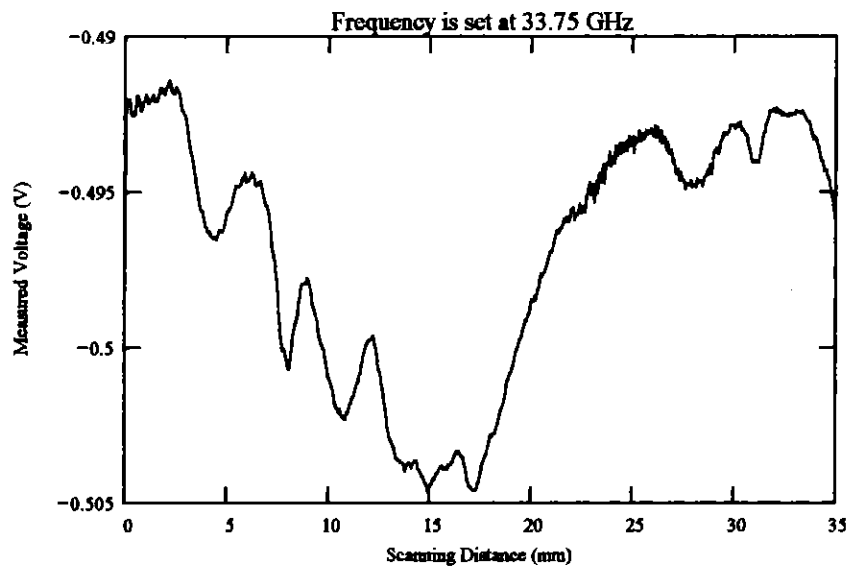


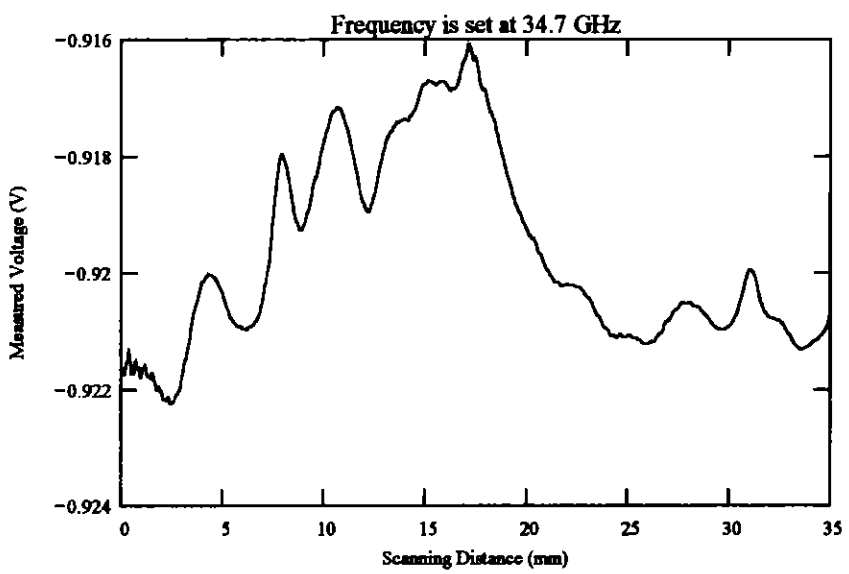
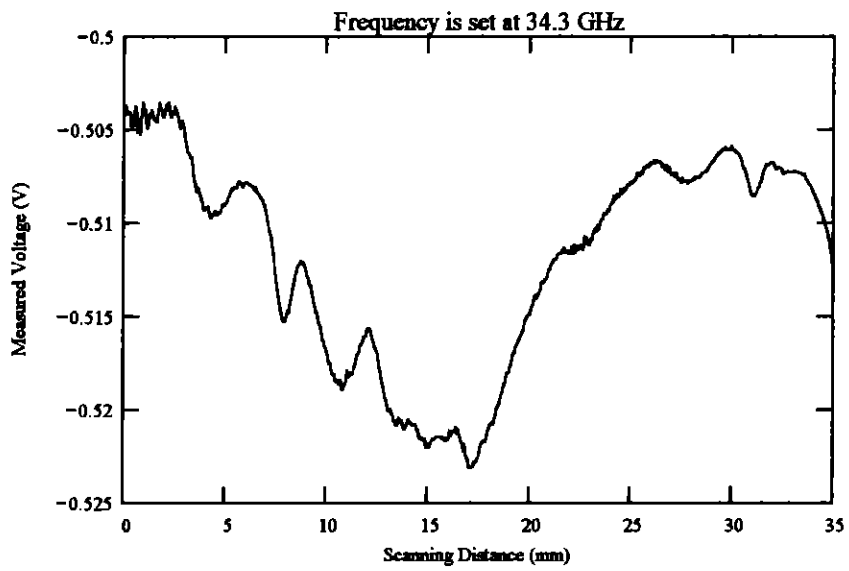


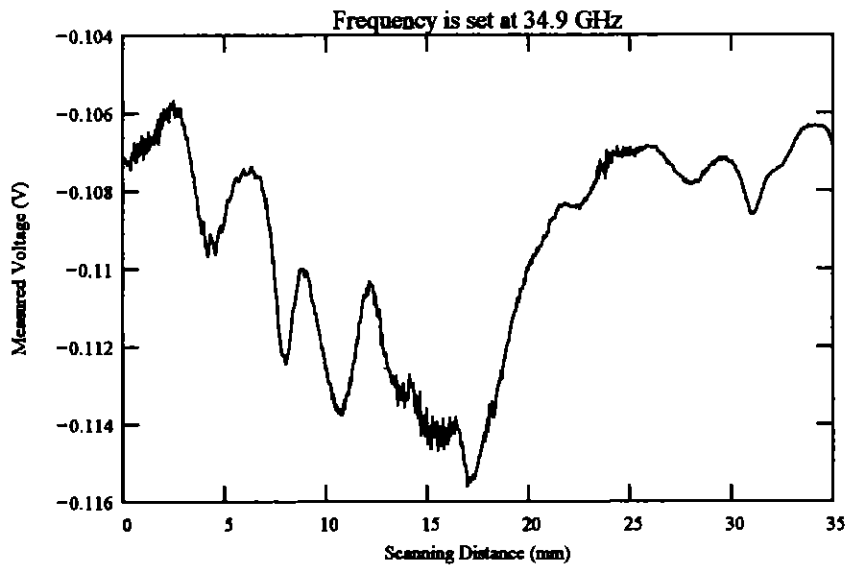
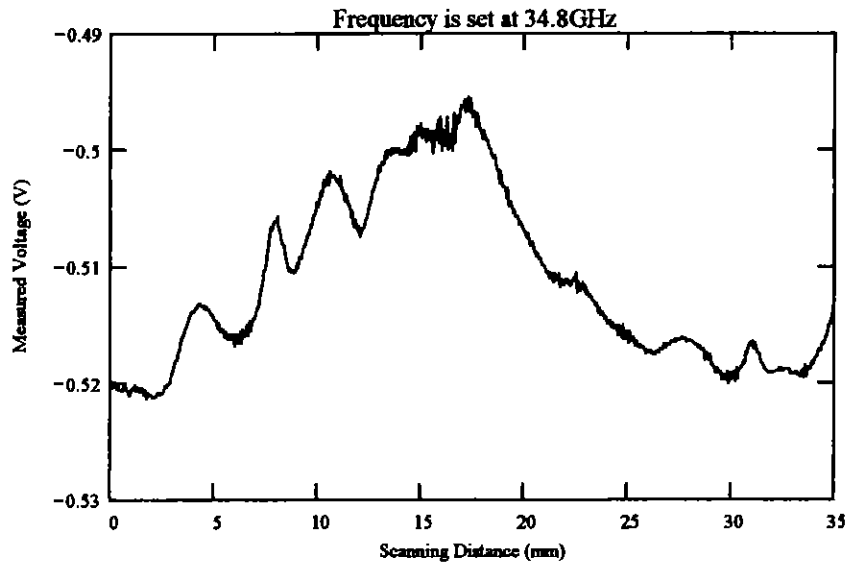


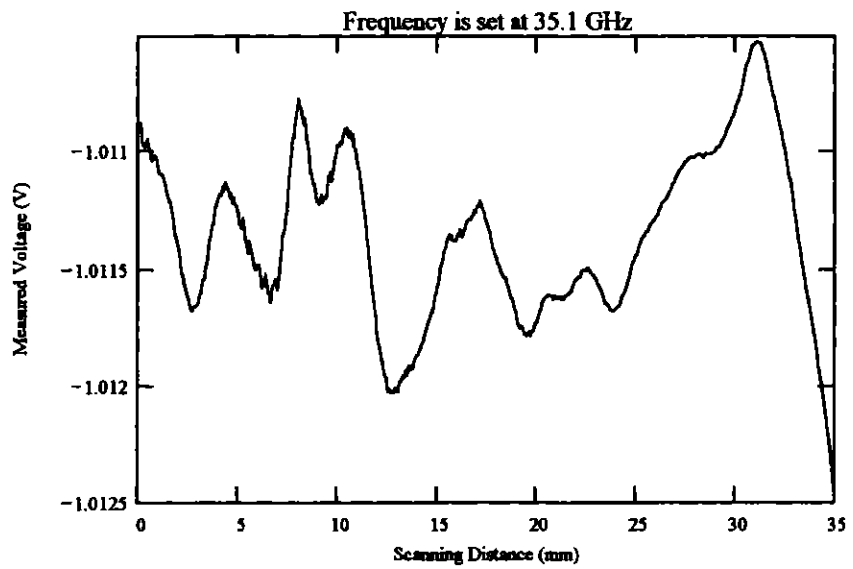
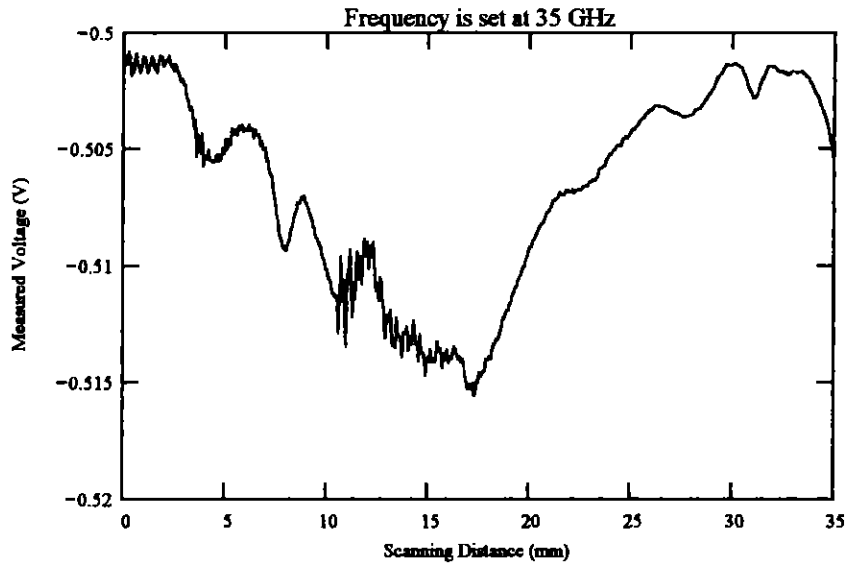


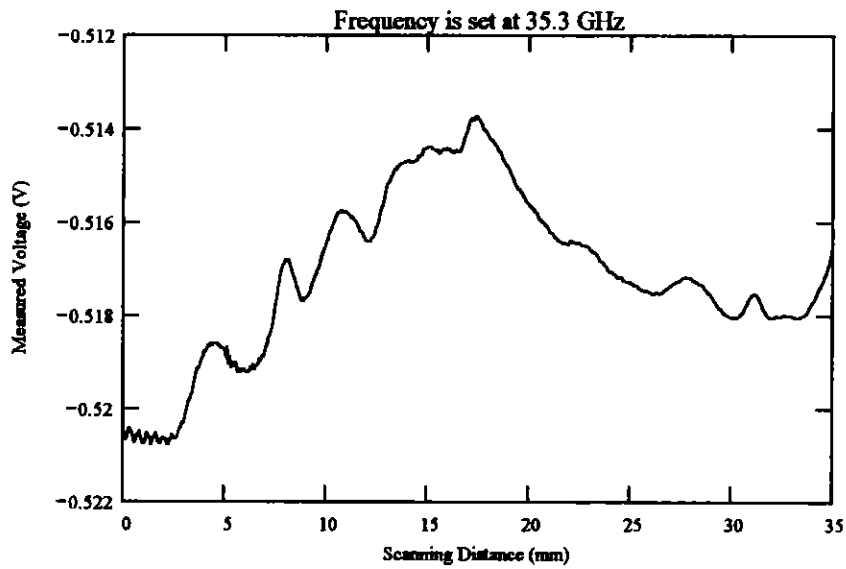
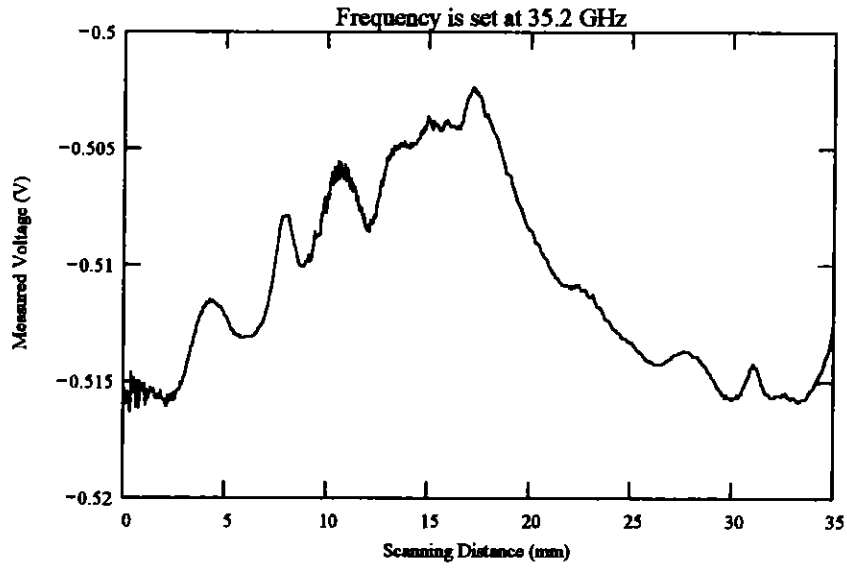


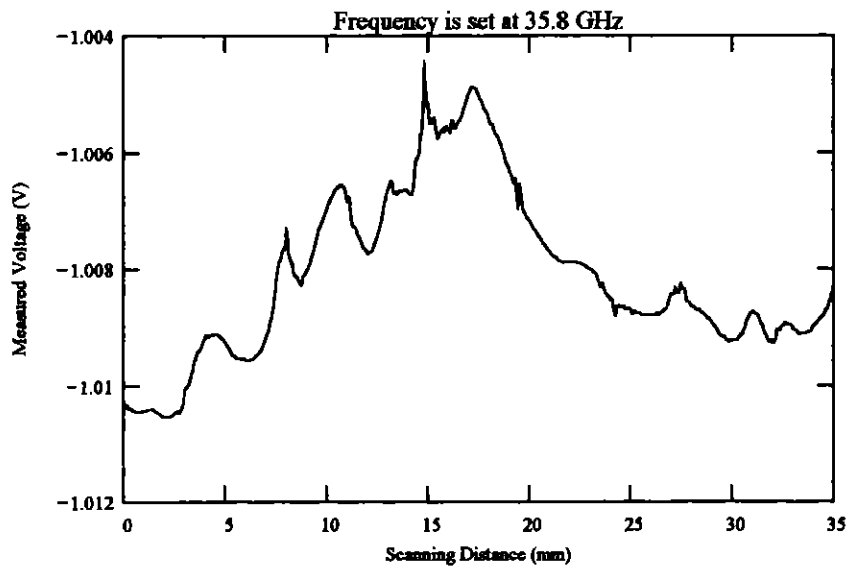
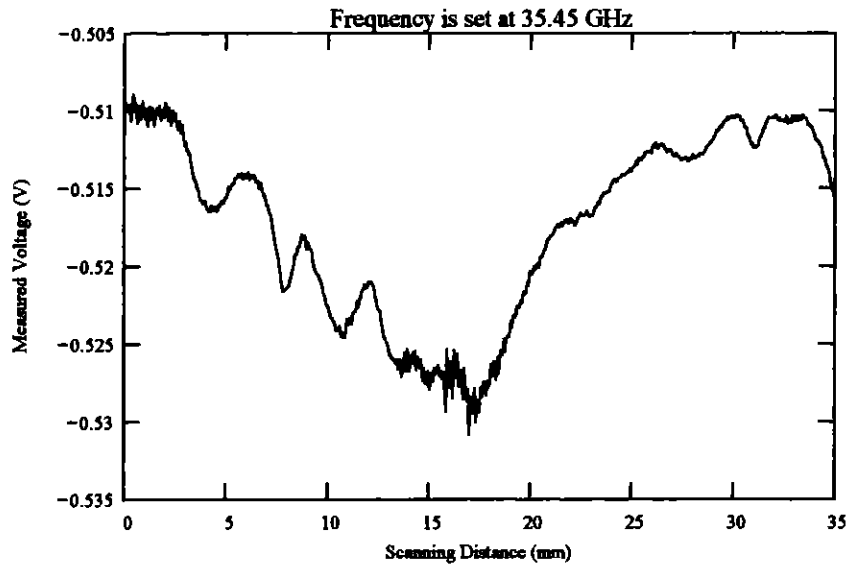


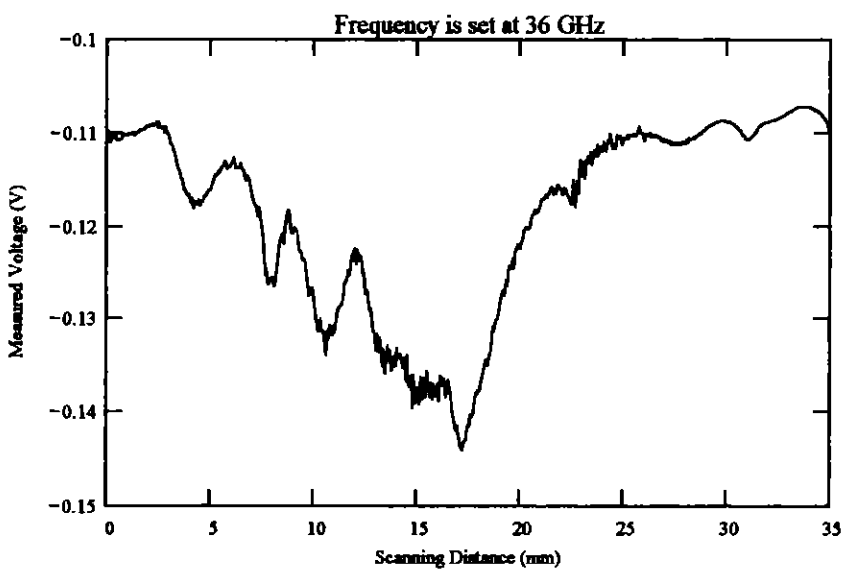
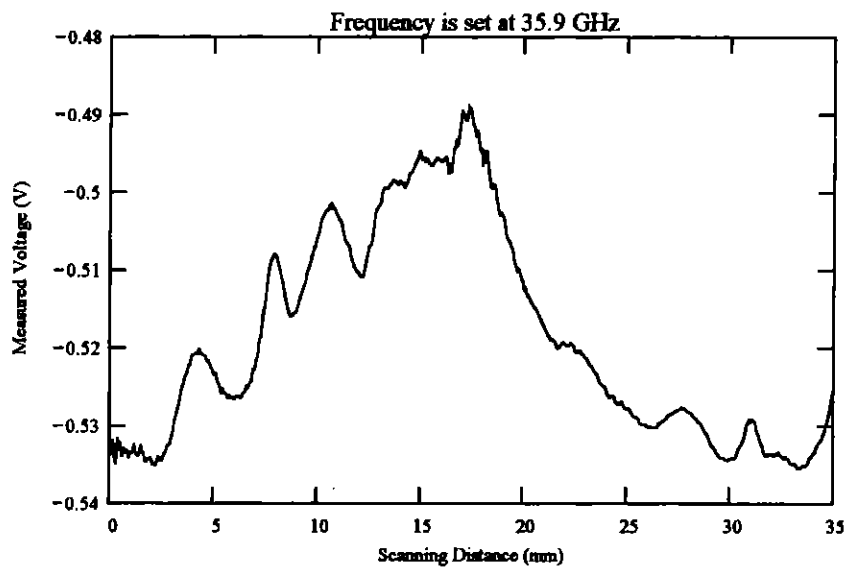








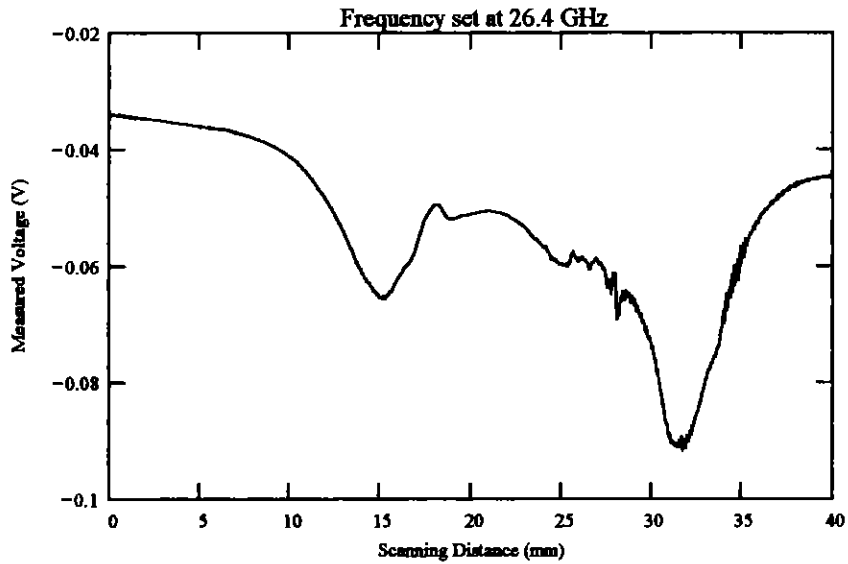


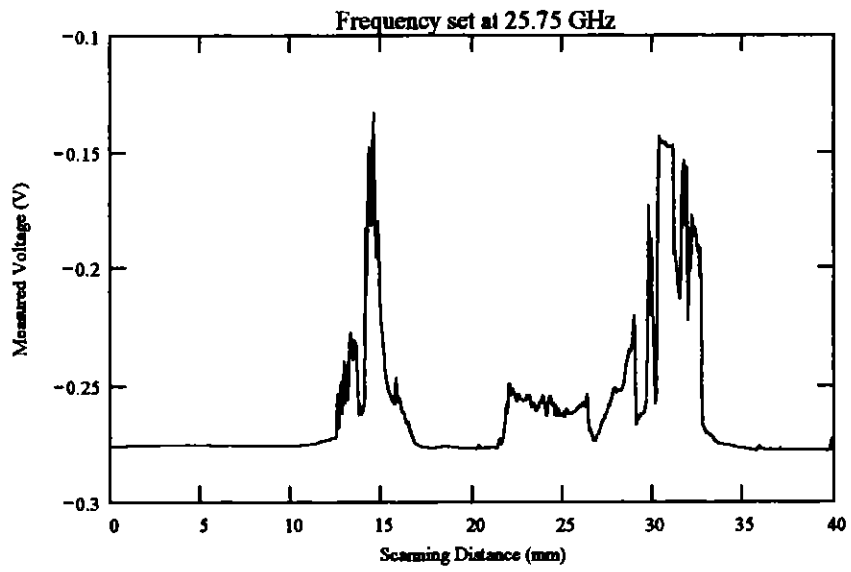
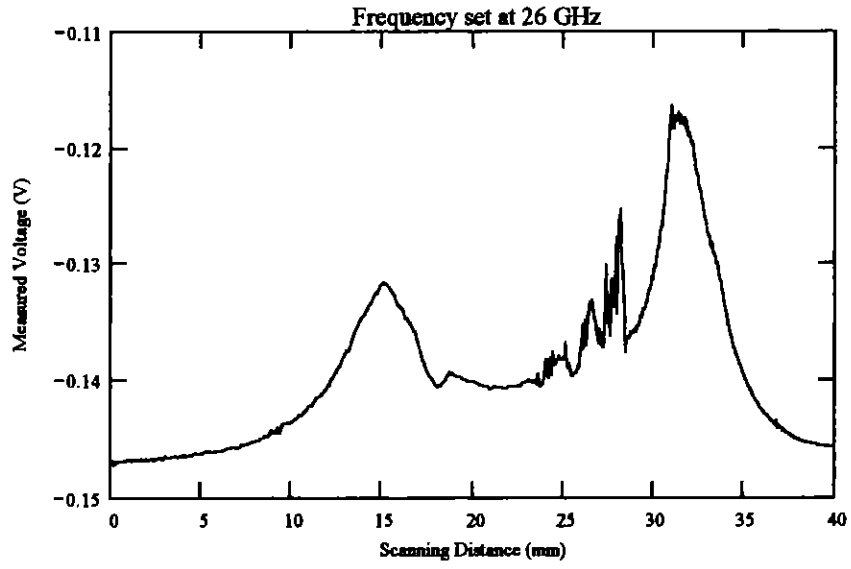


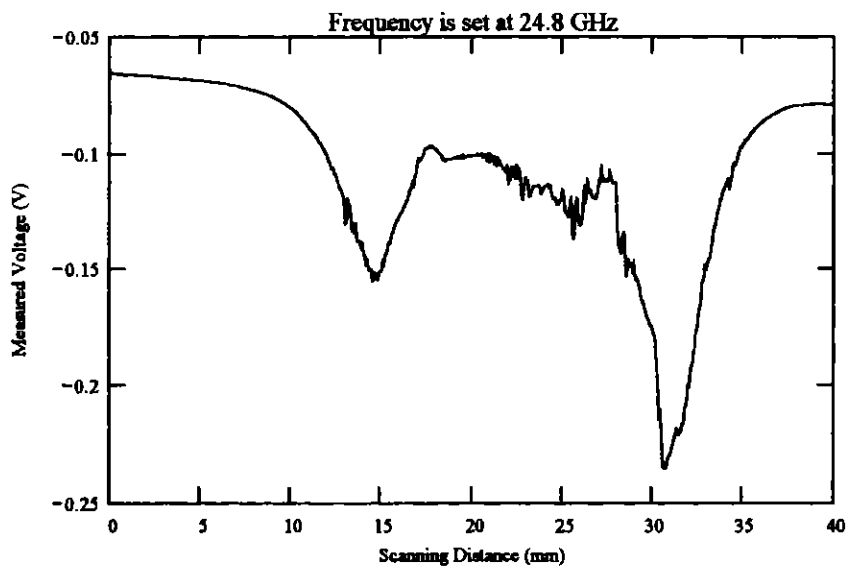
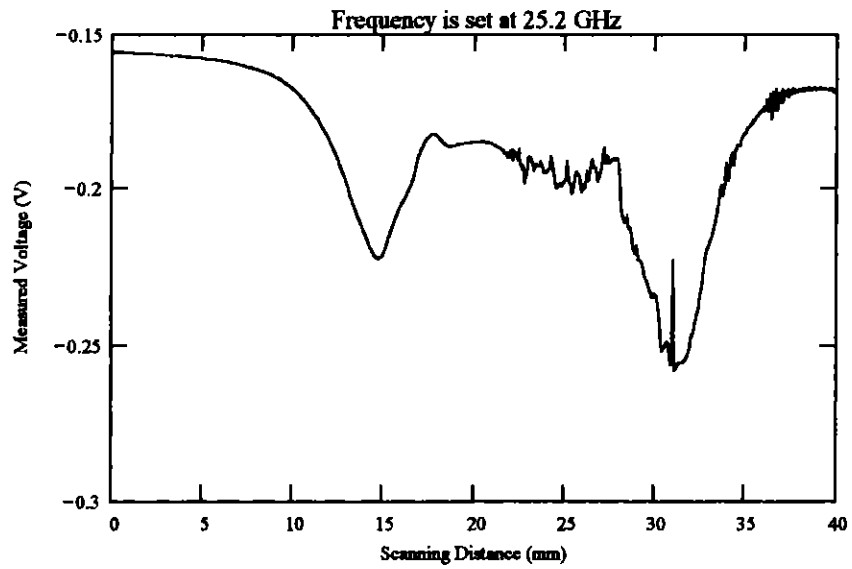
B. Crack #2

This is a Toe Indication crack. The length of the crack is 30 mm. This crack runs parallel to the welded joint.

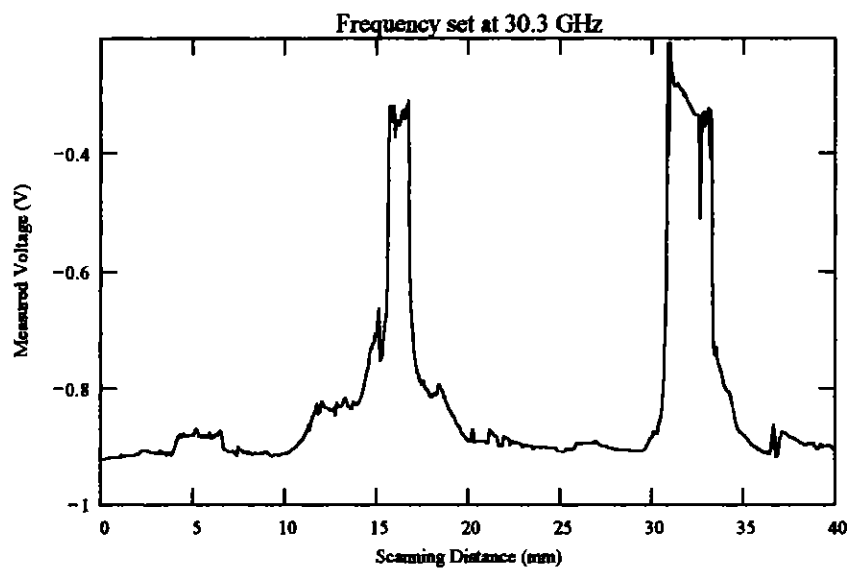
Frequency Band: K-band
Orientation: Scan parallel to crack length.
Probe: Coax no. 3
Scan Resolution: 0.064 mm per step
Scan length: 40 mm
Frequency: varies

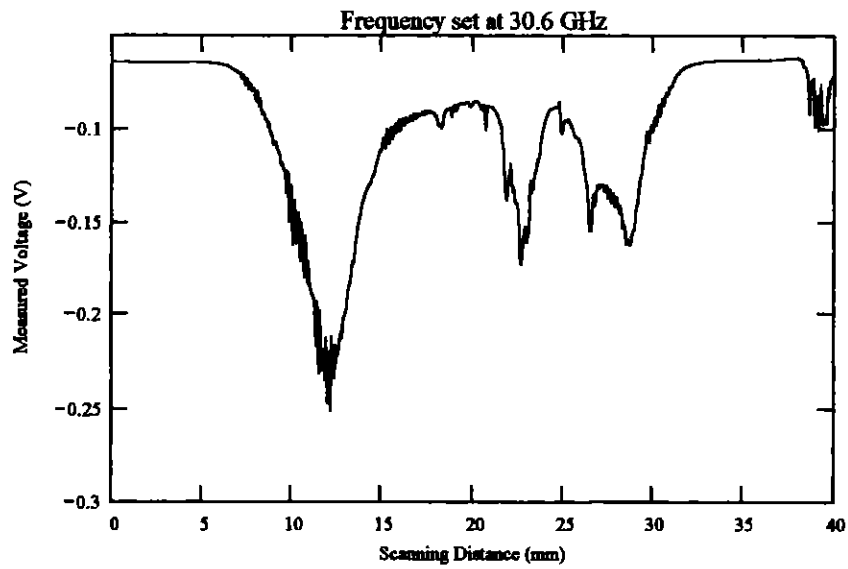
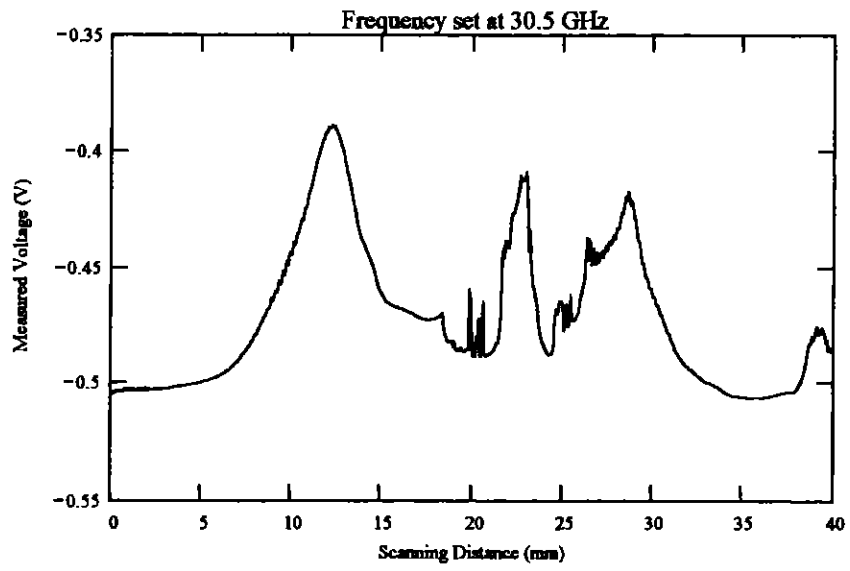


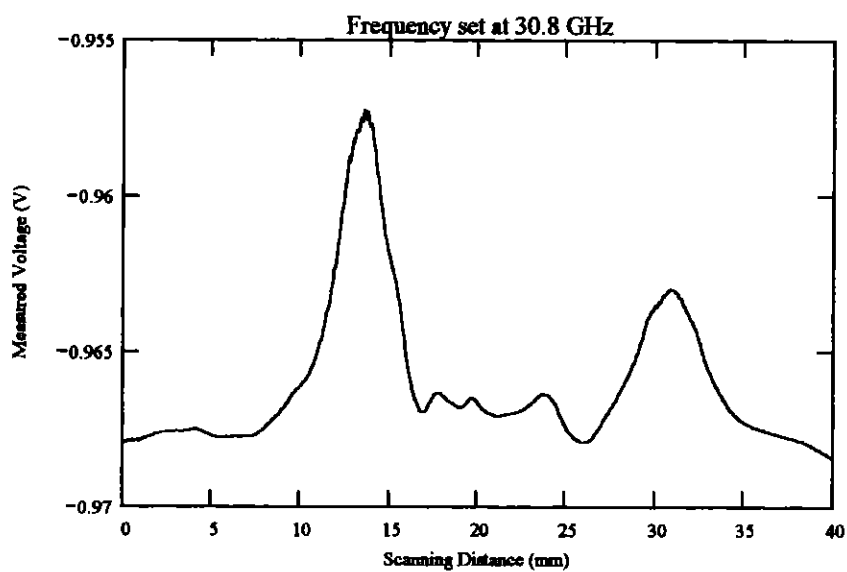
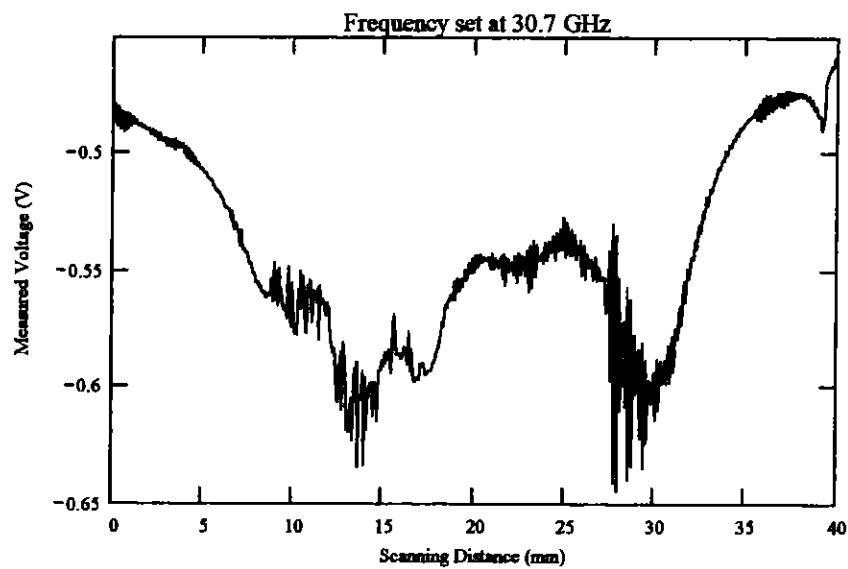


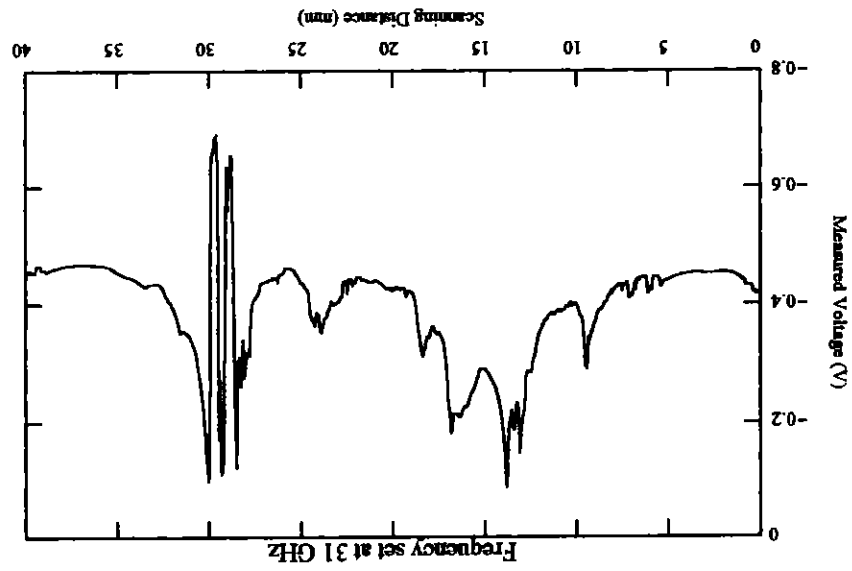
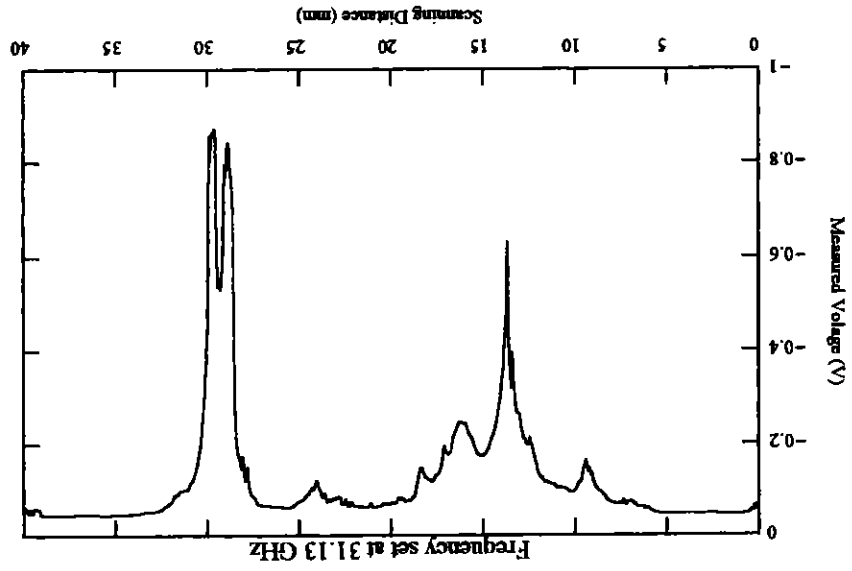


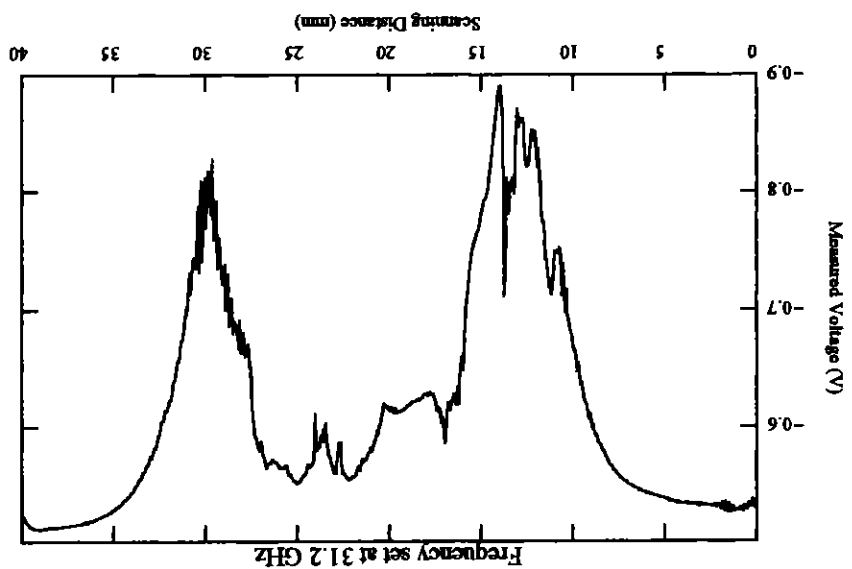
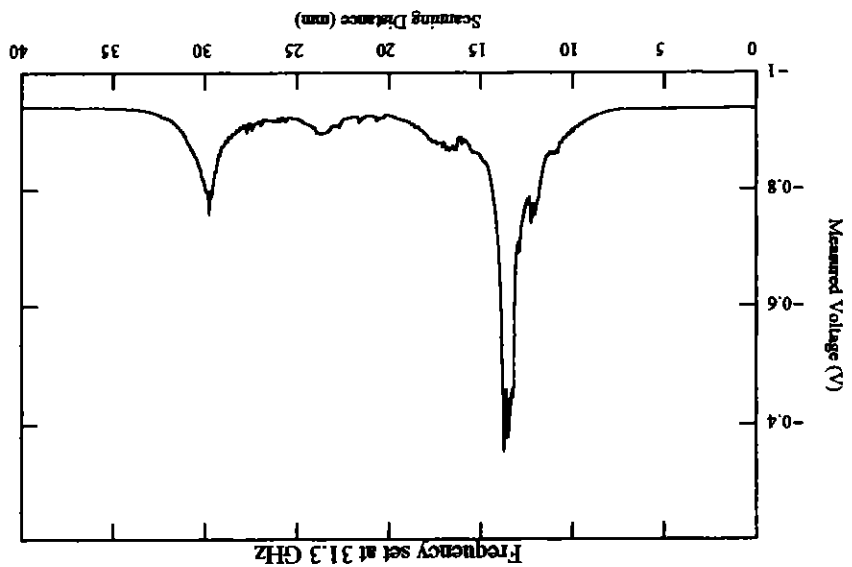
Frequency Band: Ka-band
Orientation: Scan parallel to crack length.
Probe: Coax no. 3
Scan Resolution: 0.064 mm per step
Scan length: 40 mm
Frequency: Varies

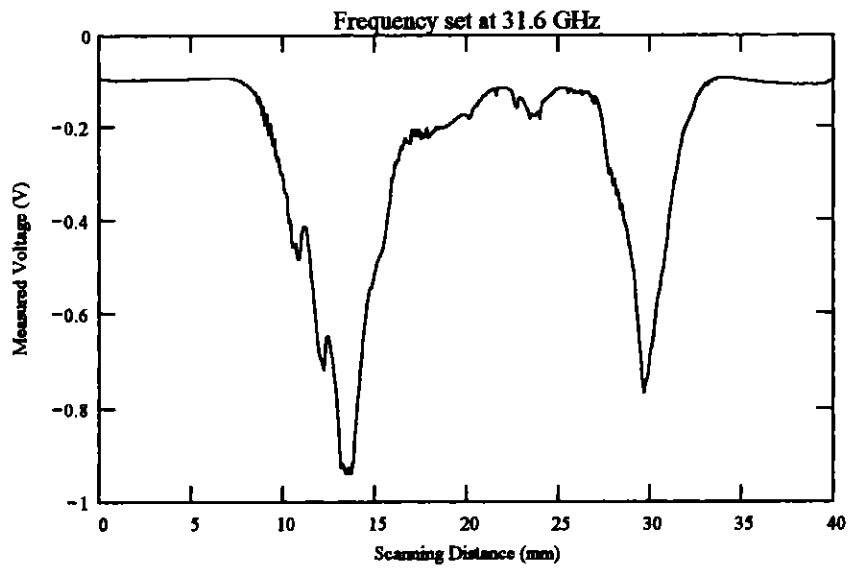
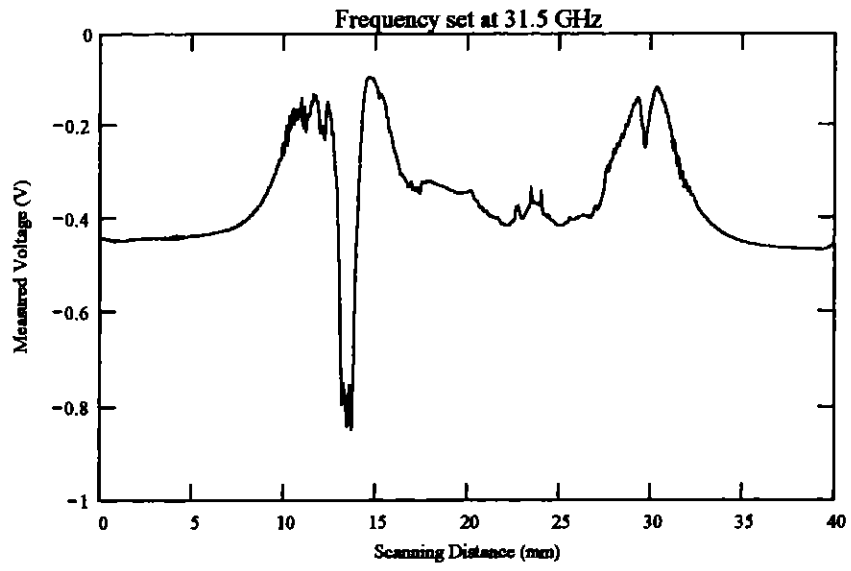


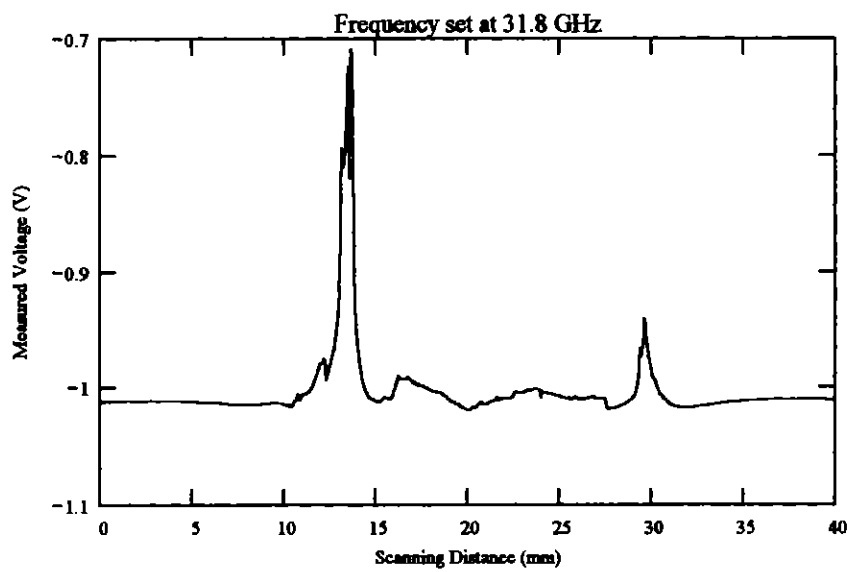
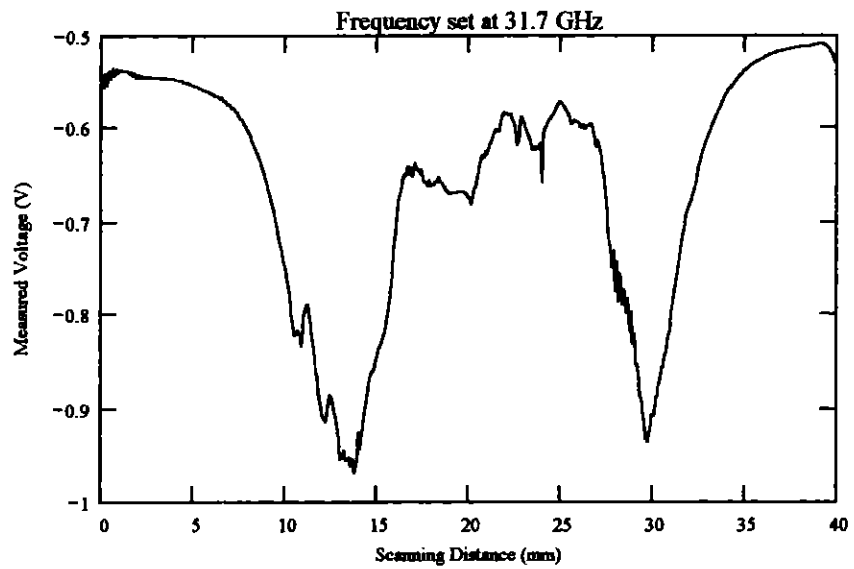


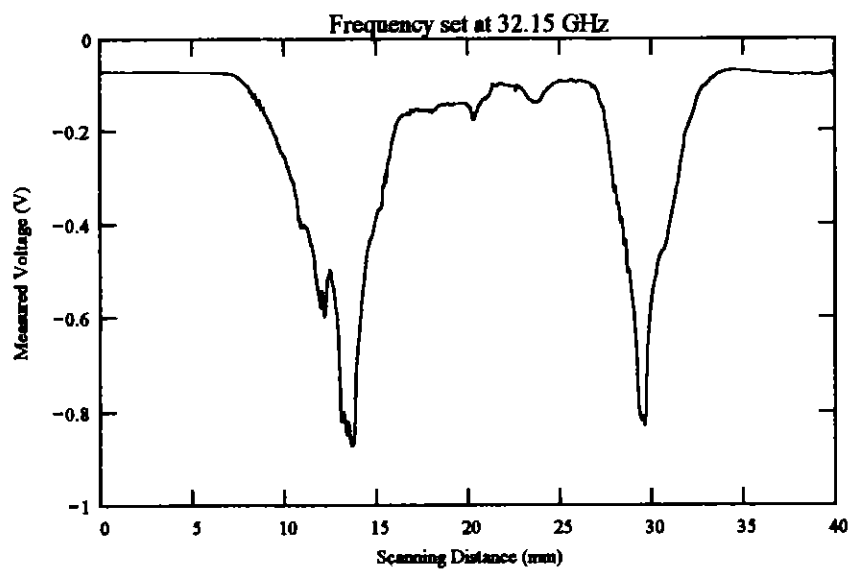
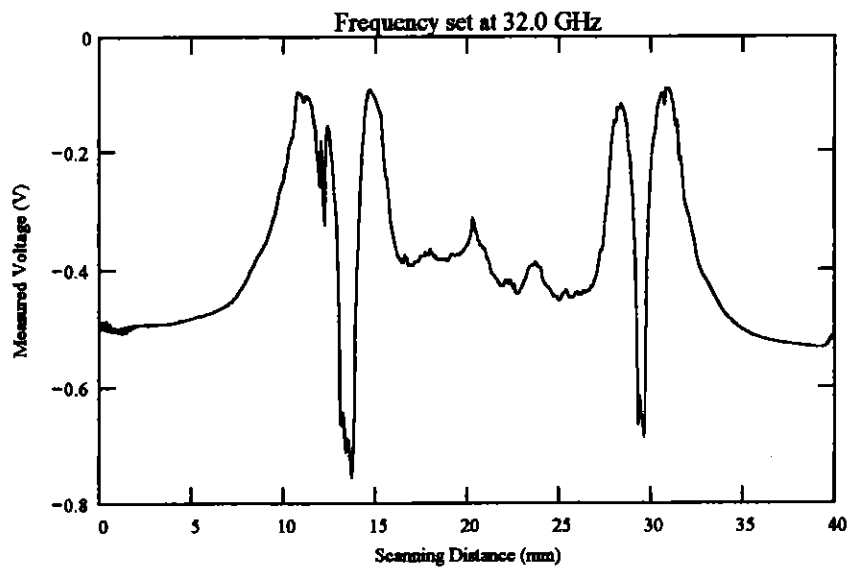


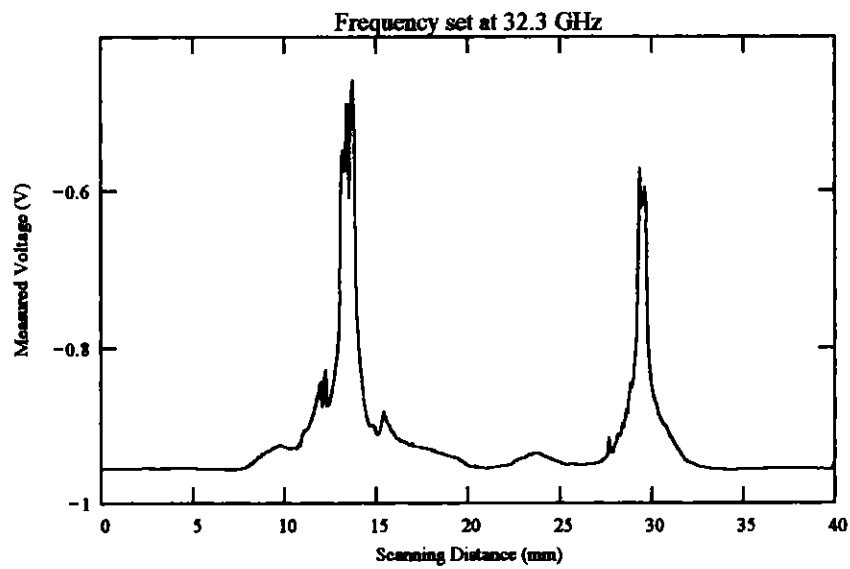
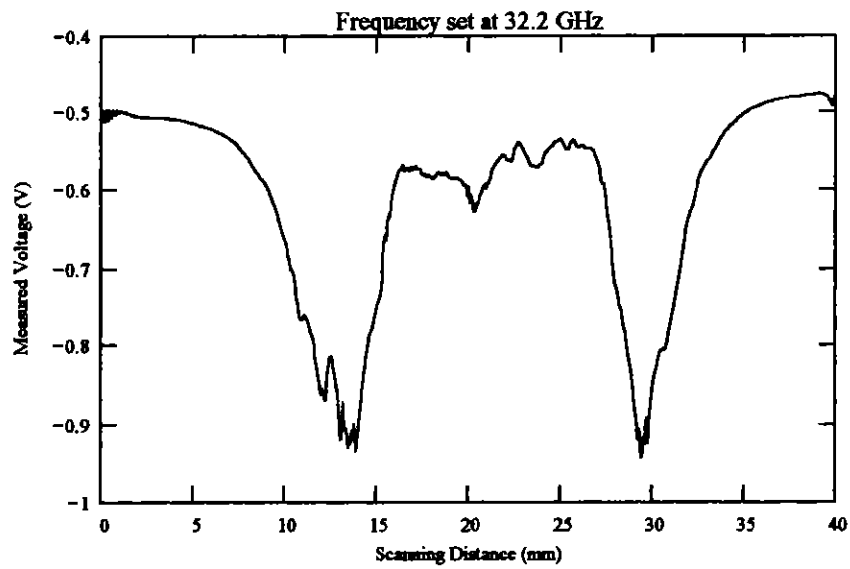


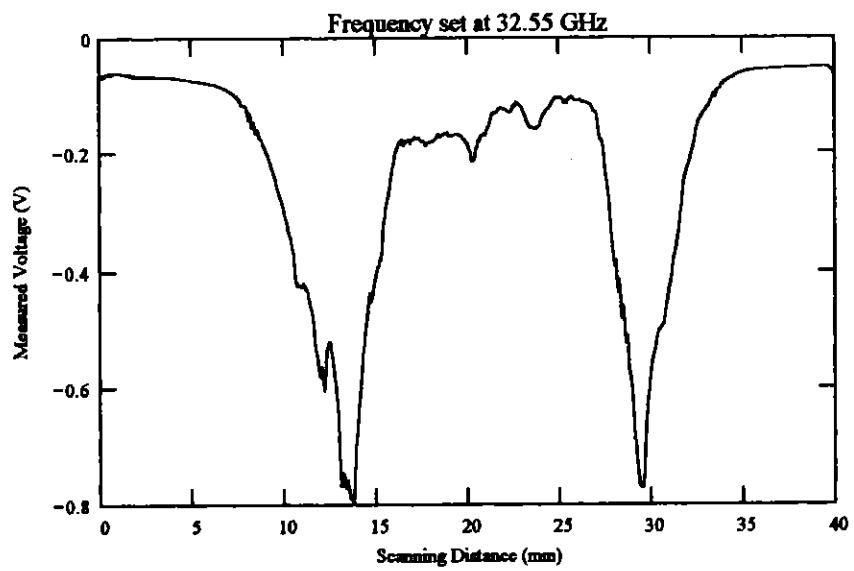
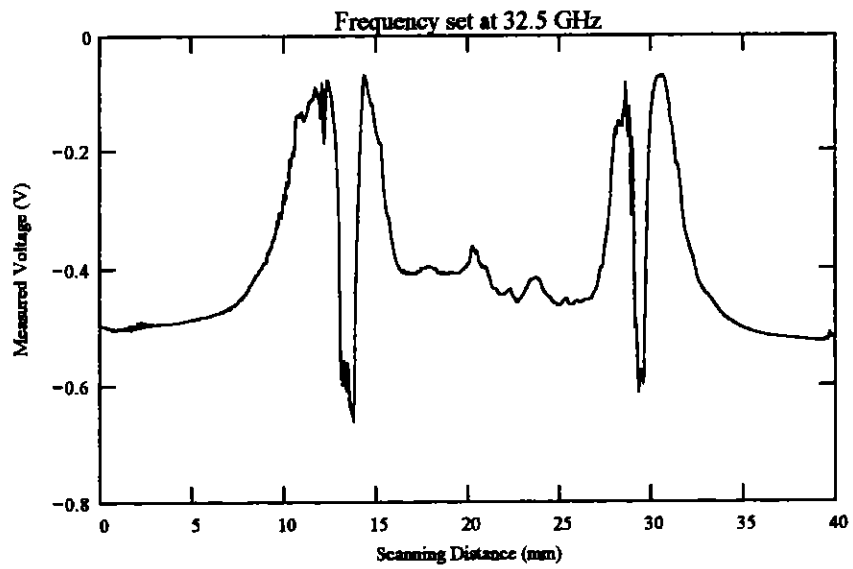


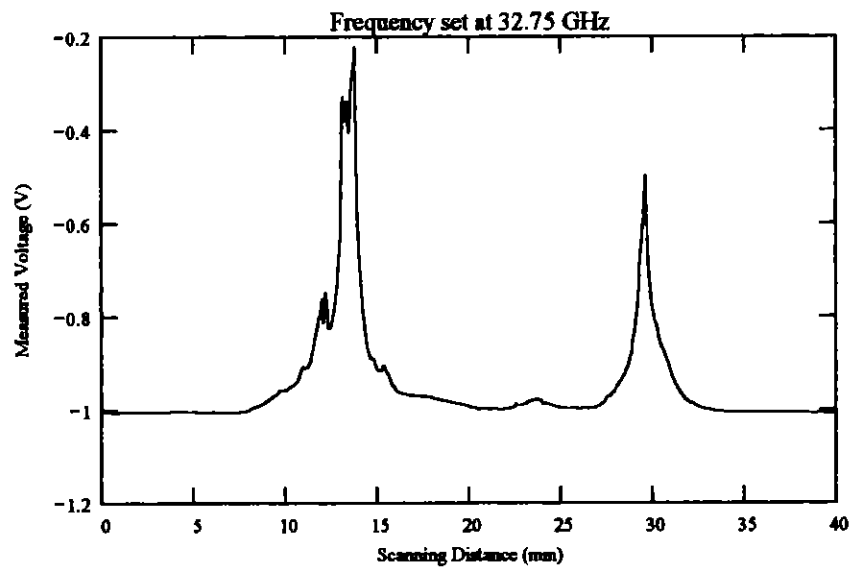
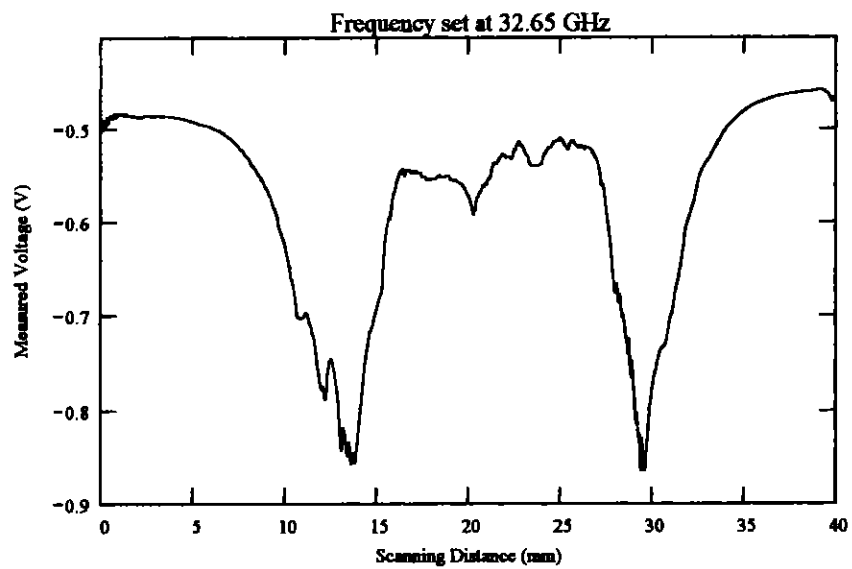


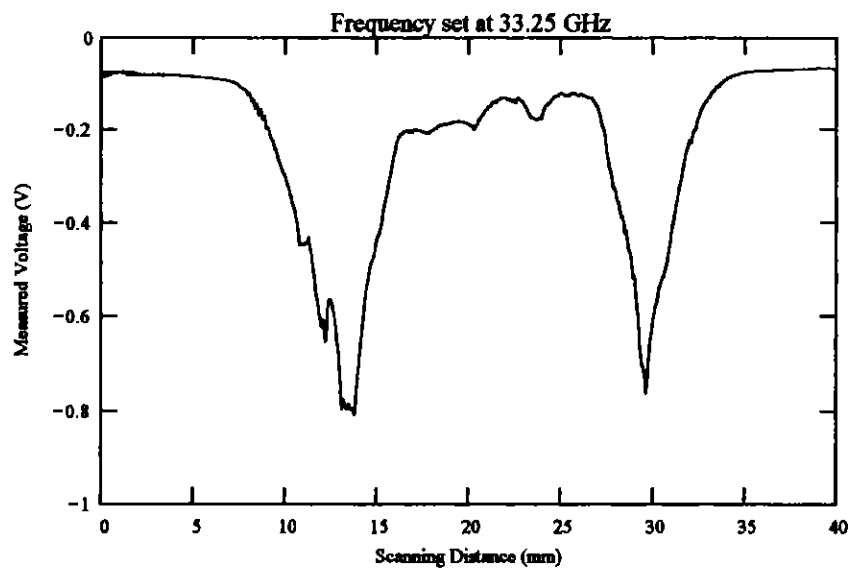
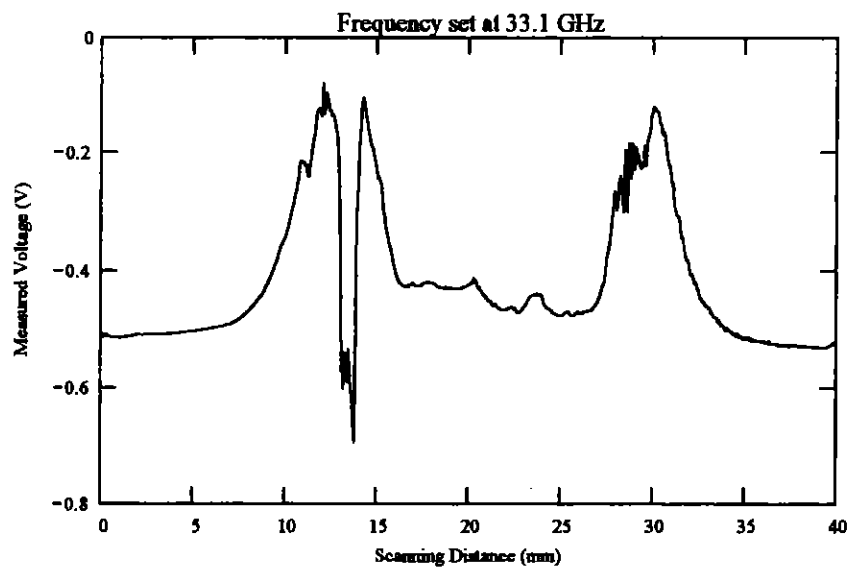


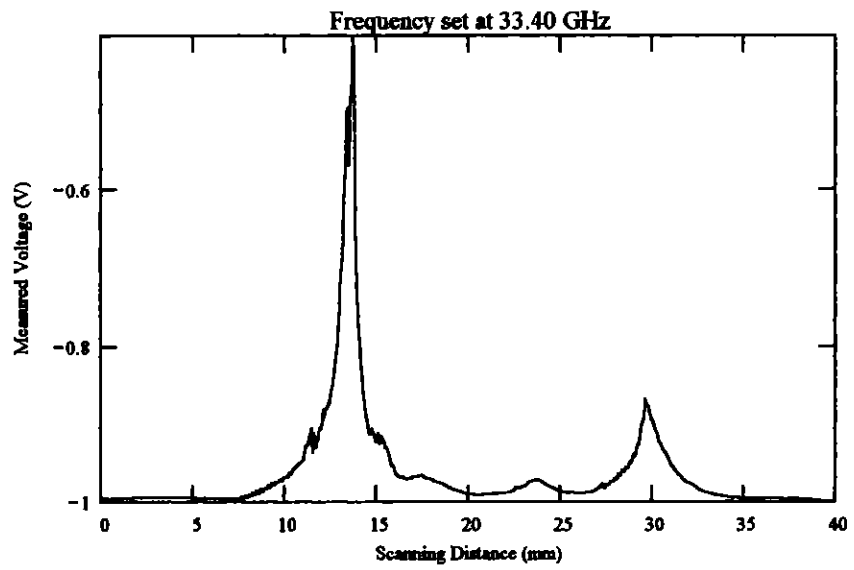
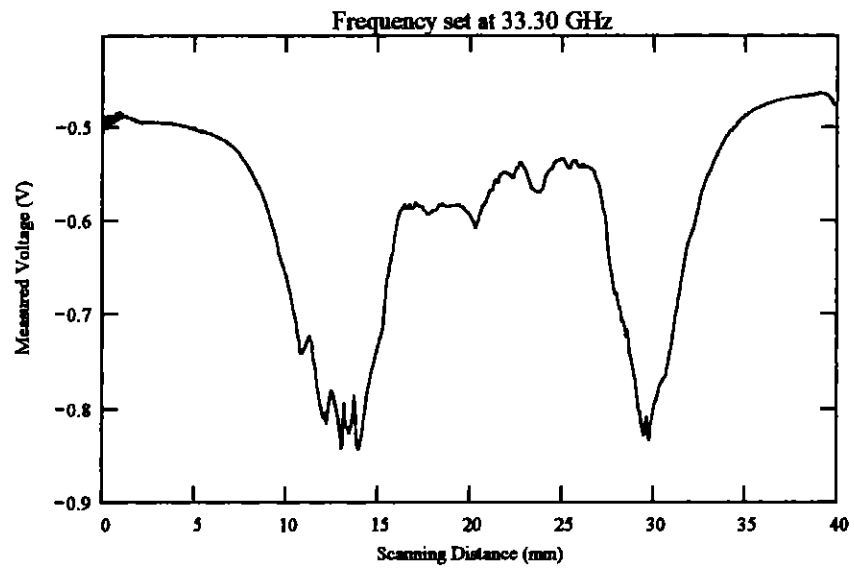


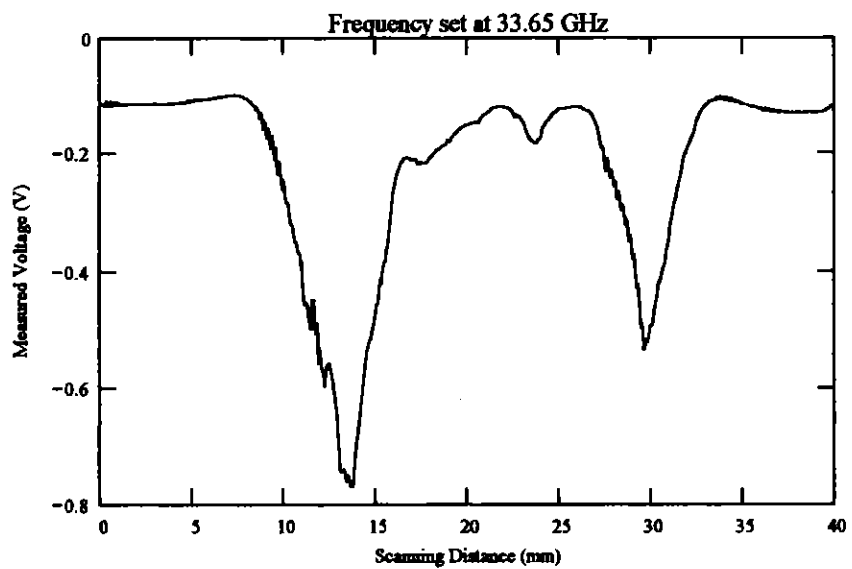
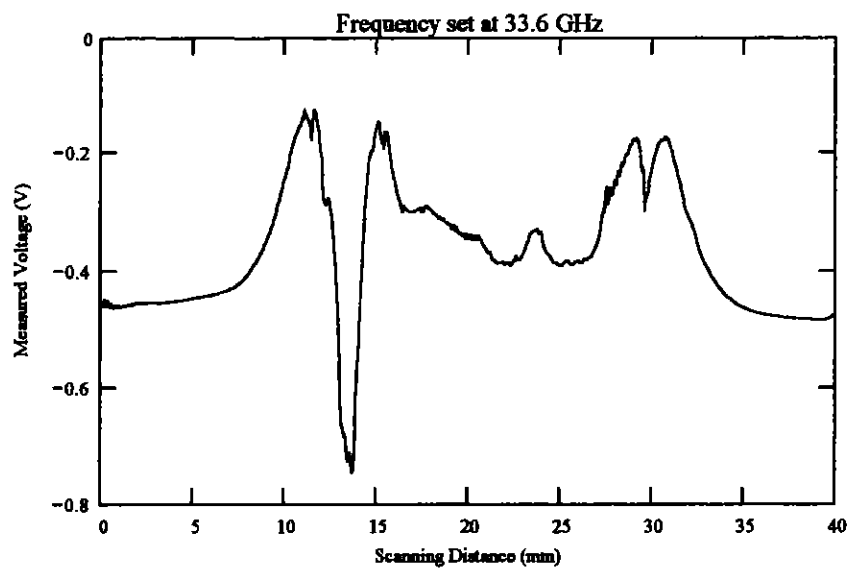


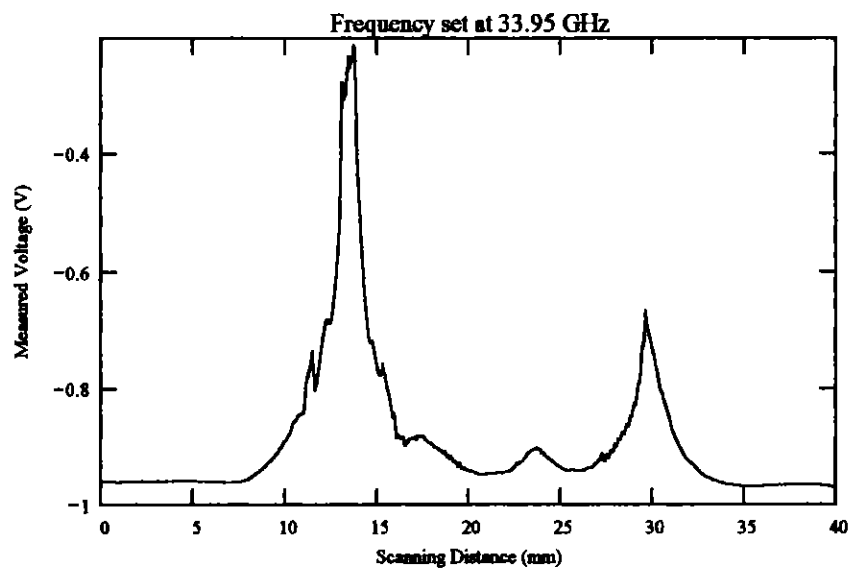
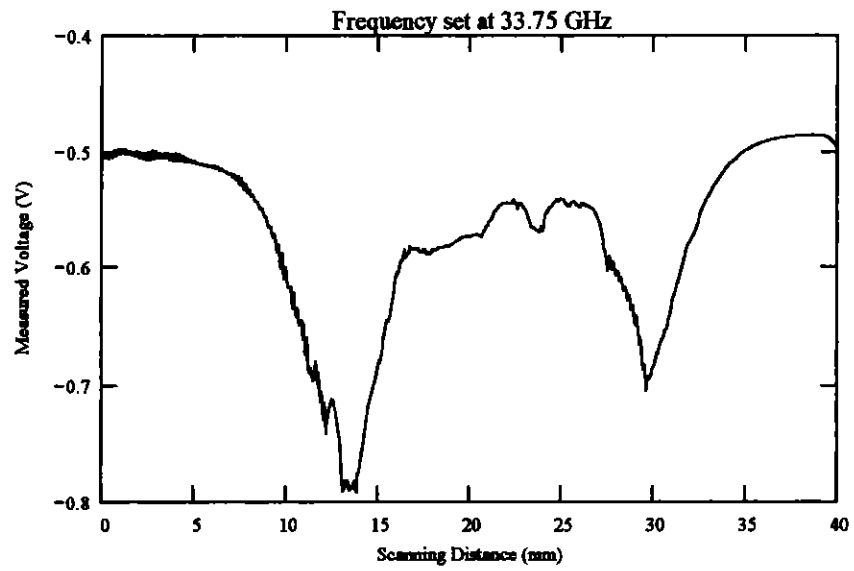


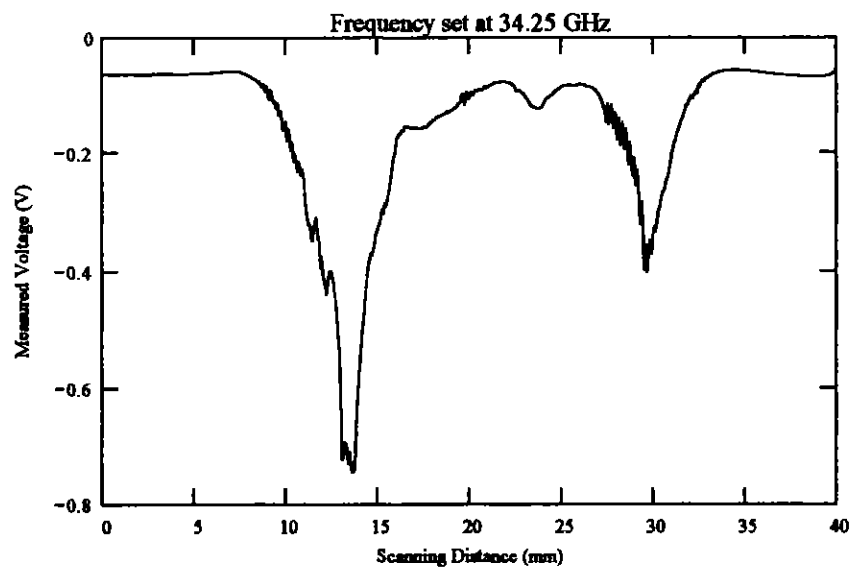
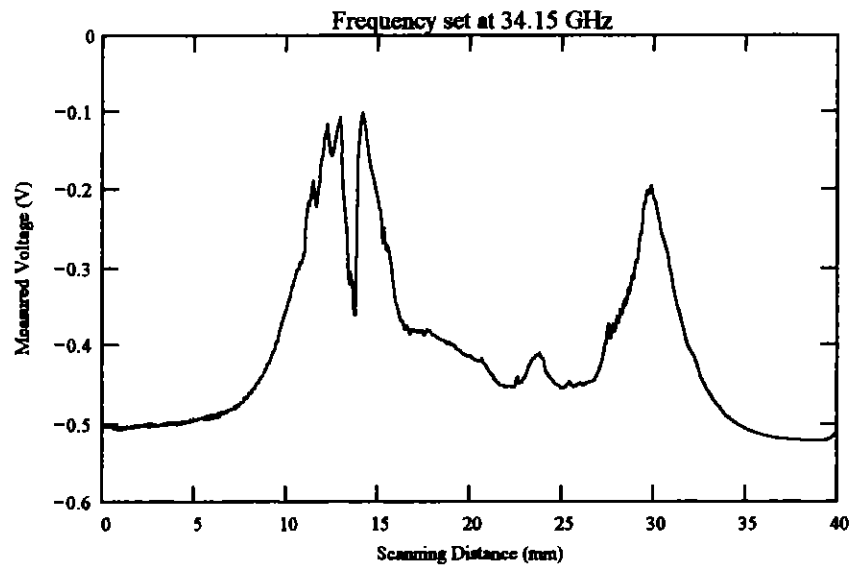


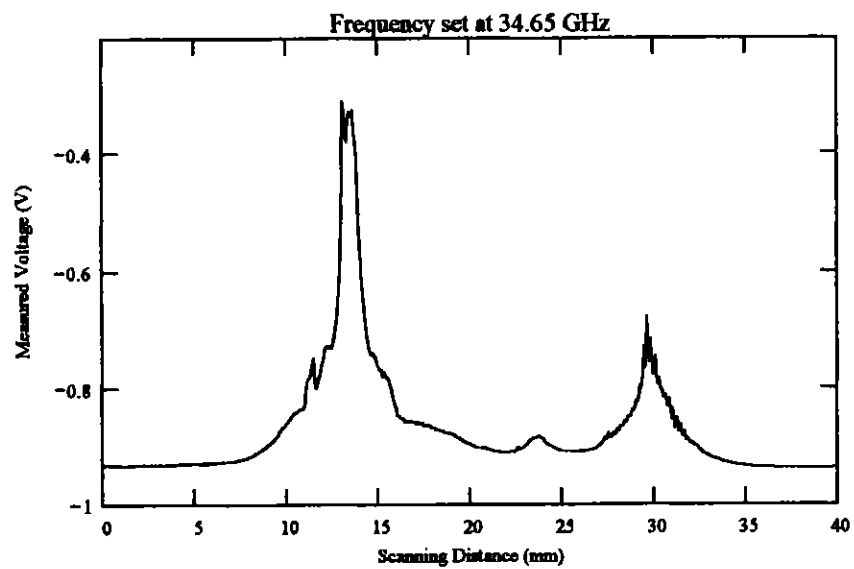
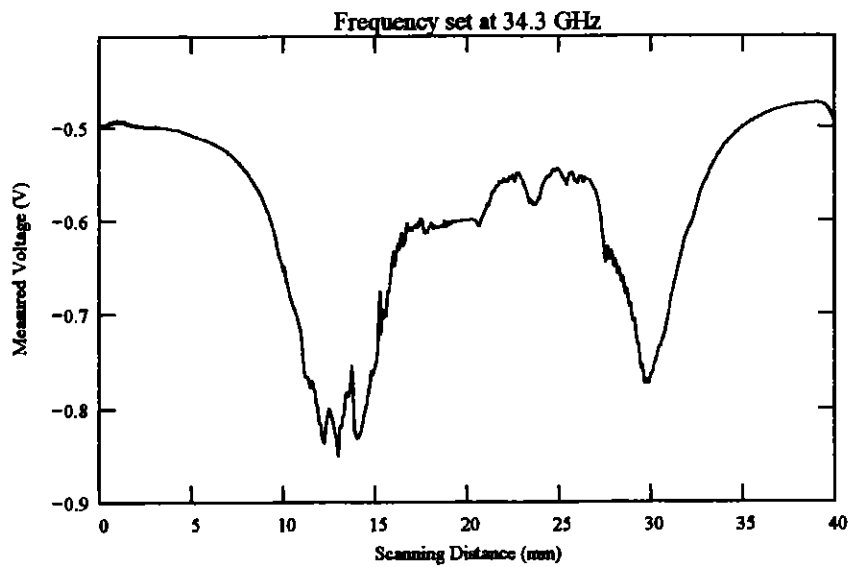


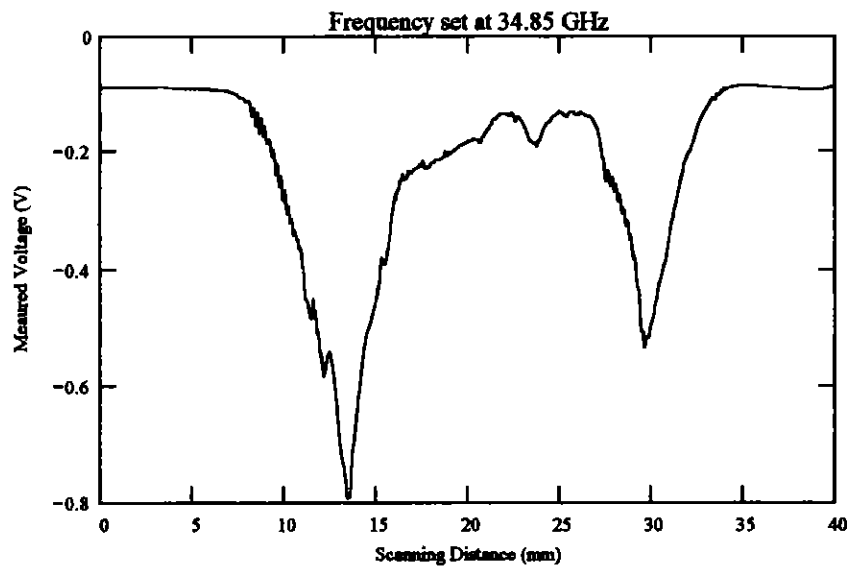
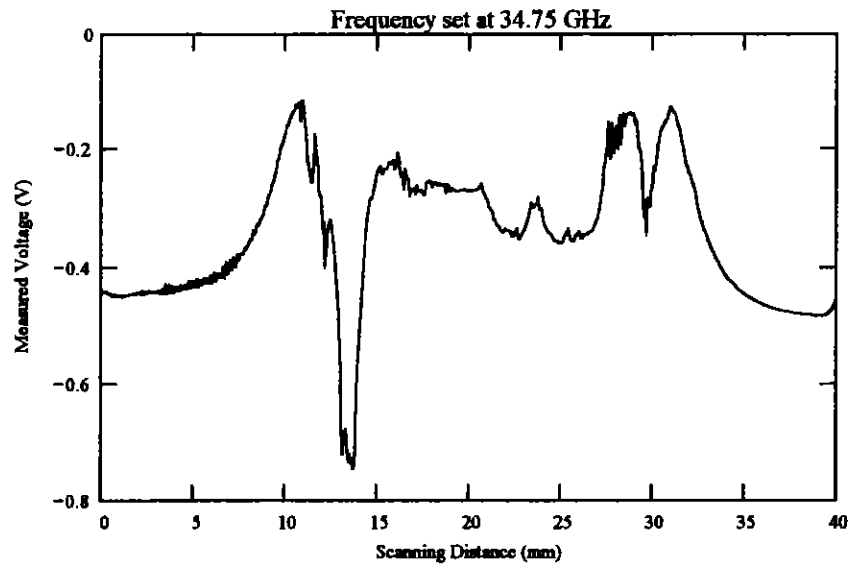


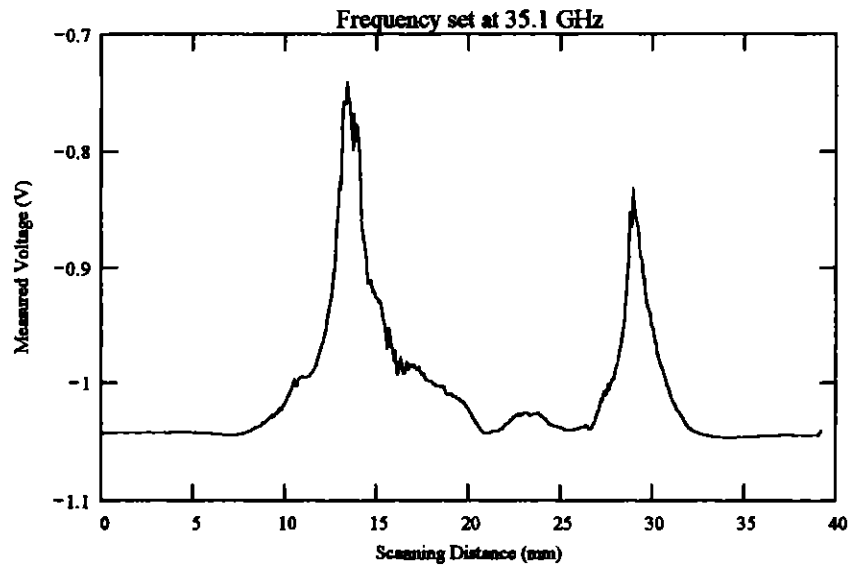
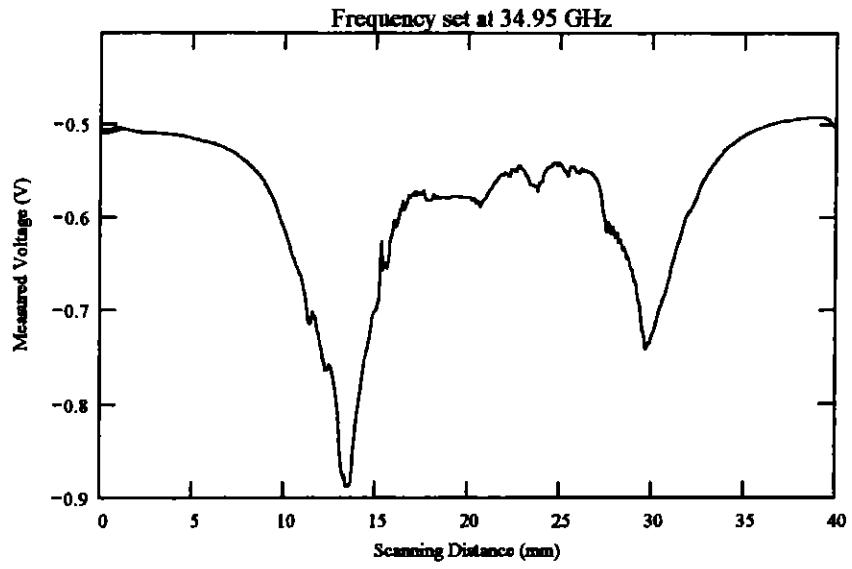


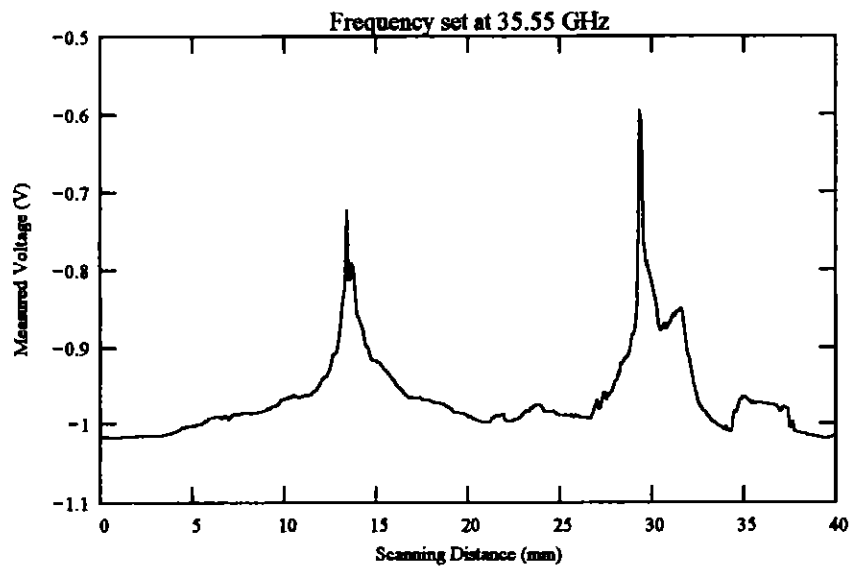
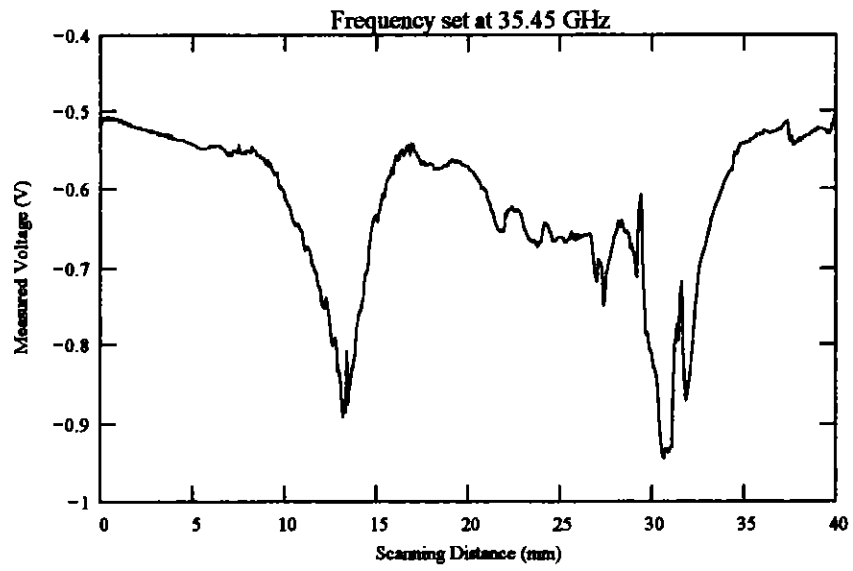


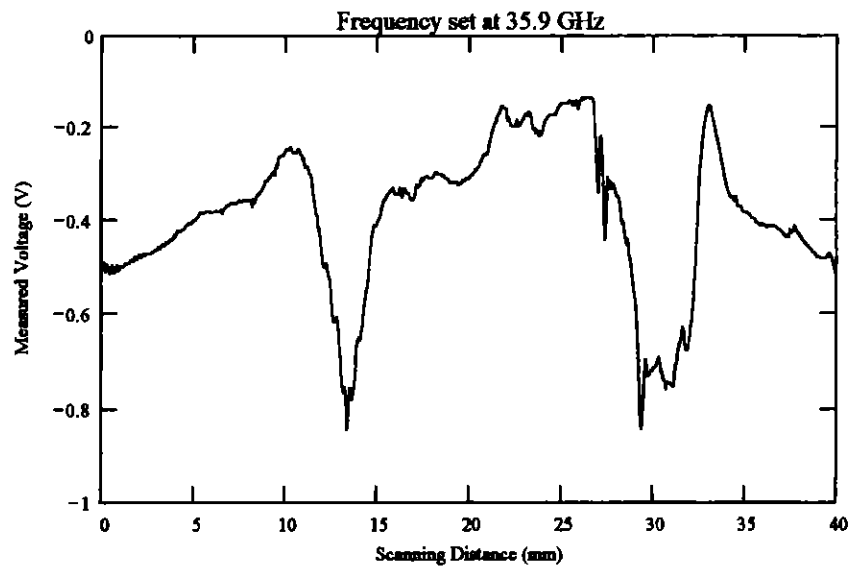












These are the results of the work done on detecting cracks in the welded joints, of the VTRC samples PL4295, PL4296, T4297, and T4298. There are four different types of cracks on these samples, and they are a Toe Indication, Root Indication, Transverse Indication, and a Centerline Indication. Sample PL4295 has two defects/cracks along the edge of the weld. Defect two is on the bottom of the sample, while defect one is on the top. Defect one is a Toe Indication with a length of 12 mm, and defect two is a Root Indication with a length of 20 mm. Sample PL4296 also has two defects that are on the weld, and both are on the top of the sample. Defect one is a Transverse Indication with a length of 13 mm, and defect two is a Centreline Indication with a length of 21 mm. Sample T4298 has two defects/cracks along the edge of the weld. Defect one is a Root Indication with a length of 12 mm, and defect two is a Toe Indication with a length of 26 mm. Sample T4297 also has two defects on the weld. Defect one is a Transverse Indication with a length of 13 mm, and defect two is a Centreline Indication with a length of 8 mm.

These cracks were detected using K-band and Ka-band setups. The setups contain mechanically tuned gun oscillator connected to an isolator, which in turn is connected to a piece of waveguide that is terminated by a waveguide to coax adapter. The coaxial lines at the end of the adapter were changed, these will be shown below. A diode detector is inserted at the middle of the waveguide (perpendicular to the a-dimension of the waveguide) to probe the standing wave pattern for variations due to the presence of a crack. The diode detector produces a dc voltage that is related to the properties of the standing waves inside the waveguide.

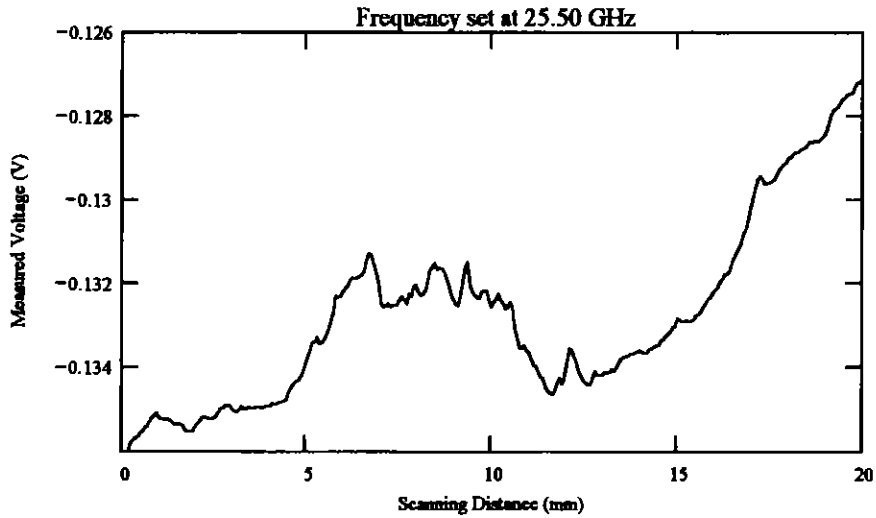
Several measurements at different frequencies were conducted to detect the presence of the cracks on this specimen. there are two different ways to scan a crack, parallel is to scan along the length of the crack and perpendicular is to scan across the length of the crack.

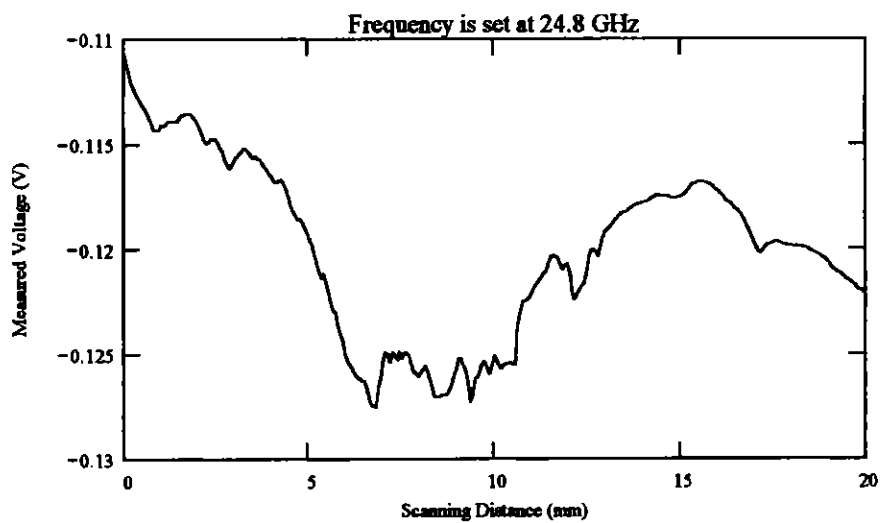
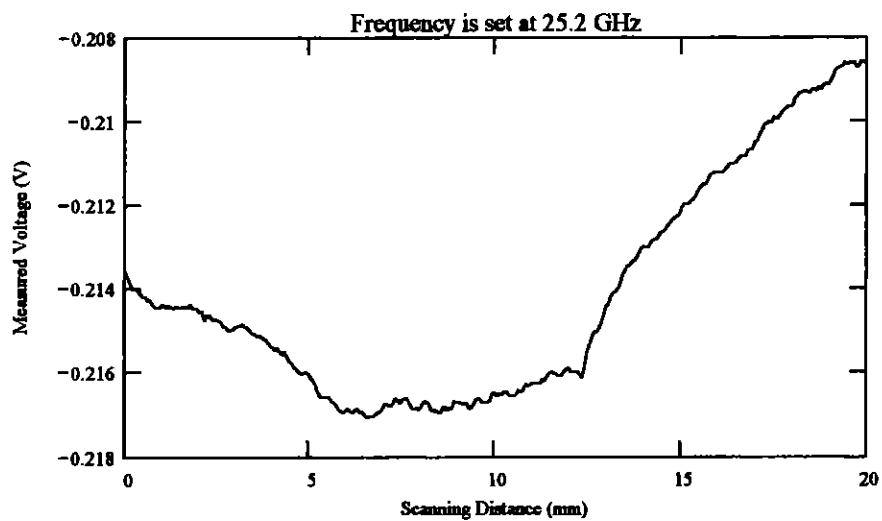
I. Sample PL4295 Painted

A. Crack #1

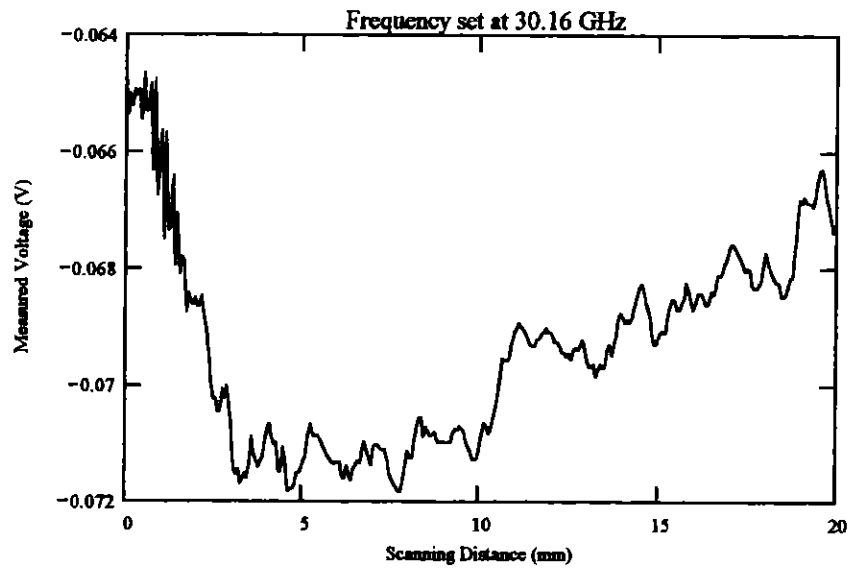
This is a Toe Indication crack. The length of the crack is 12 mm. This crack runs parallel to the welded joint.

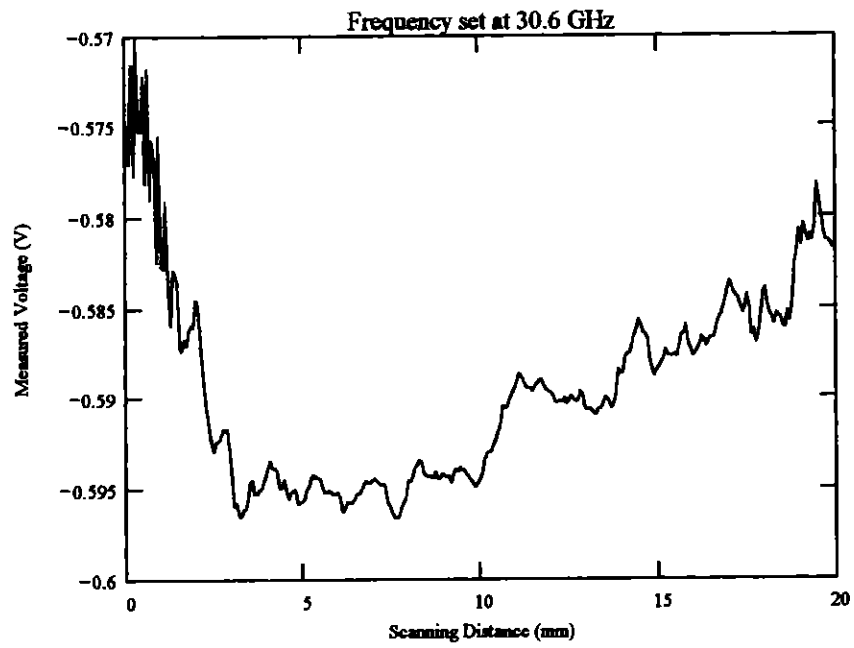
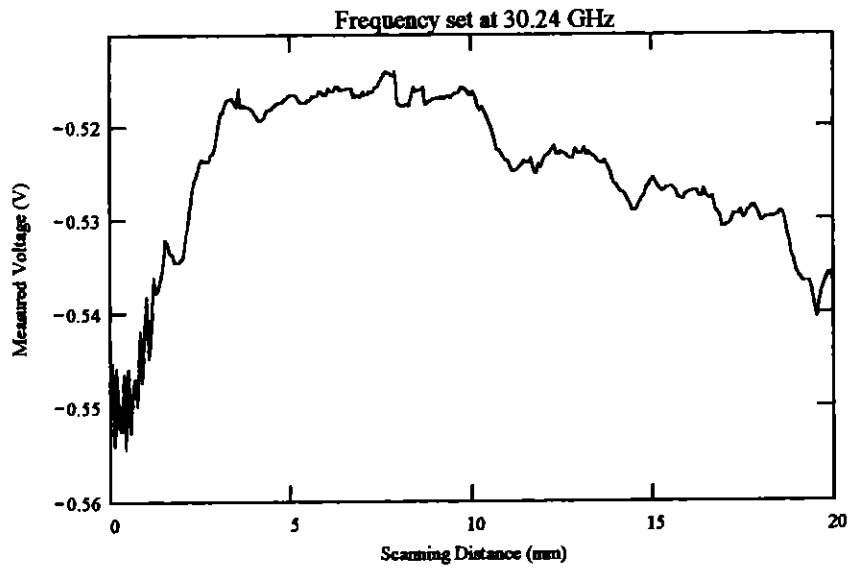
Frequency Band: K-band
Orientation: Scan parallel to crack length.
Probe: Coax no. 2
Scan Resolution: 0.064 mm per step
Scan length: 20 mm
Frequency: Varies

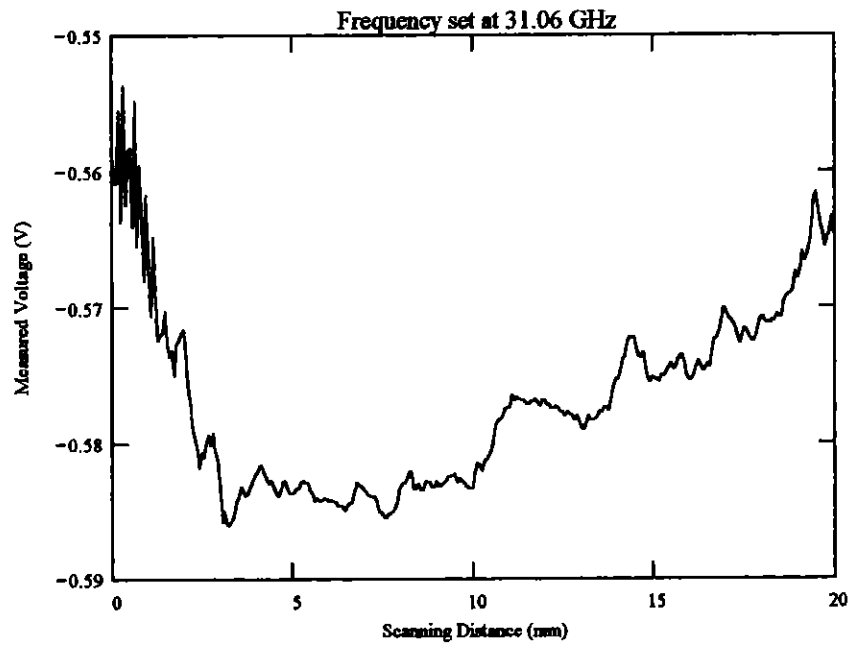
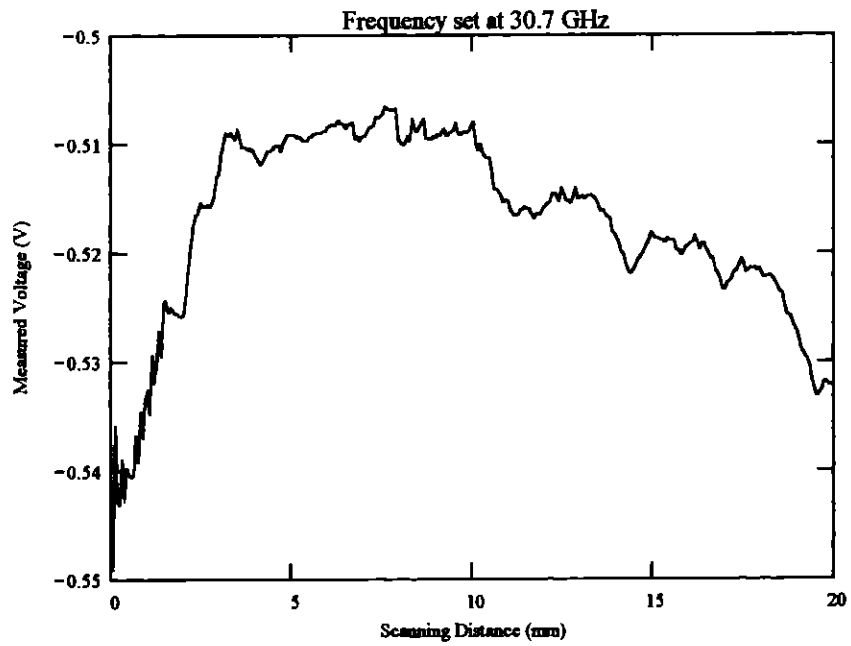


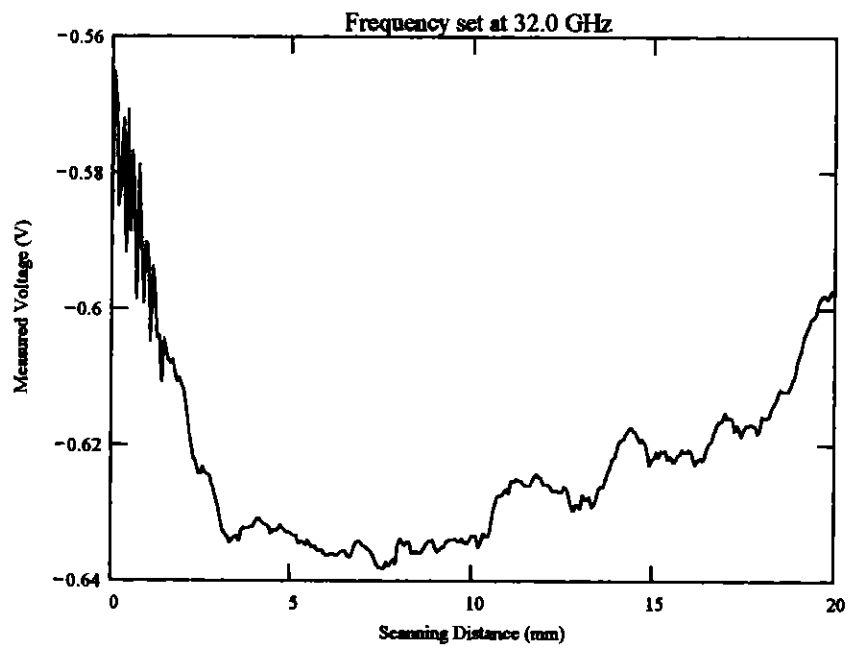
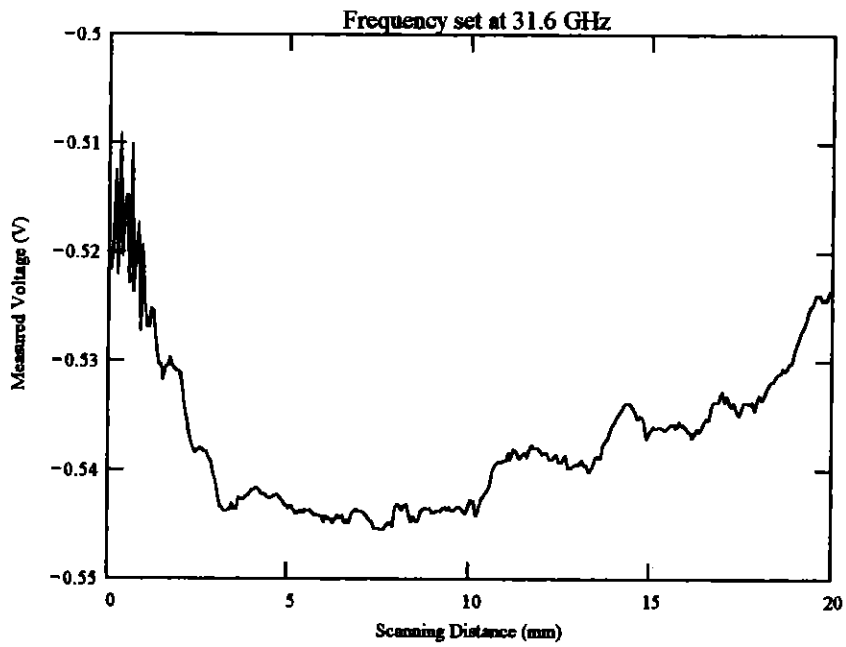


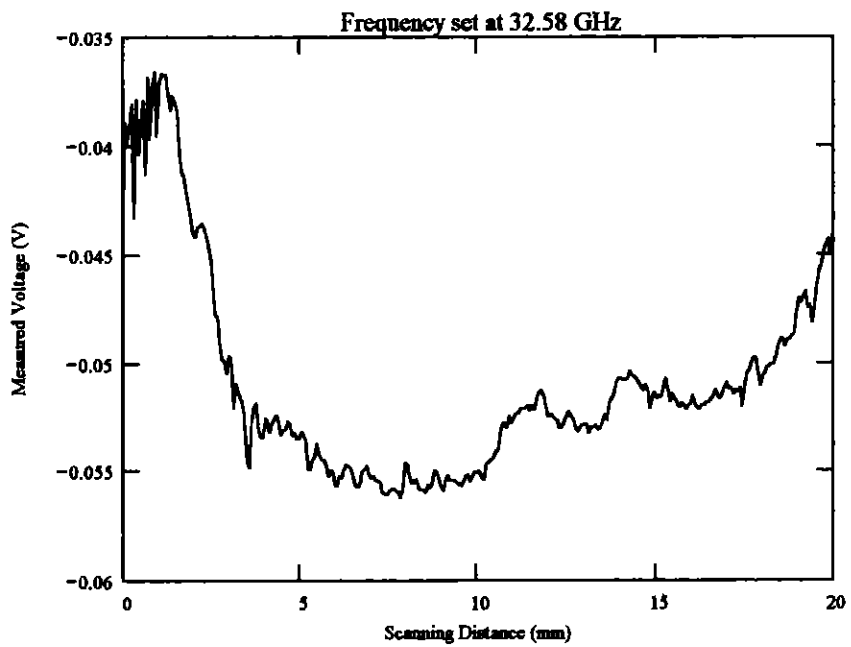
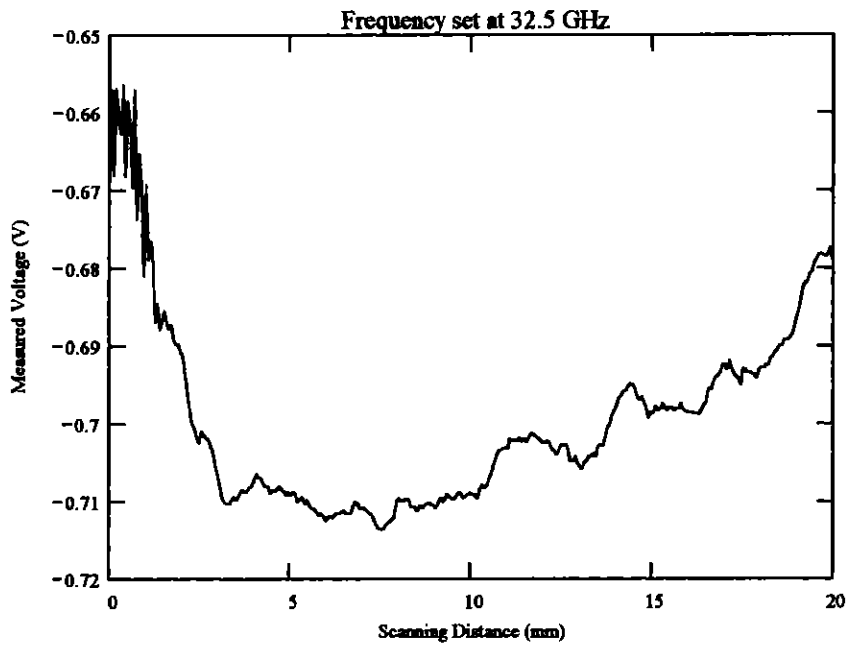
Frequency Band: Ka-band
Orientation: Scan parallel to crack length.
Probe: Coax no. 3
Scan Resolution: 0.064 mm per step
Scan length: 20 mm
Frequency: Varies

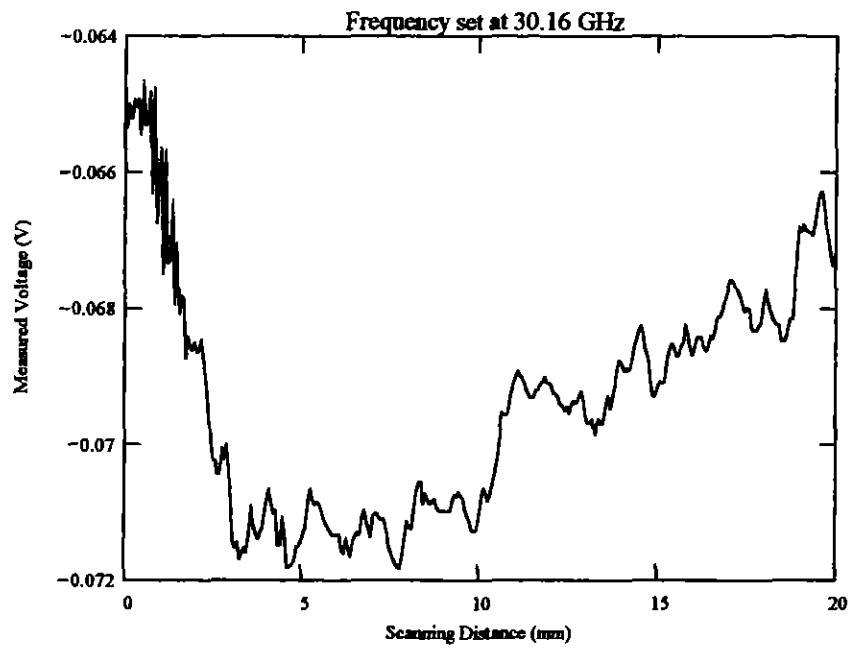








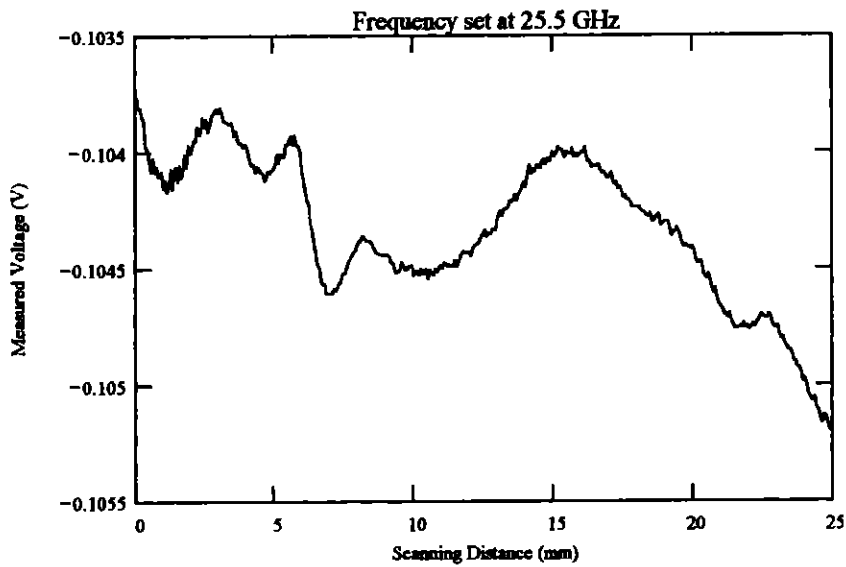


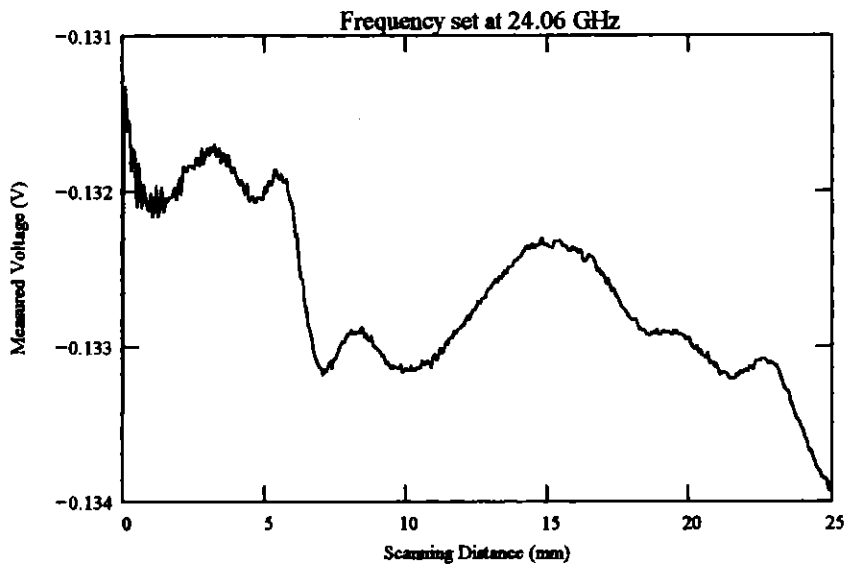
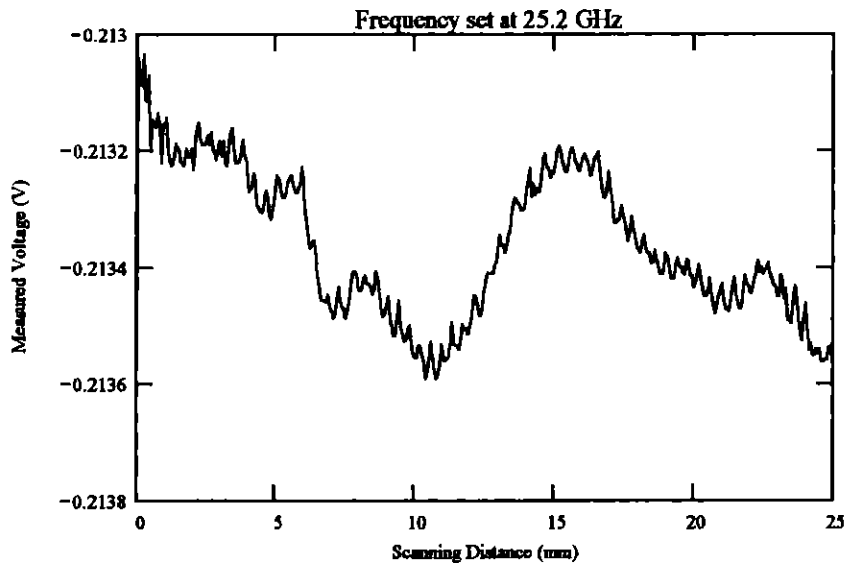


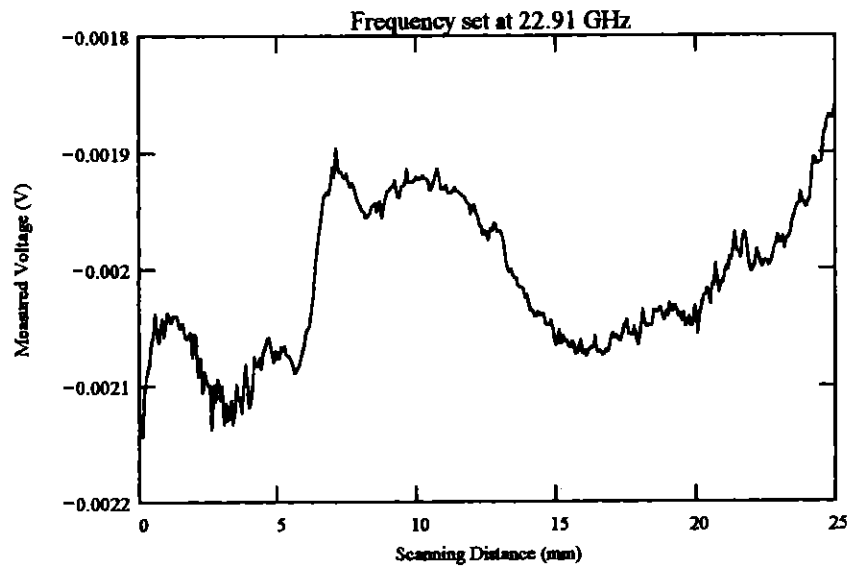
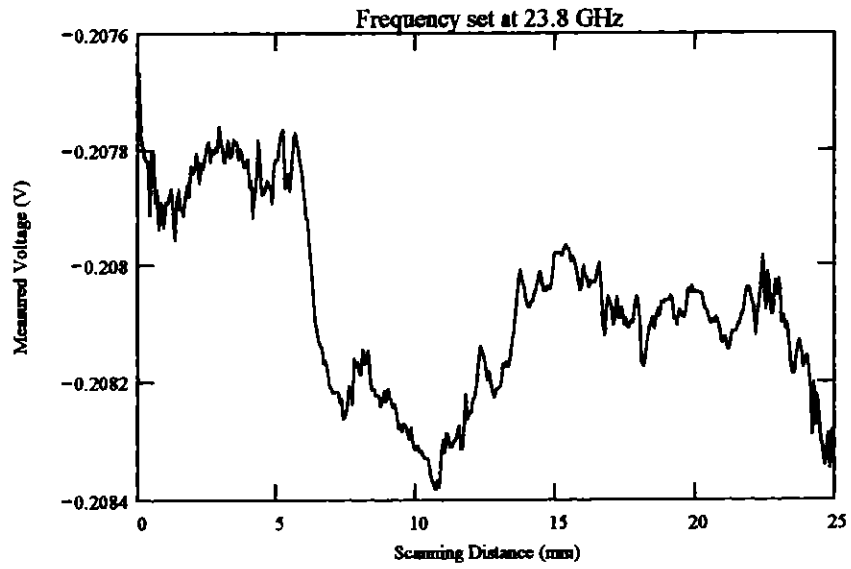
B. Crack #2

This is a Root Indication crack. The length of the crack is 24 mm. This crack runs parallel to the welded joint.

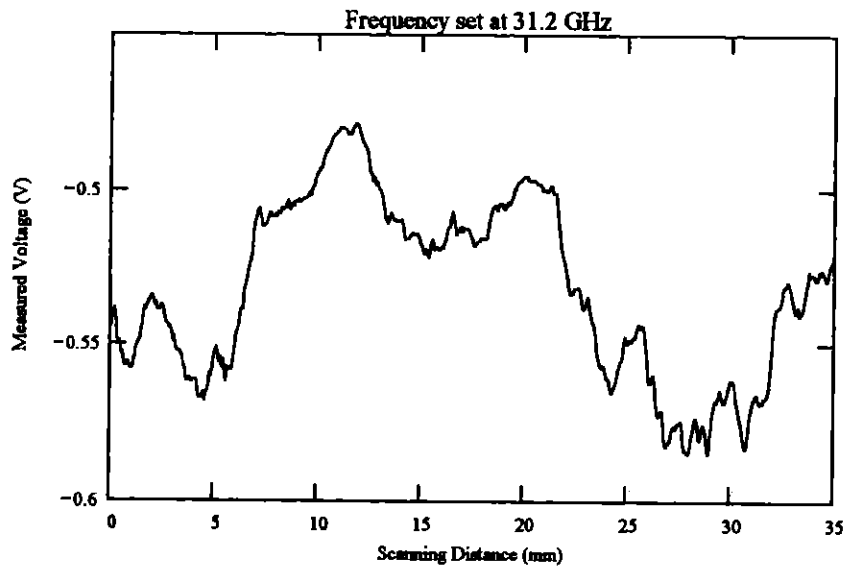
Frequency Band: K-band
Orientation: Scan parallel to crack length.
Probe: Coax no. 2
Scan Resolution: 0.064 mm per step
Scan length: 25 mm
Frequency: varies

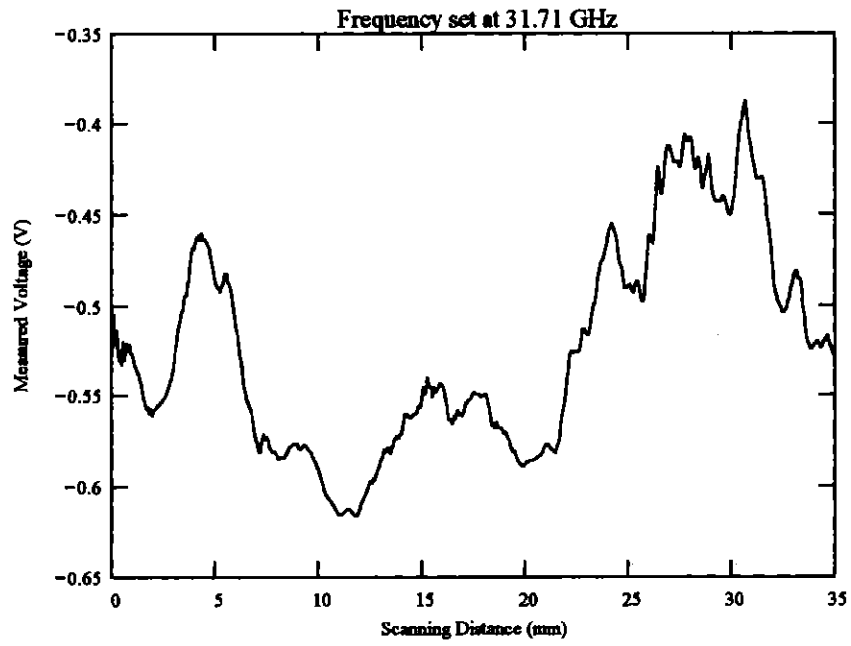
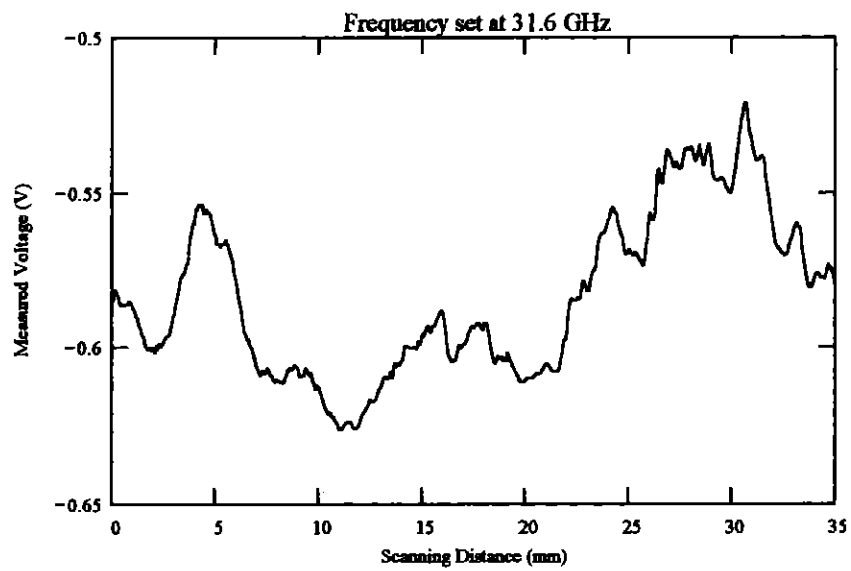


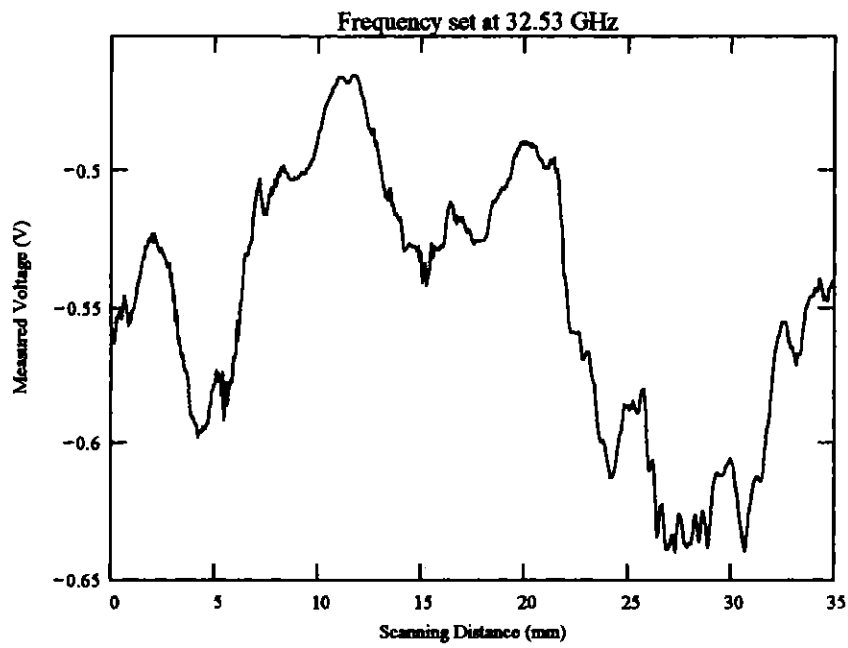
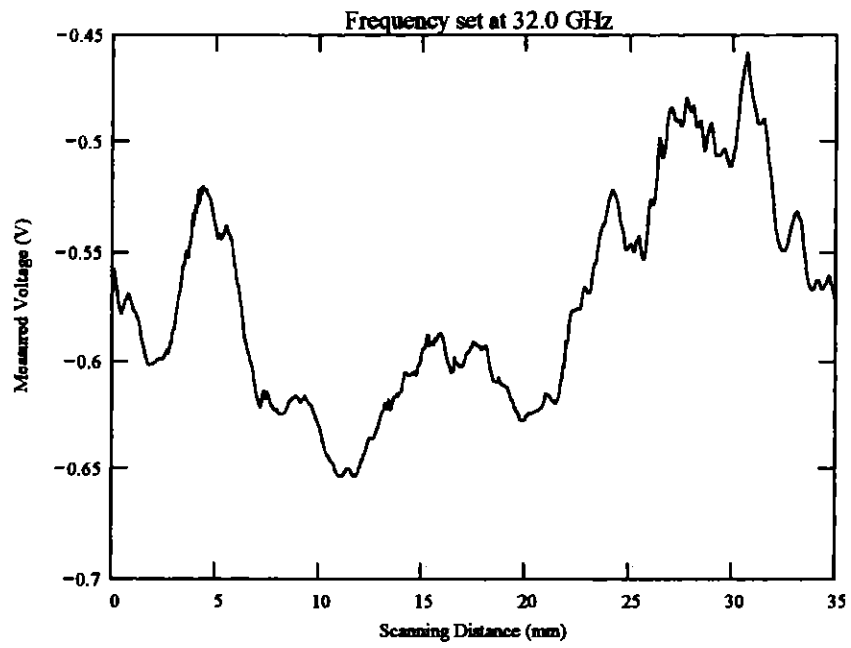


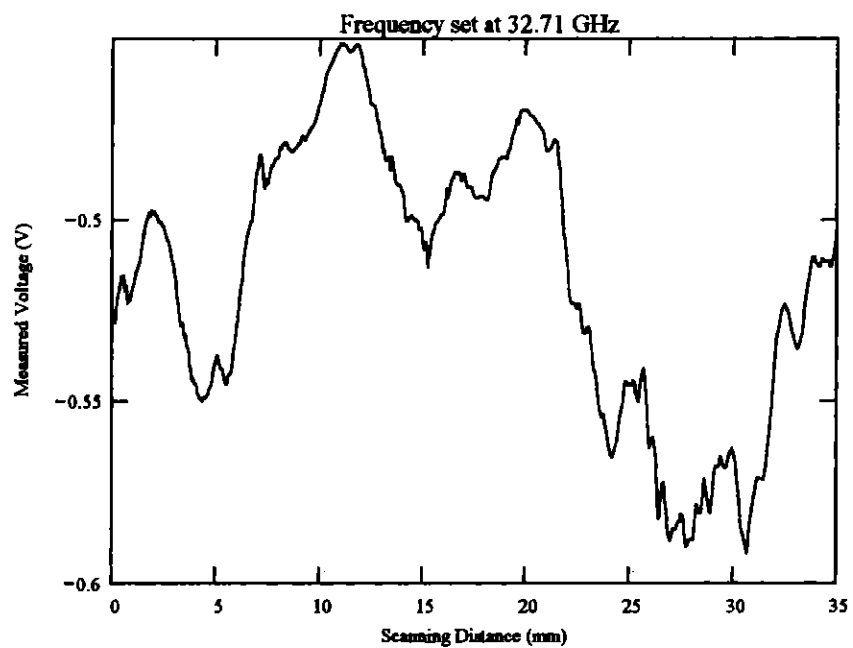


Frequency Band: Ka-band
Orientation: Scan parrallel to crack length.
Probe: Coax no. 3
Scan Resolution: 0.064 mm per step
Scan length: 35 mm
Frequency: Varies









II. Sample PL4296 Painted

A. Crack #1

This is a Transverse Indication crack. The length of the crack is 13 mm. This crack runs perpendicular to the welded joint.

Frequency Band: K-band

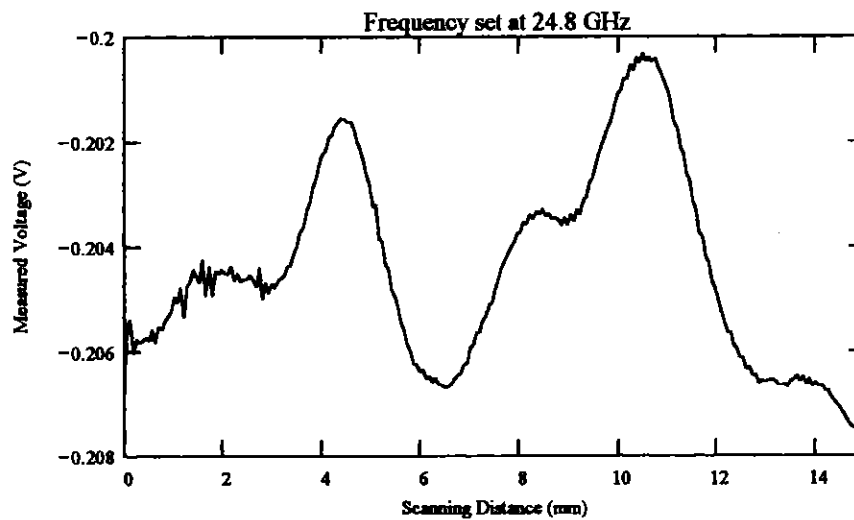
Orientation: Scan perpendicular to crack length.

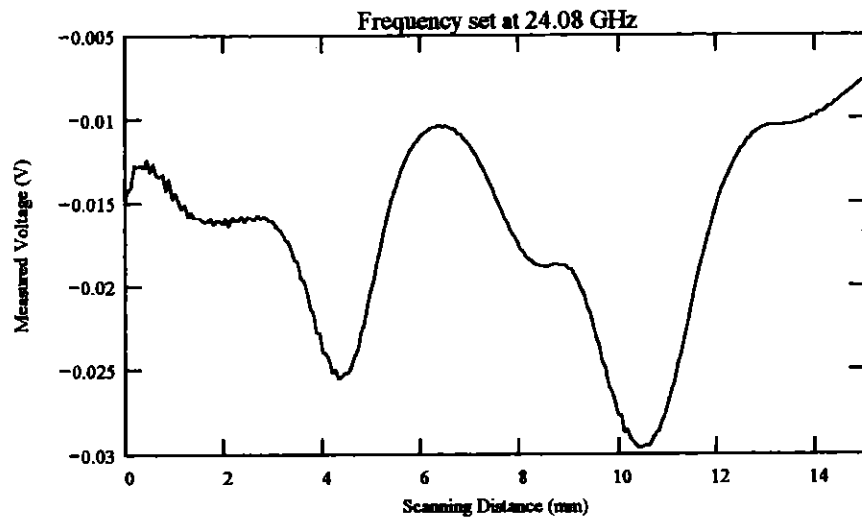
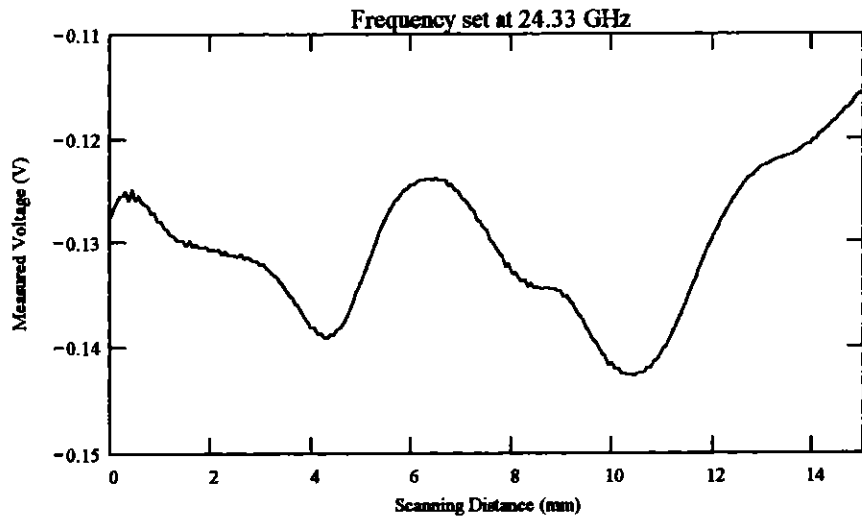
Probe: Coax no. 2

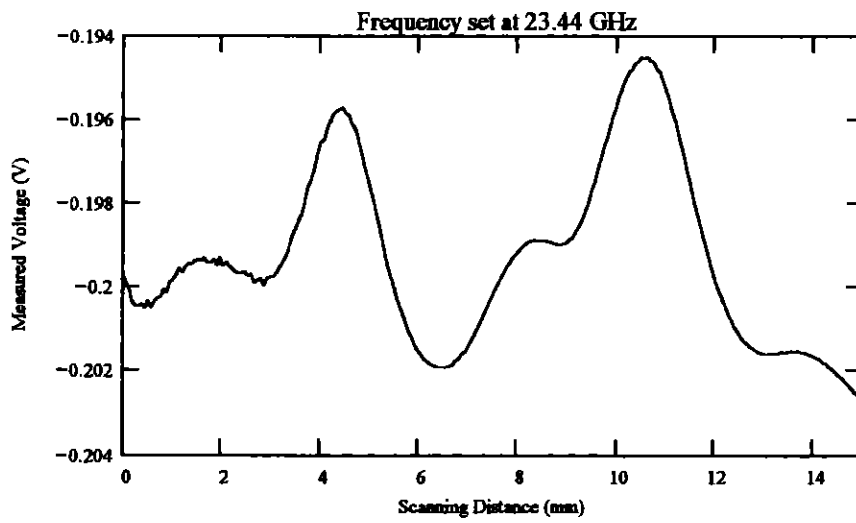
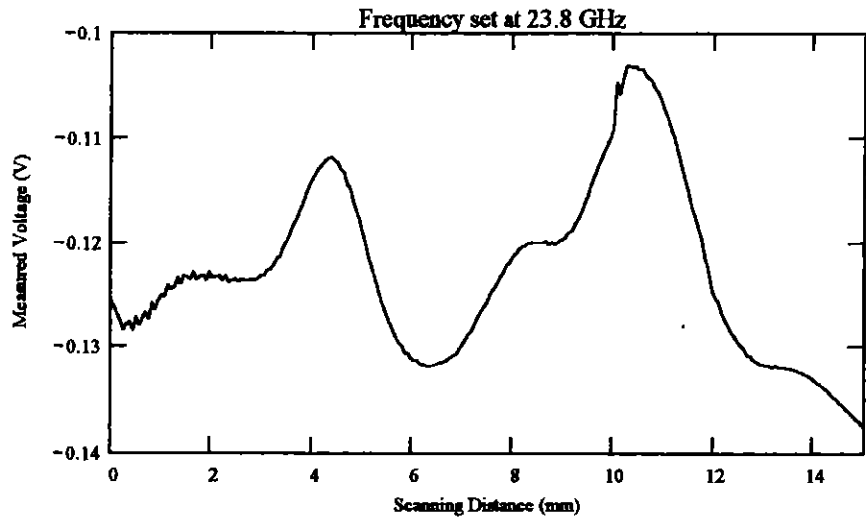
Scan Resolution: 0.064 mm per step

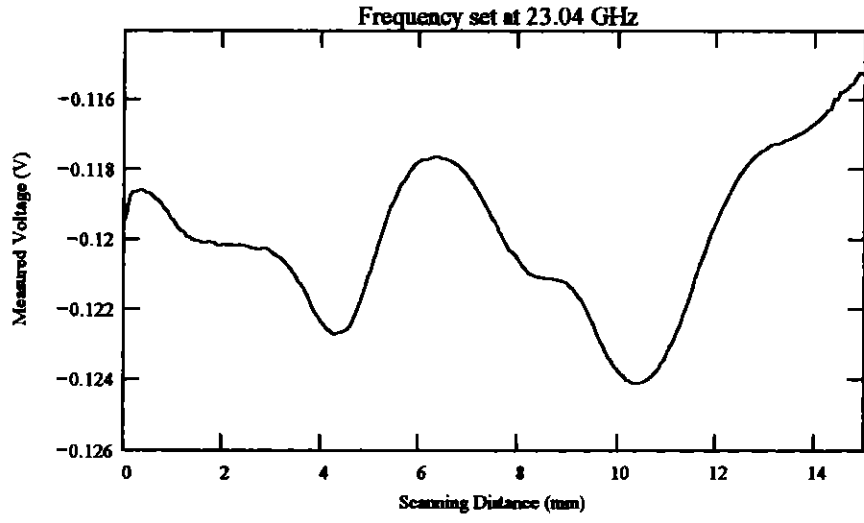
Scan length: 15 mm

Frequency: Varies

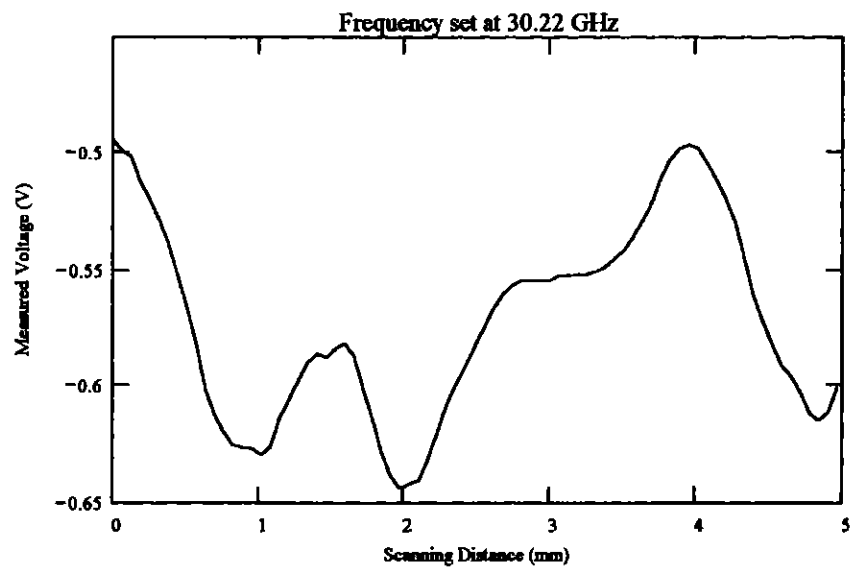


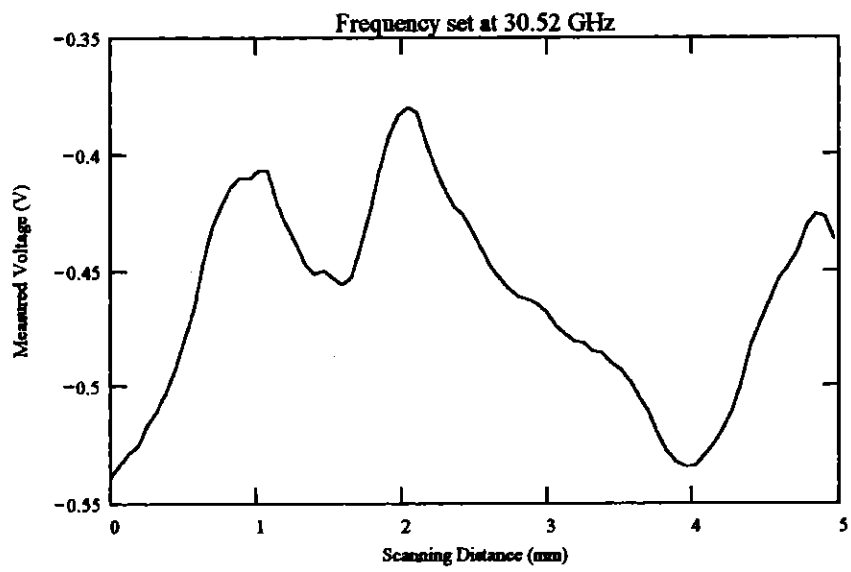
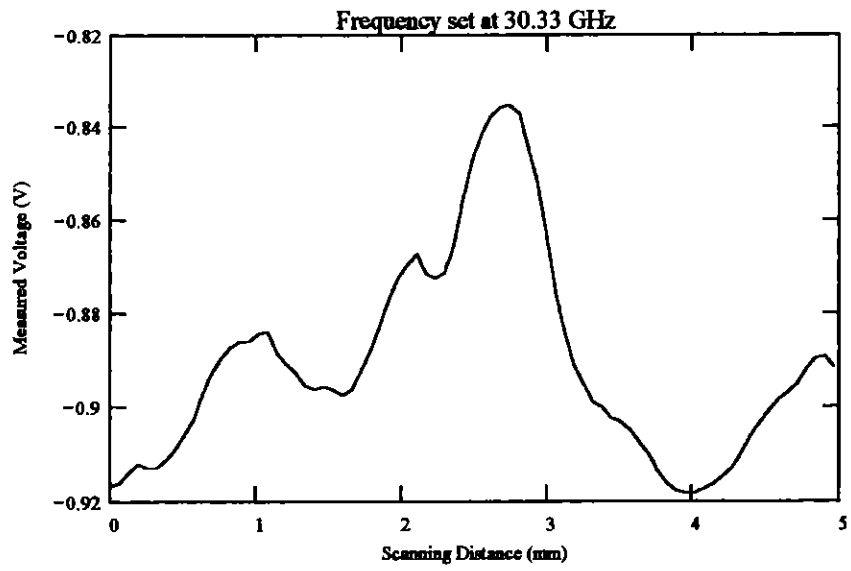


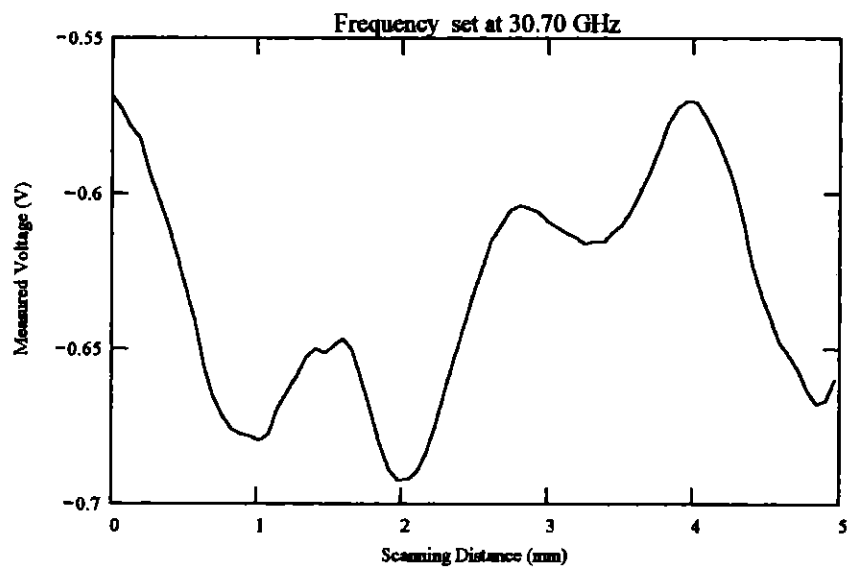
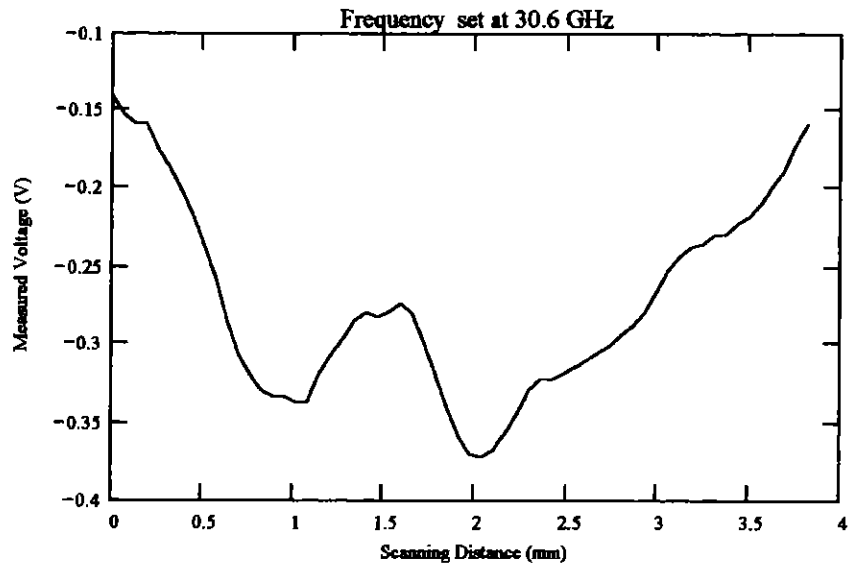


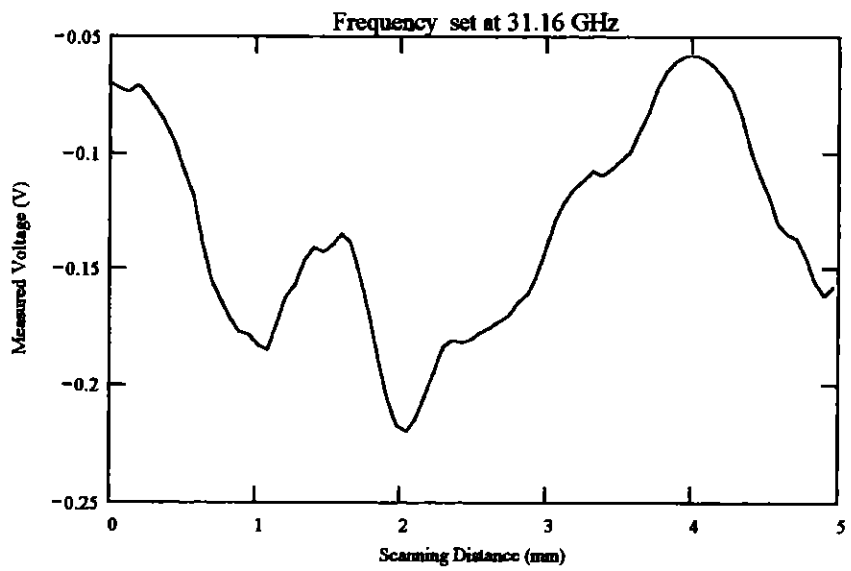
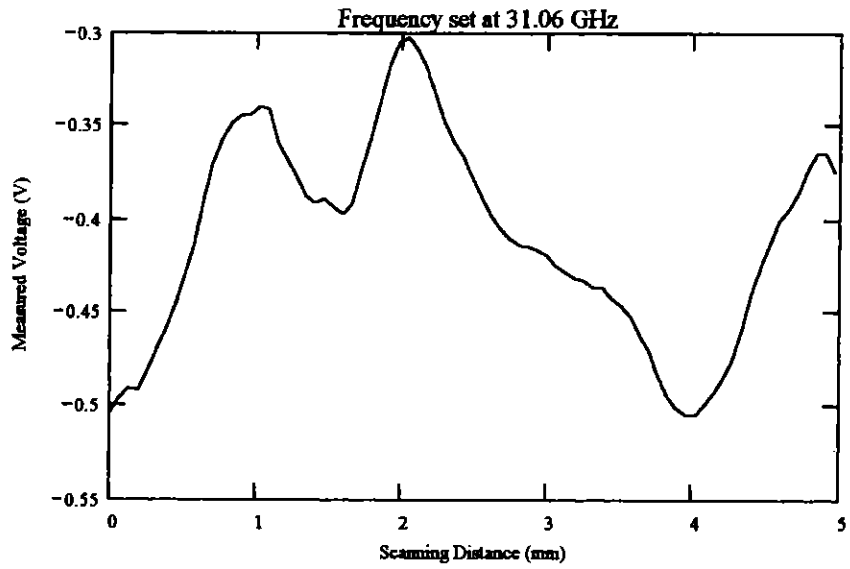


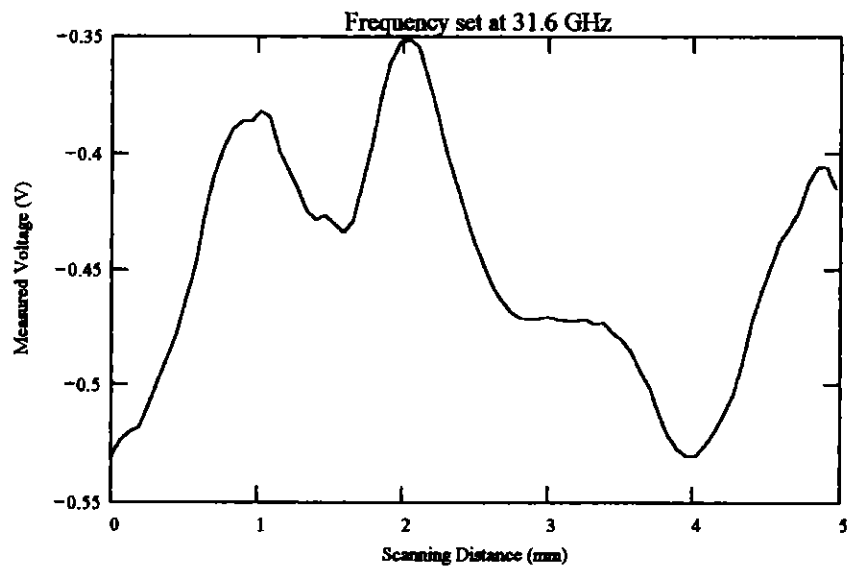
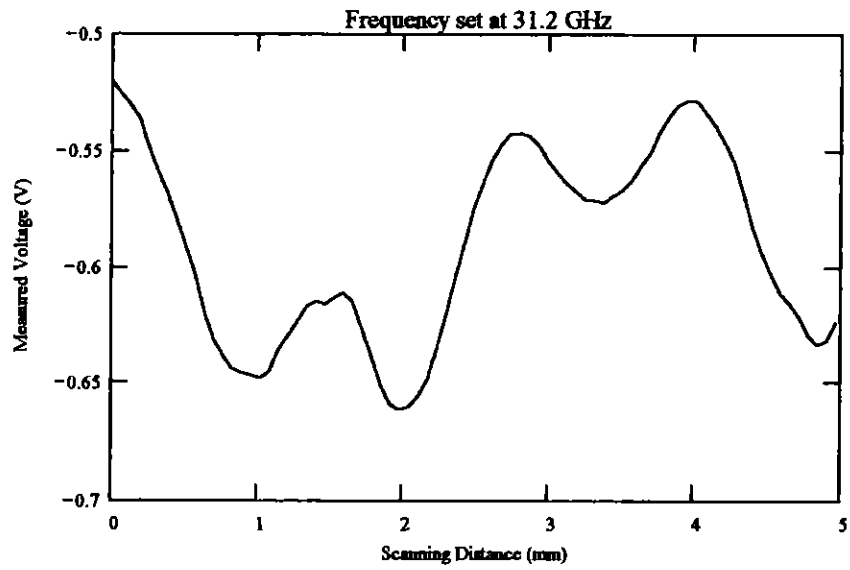
Frequency Band: Ka-band
Orientation: Scan perpendicular to crack length.
Probe: Coax no. 3
Scan Resolution: 0.064 mm per step
Scan length: 5 mm
Frequency: Varies







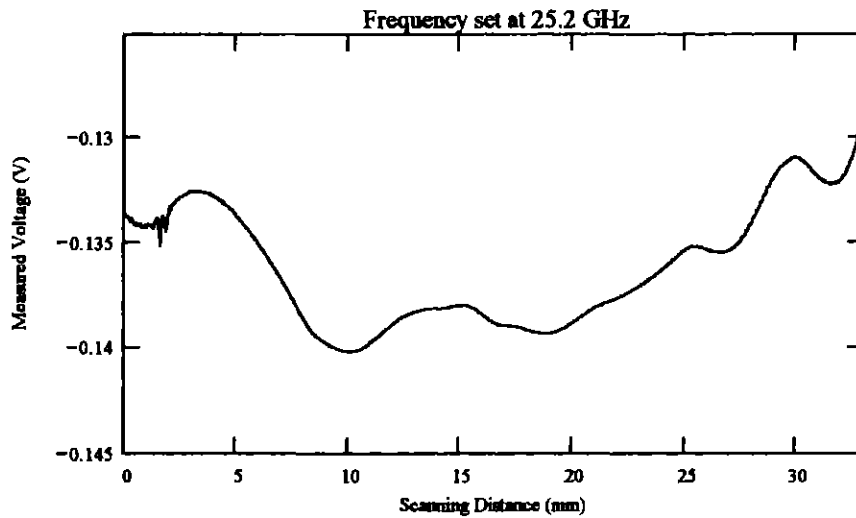


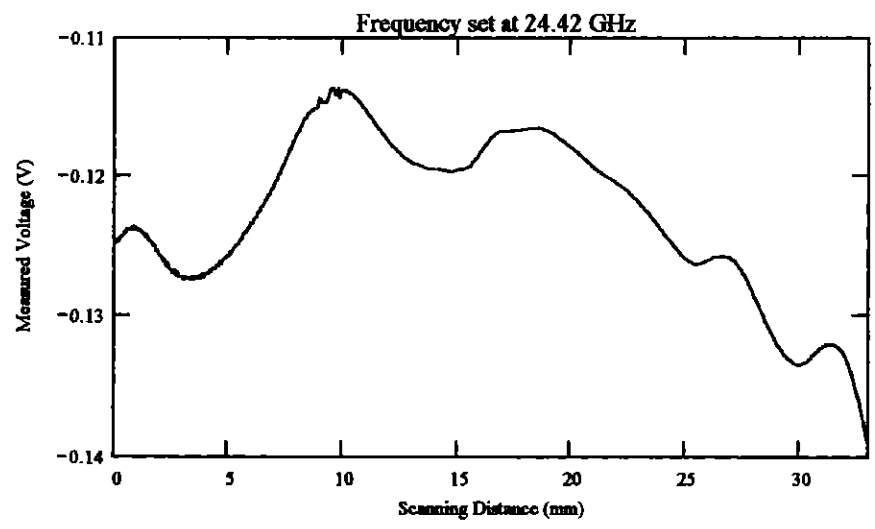
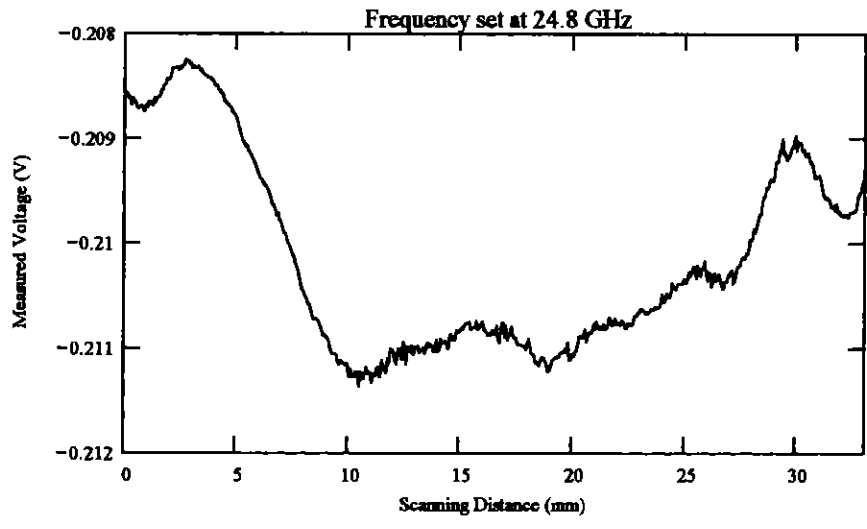


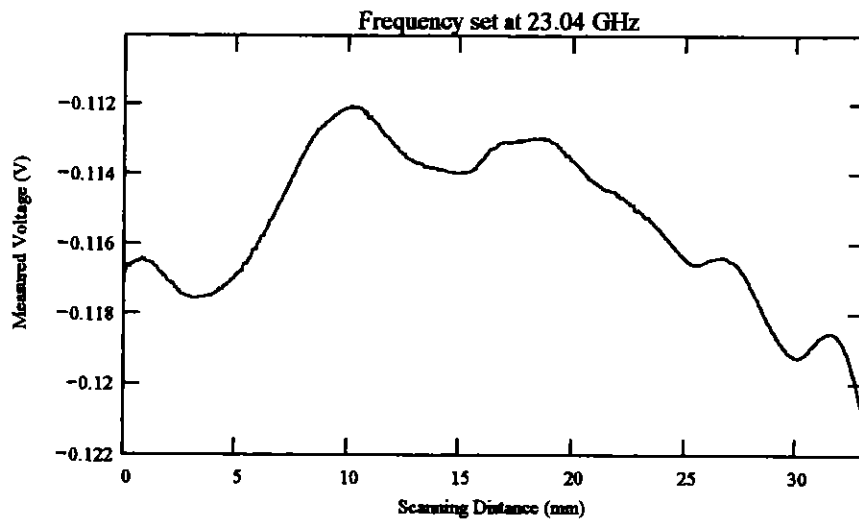
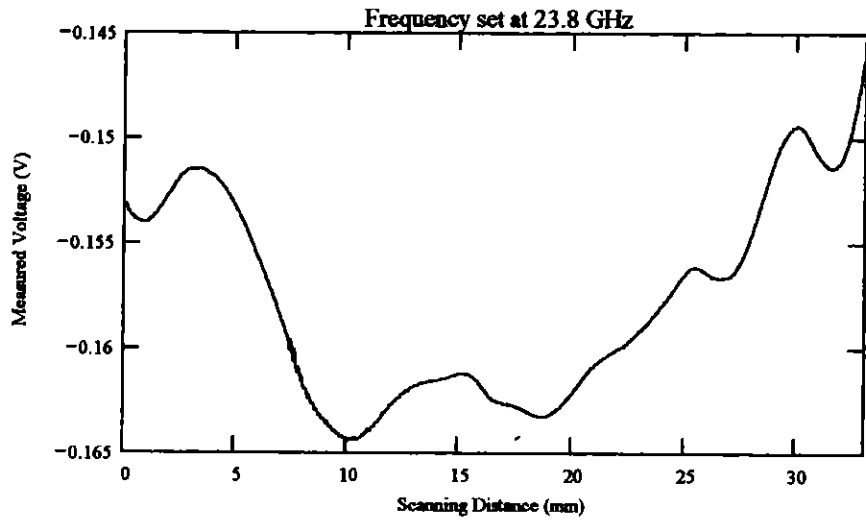
B. Crack #2

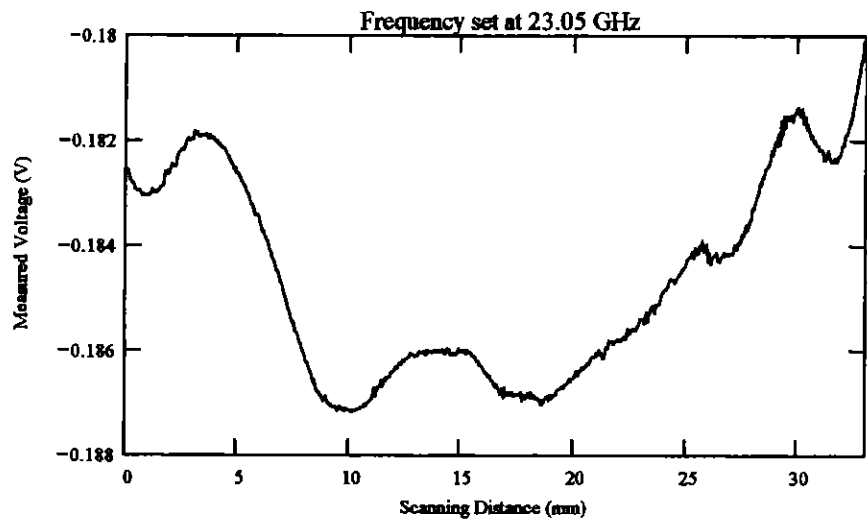
This is a Centreline Indication crack. The length of the crack is 15 mm. This crack runs parrallel to the welded joint.

Frequency Band: K-band
Orientation: Scan parrallel to crack length.
Probe: Coax no.2
Scan Resolution: 0.064 mm per step
Frequency: Varies

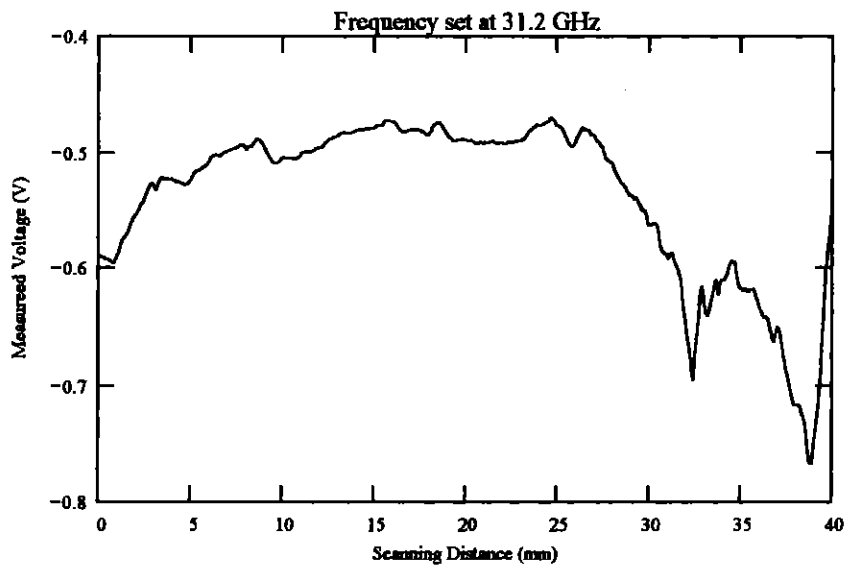


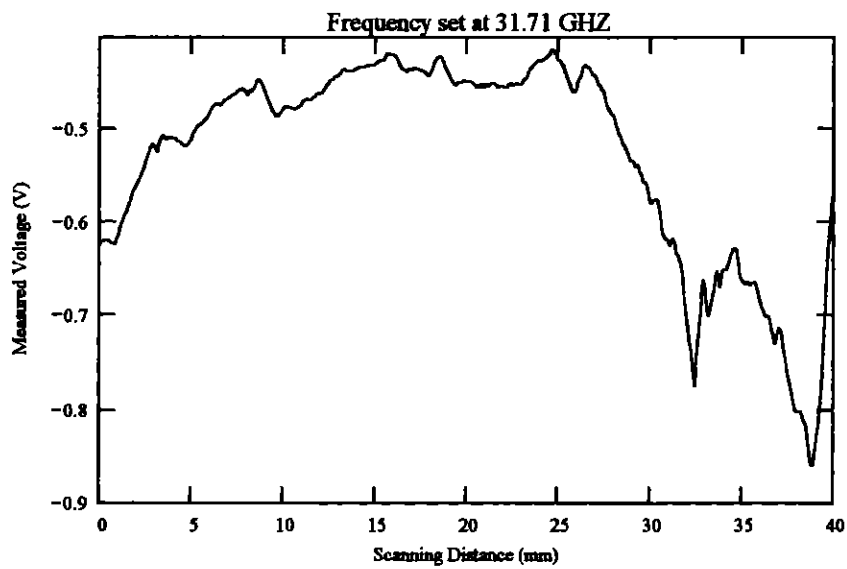
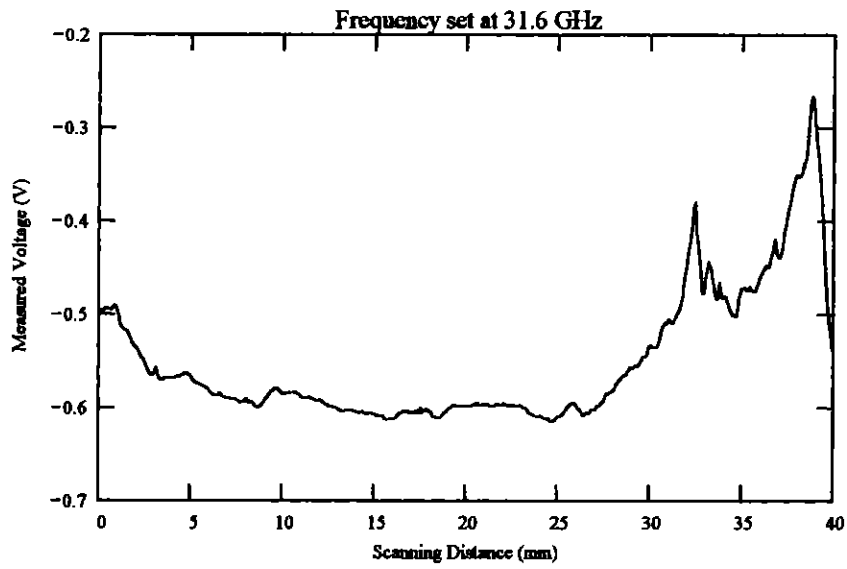


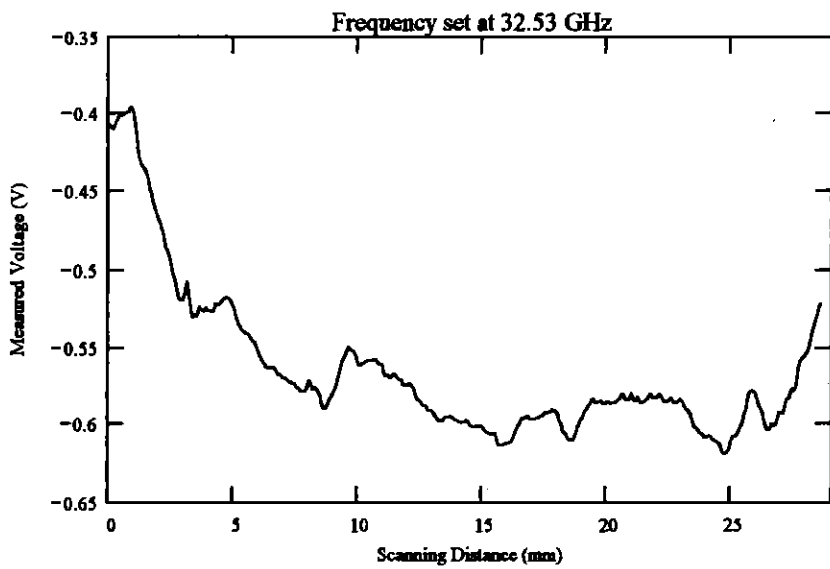
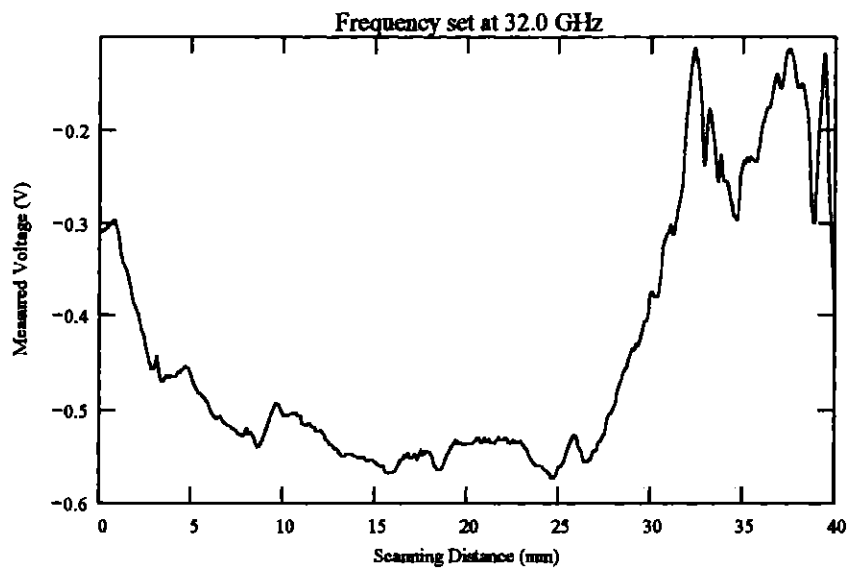


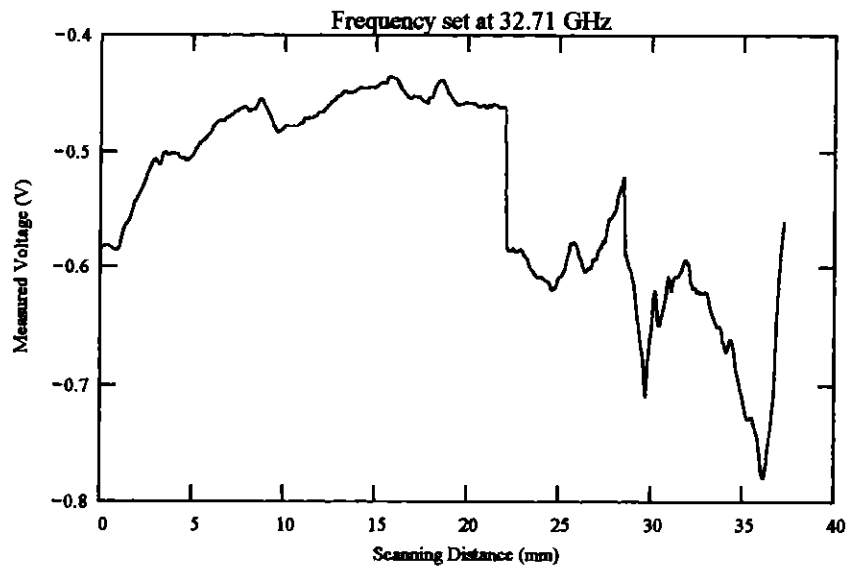


Frequency Band: Ka-band
Orientation: Scan parrallel to crack length.
Probe: Coax no. 3
Scan Resolution: 0.064 mm per step
Scan length: 40 mm
Frequency: Varies





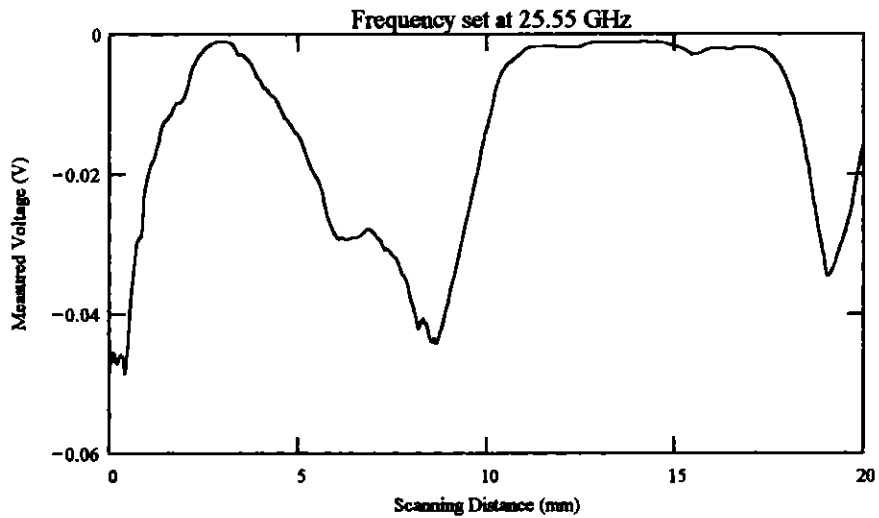


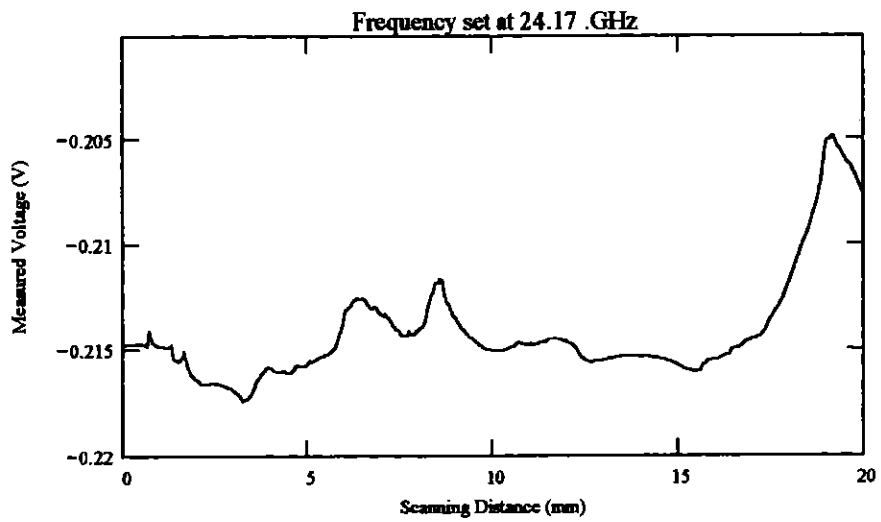
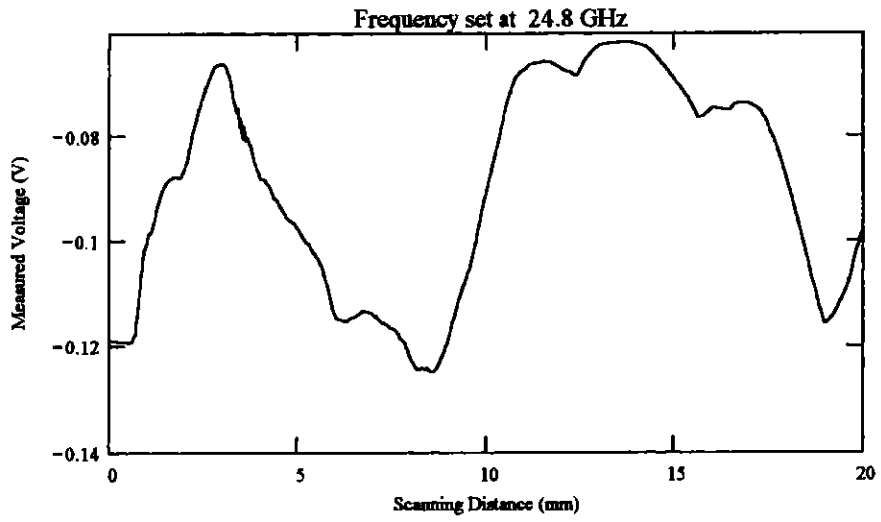


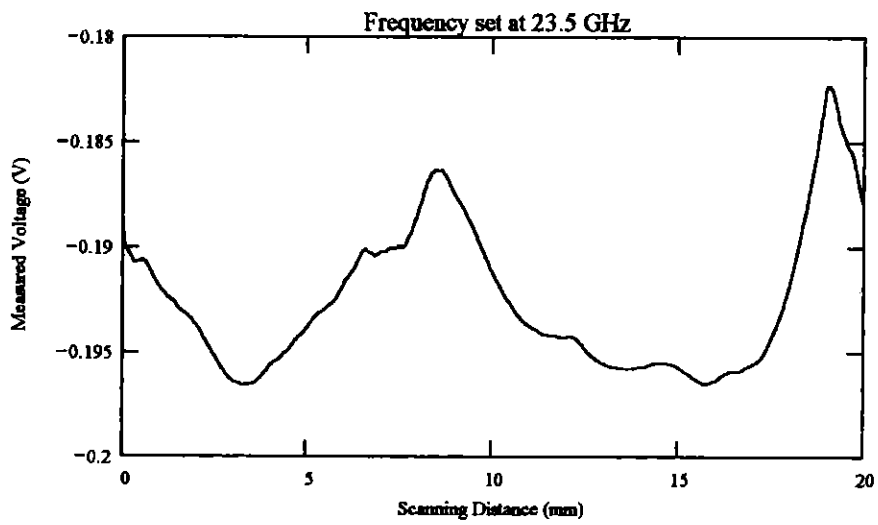
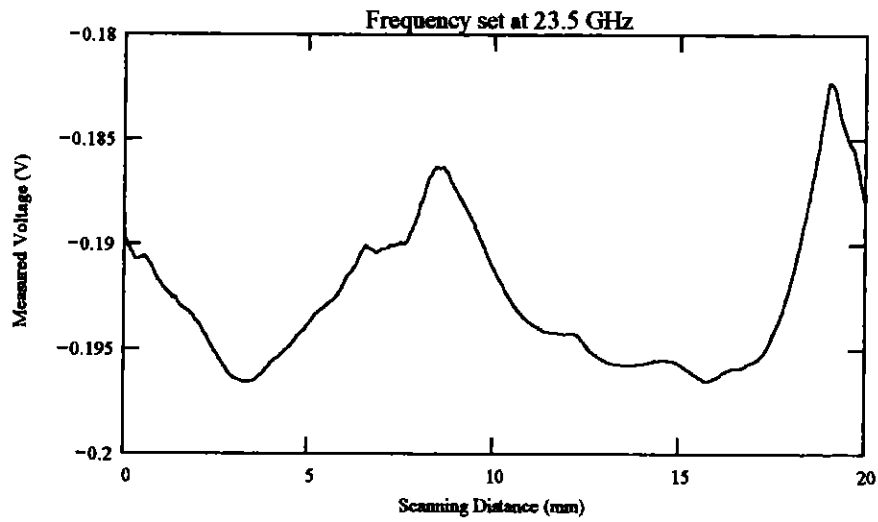
III. Sample T4297 Painted
A. Crack #1

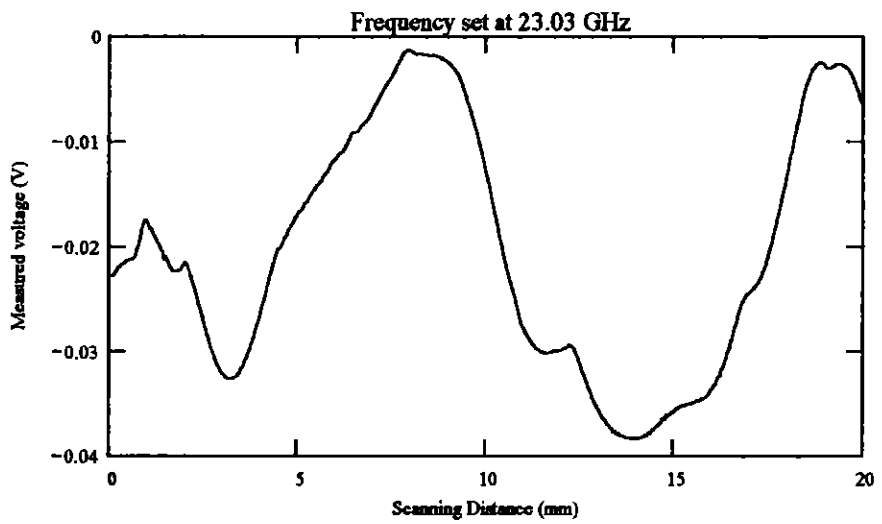
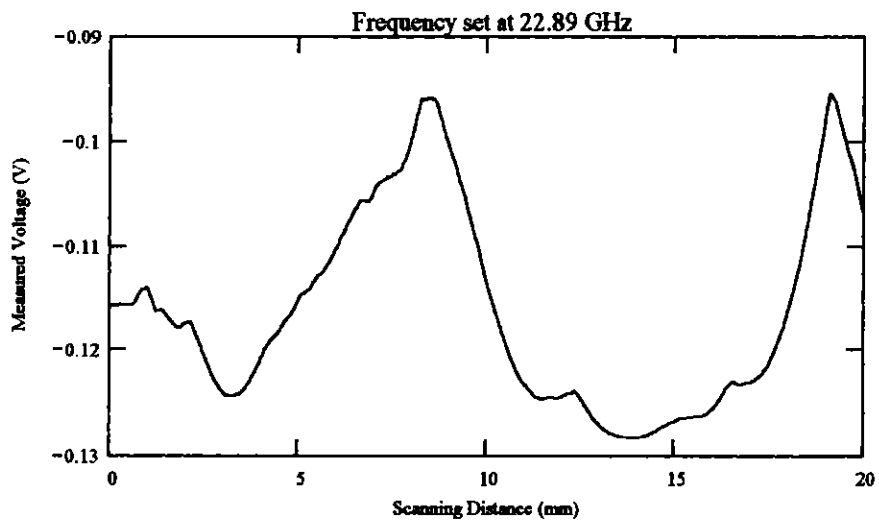
the This is a Transverse Indication crack. The length of
the crack is 11 mm. This crack runs perpendicular to
the welded joint.

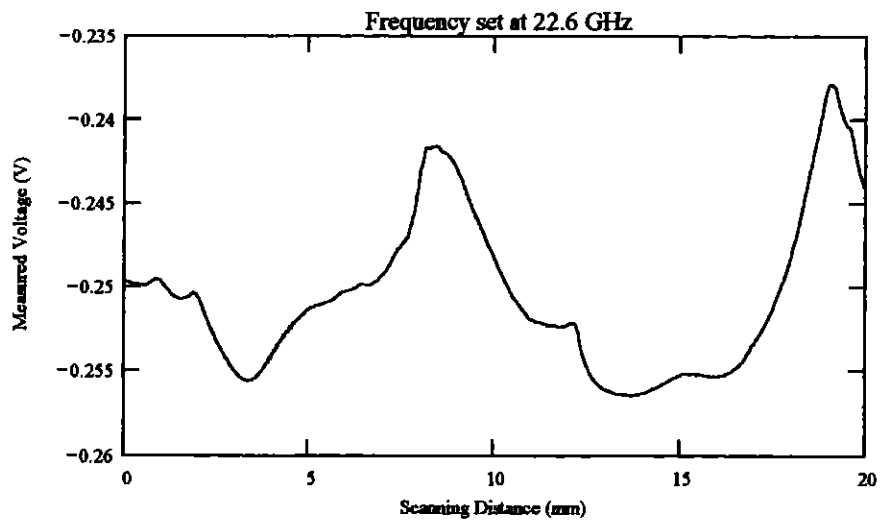
Frequency Band: K-band
Orientation: Scan perpendicular to crack length.
Probe: Coax no. 3
Scan Resolution: 0.025 mm per step
Scan length: 20 mm
Frequency: Varies



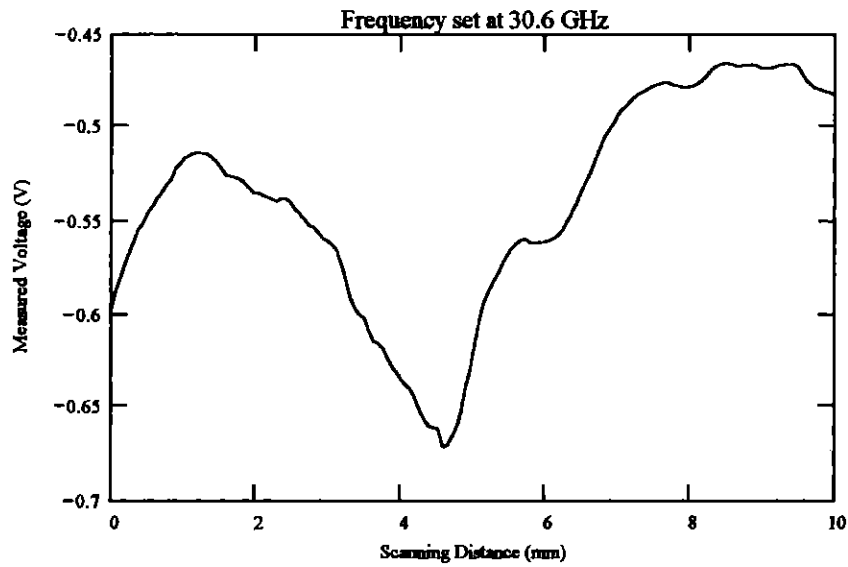


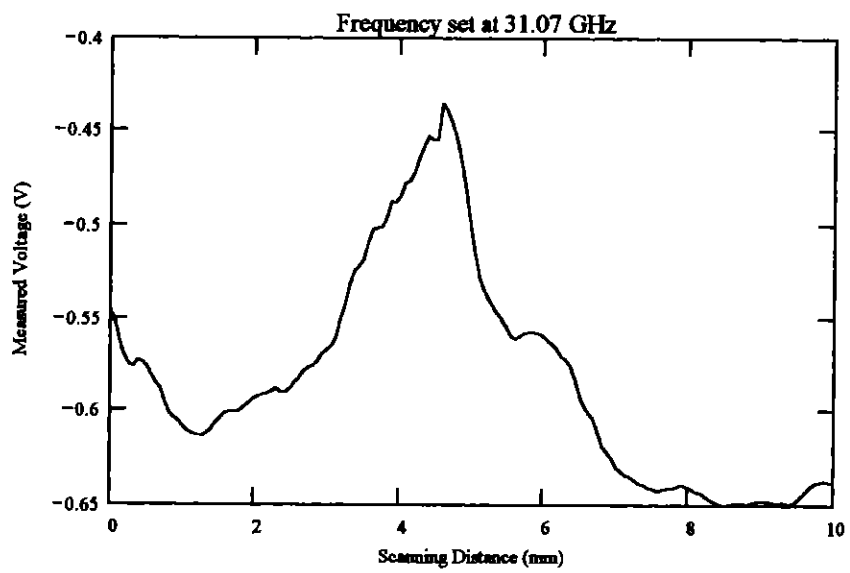
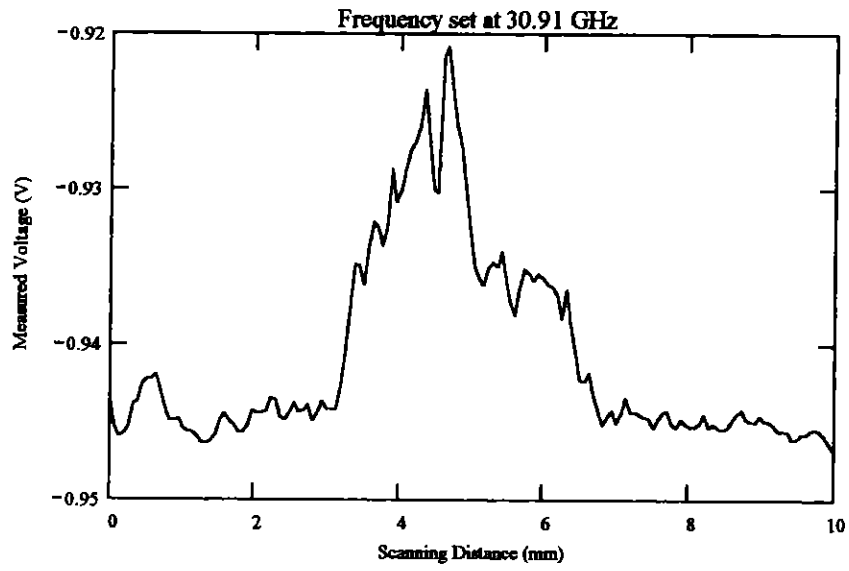


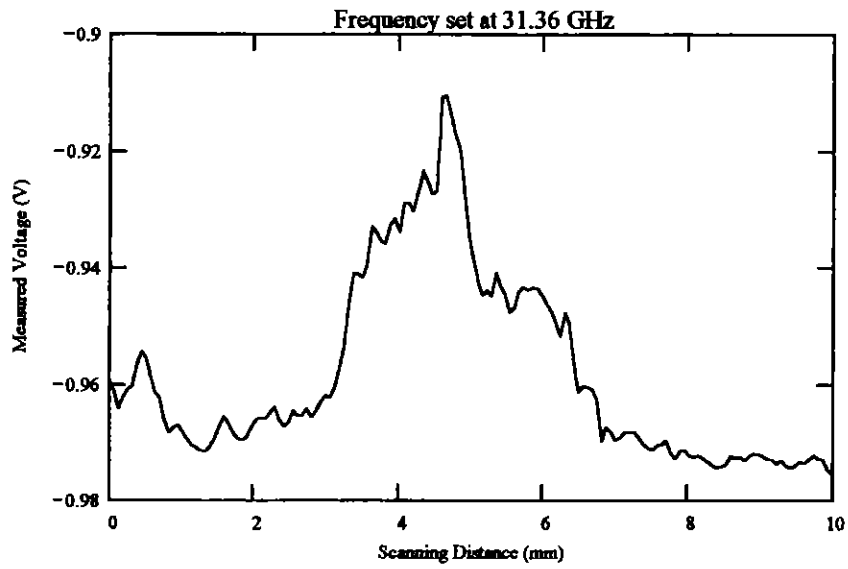
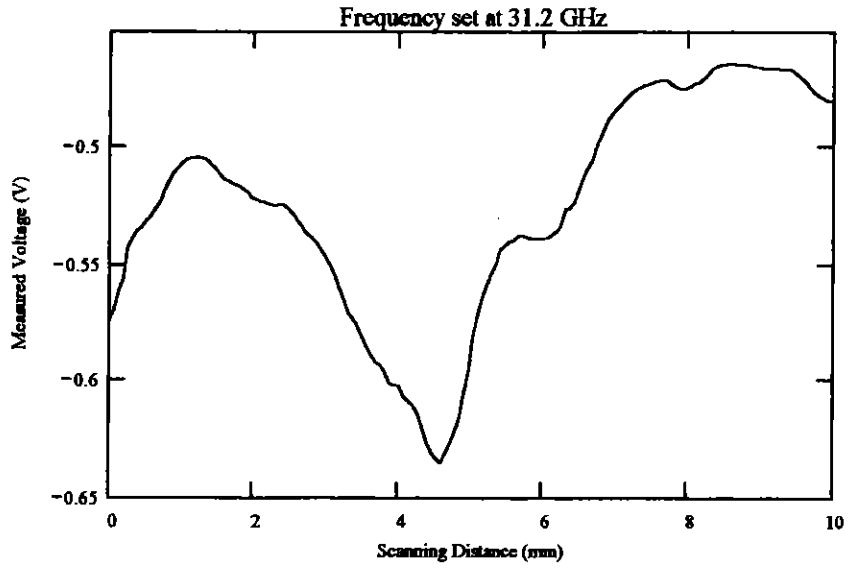


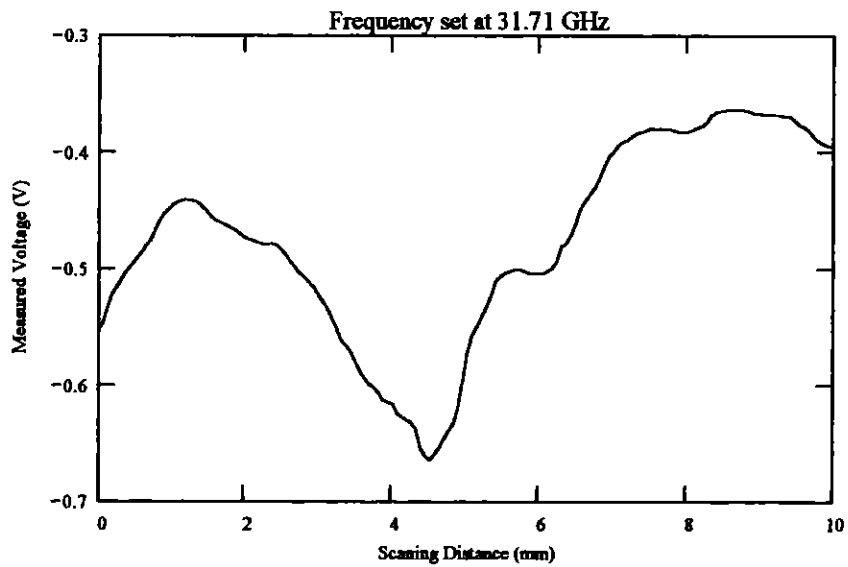
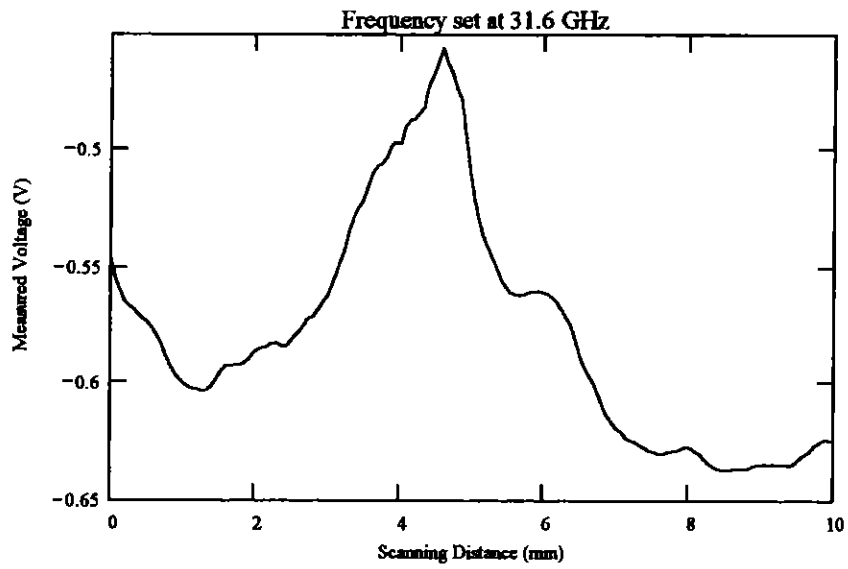


Frequency Band: Ka-band
Orientation: Scan perpendicular to crack length.
Probe: Coax no. 3
Scan Resolution: 0.064 mm per step
Scan length: 10 mm
Frequency: Varies





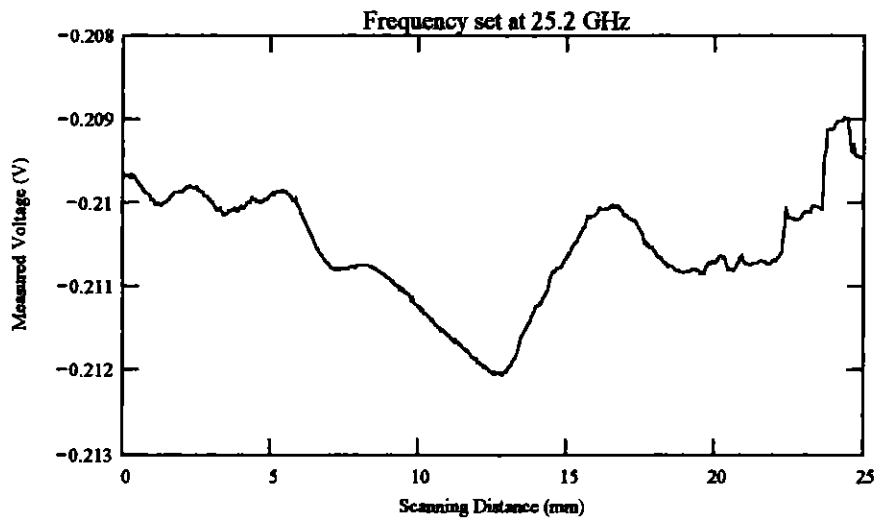


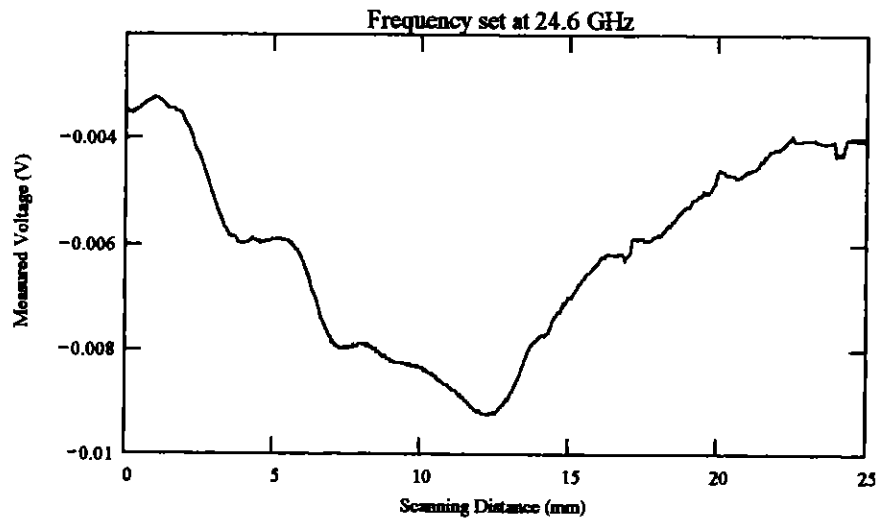
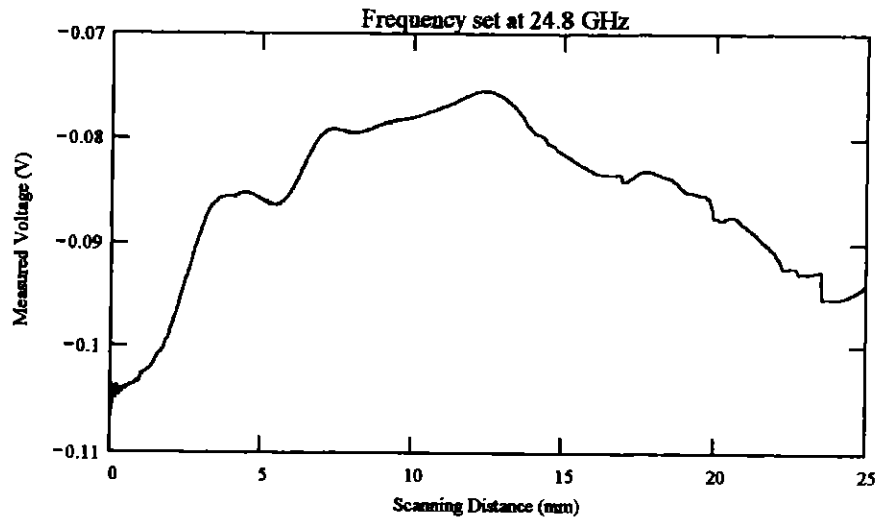


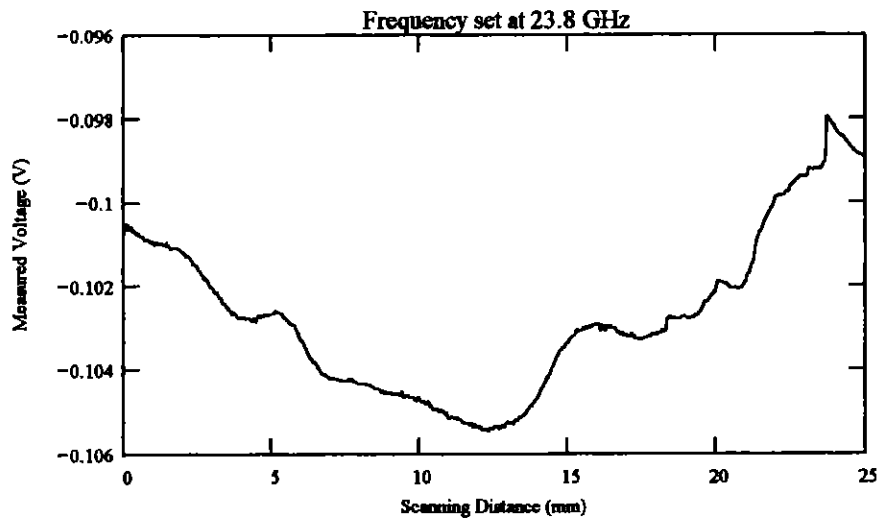
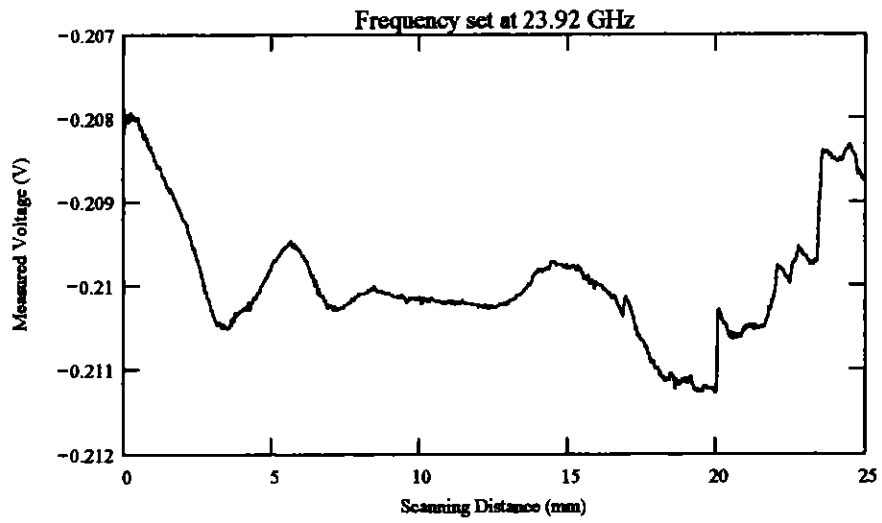
B. Crack #2

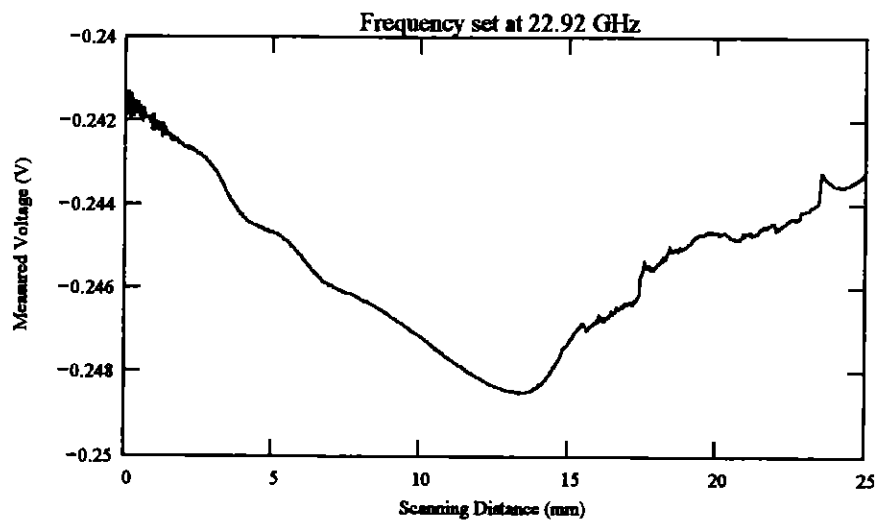
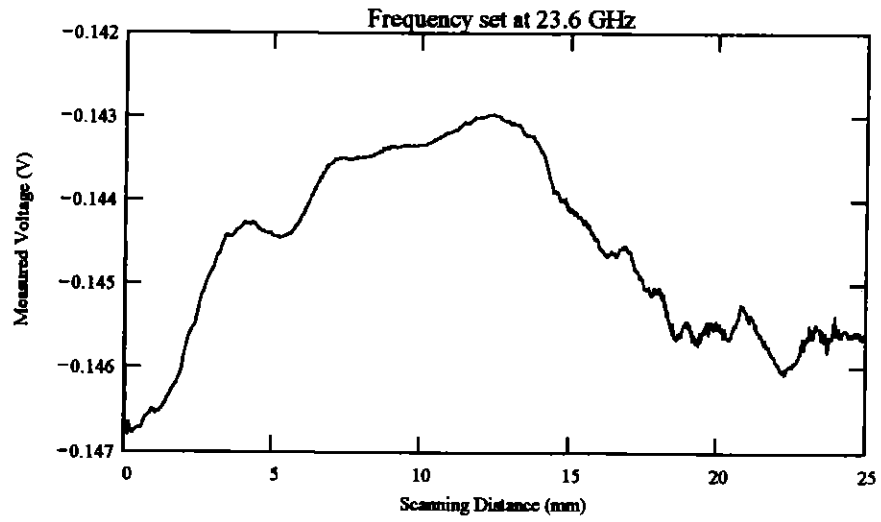
This is a Centreline Indication crack. The length of the crack is 15 mm. This crack runs parallel to the welded joint.

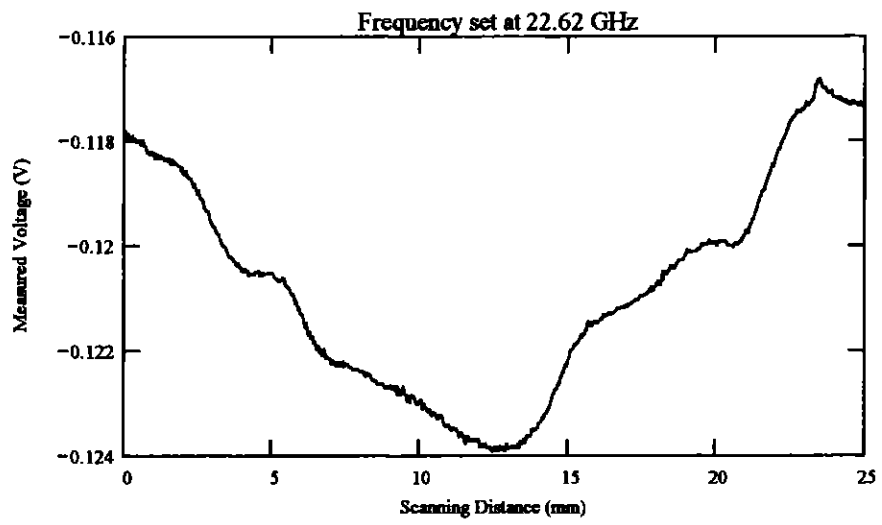
Frequency Band: K-band
Orientation: Scan parallel to crack length.
Probe: Coax no. 2
Scan Resolution: 0.032 mm per step
Scan length: 25 mm
Frequency: varies



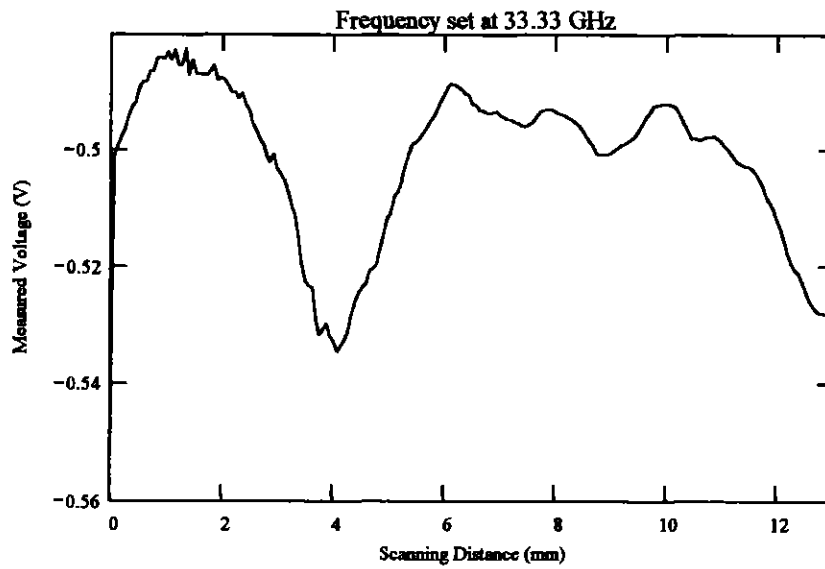


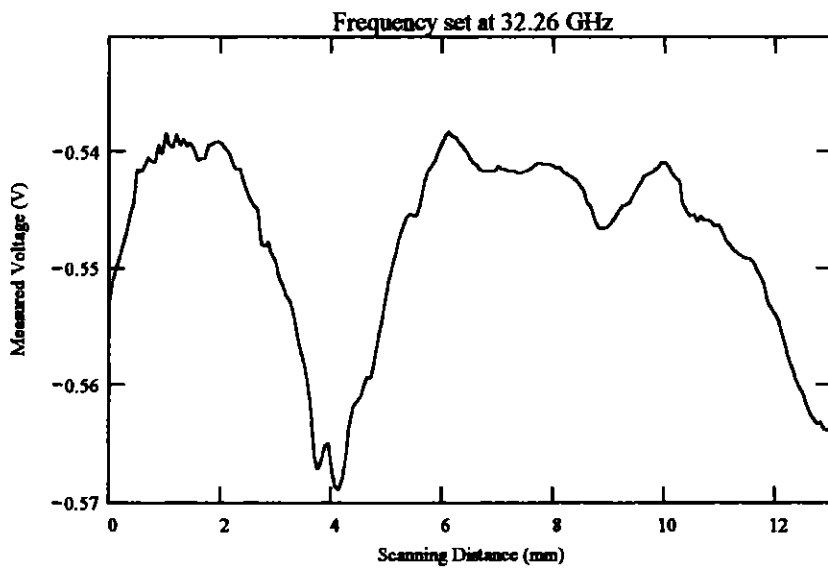
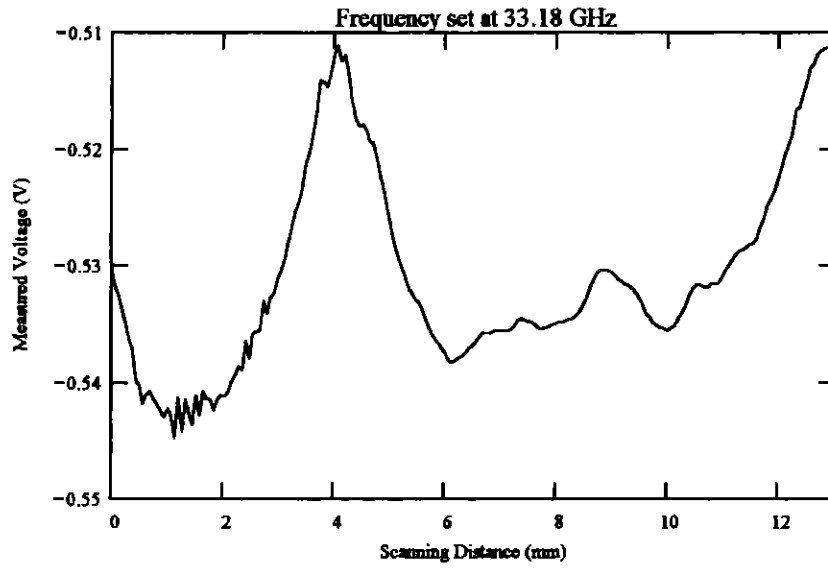


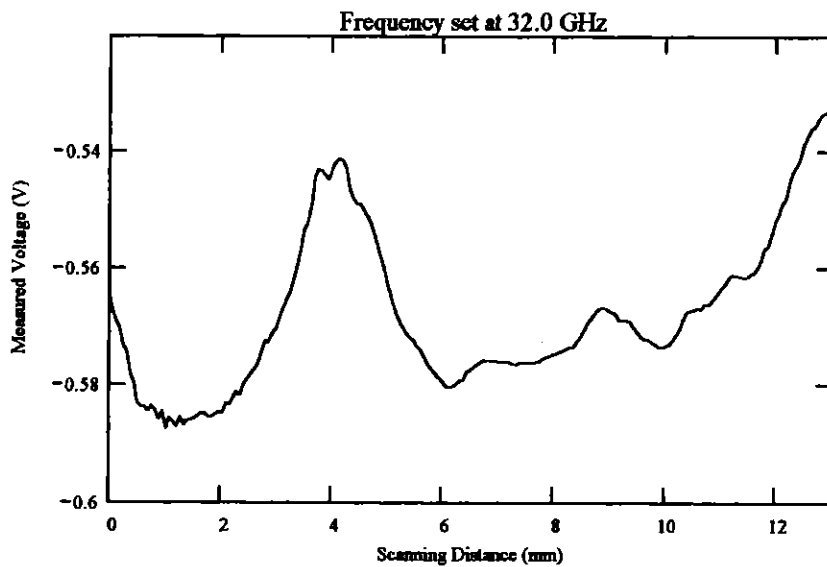
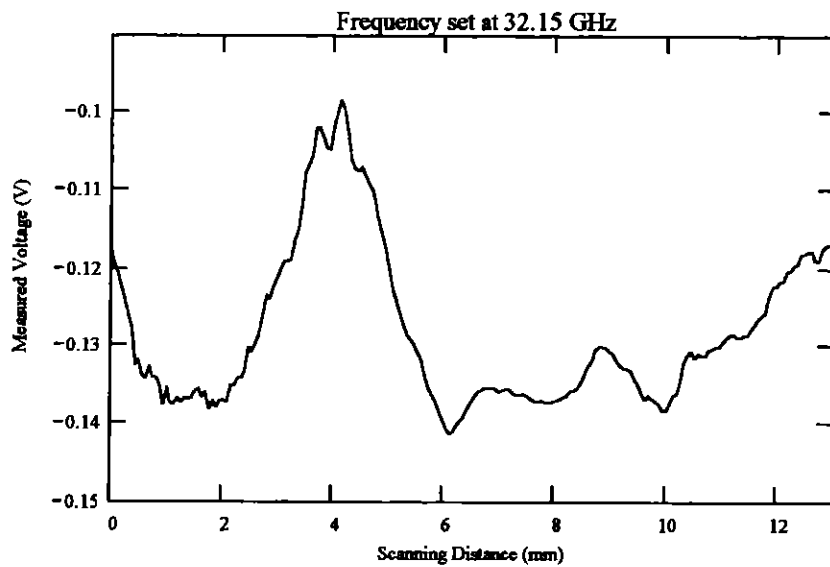


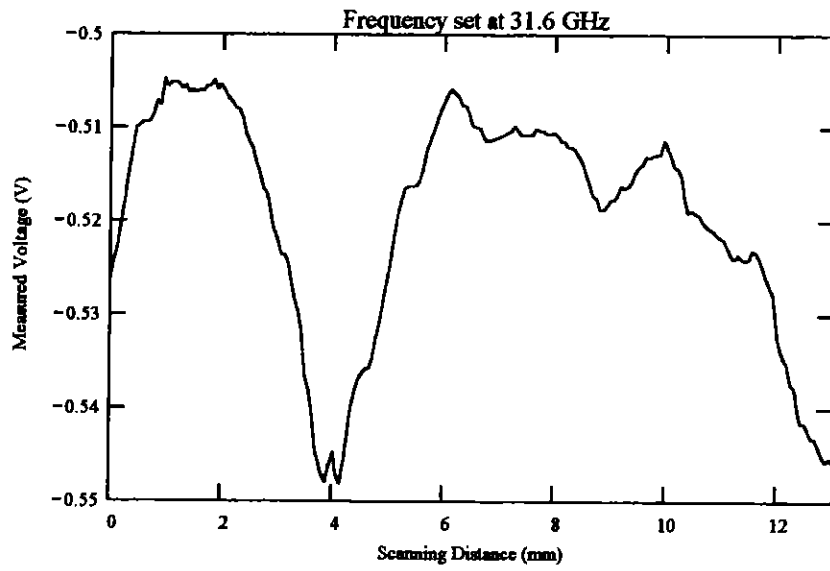


Frequency Band: Ka-band
Orientation: Scan parallel to crack length.
Probe: Coax no. 3
Scan Resolution: 0.064 mm per step
Scan length: 13 mm
Frequency: Varies







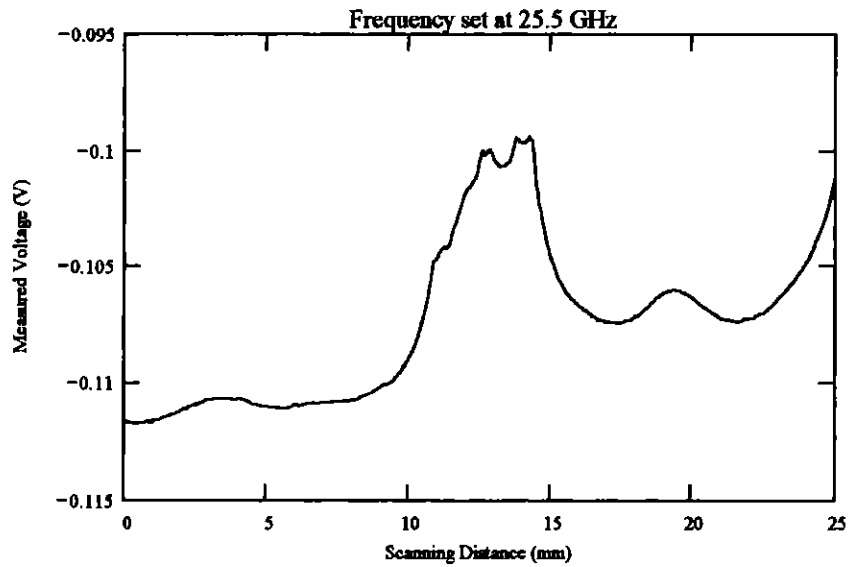


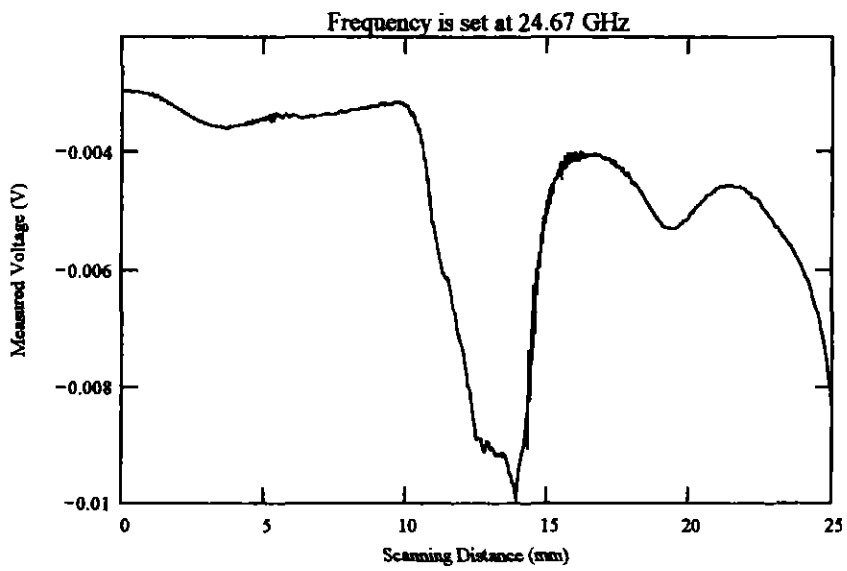
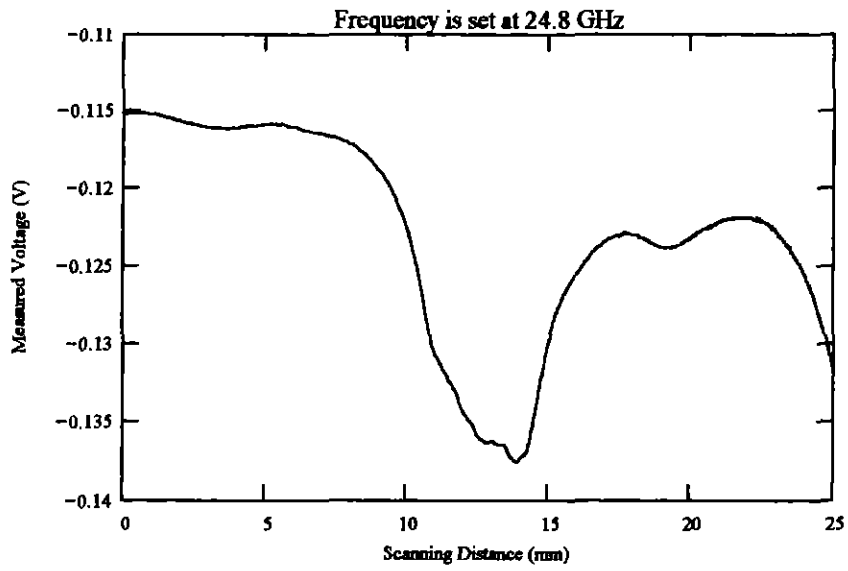
IV. Sample T4298 Painted

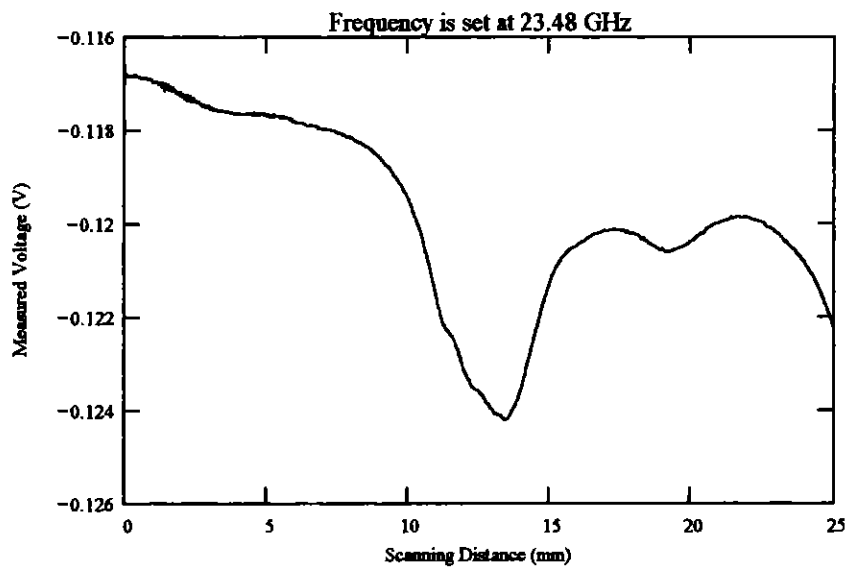
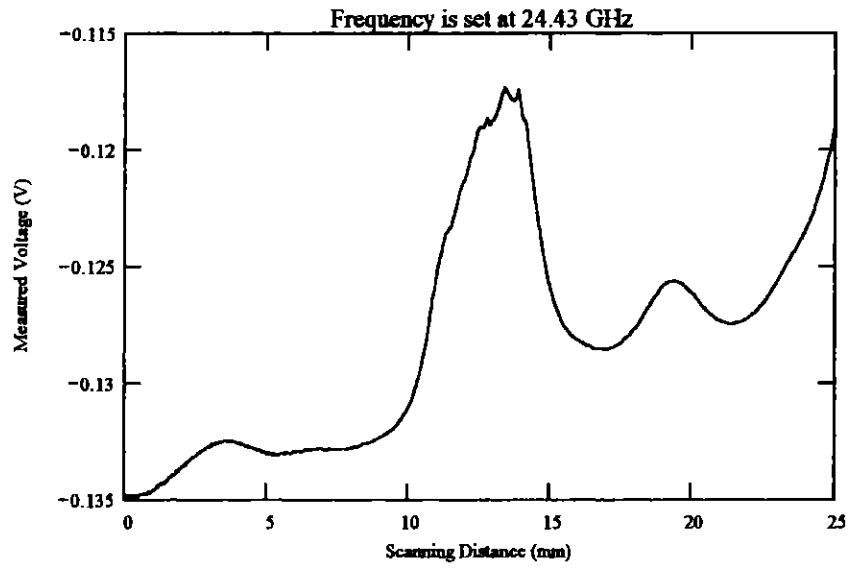
A. Crack #1

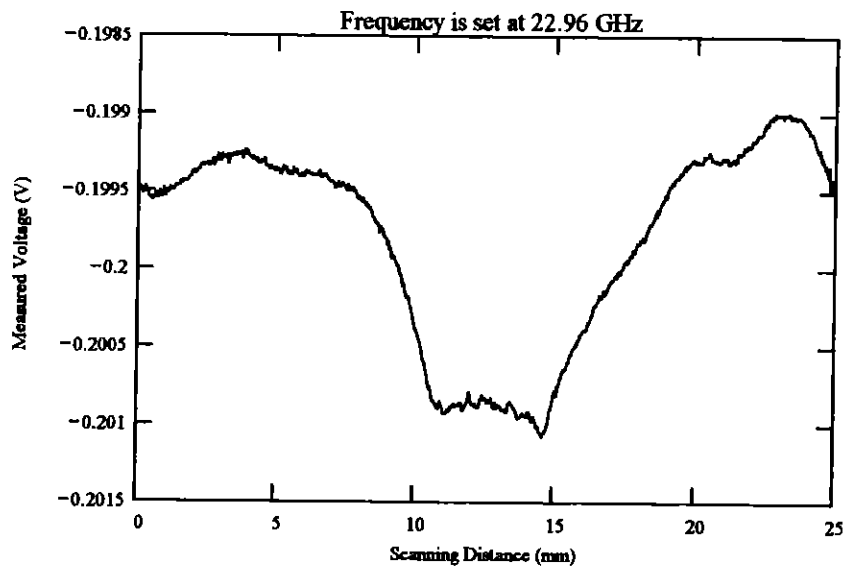
This is a Root Indication crack. The length of the crack is 17 mm. This crack runs parallel to the welded joint.

Frequency Band: K-band
Orientation: Scan parallel to crack length.
Probe: Coax no. 2
Scan Resolution: 0.064 mm per step
Scan length: 30 mm
Frequency: Varies

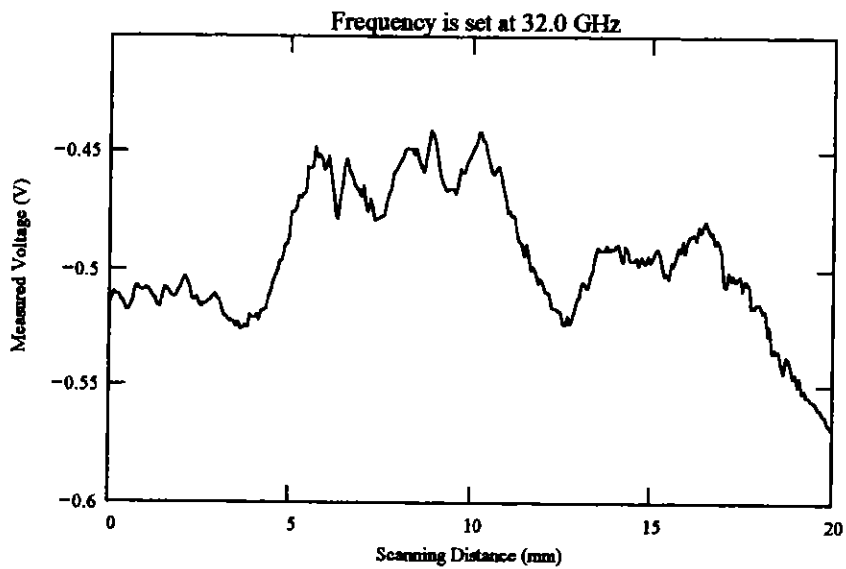


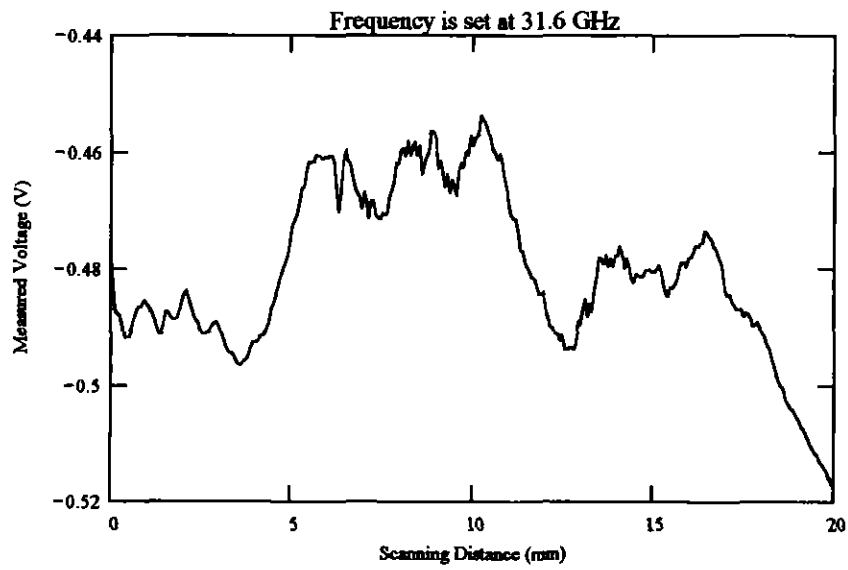
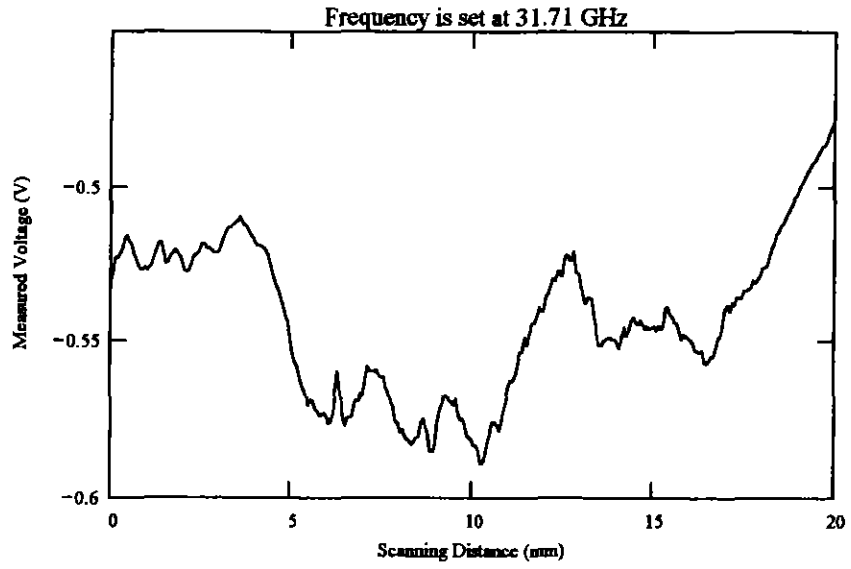


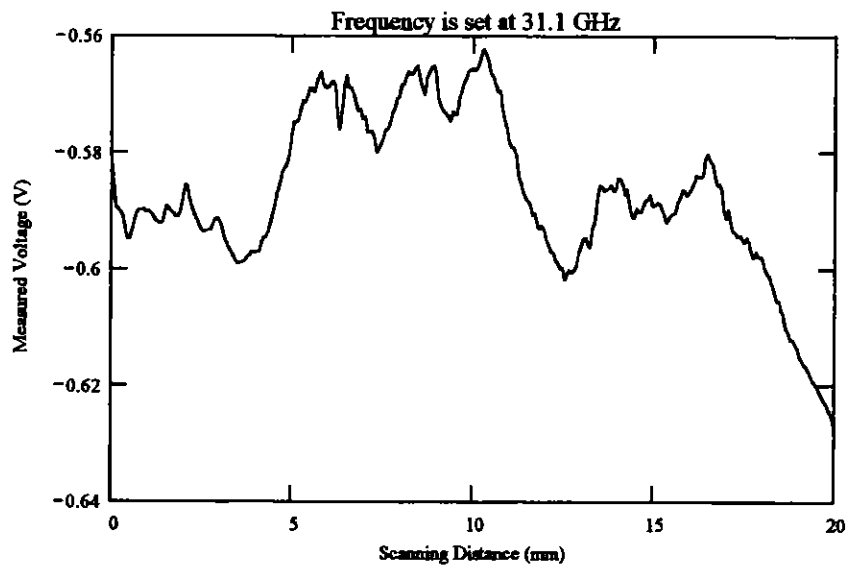
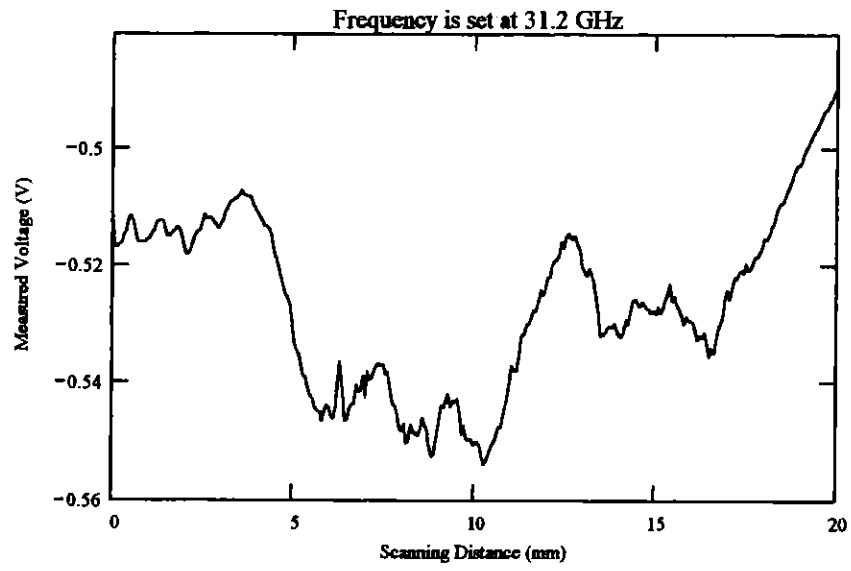


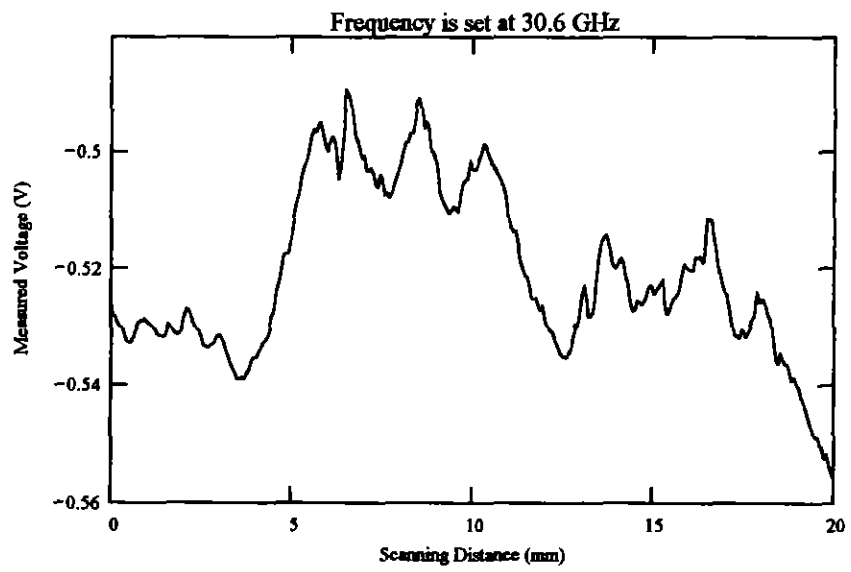
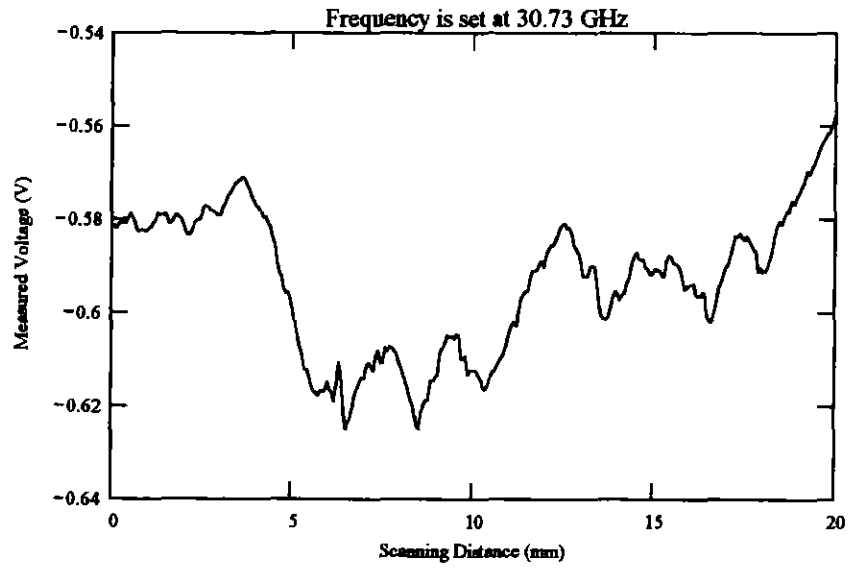


Frequency Band: Ka-band
Orientation: Scan parallel to crack length.
Probe: Coax no. 3
Scan Resolution: 0.064 mm per step
Scan length: 20 mm
Frequency: Varies





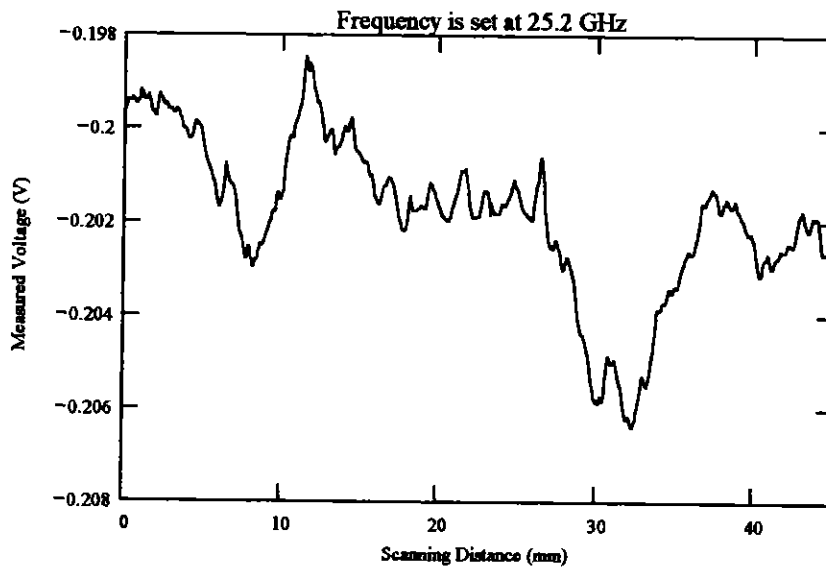


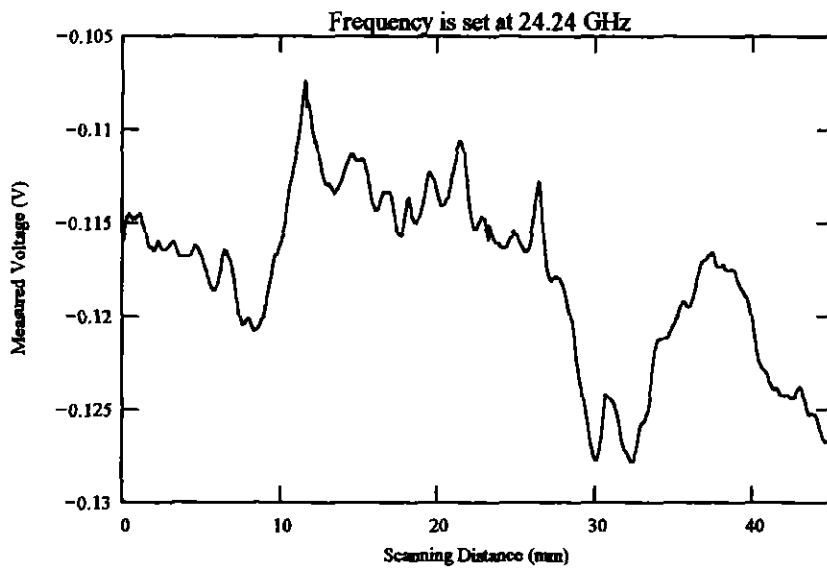
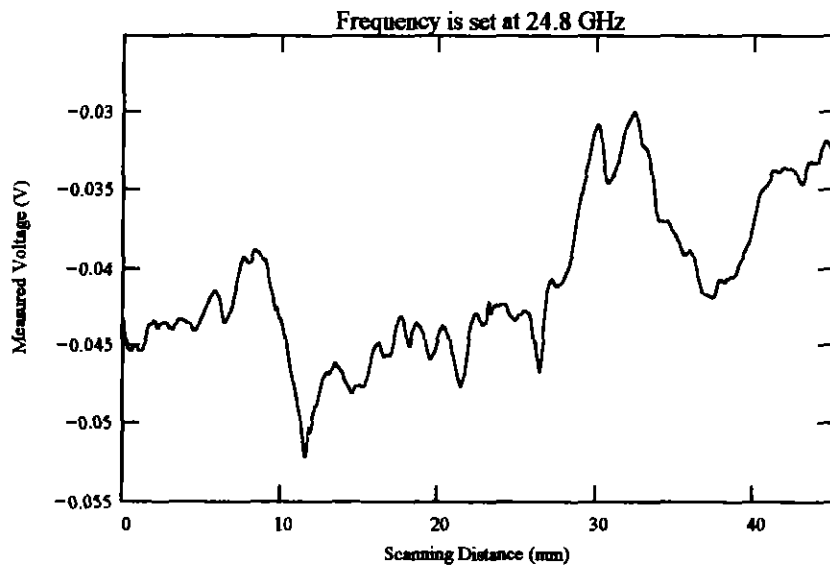


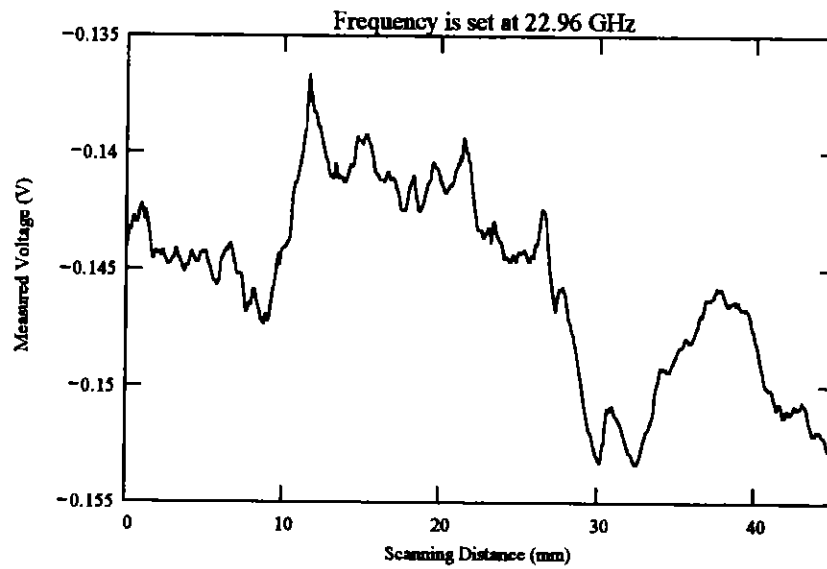
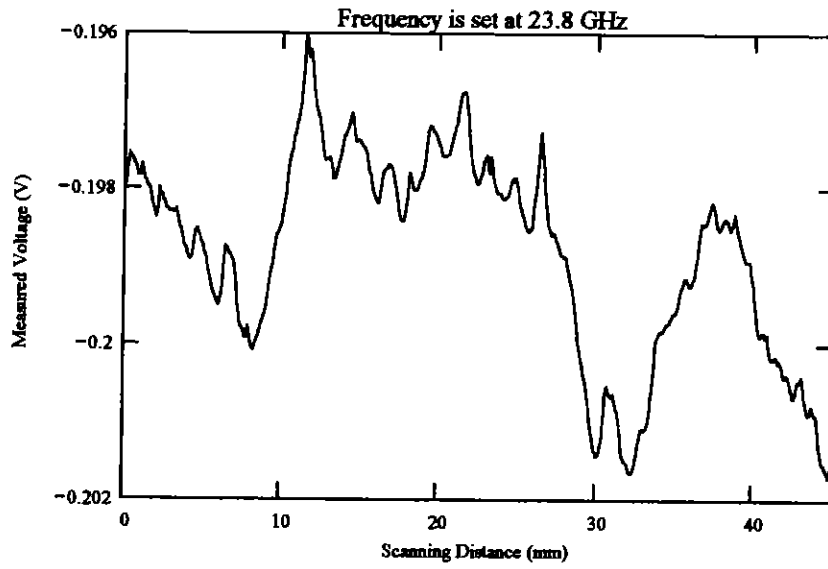
B. Crack #2

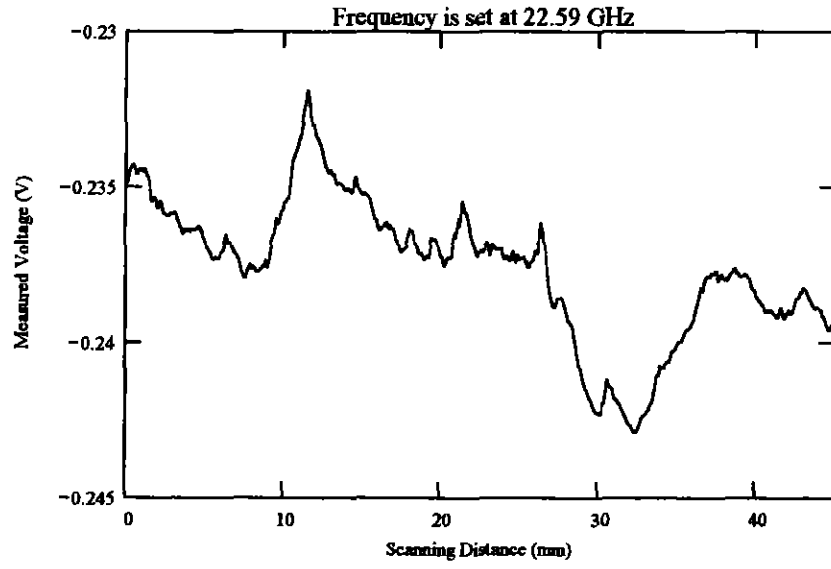
This is a Toe Indication crack. The length of the crack is 30 mm. This crack runs parallel to the welded joint.

Frequency Band: K-band
Orientation: Scan parallel to crack length.
Probe: Coax no. 2
Scan Resolution: 0.064 mm per step
Scan length: 45 mm
Frequency: varies









Frequency Band: Ka-band
Orientation: Scan parallel to crack length.
Probe: Coax no. 3
Scan Resolution: 0.064 mm per step.
Scan length: 40 mm
Frequency: Varies

